The Use of Chemistry, Isotopes and Gases as Indicators of Deeper Circulating Groundwater in the Main Karoo Basin

Report to the

Water Research Commission

by

Ricky (EC) Murray[1], Kelley Swana[2], Jodie Miller[3], Siep (AS) Talma[4], Gideon Tredoux[4], Avner Vengosh[5] and Tom Darrah[6]

[1]Groundwater Africa

[2]Student, Stellenbosch University

[3] Department of Earth Sciences, Stellenbosch University

[4]Private consultants

[5]Division of Earth and Ocean Sciences, Nicholas School of the Environment, Duke University, Durham , United States of America

[6]School of Earth Sciences, The Ohio State University, Columbus, United States of America

WRC Report No. 2254/1/15

ISBN 978-1-4312-0678-0

May 2015

GROUNDWATERAFRICA

Obtainable from

Water Research Commission
Private Bag X03
GEZINA, 0031

orders@wrc.org.za or download from www.wrc.org.za

DEDICATION

This report is dedicated to the memory of Professor Gerrit van Tonder who first raised the concern about the contamination of shallow aquifers with poor quality, deep-seated Karoo waters, and enthusiastically and at times controversially, contributed to the debate on shale gas exploration and development. He is deeply missed by the South African groundwater community.

Prof Gerrit van Tonder in 2012 at the 4169 m deep Soekor borehole SA1/66 during its opening nearly 50 years after it was drilled.

EXECUTIVE SUMMARY

Introduction

Numerous environmental concerns have been raised with the possible exploration and development of shale gas in the Karoo. One such concern is that deep borehole drilling and the hydraulic fracturing process may create conduits through which deep-seated groundwater could migrate to shallow aquifers. If this deep groundwater is of poor quality, and if shale gas development does facilitate upward migration of deep waters, then it is possible that poor-quality deep groundwater may blend with shallow Karoo groundwater that could be used for water supplies. In some areas, the deep groundwater may even issue at the surface via leaking shale gas boreholes should they lose their integrity. This upward flow to the surface or near-surface will only take place for an extended period of time if the deep-seated Karoo shales are sufficiently permeable to allow for groundwater flow, under sufficient pressure for the flow to rise to the near-surface, and hydraulically linked to an extensive area so that the flow continues over time (i.e. not a closed “reservoir”).

Should these conditions for upward flow be present in parts of the Karoo, then this is a concern if the deep-seated groundwaters are poor quality. This concern, however, is primarily a long-term one. The integrity of deep boreholes may be compromised decades or centuries after abandonment through the slow deterioration of the sealing cements used in borehole grouting and plugging. Likewise, the high-pressure fracking process may marginally open existing fractures that were previously impermeable and thus allow for the very slow upward migration of deep-seated groundwaters. Or crustal instability may only occur in years to come with the required intensity to cause upward movement of water through old or new faults and fractures.

The short-term value of knowing the quality of deep groundwater is that it will help in planning how to deal with the produced water that flows from the deep boreholes during gas extraction. If this water is not suitable for re-use in the fracking process, it needs to be treated to acceptable standards prior to disposal.

These short- and long-term concerns are however minor issues if deep-seated Karoo groundwaters are not poor quality. This project aimed to address this lack of knowledge by characterising the nature of the deeper Karoo groundwaters. At present, however, this task is problematic as there are no suitable boreholes for sampling the deep formations targeted for shale gas development. The existence of warm springs in the Karoo is the closest

approximation that is available through which one can obtain an idea of the nature of deep groundwater, and for this reason, these springs are the main sources of information in this project. Two deep boreholes were also located from which samples were collected, but in both cases it is not known if the water came from the shales or deeper, underlying formations.

The "deep" groundwater referred to in this report originated mostly from warm springs and at this stage provides a best guess of the type of groundwater to be found at greater depths but does not necessarily represent groundwater that may be found in the deep shale layers that are being considered for shale gas exploration.

Definition of deep and shallow groundwater

Eight study locations were identified that span the central and south-western areas of the Main Karoo Basin (Figure 4.2), and in each of these areas "deep" samples were collected from warm springs, deep boreholes or boreholes that had previously been suspected of containing deep groundwater. Near each of these sites, a "shallow" counterpart sample was collected from boreholes for comparative purposes. From the initial 34 sites that were investigated, 20 sites were finally selected for detailed analyses.

The determinands assessed included:

- Electrical Conductivity (EC), pH, temperature, field alkalinity, Dissolved Oxygen (DO), Oxidation-Reduction Potential (ORP)
- Major cations and anions
- Trace elements
- Oxygen and hydrogen isotopes ($\delta^{18}O$ and $\delta^{2}H$)
- Strontium isotopes ($^{87}Sr/^{86}Sr$)
- Tritium (^{3}H) and carbon-14 (^{14}C) isotopes
- Chlorine-36 isotope(^{36}Cl)
- Boron isotope ($\delta^{11}B$)
- Radium isotopes (^{226}Ra and ^{228}Ra)
- Carbon isotopes in dissolved inorganic carbon ($\delta^{13}C$-TIC)
- Carbon isotope in methane ($\delta^{13}C$-CH_4)
- Carbon isotope in carbon dioxide ($\delta^{13}C$-CO_2)

- Gases: Radon (^{222}Rn), helium (^{4}He), helium (^{3}He), argon (Ar), methane (CH_4), nitrogen (N_2), oxygen (O_2), carbon dioxide (CO_2), hydrogen sulphide (H_2S).

Some shallow samples showed clear evidence of being similar to the deep sites, so it became necessary to group samples into provisional deep and shallow categories that were not only based on temperature or borehole depth. The criteria used were temperature and the shape of the Stiff diagrams. The deep groundwater was characterised by ”Y” shaped Stiff diagrams and/or elevated temperature and the shallow groundwater was characterised by hexagon shaped Stiff diagrams and/or low temperatures. A third group became necessary, a “mixed” groundwater that typically had an ambiguous Stiff diagram shape and/or inconsistent temperature information. Figure 1 presents the samples in the Stiff diagram groups. The diagrams on the left hand side are presumed to be from deep sources, while those on the right hand side are presumed to be from shallow sources. Because of significant differences in the concentrations of the total cations and anions in the different samples, the Stiff diagrams are not all on the same scale.

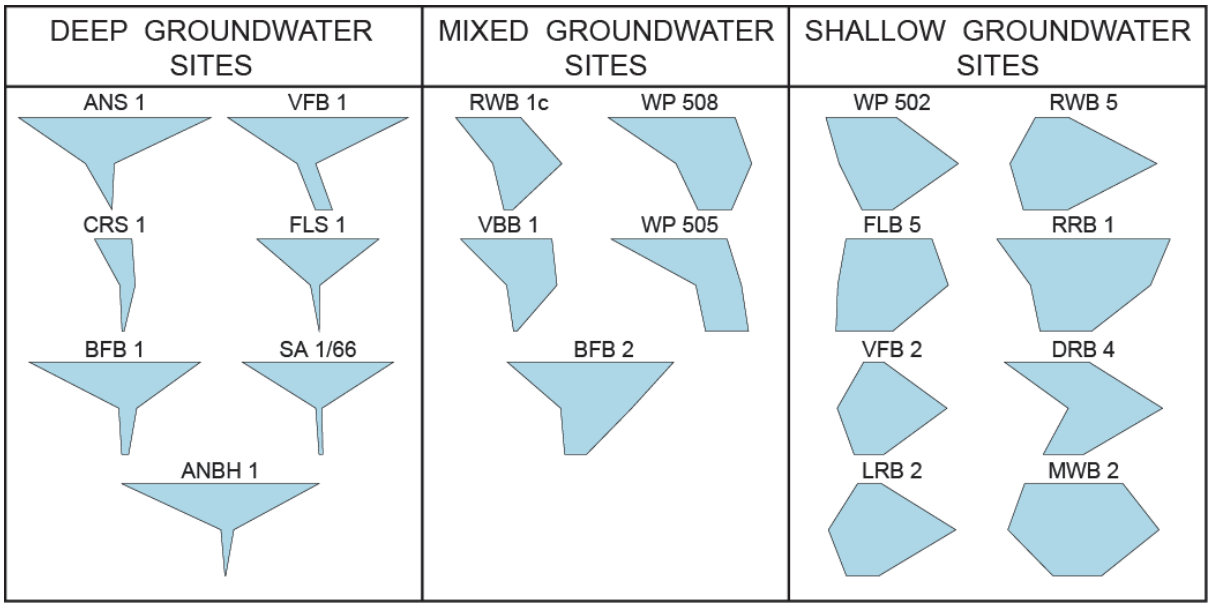

Figure 1. Groundwater samples grouped into depth categories based on Stiff diagram shapes

Groundwater temperature, which was the other main criteria for differentiating deep from shallow waters, together with ^{14}C values are shown in Figure 2.

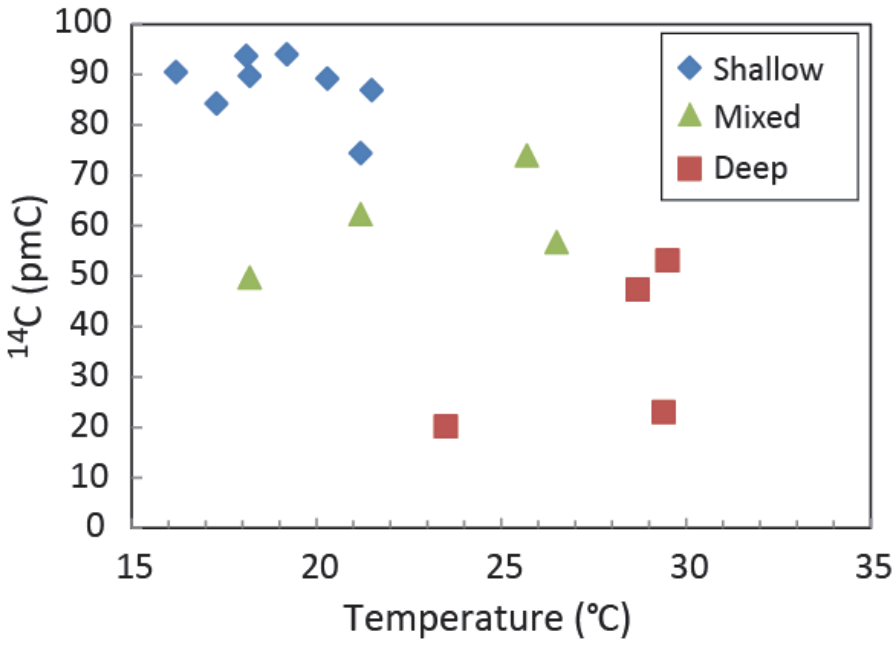

Figure 2. Plot of ^{14}C versus temperature for the three groups of sources

The data and interpretations presented suggest that for the Main Karoo Basin it is possible to define a "deep" or warm groundwater, which is distinct from a shallow or cold groundwater. For the purposes of this report, deep and shallow groundwaters were defined as follows:

- Deep Groundwater
  - "Y" shaped Stiff diagram
  - Low ^{14}C value
  - Temperature > 25°C (but not always the case)
- Shallow Groundwater
  - Hexagonal shaped Stiff diagram
  - High ^{14}C value
  - Cold temperature < 25°C

Characterisation of deep and shallow groundwater

The determinands listed above under the heading “Definition of deep and shallow groundwater” were analysed and their ability to differentiate deep from shallow groundwater assessed. Of the 20 assessed sites, seven could be confidently classified as deep or warm groundwater, whilst eight could be confidently classified as shallow or cold groundwater. The remaining five sites were classified as mixed. The common characteristics of the deep and shallow sources are listed below. While not all of these characteristics need be present in each sample, the majority should comply.

Deep groundwater can be characterised as:

- An anaerobic NaCl water type that may be warm (>25°C) but does not have to be.
- An older water characterised by low tritium and ^{14}C and by low $^{36}Cl/Cl$ and $^{3}He/^{4}He$ ratios.
- Very low nitrate as a result of denitrification.
- Low magnesium, probably due to ion exchange reactions with the aquifer matrix.
- Lower $\delta^{18}O$ and $\delta^{2}H$ than those in shallow groundwater.
- Low alkalinity possibly due to precipitation of $CaCO_3$ at higher pH.
- Low uranium and vanadium (and maybe other metals) as a result of anoxic conditions.
- Very low radon and radium as a result of low uranium concentrations in deep groundwater.
- Relatively high fluoride, possibly as a result of long term dissolution of fluorite and concomitant partial removal of calcium.
- Relatively high methane and helium gas concentrations.
- Relatively high boron levels.

Shallow groundwater can be characterised as:

- An aerobic $Ca.Mg.HCO_3$ water type that is <25°C.
- A young water characterised by moderate tritium, high ^{14}C, and higher $^{36}Cl/Cl$ and $^{3}He/^{4}He$ ratios.
- Variable nitrate levels that may be due either to anthropogenic factors or natural nitrification.
- Relatively higher $\delta^{18}O$ and $\delta^{2}H$ ratios due to recent recharge.
- Elevated alkalinity with higher uranium concentrations leading to elevated radon.

- Relatively low fluoride and bromide concentrations.
- Relatively low methane and helium gas concentrations.

Deep groundwater indicators

Based on literature and the results from this study it is evident that certain determinands provide better guidance in differentiating deep from shallow groundwaters. In this study seven determinands stood out:

i. Alkalinity
ii. Sodium as percentage of the cation total (in meq/L) ($\%Na^{+}$)
iii. Magnesium (Mg^{2+})
iv. Fluoride (F^{-})
v. Uranium (U)
vi. Oxygen-18 isotope ($\delta^{18}O$) or deuterium ($\delta^{2}H$)
vii. Radiocarbon (^{14}C).

Figure 3 shows the range and median for the deep, shallow and mixed samples for each of the seven determinands. It is clear from this that whilst the median is clearly distinct for the deep, shallow and mixed samples, the total range in values for each determinand in many cases overlaps. However, much of the overlap lies within the mixed samples and the deep and shallow samples are usually distinct from one another. There is only one exception to this and that is with fluoride where the highest value for the shallow samples and the lowest value for the deep samples overlap slightly. It is important to note that the ranges defined here and the limits described below are based on a very limited number of samples.

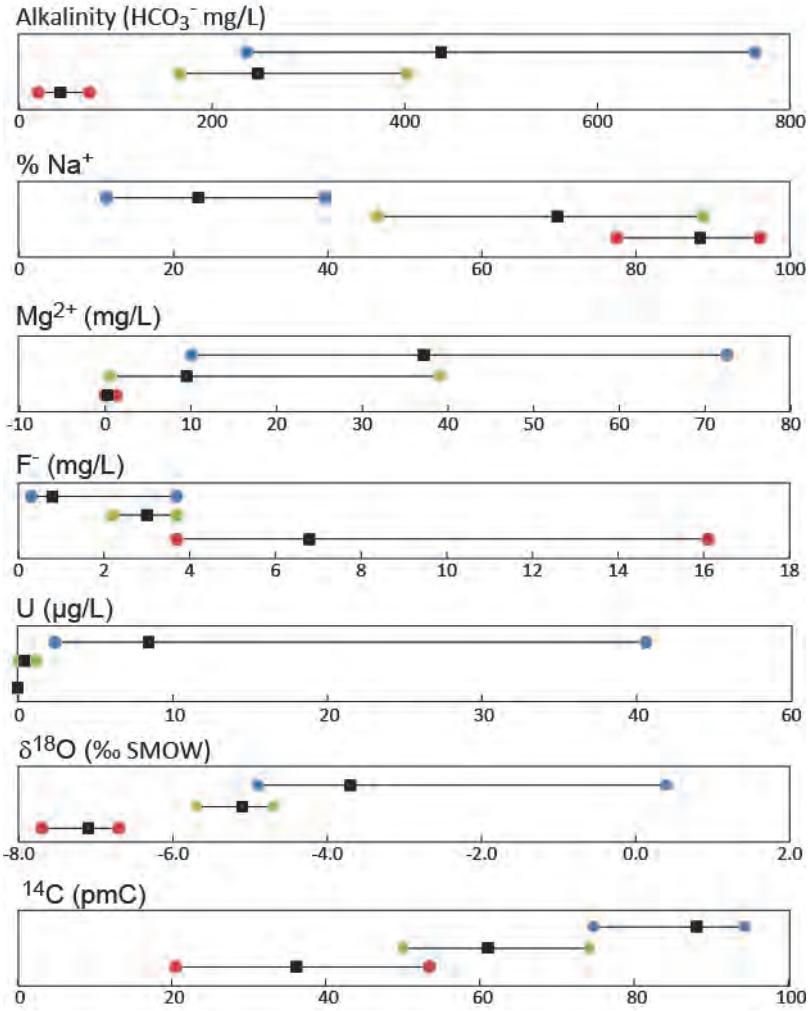

Figure 3. The ranges and medians of the seven parameters that are most successful in differentiating deep from shallow groundwater. The blue dots refer to the shallow samples; the red dots to the deep samples; and the green dots to the mixed samples. The black squares represent the median values.

Limits were set for relevant determinands in order to evaluate their reliability as depth indicators and to provide the basis for preliminary guiding criteria. These limits are listed in Table 1. Note that because of the good correlation between $\delta^{18}O$ and $\delta^{2}H$, either could be used in this classification. In this report $\delta^{18}O$ has been used.

Table 1. Indicators of deep flow

Determinand	Deep groundwater criteria	Units
^{14}C	<60	pmC
$\delta^{18}O$	<-6	‰ SMOW
F^-	>3	mg/L
$\%Na^+$	>70	%
Mg^{2+}	<10	mg/L
U	<0.05	µg/L
Alkalinity	<100	mg/L HCO_3^-
B	>300	µg/L
V	<1	µg/L
Li	>100	µg/L
$\delta^{11}B$	<+30	‰
NO_3^-	<1	mg NO_3/L
$^{36}Cl/Cl$	<100	10^{-15}
Rn	<10	Bq/L
H_2S	>1	µcc/kg
^3H	<1	TU
Na^+	>300	mg/L
pH	>9	
^4He	>30000	µcc/kg
$^3He/^4He$	<0.1	R/R_0
Temperature	>25	°C
CH_4	>10	cc/L

The ability of individual determinands to differentiate deep from shallow groundwater was then grouped based on how reliable they were in meeting the criteria in Table 1. Four groups were identified and are presented in Table 2. Groups 1 to 3 should be the first choice in any groundwater monitoring program in the Main Karoo Basin which aims to identify areas of deep groundwater flow, with Group 1 being the highest priority. Group 4, whilst not being particularly useful in this study may provide further information on contamination processes after shale-gas development and hence may have their place in future monitoring programs.

Table 2. Success rate and prioritisation of different determinands for identifying deep groundwater. A 100% success rate means that all the determinands listed meet the criteria set in Table 1.

Group	Success Rate	Determinands
Group 1	100% success rate	^{14}C, $\delta^{18}O$, fluoride, %sodium, magnesium, uranium, alkalinity
Group 2	>75% success rate	Boron, vanadium, lithium, $\delta^{11}B$, $^{36}Cl/Cl$, $^{222}Radon$, H_2S
Group 3	50-75% success rate	Sodium, pH, tritium, nitrate, temperature, ^{4}He, $^{3}He/^{4}He$, CH_4
Group 4	< 50% success rate	$^{87}Sr/^{86}Sr$, $\delta^{13}C$, rare earth elements, other trace elements

Monitoring Recommendations

Taking into account the success rates presented in Table 2, cost, availability and ease of analysis, the geochemical parameters were grouped into four sampling categories:

1. **Easy to obtain, cost effective and available in South Africa**
    a. Major cations and anions including nitrate, fluoride and boron
    b. $\delta^{18}O$ and $\delta^{2}H$
    c. Uranium
    d. Alkalinity and pH
    e. Temperature
2. **Relatively easy to obtain and available in South Africa but less useful than the above determinands**
    a. $^{222}Radon$
    b. Vanadium and lithium
    c. H_2S
3. **More difficult to analyse, time consuming and higher cost**
    a. ^{14}C and tritium
    b. $^{87}Sr/^{86}Sr$
    c. Rare earth elements
4. **Not currently available in South Africa**
    a. $\delta^{11}B$
    b. $^{36}Cl/Cl$

c. ^{4}He
d. $^{3}He/^{4}He$
e. CH_4.

Since this project used a very limited sample size, it is recommended that all of the above determinands be assessed when aiming to identify deep groundwater sources in the Main Karoo Basin. This will enable the results of this study to be improved upon, and with time, assist in the development of a more comprehensive understanding of the nature of deep Karoo groundwaters.

Conclusions

This study set out to identify indicators of deep groundwater flow in the Main Karoo Basin. It was not possible to obtain groundwater samples from the deep-seated shales that are being considered for shale gas exploration and development because no suitable deep boreholes exist. Instead, samples from warm springs and two deep boreholes that pass through the shales were obtained as the best approximation of deep-seated groundwaters in the Karoo at this stage.

Deep and shallow groundwaters were characterised and determinands were identified to differentiate these waters. A provisional guide on the limits for these determinands was provided (Table 1), and at this stage, this list can be used as guidance on differentiating deep form shallow waters. The determinands that appear to be most reliable in identifying deep groundwater were grouped (Table 2) and prioritised for future monitoring programmes.

While this project noted fairly consistent geochemical patterns throughout the vast area of the Karoo, it must be stressed that the analyses, conclusions and recommendations presented pertain to a relatively small sample number of water and gas samples derived from sources of unknown depths.

ACKNOWLEDGEMENTS

- The Water Research Commission for funding, and in particular Dr Shafick Adams for supporting the project.
- Land owners, farm managers, spring managers and municipalities who kindly gave permission for the project team members to enter their land and who offered valuable site information: Mr Boetie Botes, Merweville; Mr Fred Badenhorst, Groot Kruidfontein, Leeu Gamka; Mr Dick Viljoen, Kruidfontein, Leeu Gamka; Mr Gerome Plaatjies, Construction Site, Leeu Gamka; Mr Barry Mildenhall, Bath Farm, Fort Beaufort; Mr Unathi Mguzulwa, Cradock Spa Manager; Mr Zis Ferreira, Marlow High Agricultural School, Cradock; Mr Erik Maskell, Cradock farmer; Ms Gertrude Masumpa, Aliwal North Spa manager; Ms Marita van Wyk, Aliwal North farmer; Dr James Brink, Florisbad Spa; Mr JC van der Walt, Wildebeest Valley, Venterstad; Mr Mawethu Cawe, Rooiwal, Venterstad; Mr Mark Frewen, Vaalbank, Venterstad; Mr Mario du Preez, La Rochelle, Venterstad; and Mr PD Jacobs, Trompsburg.
- The Reference Group members: Ms Lara Sciscio, Dr Roger Diamond, Mr Mike Smart, Ms Philippa Scott, Dr Doug Cole, Dr Luc Chevallier, Ms Zoe George, Prof Yongxin Xu, Dr Chris Hartnady, Mr Peter Rosewarne, Ms Danita Hohne, Mr Maselaganye “Petrus” Matji and Ms Debbie Jooste.
- Participants of the Groundwater Shale Gas Research meeting (February 2013): Dr Shafick Adams, Mr Mike Smart, Ms Danita Hohne, Ms Adaora Okonkwo, Dr Danie Vermeulen, Prof Gerrit van Tonder, Ms Surina Esterhuyse, Prof Maarten de Wit, Ms Zoe George, Mr John Decker, Ms Jeniffer Marot, Mr Stet Mushwana, Mr Nigel Rossouw, Mr Curtis Stanley, Mr John Kidd, Dr Luc Chevallier, Ms Katie Baker and Dr Ricky Murray.
- Stellenbosch University Honours students: Ms Anya Eilers, Ms Kay-Lee Kaywitz and Mr Tyron Hartle, for assisting with field work and data compilation.
- Mr Ryno Botha, University of the Western Cape and iThemba Laboratories and Prof Richard Newman from Stellenbosch University for collecting and analysing radon.
- Ms Katie Baker, Groundwater Africa for support during the first year of the project.
- The Department of Water Affairs and Sanitation (DWS): Stephen Mulineux, Azwifaneli Mulovhedzi and Vhuthu Tshishonge for visiting potential sampling sites.

- Prof Gerrit van Tonder and Mr Fanie de Lange for sharing data from Soekor borehole SA1/66.
- Mr Kes Murray, BSc student from Stellenbosch University for assessing the Florisbad site and for data compilation and presentation.
- Mr Peter Rosewarne from SRK Consulting for the cross sections presented in the report and appendices.
- Mr Mike Butler, iThemba Laboratories, Witwatersrand University for 14C, tritium and stable isotope analyses.
- IGS laboratory at the University of the Free State.
- Central Analytical Facility at Stellenbosch University.
- University of KwaZulu-Natal for stable isotope analyses.
- Prof Keith Fifield from the Australian National University for ^{36}Cl data analyses.
- Mr Billy Eymold from Ohio State University for assistance in the field and gas sampling.
- Dr Petrus le Roux, Department of Geological Sciences, University of Cape Town, for Sr isotope analyses.

ABBREVIATIONS, ACRONYMS AND SYMBOLS

ASW	Air-saturated water
bdl	Below detection limits
CB	Charge balance
C_{ORG}	Organic carbon content
DO	Dissolved oxygen
DWS	Department of Water and Sanitation
EC	Electrical conductivity
GMWL	Global meteoric water line
IGS	Institute for Groundwater Studies
LMWL	Local meteoric water line
NGA	National Groundwater Archive
NGDB	National Groundwater Data Base
ORP	Oxidative reduction potential
PASA	Petroleum Agency SA
PDB	Pee Dee Belemnite: ^{13}C standard
pmC	Percent modern carbon
REE	Rare earth elements
R/R_0	The ratio of $^{3}He/^{4}He$ in water relative to that in air
SMOW	Standard mean ocean water
Soekor	Southern Oil Exploration Corporation
SU	Stellenbosch University
TDS	Total dissolved solids
TIC	The sum of the carbon in carbonate, bicarbonate and dissolved carbon dioxide
TU	Tritium units
UCT	University of Cape Town
UFS	University of the Free State
WMS	Water Management System
‰	Parts per thousand

TABLE OF CONTENTS

Appendices

Figures

Tables

Photos

1. INTRODUCTION

1.1 General Introduction

A major concern regarding shale gas development is that deep borehole drilling and the hydraulic fracturing process (or fracking) may create conduits through which deep-seated groundwater could migrate to shallow aquifers. If this deep groundwater is of poor quality, and if shale gas development does facilitate upward migration of deep waters, then it is possible that poor-quality deep groundwater may blend with shallow Karoo groundwater currently used for water supplies. In some areas, the deep groundwater may even issue at the surface via leaking shale gas boreholes should they lose their integrity. This concern is primarily a long-term one. The integrity of deep boreholes may be compromised decades or centuries after abandonment through the slow deterioration of the sealing cements used in borehole grouting and plugging. Likewise, the high-pressure fracking process may marginally open existing fractures that were previously impermeable and thus allow for the very slow upward migration of deep-seated groundwaters. Or crustal instability may only occur in years to come with the required intensity to cause upward movement of water through old or new faults and fractures.

The short-term value of knowing the quality of deep groundwater is that it will help in planning how to deal with the produced water that flows from the deep boreholes during gas extraction. If this water is not suitable for re-use in the fracking process, it needs to be treated to acceptable standards prior to disposal.

The potential short-term problems, like spills of produced water, or immediately apparent leaking boreholes, are also real concerns, but would most likely be picked up during the shale gas development period and dealt with in a suitable manner. The short- and long-term concerns relating to deep groundwater are however minor issues if deep-seated Karoo groundwaters are not poor quality. This project aimed to address this lack of knowledge by characterising the nature of the deeper Karoo groundwaters.

Three points are worth stressing at the outset:

i. Deep-seated groundwater will generally rise if given the opportunity (through boreholes or fractures) as this water is hot and under pressure. This does not mean that it will necessarily flow to the surface; rather, it may reach hydraulic equilibrium below ground level, and if so, would blend with the groundwater found in and around that depth. This concern was initially raised by the late Prof G van Tonder and is based on the assumption that in places, the deep Ecca Group shales are under

confining pressures and if punctured with boreholes, will allow for upward flow. At this stage insufficient information is available to know where and if the Ecca Group may regionally behave in this manner. The most likely region would be the relatively low-lying southern Karoo between the Great Escarpment and the Cape Fold Belt, but even in this area, the groundwater source may not be the Ecca Group shales, but rather the underlying Table Mountain Group sandstones/quartzites which receive recharge in the mountains of the Cape Fold Belt.

Evidence of areas where there is proof of upward flow is the widely dispersed warm springs throughout the Karoo (including in the higher-lying areas on the escarpment). While these warm springs prove a continuous upward flow from ~1km depths in some areas, they do not necessarily prove there will be a continuous flow from much greater depths if deeper boreholes do encounter water. Van Wyk (2013) noted that the western Karoo Basin only partially meets the hydraulic requirements for confined or semi-confined conditions. If this is correct and the deep-seated shales are not linked to greater groundwater flow systems, then confined areas would become de-pressurised with time and the upward flow would diminish and ultimately stop. However, besides two reported cases where deep artesian boreholes drilled into the shales either stopped flowing or their salinity decreased significantly (Van Wyk, 2013), at present this is not known, and thus the concern remains that deep water (in specific areas where hydraulic conditions are favourable) may rise, and undetected, migrate sideways at a depth commonly used for water supplies.

ii. The permeability of Karoo rocks at the depths targeted for shale gas exploitation is exceptionally low. For this reason natural migration of deep waters to the near-surface either takes place very slowly (over geologic timelines) or does not happen at all throughout much of the Karoo. The exceptions are areas with secondary permeability where fractured rocks provide conduits for rapid upward movement. While some of these areas are known and can be seen where warm water daylights as springs, they would remain undetected where the artesian pressures do not allow for surface expression. Thus there may be many areas throughout the Karoo where deep, warm waters are naturally blending with near-surface waters to produce a chemistry that reflects neither typical shallow nor deep waters, but rather a mix that is dependent on the quality of the end-members (deep and shallow) and the permeabilities of the rocks. While the chemistry of the end-members governs what is

available to be mixed, formation permeability to a large degree, dictates the blending ratios.

iii. At present there are no suitable deep boreholes that can be used to sample and establish the chemistry of groundwater from the ~2-3 km deep Ecca Group layers. The existence of warm springs in the Karoo is the closest approximation that is available through which one can obtain an idea of the nature of deep groundwater. The minimum depths of the warm springs that are known in the Karoo are in the order of 500-1500 m (Kent, 1949 and Kent et al., 1966). If there is a vertical flow of water from greater depths, then the water emanating from the springs are the most likely places to find it. An investigation of the constituents of such spring water is therefore likely to give a best guess of the type of water to be found at greater depths.

For the sake of this study, and because it was not possible to obtain samples from truly deep sources, the three depth categories used are:

i. Shallow: Cool groundwater with a chemistry that indicates shallow circulation and no obvious blending with deeper sources.
ii. Deep: Warm or cool groundwater with a chemistry that is clearly different from “Shallow groundwater” and includes indicators of long residence times and/or deep flow.
iii. Mixed: Cool or warm groundwater that contain indicators of both “Shallow” and “Deep” groundwaters.

The “deep” groundwater referred to in this report originated mostly from warm springs and at this stage provides a best guess of the type of groundwater to be found at greater depths but does not necessarily represent groundwater that may be found in the deep shale layers that are being considered for shale gas exploration.

1.2 Aims

The overall aims of the project, as stated on inception, are listed below:

i. In selected areas in the Main Karoo Basin where shale gas exploration is envisaged, characterise shallow (cold) and deep (warm) groundwater by analysing the waters (borehole and spring) for chemistry including trace elements, heavy metals, rare earth elements, isotopes, radioactivity and, where possible dissolved gases (e.g. methane and helium).
ii. Identify specific determinands (out of the above) that distinguish shallow from deep groundwater and whether specific areas associated with shallow water samples contain traces of deep groundwater.
iii. For regulatory purposes, develop a list of determinands that should be analysed in both shallow and deep boreholes in future shale gas exploration and development areas.

1.3 The study area: The Main Karoo Basin

The Main Karoo Basin covers about 700 000 km^2 and a considerable portion of this has been earmarked for shale gas exploration (Figure 1.1). A challenging task was locating warm boreholes and springs, and boreholes with chemical indicators of deep flow. The approach taken is summarised in Chapter 4.

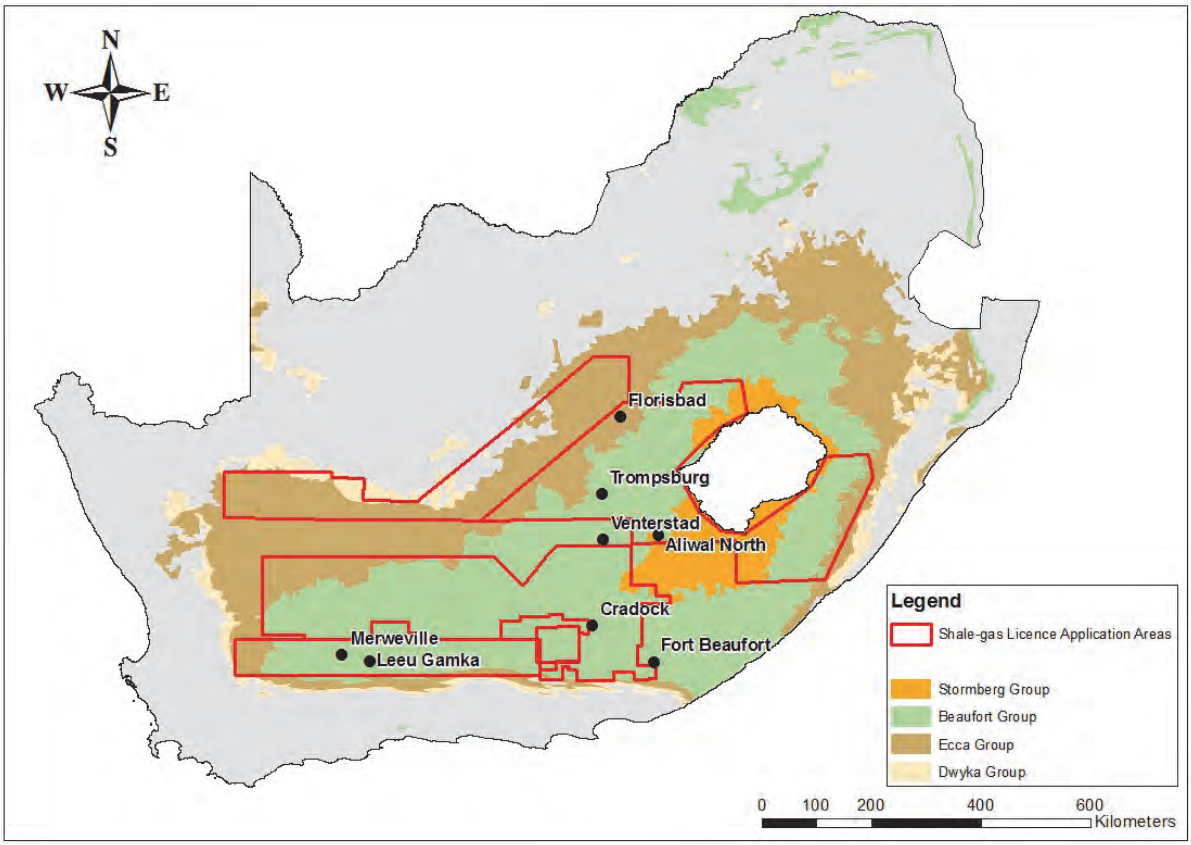

Figure 1.1. Main Karoo Basin showing the four lithostratigraphic groups and shale gas license application areas

1.4 Research methodology

This research project provided two major challenges. The first was to obtain groundwater samples that reflect deep flow paths, and the second was to identify the parameters or tracers that demonstrate this. The approach taken is summarised below:

1) *Identify "deep" groundwater sampling sites*

   Considering that no suitable boreholes exist from which samples can be obtained that reflect (with certainty) the water quality of the deep Ecca Group shales, a process to locate warm springs and boreholes that may reflect this deep water was undertaken. On the assumption that deep shale waters may be highly saline, areas where the ionic concentrations are significantly higher than the average were identified using a GIS-based study approach. Unfortunately it was not possible in the time frame to identify deep-flow sites with certainty, and the focus turned to specific springs and boreholes documented in reports or known to hydrogeologists with warm water or uncharacteristic chemistry. The number of locations were short-listed, visited in order to assess sampling suitability, and then finalised. "Shallow" borehole

sources within several kilometres of the deep sites were also identified for comparative purposes.

2) *First sampling run*

Field parameters were measured and samples collected for the analysis of major anions and cations, trace elements, rare earth elements and some isotopes. The data collected during the first sampling run included:

- Electrical Conductivity (EC), pH, temperature, field alkalinity, Dissolved Oxygen (DO), Oxidation-Reduction Potential (ORP)
- Major cations and anions
- Trace elements
- Rare earth elements
- Oxygen and hydrogen isotopes ($\delta^{18}O$ and $\delta^{2}H$)
- Strontium isotopes ($^{87}Sr/^{86}Sr$)
- Radon noble gas (Rn)

3) *Short-listing sites for detailed analyses*

Following data analysis from the first sampling run, pairs of deep and shallow sites were identified for each area where more detailed analyses would be conducted.

4) *Second sampling run*

In the second sampling run only the pairs identified in the first sampling run were visited. For all these sites, a full suite of geochemical parameters where measured. Some were repeats to ensure no temporal variation and some were additional, particularly isotopes and gases. The data collected in the second sampling run included:

- EC, pH, temperature, field alkalinity, DO, ORP
- Major cations and anions
- Trace elements
- Oxygen and hydrogen isotopes ($\delta^{18}O$ and $\delta^{2}H$)
- Strontium isotopes ($^{87}Sr/^{86}Sr$)
- Tritium (^{3}H) and radiocarbon (^{14}C) isotopes
- Chlorine-36 isotope (^{36}Cl)
- Boron-11 isotope ($\delta^{11}B$)
- Radium isotopes (^{226}Ra and ^{228}Ra)

- Carbon isotopes in dissolved inorganic carbon ($\delta^{13}C_{-TIC}$)
- Carbon isotope in methane ($\delta^{13}C_{-CH4}$)
- Carbon isotope in carbon dioxide ($\delta^{13}C_{-CO2}$)
- Gases: Radon (^{222}Rn), helium (^{4}He), argon (Ar), methane (CH_4), nitrogen (N_2), oxygen (O_2), carbon dioxide (CO_2), hydrogen sulphide (H_2S).

5) *Grouping of sites into deep, shallow and mixed groundwaters*

All data obtained was both quantitatively and qualitatively assessed in order to group the sites into deep, shallow and mixed categories.

6) *Assessment of deep groundwater indicators*

Deep and shallow groundwaters were characterised and determinands were identified to differentiate these waters. A provisional guide on the limits for these determinands was developed and the determinands that appear to be most reliable in identifying deep groundwater were grouped and prioritised for future monitoring programmes.

2. GEOCHEMICAL TRACERS AND INDICATORS OF DEEP GROUNDWATER

The central objective of this project was to characterise and thus improve the understanding of the geochemistry of deep groundwater systems within the Main Karoo Basin. This is required to provide a baseline from which potential blending or contamination of shallow groundwater can be monitored. This chapter provides an introduction to geochemical tracers and possible indicators of deep groundwater circulation.

2.1 Geochemical components of shales and groundwater

In any area being considered for shale gas development there are several important geochemical components to the system. Understanding and recognising the geochemical signature of each is necessary so that the impacts of shale gas development and the interaction between these components can be monitored. Three basic components can be identified: (1) the host rocks which are predominantly shales; (2) groundwater of variable composition; and (3) the fracking fluids introduced into the system. The geochemical characteristics of the first two are briefly described below.

2.1.1 Shale Geochemistry

Shales generally consist of quartz and clay minerals as well as heavy metals and chemical compounds that are associated with organic matter within the shale layers. Dissolved gases such as methane, carbon dioxide, hydrogen sulphide, nitrogen and helium are also commonly present together with numerous trace elements.

A typical shale within the Ecca Group of the Karoo Supergroup consists of quartz, muscovite, clay (illite), chlorite, plagioclase and pyrite as an accessory mineral. More specifically, the Whitehill Formation (of the Ecca Group), which is considered a prime target for shale gas development, contains fine grained and finely layered black shale that consists mostly of clay (illite) with a high organic content averaging 4.5% (Geel et al., 2013). This formation weathers white due to the presence of gypsum from pyrite oxidation (hence the name). Besides the predominant shales, dolomite is found near the base of the formation (Geel et al., 2013).

2.1.2 Groundwater Compositions

Most borehole in the Main Karoo Basin are <300 m deep and supply farmers and towns. The aquifers within this depth range are often referred to as the “shallow” aquifers and it is in this zone that most existing research has been done (see Woodford and Chevallier, 2002). Groundwater levels generally lie within a weathered aquifer zone which is usually between 10 and 50 m, and below this a deeper, fractured aquifer zone is usually present to depths of about 100-160 m (Woodford and Chevallier, 2002). Groundwater quality maps of the Karoo Basin (and South Africa) for numerous determinands that reflect the shallow aquifer are contained in Murray et al., 2012. The electrical conductivities (EC) of the shallow groundwater generally ranges between <70-370 mS/m throughout the Basin.

Warm springs indicate groundwater circulating from depth in an intermediate zone of ~300-1000 m and possibly a deeper zone of >1000m. With the exception of the Soekor boreholes drilled in the 1960s and a few other deep mining exploration boreholes, little is known about the deep zone.

2.2 Geochemical tracers

A variety of parameters can be used as geochemical tracers and indicators of groundwater flow. The most important and relevant to the current study are discussed in the sections below.

2.2.1 Chemical constituents and their ratios

The chemical composition of groundwater is determined by the physical and chemical conditions in the vadose zone during recharge and by subsequent chemical changes during groundwater residence and flow underground. In this project there is a specific interest in those constituents that change during residence in the aquifer since they can be used to indicate differences in provenance of the groundwater. Chemical ratios have been used to standardize differentiation between water sources, as well as between deep and shallow groundwater as certain constituents will exist in higher concentrations in deeper groundwater due to extended interaction time with the host rocks (Tredoux & Kirchner, 1981, Talma 1981, Vengosh et al., 2013).

2.2.2 Isotopes

Environmental isotopes are excellent tracers of solutes and water in catchments as they are unreactive towards catchment materials in comparison to most chemical tracers. These

isotopes are of particular interest as they can potentially be used for the following (Weaver et al., 1999; Mook, 2006; Aggarwal, et al., 2005):

- To characterise various water types.
- To recognise when mixing of different water types has occurred.
- To determine the residence time of groundwater.
- To determine the travel times and flow rate of different groundwater types.
- To provide insight into the occurrence of water-rock interactions with particular reference to weathering reactions that cause mobility of certain solutes along a flow path.

The isotopes analysed for this project are discussed below.

2.2.2.1 Stable isotope ratios

Oxygen and Hydrogen. The ratios of $^{18}O/^{16}O$ and $^{2}H/^{1}H$ in water are altered along the pathways of the hydrological cycle. These produce characteristic isotope patterns in rainfall which are transferred into the ground/soil during recharge. The isotope ratios of hydrogen and oxygen in natural water closely parallel each other except under conditions of open-pan evaporation. Since these conditions are time and locality dependent, isotope ratios become useful as tracers of groundwater flow, as well as estimating evaporation, determining the origin of groundwater and estimating recharge rates (Mook, 2006; Aggarwal, et al., 2005; Weaver et al., 2007). Studies conducted on produced waters associated with shale gas drilling from the Marcellus Shale Formation, as well as overlying shallow aquifers and surrounding surface water showed significant differences in the composition of O and H isotopes between the different water types (Sharma et al., 2014).

Boron. Boron has two naturally occurring stable isotopes, ^{11}B which has an abundance of 80.1% and ^{10}B which has an abundance of 19.9%. The ratio $^{11}B/^{10}B$ has been used to identify sources of dissolved boron and to differentiate between marine and non-marine sources. Boron in groundwater originates from leaching of country rocks, mixing with other water bodies or contamination from anthropogenic sources. Each natural source of boron has a distinguishing isotopic composition. For example, the average continental crust has a $\delta^{11}B$ value of 0 ± 5‰, whereas seawater has a $\delta^{11}B$ value of +39‰ (Vengosh et al., 1994).

Carbon isotopes. The two stable isotopes of carbon have mass 12 and 13. The ratio of $^{13}C/^{12}C$ is indicative of the source of the carbon and its geochemical history. $\delta^{13}C$ of the total inorganic carbon in groundwater, TIC, is a combination of the isotope composition of soil

CO_2 and of the carbon derived from dissolution of carbonate in the soil and in the aquifer (Clark and Fritz, 1997). Note that TIC is mainly bicarbonate, in addition to small amounts of carbonate and dissolved carbon dioxide. $\delta^{13}C\text{-}CH_4$ values are indicative of the formation process and can aid in distinguishing between biological fermentation and dry thermogenesis (Schoell, 1980; Whiticar, 1996).

2.2.2.2 Radiogenic isotopes

Helium isotopes. Two isotopes of helium are found in nature: ^{3}He and ^{4}He. Both isotopes are stable and have multiple sources in the hydrogeological cycle. Both isotopes are incorporated into recharged meteoric water from the atmosphere, known as air-saturated water (ASW). ^{3}He is also produced by radioactive decay of tritium (^{3}H) which decays with a half-life of 12.4 years. ^{4}He is produced by the radioactive decay of U and Th, although large contributions to groundwater are also sourced from radiogenic ^{4}He that previously built up in sedimentary grains and is released by diffusion into circulating groundwater or produced from the entrainment of exogenous migrated fluids; each of these processes are distinguishable by measuring heavier noble gas isotopes (e.g., Ne and Ar) (Hunt et al., 2012; Darrah et al., 2014, 2015). In addition ^{4}He concentrations in water appear to increase with increasing residence times underground (Heaton, 1984). Because the sources of the two isotopes are different they result in different $^{3}He/^{4}He$ ratios for deep and shallow water (Solomon et al., 1995 & 1996). Young meteoric (air-saturated) water has $^{3}He/^{4}He$ of 1.5×10^{-6}, while crustal rocks (and old crustal fluids) typically give a ratio of 1×10^{-8} and mantle rocks (and associated fluids) will usually yield a much higher ratio of $\sim 1.2 \times 10^{-5}$ (Lupton and Craig, 1978). As a result, both isotopes are good tracers of groundwater flow, residence time, or the presence of migrated exogenous fluids (Ballentine et al., 2002; Darrah et al., 2014, 2015; Phillips & Castro, 2003), but require careful interpretation.

Strontium. There are four isotopes of strontium but only ^{87}Sr, which is produced by radioactive decay of ^{87}Rb, is considered for isotope tracing of groundwater. Strontium is commonly found in carbonate rocks and most silicate minerals, and is released into water through weathering. The ratio $^{87}Sr/^{86}Sr$, where ^{86}Sr is a stable isotope and not produced by radioactive decay, can be used to distinguish between water that has been sourced from a marine environment (low ratio) in comparison to that sourced from a terrestrial environment (high ratio) (Johnson and DePaolo, 1994; Weaver et al., 1999; Eglington et al., 2001). The ratio can also indicate the lithology through which groundwater has travelled, potentially providing the depth of the groundwater source (Vengosh et al., 2013). Strontium isotopes are

conservative tracers only in the sense that they are not affected by biochemical processes or changes in elemental strontium concentrations caused by precipitation or adsorption.

2.2.2.3 Radioactive isotopes

Radiocarbon (^{14}C). Radiocarbon is produced in the stratosphere and reaches groundwater through soil carbon dioxide that is released by plants (Mook, 2006; Aggarwal et al., 2006). The ratio $^{14}C/^{12}C$ as determined in a laboratory is reported in pmC (percent modern carbon). 100 pmC is the $^{14}C/^{12}C$ ratio of atmospheric carbon dioxide in the past and is the starting point for geochemical processes. ^{14}C has a half-life of 5730 years and can practicably "date" water up to the age of 40 000 years. The ^{14}C content of atmospheric carbon dioxide spiked between 1954 and 1962 due to nuclear weapons testing at that time (up to 160 pmC in the southern hemisphere). High levels of ^{14}C in groundwater (>85 pmC) usually indicate contribution of recharge after 1955. In addition, ^{14}C levels in groundwater (as isotope ratio) can be reduced by dissolution of (older) aquifer carbonate into groundwater. To some extent this "dead carbon" effect can be quantified through analysis of the $^{13}C/^{12}C$ ratio of dissolved inorganic carbon and evaluation of the chemical patterns in the aquifer (Clark & Fritz, 1997). As with other tracers, an assessment of groundwater residence time is only relevant when there is piston flow. In most cases there is mixing between young and old water, producing a ^{14}C content between the two end members (Clark and Fritz, 1997; Aggarwal, et al., 2005; Talma and Weaver, 2003).

Tritium (^{3}H). Tritium has a half-life of 12.26 years, and is therefore used to date groundwater up to a few decades. The ratio $^{3}H/^{1}H$ is reported in tritium units (1 TU = 10^{-18}). Once groundwater has reached the saturated zone, the tritium will decay and enable a "date" to be determined. This is however complicated by the fact that the nuclear weapon tests of the 1950's introduced large amount of tritium in the atmosphere and this found its way into groundwater. Tritium is therefore nowadays mainly used to distinguish pre-1995 water from younger recharge water (Weaver et al., 1999; Mook, 2006; Aggarwal, et al., 2005).

Chlorine-36 (^{36}Cl). Chlorine is a conservative tracer found in atmospheric rain water but not commonly found in rocks. It is therefore a useful tracer to determine the recharge of groundwater after heavy rainfall events (Healy, 2010). ^{36}Cl has a half-life of 301 000 years (Davis et al., 2003) which makes it useful for identifying very old water. ^{36}Cl is non-volatile and its movement in the subsurface is restricted to water (Scanlon, 1992; Davis, 2003). As a result of its anionic form, ^{36}Cl behaves conservatively in that it does not absorb onto negatively charged silicates and does not take part in any geochemical or biochemical

reactions (Healy, 2010). ^{36}Cl is normally expressed as a concentration (in the order of 10^{-12}) or as a ratio relative to total Cl ($^{36}Cl/Cl$ in the order of 10^{-15}).

Radon. ^{222}Rn is the product of radioactive decay of radium (itself derived from uranium). It has a very short half-life (3.8 days). In water it can be present as "supported" by an equal activity of its mother isotope ^{226}Ra. Most radon in groundwater is unsupported and the mother radium is located within the aquifer material from which the sample derives (Cecil and Green, 2000). The short half-life implies that the radon level in groundwater reflects conditions fairly close to the sampling point.

2.2.3 Dissolved Gases

Hydrogen sulphide. H_2S occurs in both deep and shallow wells and is often present in areas underlain by acidic bedrock, most commonly shale or sandstone. The occurrence of H_2S in groundwater is an indicator of reducing conditions, i.e. it occurs as a consequence of the activities of sulphur reducing bacteria which become active once all the dissolved oxygen in groundwater has been consumed (Heaton and Vogel,1980; Swistock et al., 2001).

Methane (CH_4). Methane is a naturally occurring dissolved gas in groundwater. There are two types of methane: (1) thermogenic; originating from the burial of sedimentary organic matter (kerogen) at high temperature; and (2) biogenic; originating from bacterially-mediated reduction of carbon dioxide or bacterial fermentation. Factors affecting dissolved methane concentration in groundwater include dilution (mixing of fluids from different water-bearing layers in a well), bacterially-mediated methane oxidation, and mixed methane sources (where both thermogenic and biogenic methane sources are present). The source of methane can be determined by analysing the groundwater for its $\delta^{13}C$ methane isotopic ratio. Methane of thermogenic origin has $\delta^{13}C_{-CH_4}$ values that are higher than -50‰, and those of biogenic origin have $\delta^{13}C_{-CH_4}$ values less than -64‰ (Schoell, 1980; Gorody et al., 2005, Talma and Esterhuyse, 2015).

2.3 Indicators of deep groundwater

Of the wide variety of chemical and isotopic environmental tracers mentioned above, many can be used to identify deep groundwater. Some are generic to deep groundwater (as in temperature) but some can be site specific (e.g. enrichment in a particular element). In this study, the presence of deep groundwater was initially assessed using the eleven parameters listed below. Most of these relate more to residence time rather than circulation depth and cannot be taken to indicate deep flow on their own. Although there are many other potential

indicators of deep groundwater, the ones listed here have previously been recognised (in the Karoo or elsewhere) to suggest deep flow and were selected to provide the first assessment of potential deep groundwater circulation for this study. The reasoning for each parameter is given below.

2.3.1 Temperature

As a result of the earth's geothermal gradient, groundwater found at depth in the Karoo Basin has a higher temperature than shallow groundwater. Groundwater that migrates slowly from depth to the surface may cool to such an extent that a deep source can no longer solely be characterised by higher temperature. However, groundwater with an elevated temperature in the Karoo Basin can be assumed to indicate a deep source since there are no significant shallow heat sources in this area (such as granites or other "hot" intrusive rocks).

2.3.2 Sodium

Sodium (Na) concentrations in groundwater can increase due to NaCl leaching from the aquifer material. Ion exchange within clay rocks leads to replacement of Ca and Mg with Na. Groundwater that has been underground longer should therefore have a higher Na concentration and higher (Na+K)/(Ca+Mg) ratio. This has earlier been established in Karoo aquifers (Vogel et al., 1980; Talma, 1981; Tredoux and Kirchner, 1981).

2.3.3 Magnesium

In contrast, the behaviour of magnesium (Mg) is opposite to that of Na. The divalent bonds of Mg atoms are bound more tightly during ion exchange within clays, resulting in low concentrations of Mg in deeper groundwater (Vogel et al., 1980).

2.3.4 Boron

Ryan and Langmuir (1993) stated that boron has great potential as a tracer of deep earth fluids and in the recycling of crustal materials in the solid earth geochemical cycle. Harder (1970) noted that the boron contents in sediments depended on depositional temperature, the abundances of illite and micas, and on the grain size of the clays, and that diagenetic processes reduce boron contents. Shales and marine sediments average about 100 ppm B, with lacustrine shales showing lower values. Carbonate rock boron contents are variable between 2 and 60 ppm (Harder, 1970).

2.3.5 Helium

Helium (He) in groundwater is reported as the concentration of ^{4}He and the ratio of $^{3}He/^{4}He$ (R/R_0) (IAEA 2013). ^{4}He is produced by radioactive decay of ^{235}U, ^{238}U and ^{232}Th and its daughters. This occurs in the aquifer but also as deep helium transported upwards either directly through igneous intrusions, or by water transport processes such as dispersion and advection (Heaton, 1984). ^{3}He in groundwater, in the first instance, originates from atmospheric helium. Young water therefore has a low ^{4}He level ($40x10^{-6}$ cc/kg) but high $^{3}He/^{4}He$ ratio. In the first 40 years underground, the decay of tritium will add some ^{3}He to the water. Thereafter the water continuously collects ^{4}He from the subsurface rocks and R decreases rapidly (Darrah et al., 2014). The ratio R together with the ^{4}He concentration can therefore indicate residence times of water underground on the time scale of 1000 to 10 million years (IAEA, 2013).

2.3.6 Nitrate

Elevated nitrate (NO_3) concentrations in groundwater generally result from agricultural or human activities. In (semi-)arid regions shallow groundwater also contains nitrate produced by nitrogen fixing bacteria in soils (Tredoux and Talma, 2006; Tredoux, 2009). Nitrate levels can reduce in older water as a result of the reducing conditions that develop in the course of time (Heaton et al., 1983).

2.3.7 Fluoride

Kent (1949) and Vogel et al. (1980) reported that higher fluoride (F) concentrations occur in warmer groundwater, than in nearby cool water. Woodford and Chevallier (2002) found evidence to suggest a relationship between fluoride concentrations and age, origin and temperature of groundwater throughout the Karoo Basin. Elevated fluoride concentrations were found to be associated with sub-thermal groundwater of a deep origin. Fluoride in groundwater is generated by the slow dissolution of fluorite (CaF_2). This dissolution is enhanced by the removal of Ca by precipitation or ion-exchange but also when salinity increases. Both processes can cause fluoride levels in groundwater to increase with time.

2.3.8 Lithium

A study by Kunasz (1974) investigated lithium concentrations in brines in Nevada, USA. As a result of the unreactive character of lithium, elevated concentrations in groundwater were found to originate from deep sources. Previous research in the Karoo also indicated higher Li

concentrations in deep groundwater compared to shallow groundwater (Kent, 1949). Warner et al. (2014) showed that lithium and its stable isotope ^{7}Li have the potential to be used as tracers in shale gas exploitation areas.

2.3.9 Oxygen-18

It is a worldwide phenomenon that palaeowaters (groundwater recharged in the past) have lower oxygen-18 ($\delta^{18}O$) values than recent groundwater because of differences in climatic conditions in comparison to those of the present (Mook, 2006). This is especially so when comparing recharge from the Pleistocene with that of the Holocene and has also been observed in southern Africa (Heaton et al., 1986; Kulongoski et al., 2004). However, lower $\delta^{18}O$ values in groundwater can also be the result of changes of the recharge pattern in a specific location: stormy or aridity changes (Mook, 2006).

2.3.10 Carbon-14

Deep groundwater is not in contact with the atmosphere from where carbon-14 (^{14}C) is derived. The original ^{14}C present in the groundwater then merely decays over time, resulting in decreased ^{14}C concentrations with longer residence times. Dissolution of carbonate rocks, which contain no ^{14}C, results in further lowering of the $^{14}C/^{12}C$ ratio. Both processes therefore reduce the ^{14}C content in groundwater with increasing residence time underground.

2.3.11 Tritium isotope

The same decay process as ^{14}C occurs with tritium (^{3}H). The ^{3}H present in the groundwater at the time of recharge decays to ^{3}He over time, resulting in low to negligible tritium concentrations in deeper, older groundwater (Weaver et al., 1999; Aggarwal, et al., 2005). Large amounts of atmospheric tritium were injected into the atmosphere by the hydrogen bomb testing in the 1950s. Tritium values in southern African rainfall were as high as 100 TU in the 1960s but have steadily decreased to the present 2-3 TU (Talma and van Wyk, 2013). Tritium is used as indicator of the presence of recent (post-1960) recharge (Weaver et al., 1999; Mook, 2006; Aggarwal, et al., 2005).

Due to decay of the tritium spike since 1955 to the present (2014), the interpretation of tritium in groundwater for the southern hemisphere now is:

- Water containing less than 1 TU predominantly recharged before 1960.
- Water containing 1 to 4 TU recharged after 1960.

- Water containing more than 4 TU is somehow contaminated (e.g. by wastes).

2.3.12 Chlorine isotope ratio (^{36}Cl/Cl)

The initial ^{36}Cl content of groundwater is set by the levels in rainwater. During underground flow most aquifers cause Cl (the sum of ^{35}Cl and ^{37}Cl) to increase due to leaching from the aquifer rock. The complexity of the evolution of the Cl content and its isotope ratio reflects the complexity of its geochemistry over time. Nevertheless, many aquifers show decreasing ^{36}Cl/Cl ratio with time/downflow, making it a useful tracer for subsurface residence time (IAEA, 2013).

3. THE MAIN KAROO BASIN

3.1 An overview of Karoo geology

The Karoo Supergroup was deposited during the late Carboniferous to the Middle Jurassic period and consists mostly of marine glacial to terrestrial deposits of sandstone and shale. These sediments were deposited into two major basins, the Kalahari Basin, which stretches across Botswana, Namibia and central north South Africa and the Main Karoo Basin which stretches across most of central South Africa (Figure 3.1). Within these sediments, the formation considered to be most promising for shale gas development is the Whitehill Formation that is underlain and overlain by the Prince Albert and Collingham Formations respectively. All three formations fall within the Ecca Group (Figure 3.2).

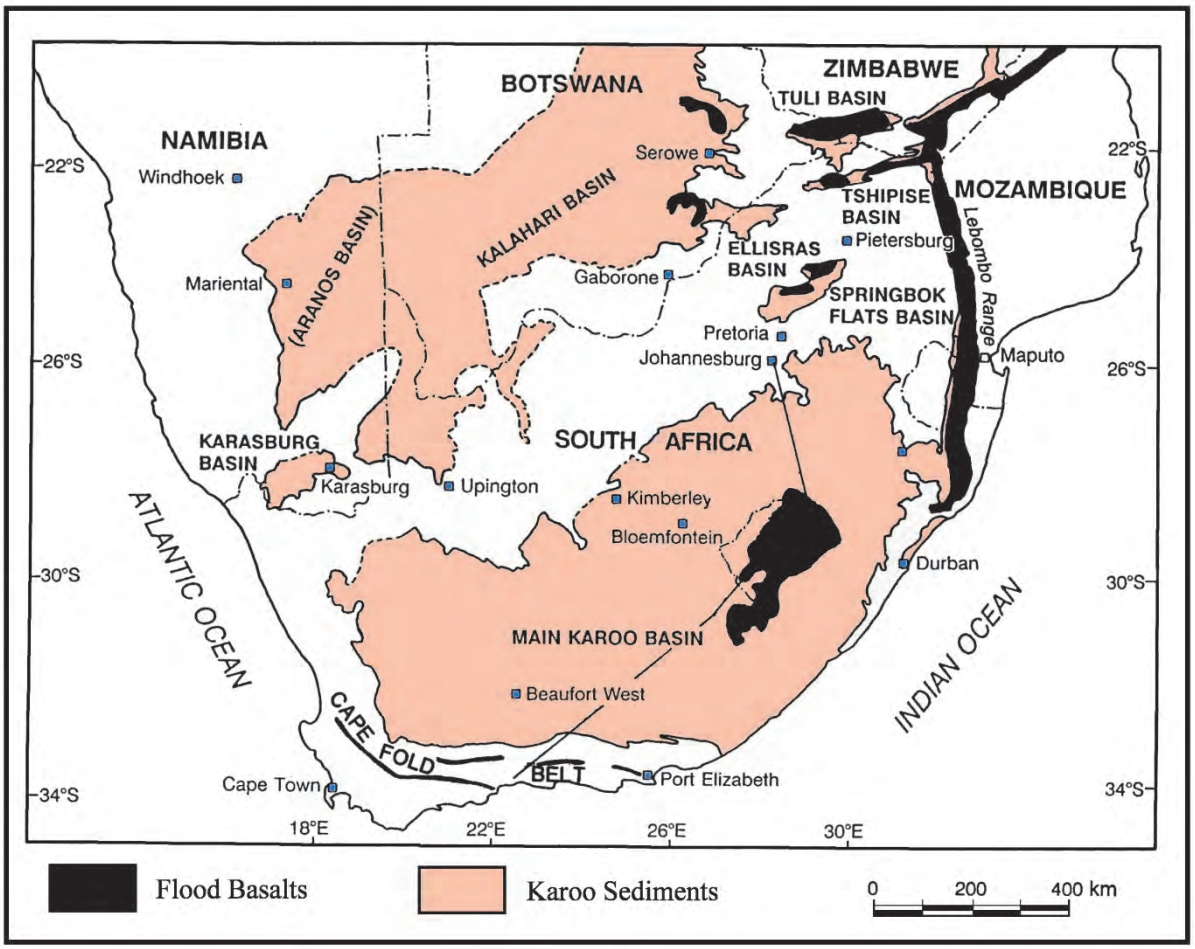

Figure 3.1. Extent of Southern African Karoo Basins (Woodford and Chevallier, 2002)

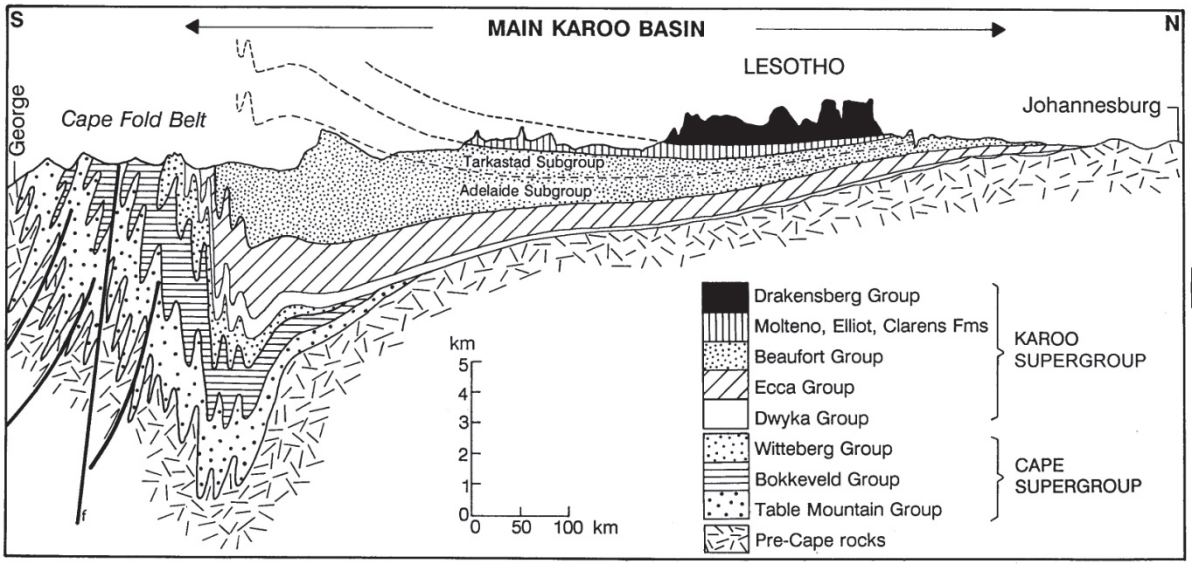

Figure 3.2. Cross section of the Main Karoo Basin (see section line, Figure 3.1) (after Woodford and Chevallier, 2002)

The Prince Albert Formation (Lower Ecca) extends across the south-western part of the Main Karoo Basin and accumulated in a deep water environment. The formation ranges in thickness from 40 to 150 m, but has been known to reach a maximum thickness of 300 m (Veevers et al., 1994). The formation can be divided into a northern facies and a southern facies based on rock composition. The northern facies consists of grey to green micaceous and silty shale, black carbonaceous shale (with a C_{org} value reaching 5.1%), fine to medium grained feldspathic arenite and wacke (Branch et al., 2007). The southern facies consists of grey pyrite-bearing shale, siltstone, chert and phosphatic nodules and lenses (Woodford and Chevallier, 2002).

The Whitehill Formation (Lower Ecca) ranges in thickness from 10 to 80 m and consists of black carbonaceous pyrite-bearing shale (up to 14% carbonaceous material) with lenses of dolomite. The carbonaceous shale formed by suspension settling in an under-filled foreland basin, in a highly anoxic environment. Within the shale cleavages, gypsum ($CaSO_4.2H_2O$) is present, which typically forms in highly evaporative conditions through reactions between sulphides (pyrite), water and dolomite. The lithology becomes less distinct towards the north-east where the lower section consists of siltstone and fine grained sandstone (Woodford and Chevallier, 2002). Generally, the C_{org} content is 3% higher in the south than in the north due to the gasification effect of the dolerite dykes in the north (Branch et al., 2007).

The Collingham Formation (Upper Ecca) ranges in thickness from 30 to 70 m. It consists of alternating hard, grey, siliceous mudrock and soft, yellowish tuff (K-bentonite). The western part of the formation consists of the Matjiesfontein Chert Bed (0.2 to 0.6 m thick), located towards the base of the formation, and an upper sandstone and siltstone unit (Woodford and Chevallier, 2002). The C_{org} content in this formation reaches 7.9% (Branch et al*.,* 2007).

3.2 Karoo dolerites

The Jurassic Karoo volcanics intruded into the Karoo sediments around 183 Ma and display significant tectonic complexity. The interconnected network of these intrusions, comprising dykes and sills, results in an inability to single out any specific intrusive event. For example, a single dyke can be the feeder of more than one sill, or one sill can be fed by numerous dykes. It therefore appears that numerous fractures were intruded by magma concurrently and the dolerite network acted as a shallow reservoir (Woodford and Chevallier, 2002).

3.2.1 Dolerite dykes

Figure 3.3 shows the distribution of the dykes throughout the Karoo Basin. According to Woodford and Chevallier (2002) there is a lithological control on the distribution of the dykes in the western portion of the basin where a sharp density increase of the dykes occurs at the lower and upper Ecca Group contact. This corresponds to the first appearance of sandstone units in the Karoo Basin. The majority of the dykes are stratabound within the Upper Ecca and Beaufort groups.

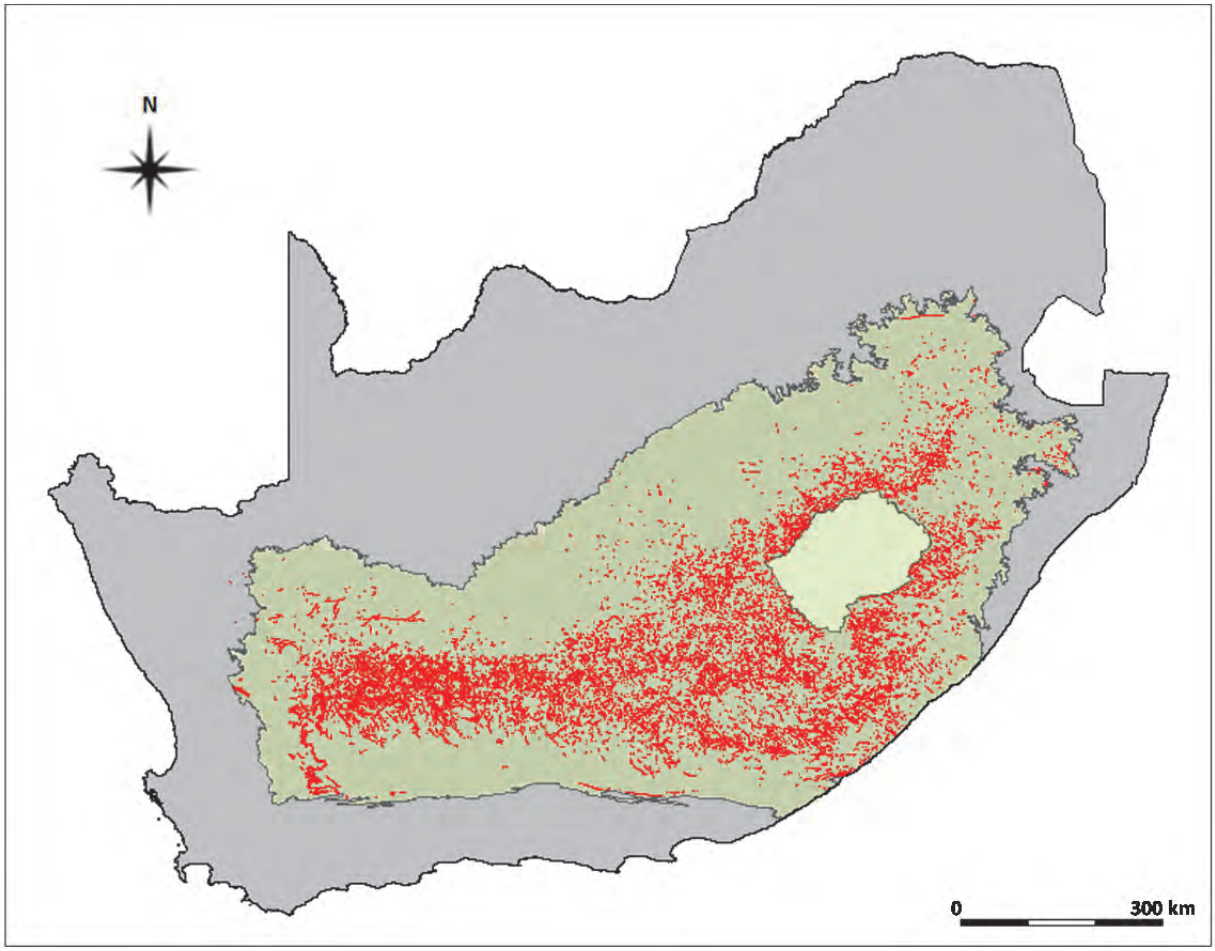

Figure 3.3. Dolerite dykes of the Karoo Basin – extracted from 1:250 000 maps (after Murray et al., 2012)

Dykes are generally steeply dipping, with dips usually exceeding 70°, and can extend tens of kilometres with the larger dykes reaching lengths of over 100 kilometres. Numerous borehole log records indicate that the attitude of dykes changes with depth, i.e. it curves, and this may have been caused by the interconnection of dykes between sediment layers. On average, the width of dykes ranges from 2 to 10 m; however major dykes such as the Middelburg dyke are known to reach 80 m (Woodford and Chevallier, 2002), and some of the major “gap” dykes in the Eastern Cape Province exceed 100 m.

It is common for the host rock to be fractured during and after dyke intrusion. Joints form parallel to the strike of the dyke over a distance ranging from 5 to 15 m. The dyke itself can also experience thermal or columnar jointing perpendicular to their margins (Woodford and Chevallier, 2002).

3.2.2 Dolerite sill and ring structures

The Karoo dolerite sills and ring structures, shown in Figure 3.4, have the same geographical distribution as the dolerite dykes. The ring structures are round, oval or irregular-shaped and can consist of smaller units within the outer unit. This can result in a complex array of "ring-within-ring" patterns. There are five major regional ring complexes across the Karoo extending from the western to the eastern parts of the Karoo and include the Sutherland, Victoria West, Middelburg, Queenstown and the Umtata regional ring complexes. The emplacement of the sills was primarily controlled by the lithology of the country rock, and as a result there appears to be horizons of preferential emplacement. These are laterally extensive undulating sills in the Dwyka-Prince Albert Formation contact and the Prince Albert-Whitehill Formation contact and well developed saucer-type sills in the Upper Ecca-Lower Beaufort Group contact (Woodford and Chevallier, 2002).

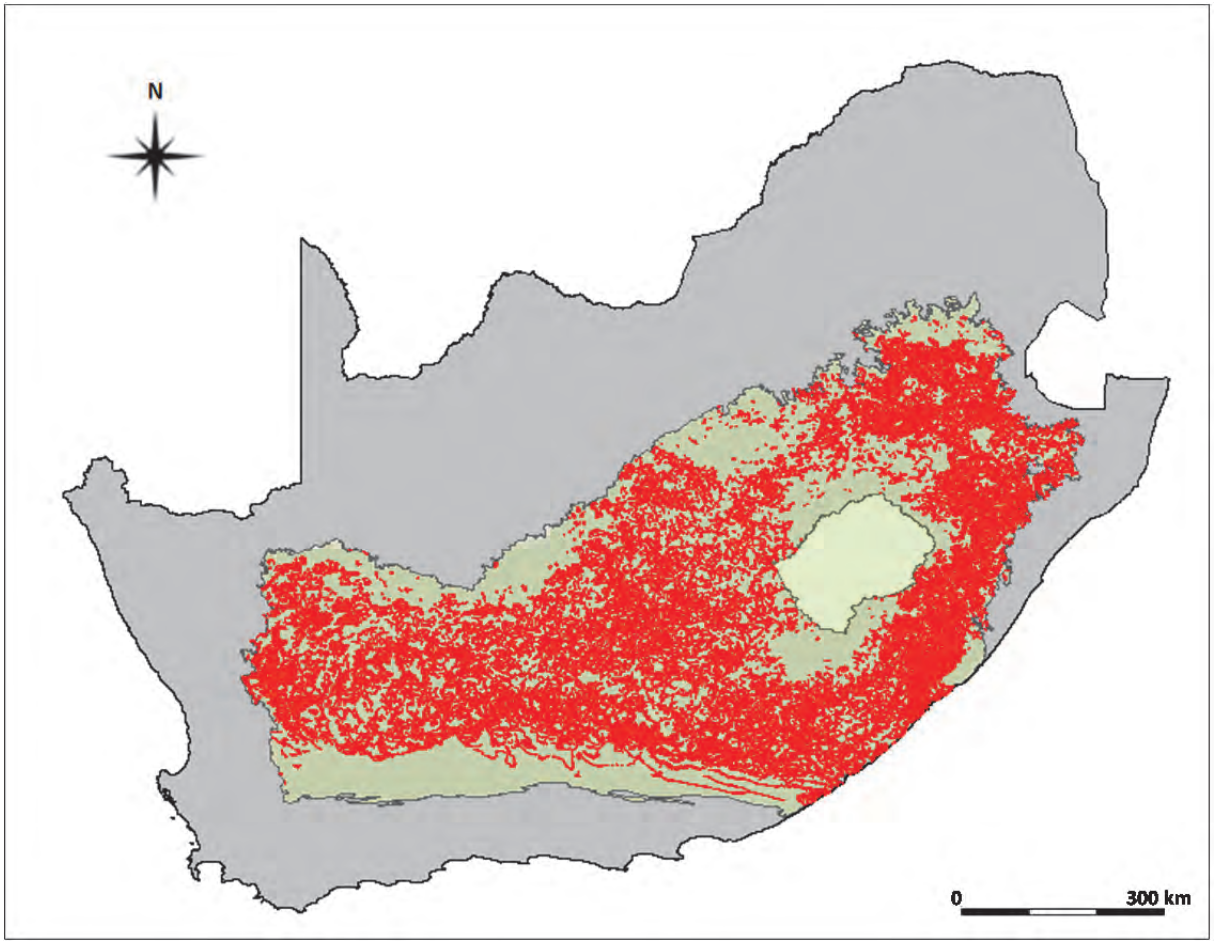

Figure 3.4. Dolerite sills and ring structures of the Karoo Basin – extracted from 1:250 000 maps (after Murray et al., 2012)

According to Chevallier et al. (2001) there are three major types of fracturing associated with sill and ring complexes:

1) Vertical thermal columnar jointing, which is well developed in flat lying sills
2) Fractures, which are parallel to the strike of the intrusion and are common in inclined dolerite sheets
3) Sub-horizontal fractures which are well developed in curved portions of a sill and are filled with calcite in the western and eastern parts of the Karoo.

The country rock above a sill or inclined sheet often experiences vertical jointing (Woodford and Chevallier, 2002).

3.3 An overview of Karoo hydrogeology

The most comprehensive studies on Karoo hydrogeology are contained in the reports by Woodford & Chevallier (2002) and Murray et al., (2012). The former study compiled information from numerous research and consulting projects and provides in-depth descriptions of geological processes, the physical and chemical nature of Karoo aquifers and insights into groundwater flow mechanisms. The latter study focussed on providing hydrogeological planning “tools” for Karoo aquifers and included electronic water quality and transmissivity maps, numerical models for quantifying regional and local groundwater yields, and a spreadsheet-based tool for estimating wellfield development and groundwater supply costs. The summary provided below has been taken from the Murray, et al., (2012) report and refers to relatively shallow groundwater resources within ~300m of the surface.

3.3.1 Groundwater quality

The groundwater quality of the Main Karoo Basin changes throughout the area from the local to the regional scale and is predominantly a function of soil type, host rock lithologies, rainfall and climate. The regional pattern, which mirrors the precipitation pattern, shows that salinity increases towards the west (Figure 3.5).

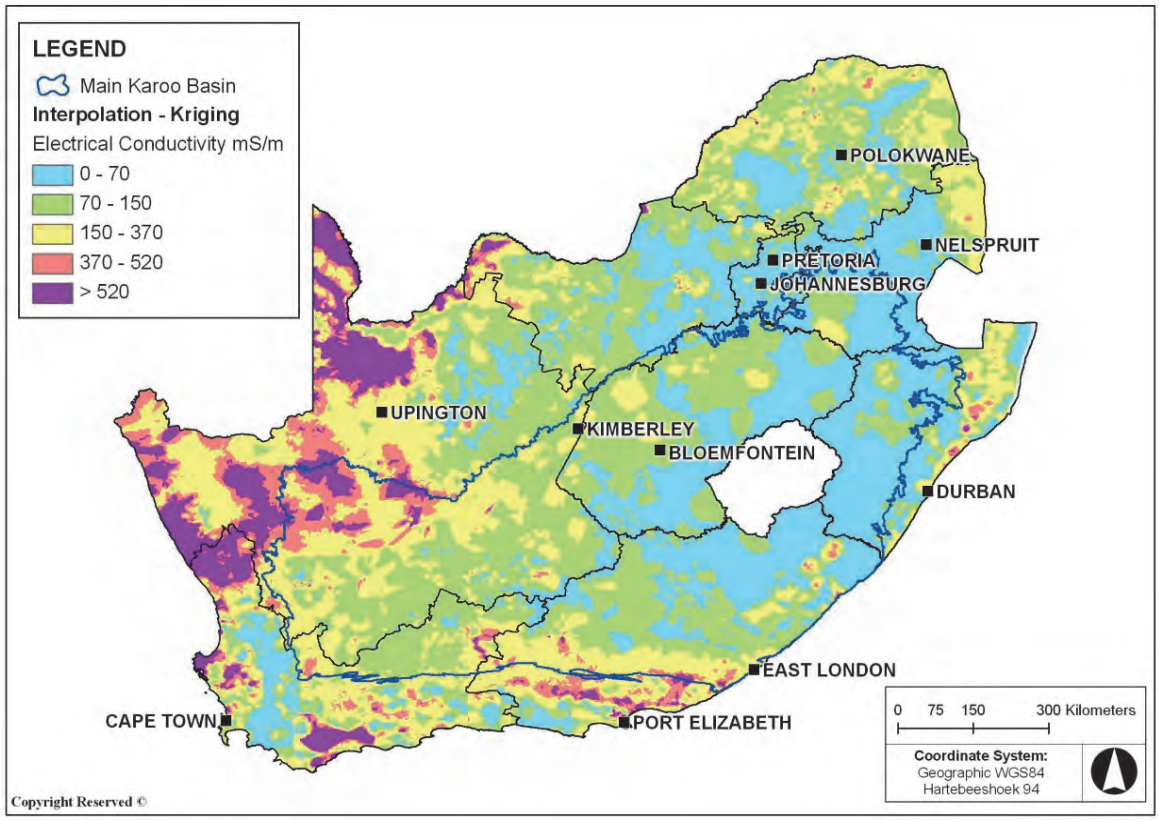

Figure 3.5. Interpolated groundwater electrical conductivity (after Murray, et al., 2012)

3.3.2 Permeable areas in the Main Karoo Basin

Karoo aquifers are mostly hard-rock, fractured aquifers with preferential flow paths that are dictated by secondary permeability. Natural and induced flow through Karoo formations can be conceptualised as being slower through the unfractured matrix, and faster through fractured zones. For this reason, the water quality from boreholes that intercept highly permeable areas can be different to those that intercept relatively impermeable areas. The greater throughflow in permeable areas can result in younger and less saline waters than in the less permeable areas. The permeable areas are predominantly associated with:

- Dolerite dykes
- Dolerite rings
- Dolerite sill margins (especially inclined sheets)
- Thick alluvial deposits
- Folded and faulted formations

Dolerite intrusions can have the effect of baking, deforming and fracturing the sedimentary rocks thereby allowing transmissive zones to develop along these geological contacts.

Unconsolidated or poorly consolidated alluvial deposits, if sufficiently coarse grained, allow for easy flow through aquifers. While large deposits are uncommon, where they are expansive, thick and permeable, they form highly productive aquifers, and where these deposits overlie fractured hard-rock aquifers, the groundwater potential is substantial.

Folded and faulted formations owe their permeability to deformation and fracturing. While faulting in the Main Karoo Basin is rather limited, the southern margin of the Basin is highly folded where it meets the excessively deformed Cape Fold Belt.

The other factor that dictates hydraulic conductivity is the type of host rock that has undergone deformation. From the borehole yield data it is evident that fractured sandstones are more permeable than fractured mudstones and shales, and fractures within sandstones are more extensive than in the fine-grained mudstones and shales.

Areas of high permeability are localised and related to the occurrence of the abovementioned structures. Nonetheless, Murray et al., (2012) produced transmissivity maps at 1:250 000 scale for the entire Main Karoo Basin to facilitate first-level water supply planning. The Basin was divided up into domains that reflect lithological, metamorphic and depositional areas of commonality, and together with maps/data sets of favourable geological structures, they were used to delineate the potentially high transmissive areas. An example of a transmissivity map in an area with an extensive alluvial deposit and numerous dolerite dykes is shown in Figure 3.6.

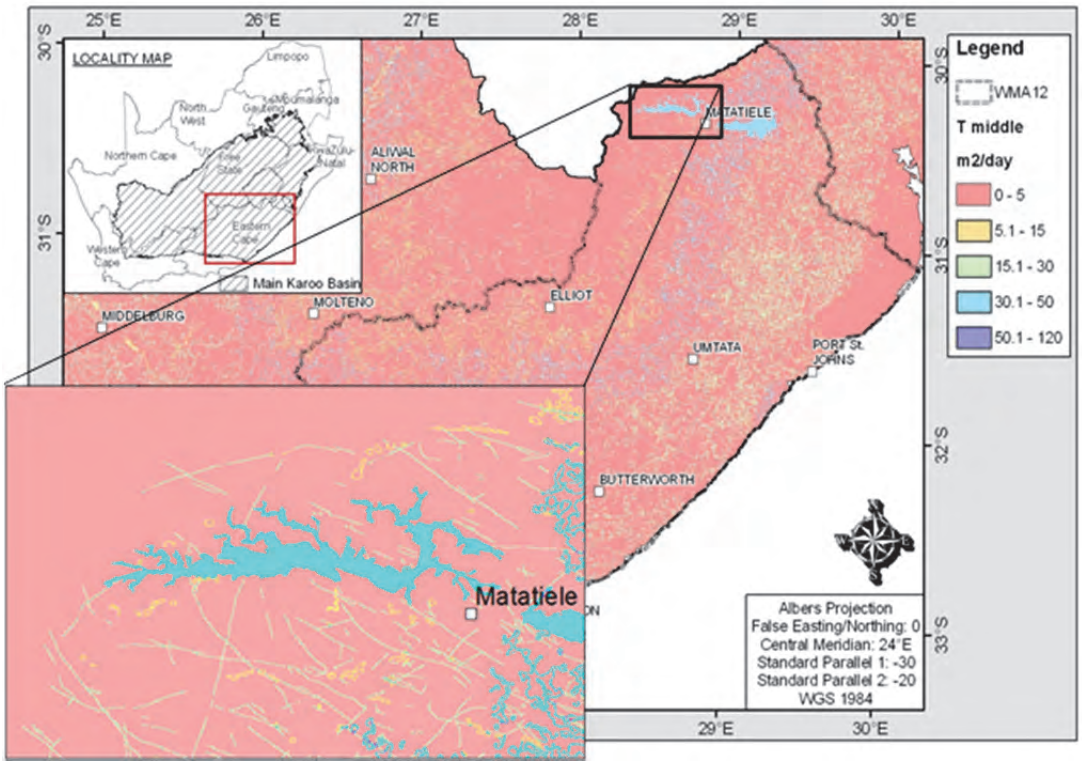

Figure 3.6. An example of the transmissivity maps produced by Murray, et al. (2012).

3.3.3 Preferential flow paths linking deep and shallow groundwater systems

If groundwater naturally migrates from deep (>1 500 m) to shallow (<500 m) Karoo groundwater systems, or if fracking activities induces such flow, then the likely routes would be via specific geologic structures that form preferential flow paths. This excludes the possibility that faulty deep shale gas boreholes may themselves provide for such conduits. It is unlikely that a single geological structure would result in direct hydraulic connectivity between deep and shallow groundwater systems. Rather, it is more likely that a number of interconnected structural features form preferential flow paths. The following structural features are considered to be potential conduits for upward movement:

- Fractures within or along contacts of dolerite intrusions, especially regional dykes and ring-sill complexes associated with feeder dykes or inclined sheets.
- Sub-vertical or vertical fault or fracture zones (e.g. fractures that resulted in the flooding of the Orange-Fish Tunnel (Whittingham, 1970).
- Bedding planes (these are unlikely to be important at depths below about 500 m, but if present, could result in horizontal connections between various vertical conduits).
- Sandstone layers with secondary permeability.
- Kimberlite fissures, pipes and breccia plugs.

3.4 Deep boreholes and warm springs

3.4.1 The Soekor boreholes

In 1965, the South African government formed a State owned oil and gas exploration company named Southern Oil Exploration Corporation (Soekor) (Pty) Ltd. The company set out to establish whether there were economic accumulations of oil or gas in South Africa. The company commenced its search by drilling a number of deep boreholes (up to 5.5km deep) in the Algoa and Zululand Basins, as well as the southern Karoo Basin. The target areas in the southern Cape-Karoo Basin included the Bokkeveld and Table Mountain groups, the Ecca and Beaufort groups, and the Dwyka Group as a secondary option. Extensive field work was carried out as well as petrographic, petrophysical and geochemical analyses to determine the potential of the source rock (Rowsell and De Swardt, 1976). The results of the drilling and analytical work were not promising and from 1969 the research areas shifted towards the northern Karoo Basin and the Cretaceous Basin. The most active period of exploration drilling was between the years 1981 and 1991, during which a total of 181 exploration boreholes were drilled (Petroleum Agency SA, 2010). In 1999, the Petroleum Agency SA (PASA) was formed and two years later a new state oil company through the merger of Soekor and Mossgas was founded, named PetroSA. Figure 3.7 shows the positions (or estimated positions) of Soekor boreholes in the Main Karoo Basin (the numbered boreholes are those referred to in the text). Borehole information such as coordinates and depths are presented in Appendix 1.

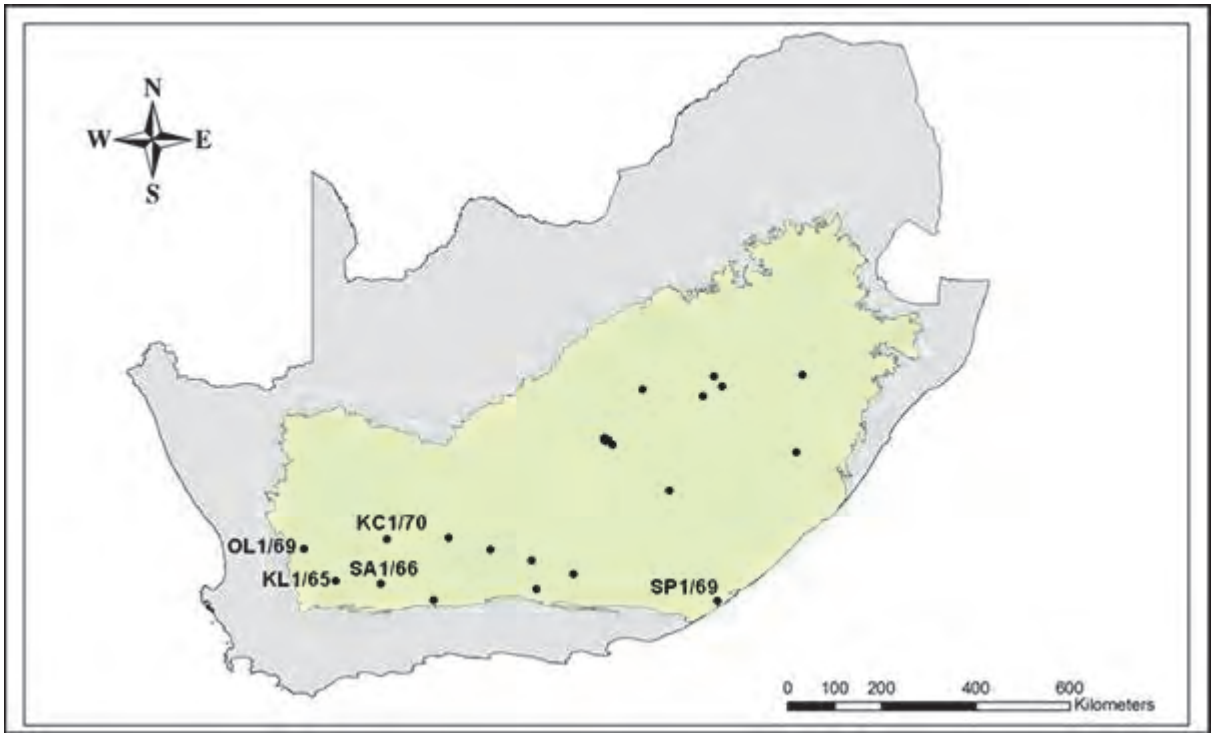

Figure 3.7. Location of Soekor boreholes in the Main Karoo Basin (after Rowsell and De Swardt, 1979)

Most core samples, as well as surface outcrop, were analysed for their organic carbon content (C_{org}) and the results are also provided in Appendix 1. Results indicate that the highest C_{org} content occurs in the lower Ecca and/or Dwyka shales of the southern Karoo, in particular within boreholes OL 1/69, KC 1/70 and SP 1/69. In the northern part of the Main Karoo Basin, C_{org} values are very low, which may be the result of changes in facies and lithology related to the formation of the basin. In the northern part of the basin, the C_{org} content in the Upper Ecca is lower than in the Lower and Middle Ecca.

Additionally, the vitrinite reflectance was determined in some samples. The study of vitrinite reflectance is a method for identifying the thermal maturity or maximum temperature history of sediments in a sedimentary basin. The results indicated that the sediments of the southern Karoo are too metamorphosed for the occurrence of oil. The samples are in the “late dry-gas” stage (except for borehole KL1/65), which indicates that sediments have been exposed to a palaeotemperature of 180°C to 250°C as a result of burial and dolerite intrusion. The results indicate that the Beaufort, Ecca and Dwyka sediments in the Main Karoo Basin are capable of containing dry gas, which consists mainly of methane and occurs in the absence of liquid hydrocarbons, as opposed to wet gas which is present with hydrocarbon compounds such as ethane and butane (Rowsell and De Swardt, 1976).

Two SOEKOR boreholes (Table 3.1) in the southern Karoo reached deep seated thermal artesian water at the time of drilling. The temperatures of the artesian outflows give a minimum geothermal gradient of 1.5°C/100 m (using the first temperature/depth measurement and an ambient surface temperature of 20°C).

Table 3.1. Soekor boreholes with thermal artesian water (after Kent (1969) in Woodford and Chevallier (2002)).

Name (Date drilled)	Depth of water strike (m.bgl)	Artesian flow (ℓ/s)	T (°C) at surface	Total dissolved solids (mg/ℓ)	pH	Lithology and predominant rock type
KL1/165	1006	0.3	n.d.	1390	8.9	Ecca Gp shales
(1966)	2347 & 3184	1.2	76.7	10010	7.5	Table Mountain Group sandstone
SA1/66	2975	3.7	65.5	6460	8.0	Dwyka Gp tillite
(1966)	3029	1.2	43.3	n.d.	n.d.	Dwyka Gp tillite
	3206	3.0	46.1	n.d.	n.d.	Dwyka Gp tillite

3.4.2 Warm springs and boreholes

The terms thermal, sub-thermal and warm have not been used consistently in the past when referring to spring and groundwater temperatures. Kent (1949) chose 25°C as the temperature to distinguish thermal from non-thermal springs. In this report 25°C has also been used to distinguish “ambient” or “cold” from “warm” waters. The term “thermal” is used here to describe the exceptionally high temperatures like those presented in Table 3.1 (>34°C), and the term “warm” is a general description for waters >25°C.

Research on warm waters in South Africa was carried out by Kent (1949), Kent et al., (1966), Kok (1992) and Olivier et al., (2008). According to Kok (1992), springs in the Karoo Basin often occur at the contact between dolerite dykes or sills and Karoo shales, and this contact can be highly fractured and cater for flows of up to 50 L/s. Kent (1949) pointed out that certain determinands from warm sources, such as fluoride and TDS, had elevated concentrations (Table 3.2 and Figure 3.8). Table 3.2 provides a rough estimate of circulation depths based on a 1.5°C/100m thermal gradient and a surface temperature of 20°C.

Referring to the origin of warm waters, Kent’s views are still widely believed to hold true: He stated that “it has been possible to explain the origin of all the thermal springs that have been

investigated in detail by structures permitting water of meteoric origin to descend to depth, take up earth heat, and then return to the surface at such a rate that much of this heat is retained"; and "....it is not necessary to postulate the presence of juvenile water, but the possibility cannot be ruled out that such water may contribute to the discharge of some springs" (Kent, 1949).

Table 3.2. Warm springs and boreholes in the Main Karoo Basin (Kent (1949); Kent et al., (1966))

Locality	Source	Fluoride (mg/ℓ)*	Total dissolved solids (mg/ℓ)*	T (°C)	Estimated depth of origin based on a geothermal gradient of 1.5°C /100m and a surface temp. of 20°C
Stinkfontein (Leeu Gamka)	Spring	-	-	28.7#	580
Bath Farm (Fort Beaufort)	Spring	13.2	520	27.0-29.0#	470-600
Cradock	Spring	5.8	181	29.0-31.3#	600-750
Rooiwal (Venterstad)	Spring	-	-	30.0#	670
Badsfontein (Venterstad)	Spring	5.3	412	27.1*	470
Aliwal North	Spring	4.8	1214	36.9#	1 130
Florisbad	Spring	6.0	2189	28.3*	550
Trompsburg	Bh	-	-	37.2#	1 150
Odendaalsrus	3 x Bh	-	-	28.8-34.0#	580-930

#Kent (1949); *Kent et al., (1966); Bh = borehole

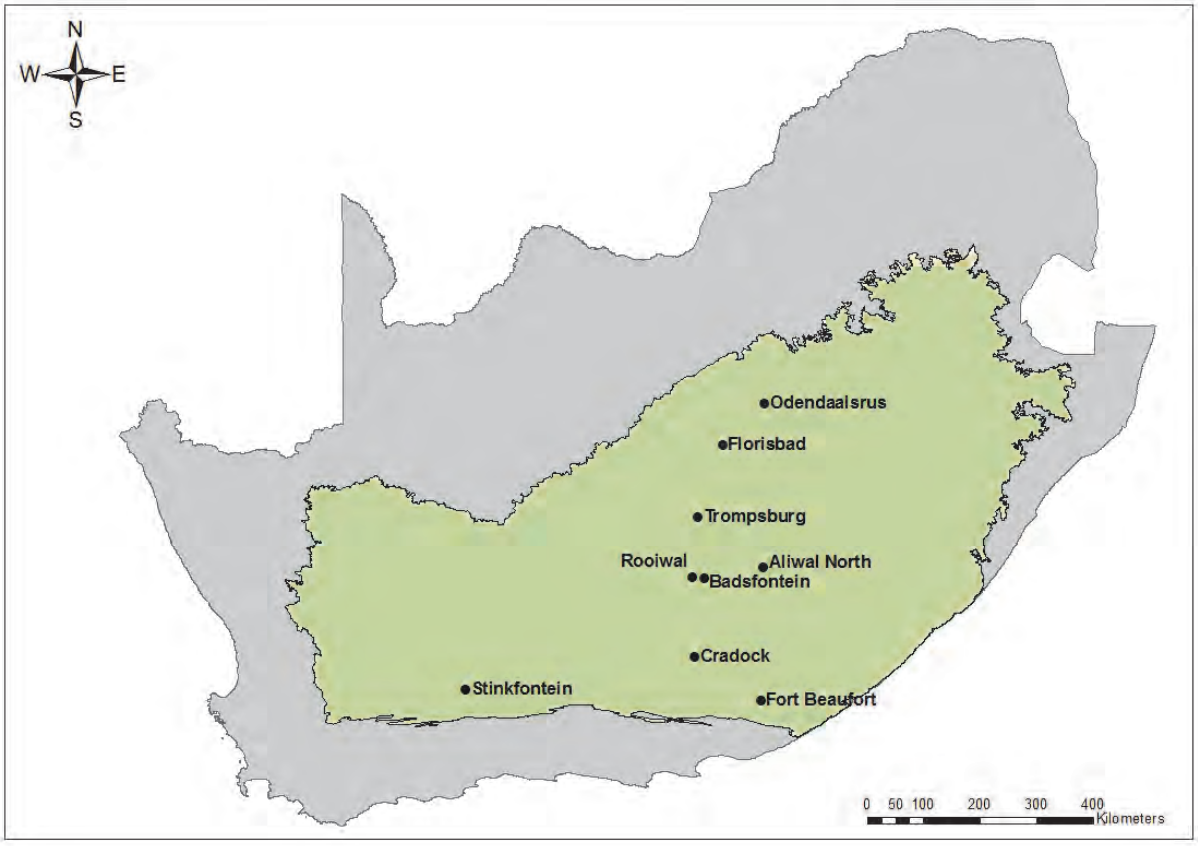

Figure 3.8. Warm springs and boreholes in the Main Karoo Basin (after Kent, 1949 and Kent et al.,1966)

4. STUDY SITES

Given the vast number of boreholes in the main Karoo Basin, the first major task was to select suitable sampling sites. Borehole and spring locations and associated hydrochemistry were obtained from the Department of Water and Sanitation's (DWS) National Groundwater data Base (NGDB), the National Groundwater Archive (NGA), and the Water Management System (WMS). After an initial visit to all the selected potential locations, specific sites were selected for further study, and two sampling field trips were organised. A brief outline on site selection is given below, along with a description of each of the final sampling sites. A comprehensive description of each area is provided in Appendix 3.

4.1 Selection of study areas

Selection of potential study sites was based on the following criteria:

- Host lithologies (i.e. needed to be in the Main Karoo Basin and with Karoo Formations)
- The presence of warm water
- Unusual groundwater chemistry with similarities to known warm boreholes or springs

The existing databases and relevant data that were used in the identification of study areas and sampling sites (boreholes/springs) are given in Table 4.1.

Table 4.1. Existing data sources

Database	Data
Borehole information	
NGDB	Borehole depth, borehole in use/equipped, yield/discharge rates, owner name, water level (and date of measurement)
WARMS	Discharge rates (registered use) Owner name, Property (Farm) name
Water Quality	
NGDB	Electrical conductivity (EC)
WMS	Temperature, electrical conductivity and water chemistry
Geology	
WRC K5/1763 (Murray et al., 2012)	Lithological, metamorphic and depositional domains; and dolerite dykes and sills (derived from the Council for Geoscience published 1:250 000 geological maps)

An initial assessment of all data within these databases involved a GIS-approach to determine locations of unusual groundwater chemistry. For example, plotting EC against number of boreholes gave a bell curve with a dramatic decrease at around 50 mS/m, tapering off at around 350 mS/m. Using this process to isolate high EC boreholes and springs it was possible to successfully identify specific areas with exceptionally high EC values such as Brandvlei and Van Wyksvlei in the north-western edge of the main Karoo Basin (Figure 4.1). However, attempts to further refine the data in this way proved difficult and the data was found to be insufficient to present a reliable statistical analysis. Plotting specific determinands such as chlorine, fluorine and arsenic also did not help to further refine the selection of sampling sites. Instead, study sites with warm boreholes, warm springs and those with uncharacteristic chemistry were identified through liaison with hydrogeologists, drillers, test pump contractors, municipalities and other experts with historical knowledge of such sites.

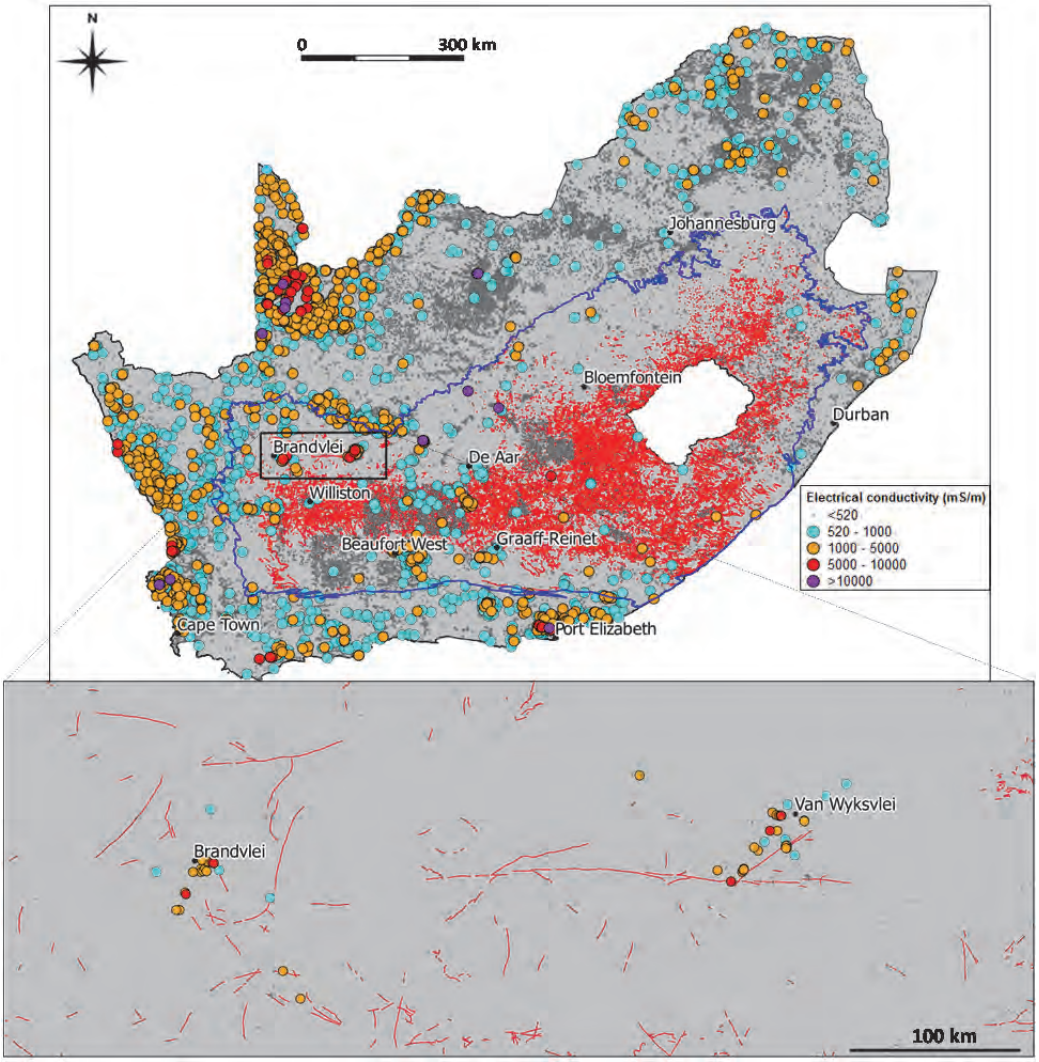

Figure 4.1. Borehole EC distribution with dolerite dykes (after Murray, et al., 2012)

Following field visits to a number of sites identified as above throughout the Main Karoo Basin, a final list of eight areas was identified as suitable for detailed investigations (Figure 4.2 and Table 4.2). Some of these areas, such as Venterstad and Leeu Gamka, had more than one suspected deep-flow site, and in total eleven suspected deep-flow sites were selected for the first round of investigation from the eight areas. These sites met the above criteria and in addition, were found to be suitable for sampling in that they were either a flowing spring, a borehole with an existing pump and a nearby sampling point, or an unused borehole into which a sampling pump could be lowered. Since most boreholes and springs did not have official numbers that were known to the project team, numbers were given to them for the sake of this study. In most cases the number reflects the sampling site name, for example, CRS1 (Cradock Spring 1) or BFB1 (Bath Farm Borehole 1). The first recorded historical temperatures of the selected sites are shown in Figure 4.3.

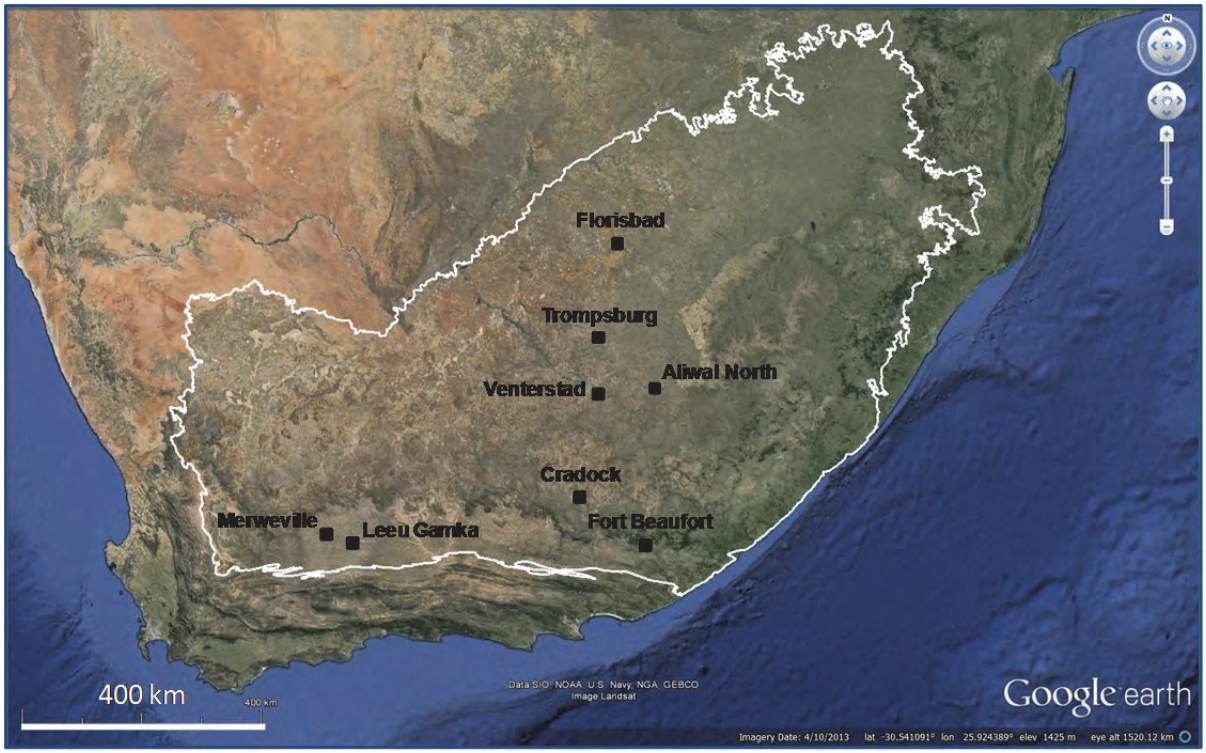

Figure 4.2. Study locations within the main Karoo Basin, outlined in white (Google Earth, 2014).

Table 4.2. Study locations within the Main Karoo Basin

Nearest Town	Site Name/Farm	Assigned Site Number for this study	Other Site Name or WMS* data base number	Main reasons for selecting the site
Merweville		SA1/66	SA1/66	4175 m deep borehole with original temperature of 46 ^{o}C
Leeu Gamka	Kruidfontein	wp508	wp508	Chemistry similar to suspected deep-flow sites near Venterstad (Vogel et al., 1980); slightly elevated temperatures; seismically active area.
	Groot Kruidfontein	wp505	wp505	
Cradock	Spa	CRS1	101267	Historic warm baths
Fort Beaufort	Bath Farm	BFB1		Historic warm baths
Aliwal North	Spa	ANS1	89868	Historic warm baths
Venterstad	Wildebeestfontein	DB11a	DB11a	Near the originally warm spring at Badsfontein; chemistry unlike nearby boreholes
	Rooiwal	RWB1B	DB15 & 171922	Originally a warm spring; now a nearby warm borehole
	Vaalbank	VBB1	DB22	Original spring site with chemistry unlike nearby boreholes
Trompsburg	Vlakfontein	VFB1	TG1	Deep borehole with an 37 ^{o}C artesian water strike at 1434 m
Florisbad	Florisbad Quaternary Research Dept.	FLS1	171921	Historic warm spring

*DWASs Water Management System

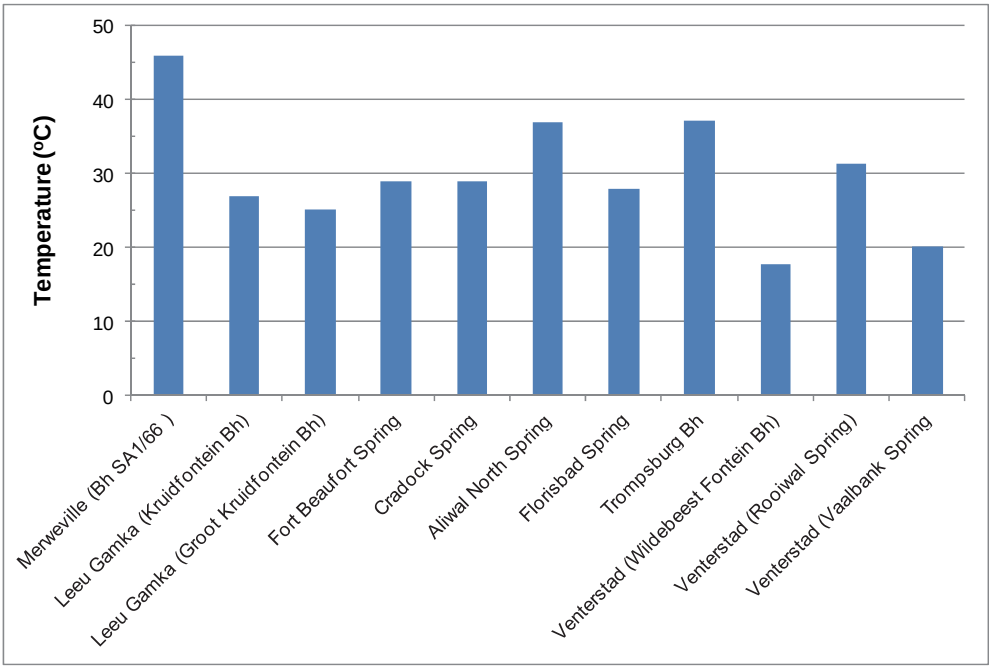

Figure 4.3. Original temperatures recorded in historical documents

4.2 The study sites

This section provides an overview of the final selected study sites. A more detailed description is presented in Appendix 3 which also describes how the final shallow-circulation sampling sites were selected. In most cases, several shallow sites were sampled during the first sampling run in order to identify a distinguishable site from the deep-circulation site.

Six of the eight areas selected for research in this project were previously assessed by Kent (1949) when he sampled 25 warm boreholes and springs across South Africa. The remaining two areas were previously assessed by Mazor and Verhagen (1983) after they sampled 16 warm springs throughout South Africa in 1971. While only dissolved ionic species were analysed in Kent's study, Mazor and Verhagen assessed ionic species together with $\delta^{18}O$, $\delta^{2}H$, tritium and radiocarbon. A selection of these initial results together with data collected during the first sampling run of this project (including field measurements), is presented in Appendix 3.

4.2.1 Florisbad

The Florisbad site, about 50 km north-west of Bloemfontein, is diverse in archaeology, palaeontology and geology, and hosts the Florisbad Quaternary Research Department of the National Museum (Bloemfontein). The spring (FLS1), which used to consist of several eyes, is located in a topographically low-lying area at the edge of a salt pan (Figure 4.4). The spring, which maintained a fairly constant temperature of 29^{o}C since first measured in the early 1900s (Rindl, 1915), now discharges into an enclosed pool (Photos 1 & 2).

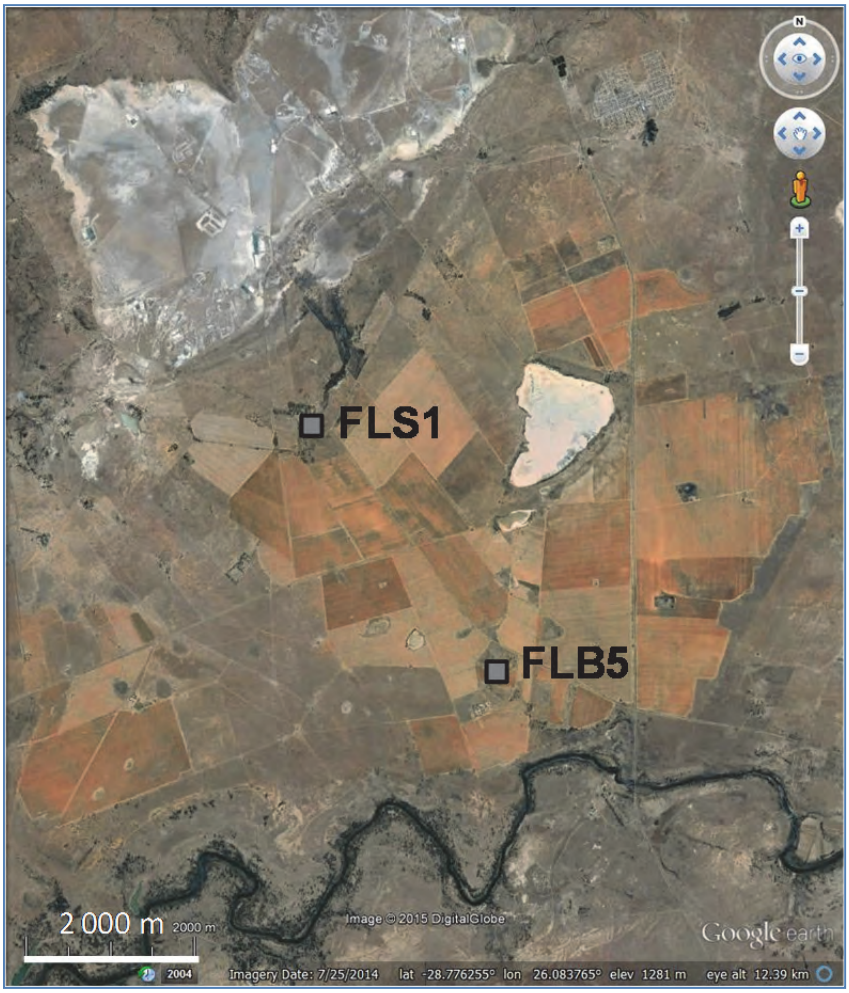

Figure 4.4. Florisbad sampling sites with the salt pan to the north-west of the spring FLS1 (Google Earth, 2014)

Photos 1 & 2. The Florisbad pool into which the spring discharges; and inserting sampling pipes into the ~10cm diameter inlets at the base of the pool (where the spring flow discharges into the pool).

The area sits on surficial Quaternary aeolian sand deposits and calcretes which are underlain by Ecca and Beaufort Group sediments (predominantly shales, siltstones and sandstones) which in turn rest on lavas of the Ventersdorp Supergroup (**Figure 4.5**). These basement lavas overlie older granites and gneisses (Loock and Grobler, 1988). While there are numerous dolerite sills and dykes in this area, Grobler and Loock (1988) located a north-west plunging dolerite sill and Dreyer (1938) uncovered a dolerite dyke within the spring area.

During the September 1912 earthquake at Fauresmith, apparently a new spring eye appeared and the flow was said to have increased, and that gas, sand, artefacts and fossils were expelled from the new eye (Anon, 1980). This observation suggests that the increased secondary permeability associated with the springs may not only be a result of dolerite intrusions, but is also likely to be associated with localised seismicity.

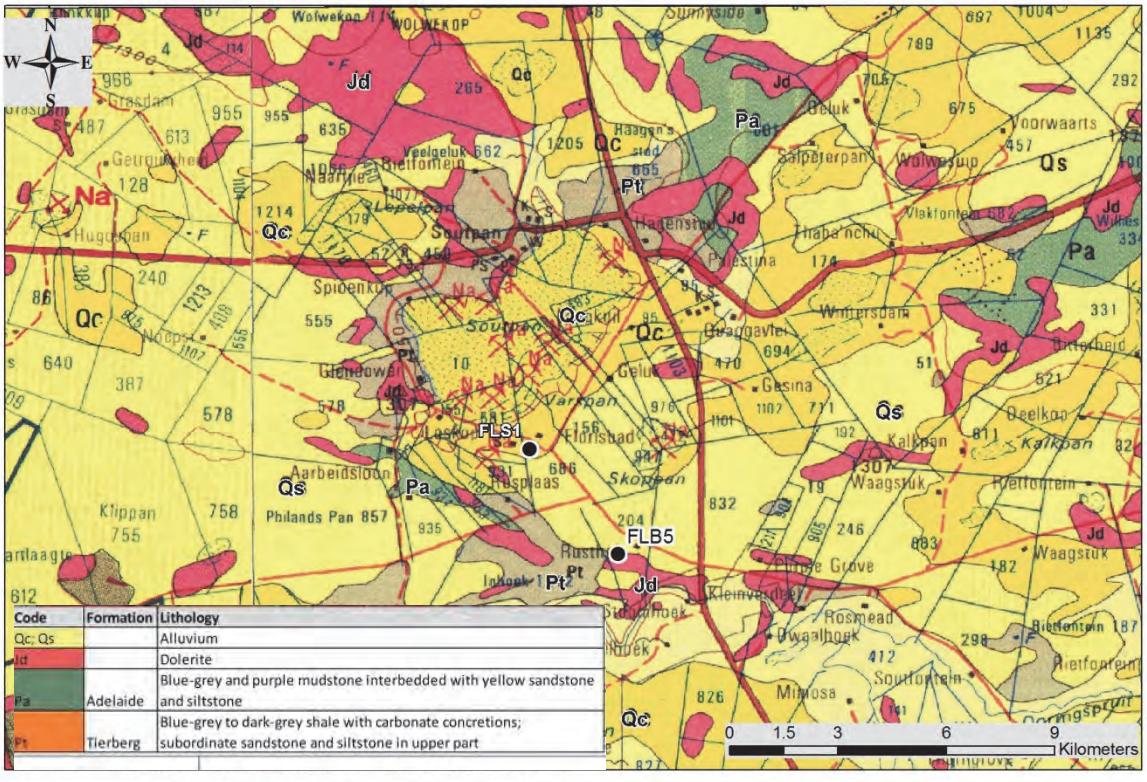

Figure 4.5. Geological map (1:250 000) of Florisbad including the final sampling sites

4.2.2 Trompsburg

The farm on which the deep, warm, artesian borehole is located lies about 15 km north-west of the small agricultural town of Trompsburg between Colesberg and Bloemfontein in the Free State Province. The borehole was drilled in the late 1940s and water was struck in the

mafic basement rocks at a depth of about 1425 m. It gave an artesian yield of 2.4 L/s which has subsequently dropped to <1 L/s, and had a temperature of 37^{o}C (Kent, 1949). The water is highly saline with an EC of 1019 mS/m. Kent (1949) postulated that much of this saline water was likely to result from “downward percolation through the Dwyka series which overlies these ancient rocks”. This supposition is based on the low chloride concentrations of these deeper rocks (Bond, 1946, in Kent, 1949). Because the Dwyka Group is only a few metres thick in this area, any downward percolation would be from the overlying shales of the Ecca Group, and this would make this site suitable for assessing the water quality of these deep shales. Figure 4.6 shows the location of the deep borehole VFB1 in relation to the surrounding dolerite ring structure.

While this site does not strictly represent deep Karoo water, it is one of only two very deep boreholes that penetrate Karoo rocks that could be located for this study, and it was retained as a study site for the project. Whether the current artesian flow is purely from the mafic basement rocks or whether it contains a portion of deep Karoo water is not known.

Figure 4.6. Trompsburg sampling sites in the centre of a dolerite ring structure which can be seen west and south of the boreholes (Google Earth, 2014).

In the late 1940s seven core boreholes were drilled in this area (Ortlepp, 1959), one of which is the borehole that was sampled during this project (Photos 3 & 4). The drilling records show that the area is underlain by Adelaide Formation sandstones (interbedded with mudstones) of the Beaufort Group to a depth of about 150 m; then Ecca Group shales to about 700m;

and then a thin lens of Dwyka Formation tillites (<25m thick). These Karoo-age rocks lie unconformably on intrusive gabbro-anorthosite basement rocks which in places have a layer of marble in between. The area has also been intruded by the relatively young Karoo dolerite dykes, sills and ring structures which are all evident at the surface.

The deep and shallow boreholes used in the water quality comparison are shown in Figure 4.7 and the deep hole's lithological log is presented in Appendix 3.

Photos 3 & 4. The artesian borehole (located next to the beacon), and its discharge into the nearby reservoir.

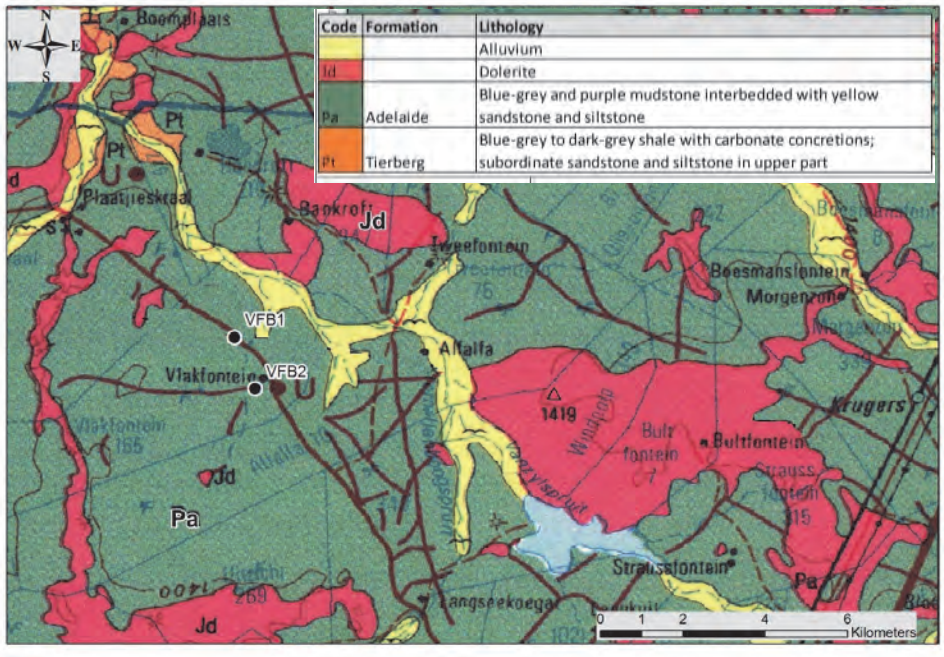

Figure 4.7. Geological map (1:250 000) of the Trompsburg area including the final sampling sites

4.2.3 Venterstad

The small agricultural town of Venterstad is situated about 10 km south of the Gariep Dam. Warm springs in the neighbourhood of the town have been used by farmers for years but are now either seeps or have dried up apparently because of over-abstraction from boreholes. The three farms on which they are specifically mentioned in the Annals of the Geological Survey (Visser, 1962), Vaalbank, Rooiwal and Badsfountain, were targeted during this study, and two (Vaalbank and Rooiwal) with boreholes adjacent to these springs, were selected for detailed analysis (Figure 4.8-4.10 and Photos 5-8).

During and after the construction of the Orange-Fish River tunnel in 1969, a great deal of research was conducted in the area after tunnelling encountered a high in-flow of groundwater. The research showed very different water types in the greater Venterstad areas, some of which were warm and old, and were considered to contain an element of deep flow (Whittingham, 1970; Vogel, et al., 1980).

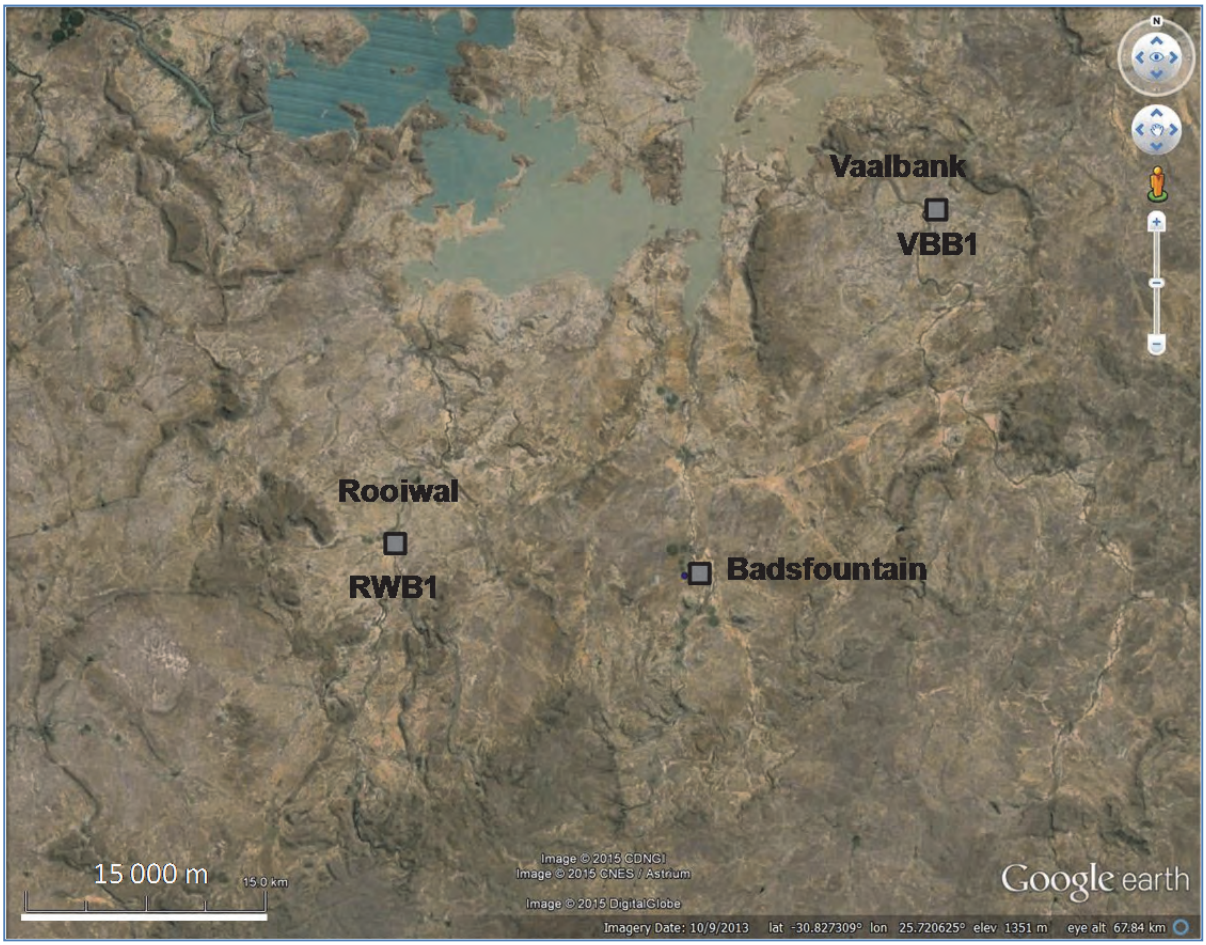

Figure 4.8. The Venterstad warm spring sites showing their proximity to dolerite ring structures and sills (Google Earth, 2014)

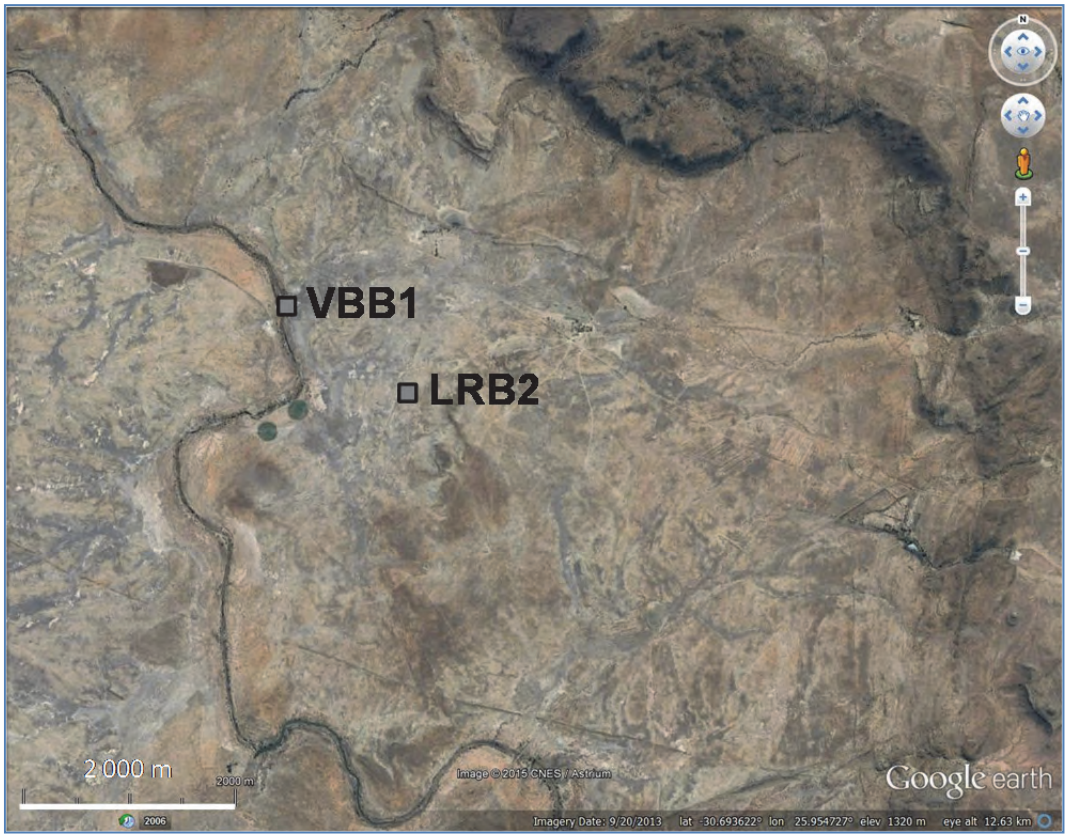

Figure 4.9. Venterstad's Vaalbank sampling sites inside a dolerite ring structure (Google Earth, 2014)

Photos 5 & 6. The borehole that was sampled near the old Vaalbank spring; and the adjacent old stoneworks that may indicate the location of the old, warm spring

Figure 4.10. Venterstad's Rooiwal sampling sites showing the NE-SW trending dyke on which the spring and borehole RWB1c are located (Google Earth, 2014)

Photos 7 & 8. Possible location of the old Rooiwal warm spring; and sampling the nearby borehole RWB1c

The Venterstad area sits in the Tarkastad Formation which consists of interbedded mudstones and sandstones. The area was intensely intruded by Karoo-age dolerites in the forms of dykes, sills and ring structures (Figure 4.11). Besides the deformation resulting from the intrusive dolerites, the area may also lie in an east-west trending neotectonic zone (Woodford and Chevallier, 2002). This latter instability, coupled with the dolerites, may account for the high density of localised deep-shallow hydraulic conductivity and the consequent warm springs in this area.

The Vaalbank area lies on the inside margin of a 20 km wide dolerite ring structure which is transected by numerous major dykes. The location of the sampled borehole (which by all accounts is next to the old spring), lies 130 m away from a large, NE-SW trending dyke. Like all other selected sites, it is not certain where the recharge area is, but it is probable that the location of the spring is associated with this nearby dyke.

The Rooiwal warm spring is also located adjacent to a major NE-SW trending dyke which crosses and merges with other dykes. The area around this has also been intruded with sills and ring structures. The spring is 19 km east of the Badsfountain warm spring and may be the product of more than one intrusive/tectonic event. The Badsfountain spring itself lies about 2 km east of the Orange-Fish River tunnel where a major fracture zone was intercepted that flooded the tunnel (at a rate of ~860 L/s) (Whittingham, 1970) and it was postulated that this fracture zone may represent reactivation of an eastward extension of the pre-Karoo Doornberg fault zone that is exposed near Prieska (Vogel, et al., 1980). Based on possibilities of geologic events from pre-Karoo, Karoo-age (dolerites) and neotectonics, it is evident that understanding the nature of deep groundwater flow in this area is a challenging task that would require considerable research.

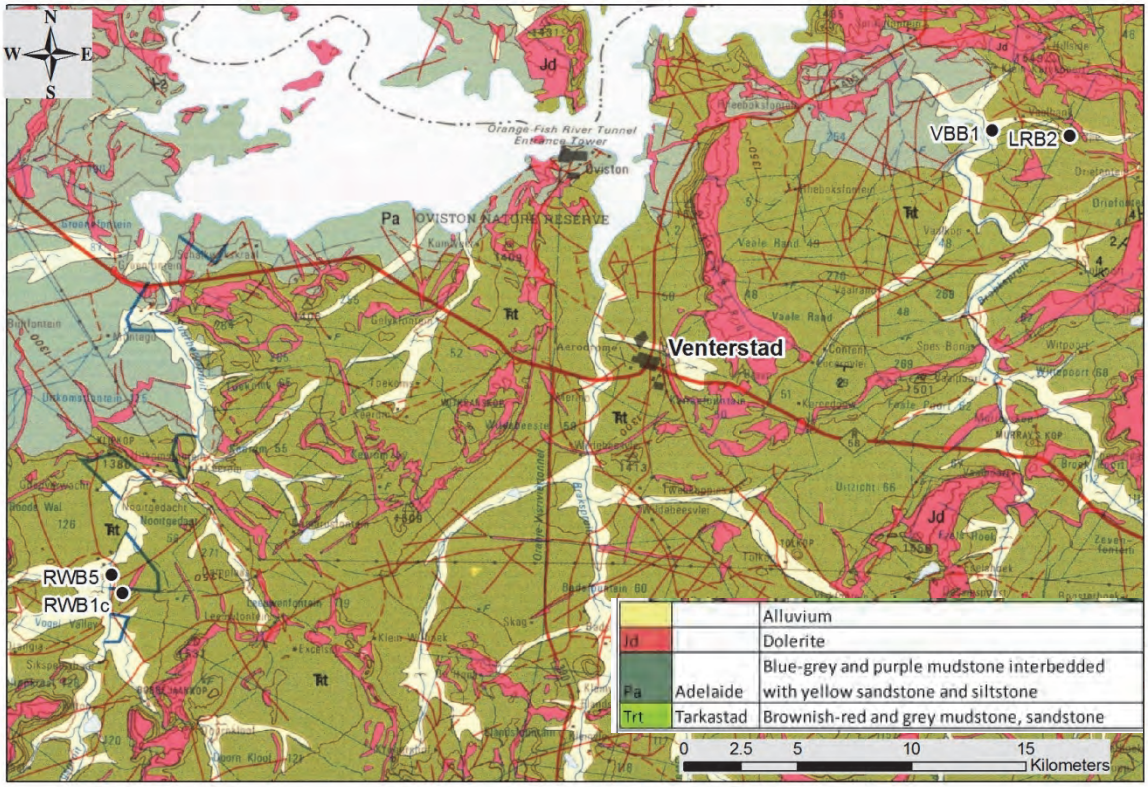

Figure 4.11. Geological map (1:250 000) of the Venterstad area including the final sampling sites

4.2.4 Aliwal North

The Aliwal North spring, together with the Cradock spring, had the highest temperatures when measured by Kent in 1949. The Aliwal North's spring temperature was 36.9°C (Kent, 1949), and this site formed the core of what was once a popular tourist attraction. The main spring discharges into the base of a disused and derelict indoor pool, and it is possible to install the intake of the sampling pipe into the submerged chamber from which water rises into pool (Photos 9 & 10).

A number of sites were visited to try and find a suitable "shallow" source with which to compare the warm spring water, but this proved difficult and a site (ANBH1) was finally found 1.8km form the spring (Figure 4.12). This site gave a broadly similar chemical composition as the spring, but with some significant differences (as can be seen in the following chapter).Unfortunately this site did not give a significant chemical contrast (as can be seen in the following chapter).

Photos 9 & 10. The Aliwal North spring, with water rising and bubbling at the surface

Figure 4.12. Aliwal North sampling sites in the south-western side of a dolerite ring structure (Google Earth, 2014).

The spring is located on the south-western side of a large dolerite ring structure. This structure is cut by a major north-south trending dyke which at surface appears to have “cut-off” the south-western part of the ring structure (Figure 4.13). There are also numerous other

dykes and sills in the greater Aliwal North area, and it forms part of the major east-west neotectonic zone postulated by Woodford and Chevallier (2002). The sub-surface geology of this area is not straight forward, and like other ring-dyke-sill complexes, it is not possible to identify particular structures that may impede flow at depth and provide conduits for upward flow.

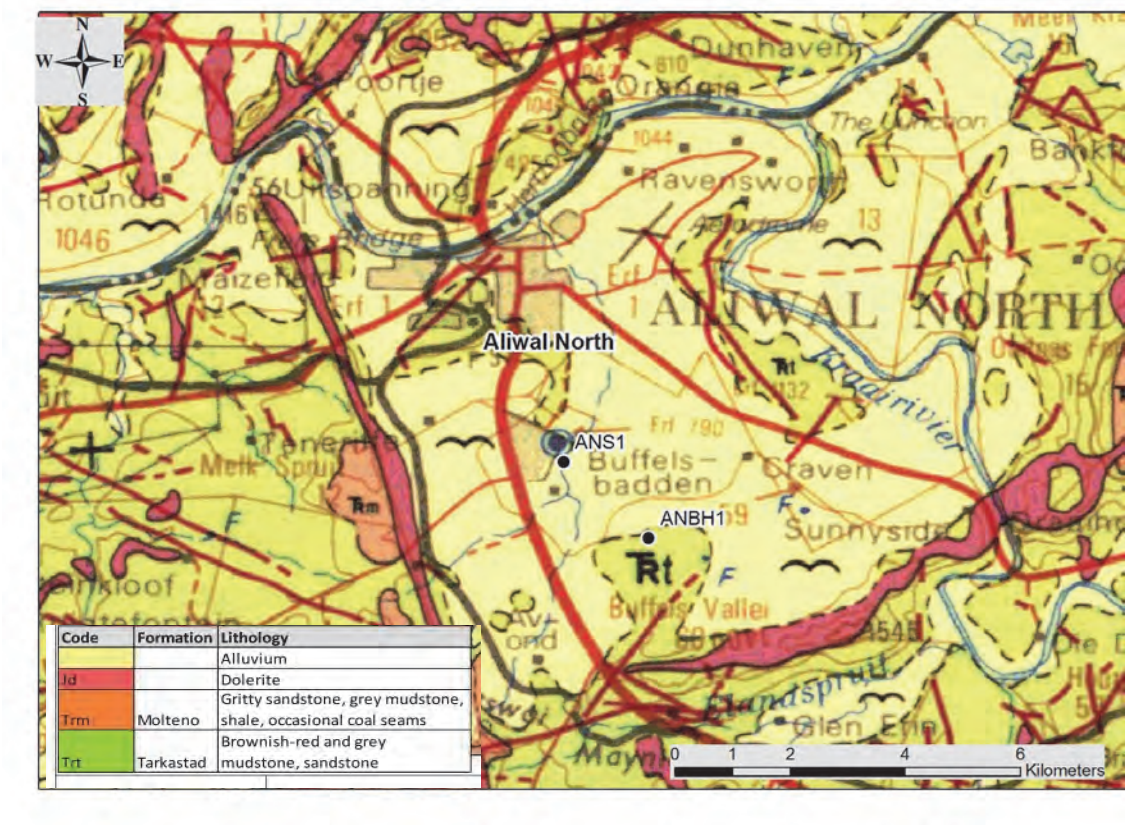

Figure 4.13. Geological map (1:250 000) of the Aliwal North area including the final sampling sites

4.2.5 Cradock

The Cradock spa is a popular resort and the pool is well maintained and suitable for sampling. The warmest temperature measured was 31°C (Kent, 1949), which is close to the 29°C measured during this project. Like at Aliwal North, the main spring discharges into a swimming pool with a sump at its base where the bubbling spring water rises (Photos 11-14). A comparative shallow-flow sampling site, borehole DRB4, was found 6.5 km from the warm spring (Figure 4.14).

Photos 11 & 12. Cradock spa swimming pool in August 2013 (after being drained for cleaning), with metal grids protecting the bubbling springflow from below (photo courtesy S Mullineux, DWA, Cradock).

Photos 13 & 14. Swimming pool in December 2012 (photo courtesy S Mullineux, DWA, Cradock); and inserting a sampling pipe into the submerged spring chamber.

Figure 4.14. Cradock sampling sites with dolerite ring structure and sills to the north-east (Google Earth, 2014).

The Cradock warm spring daylights from the Balfour Formation which consistes mostly of mudstone with intercalated fine-grained sandstone. At the surface, a fairly dense distribution of dolerite sills and dykes can be seen, with one fairly major north-west trending dyke outcropping 1 km west of the spring (Figure 4.15). The spring itself appears to be located outside the western edge of a complex ring structure.

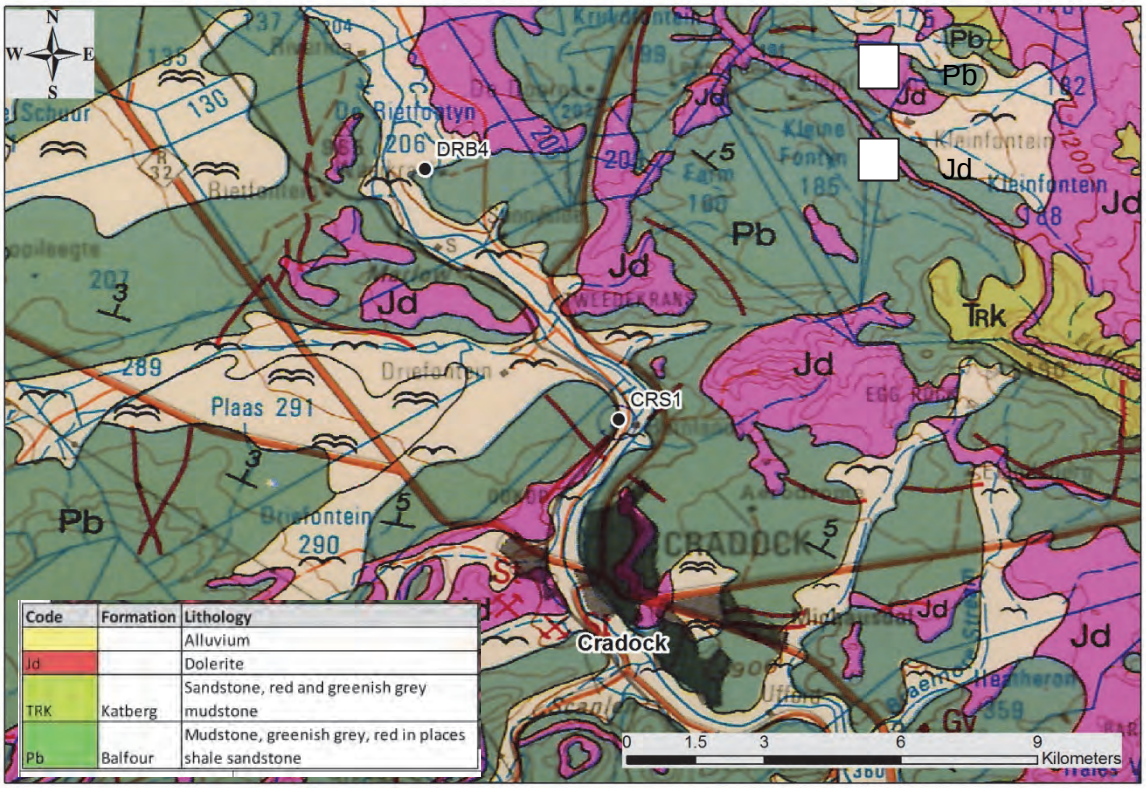

Figure 4.15. Geological map (1:250 000) of the Cradock area including the final sampling sites

4.2.6 Fort Beaufort

An artesian warm spring is situated on the private citrus farm, Bath Farm; its temperature was reported to be 27-29^{o}C in 1947 (Kent, 1949). A health spa, named Sulphur Baths, was developed at this site, and the old pools can still be seen hidden in the lush vegetation that now covers the baths. The eye of the spring could not be accessed at the base of the main pool, so a gently flowing artesian borehole (BFB1) about 30m away was sampled instead (Photos 15 & 16). The water discharging from this borehole is warm, with a temperature of 26^{o}C, and gas bubbles can be seen rising and breaking at the surface. It was considered a good alternative to the inaccessible spring.

Photos 15 & 16. The main spring (old spa bath) and the nearby gently-flowing artesian borehole from which groundwater rises and bubbles to the surface.

Fort Beaufort, like the remaining two sites, Leeu Gamka and Merweville, lies below/south of the great escarpment and thus outside the central Karoo Basin that is so distinctly defined by the dense network of dolerite dykes, sill and ring structures (Figures 4.16, 3.3, 3.4 and 4.2). The dolerites are still present in this area, and the spring site sits about 3km north of a >100km long dolerite sheet that runs into the Indian Ocean. The area is located in folded sediments of the Middleton Formation which consists of mostly mudstone with interbedded sandstone, and the spring daylights from a point between anticline and syncline axes (Figure 4.17). The source of the spring flow is not known. It is postulated that recharge takes place in the high-lying escarpment some 20 km north of the spring, and that the dolerite sheet immediately south of the spring acts as a barrier to flow which then forces the water to migrate upwards along joints and fractures associated with the folded Middleton Formation sediments.

Figure 4.16. Artesian borehole (BFB1) adjacent to the spring with the high-lying escarpment to the north and the WNW-ESE trending dolerite sheet immediately south of the site (and running through BFB2)

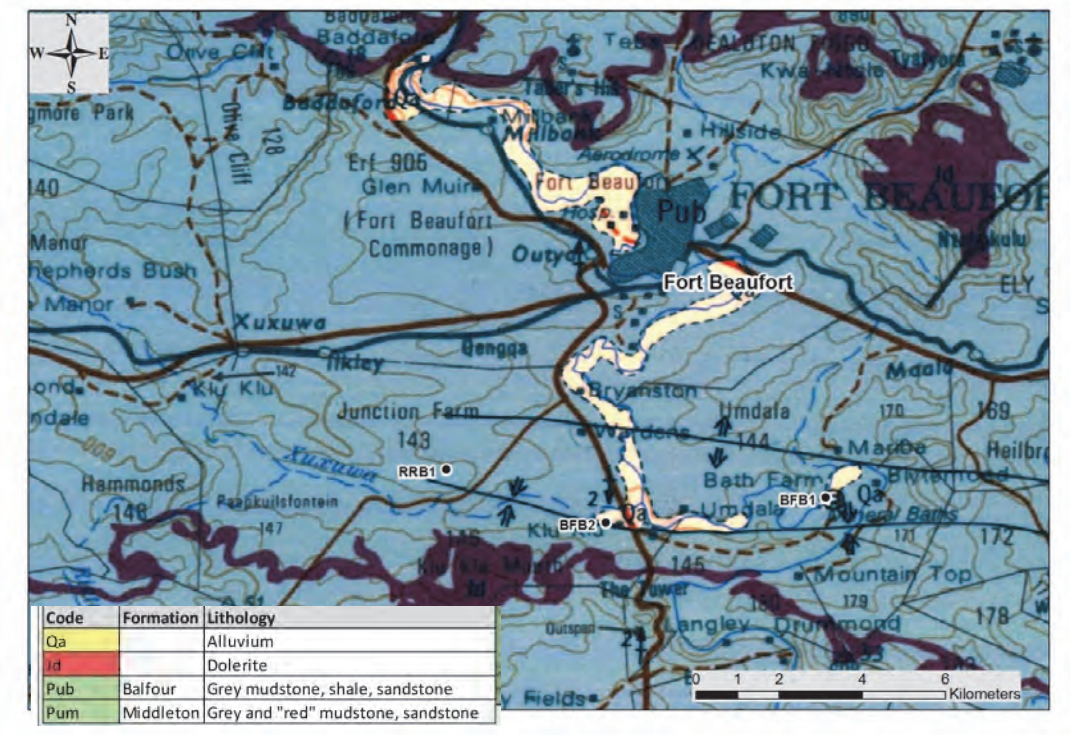

Figure 4.17. Geological map (1:250 000) of the Fort Beaufort area including the final sampling sites

4.2.7 *Merweville*

The Merweville and Leeu Gamka sites lie in similar geological settings. The Cape Supergroup, defined by the Cape Fold Belt in the south, forms the basement for the Karoo Supergroup in this area (Figure 4.18). The area is relatively low-lying when compared to the great escarpment to the north and the Cape Fold belt to the south (Figure 4.19), and like other areas sandwiched between these two prominent geologic features, is in a setting conducive to artesian pressures at depth. These are areas where the hypothesized Karoo artesian basin likely holds true.

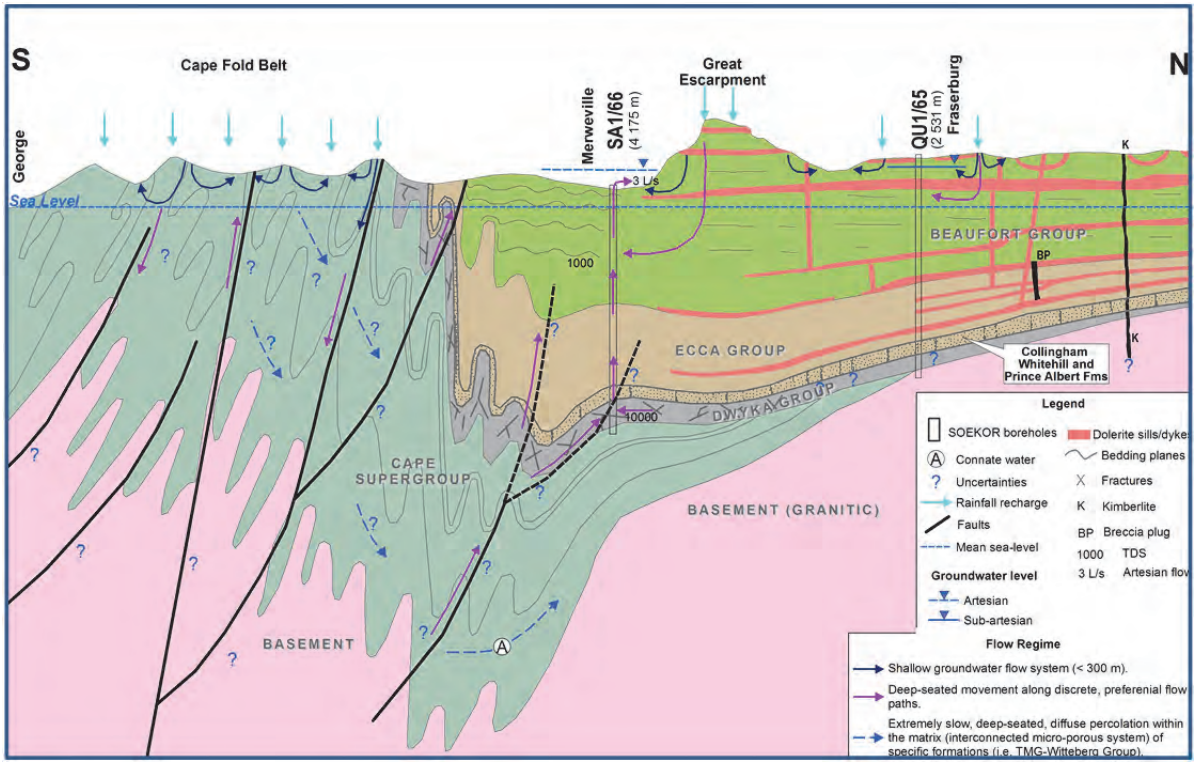

Figure 4.18. Schematic cross section through the Merweville area (Leeu Gamka is at a similar latitude to Merweville)

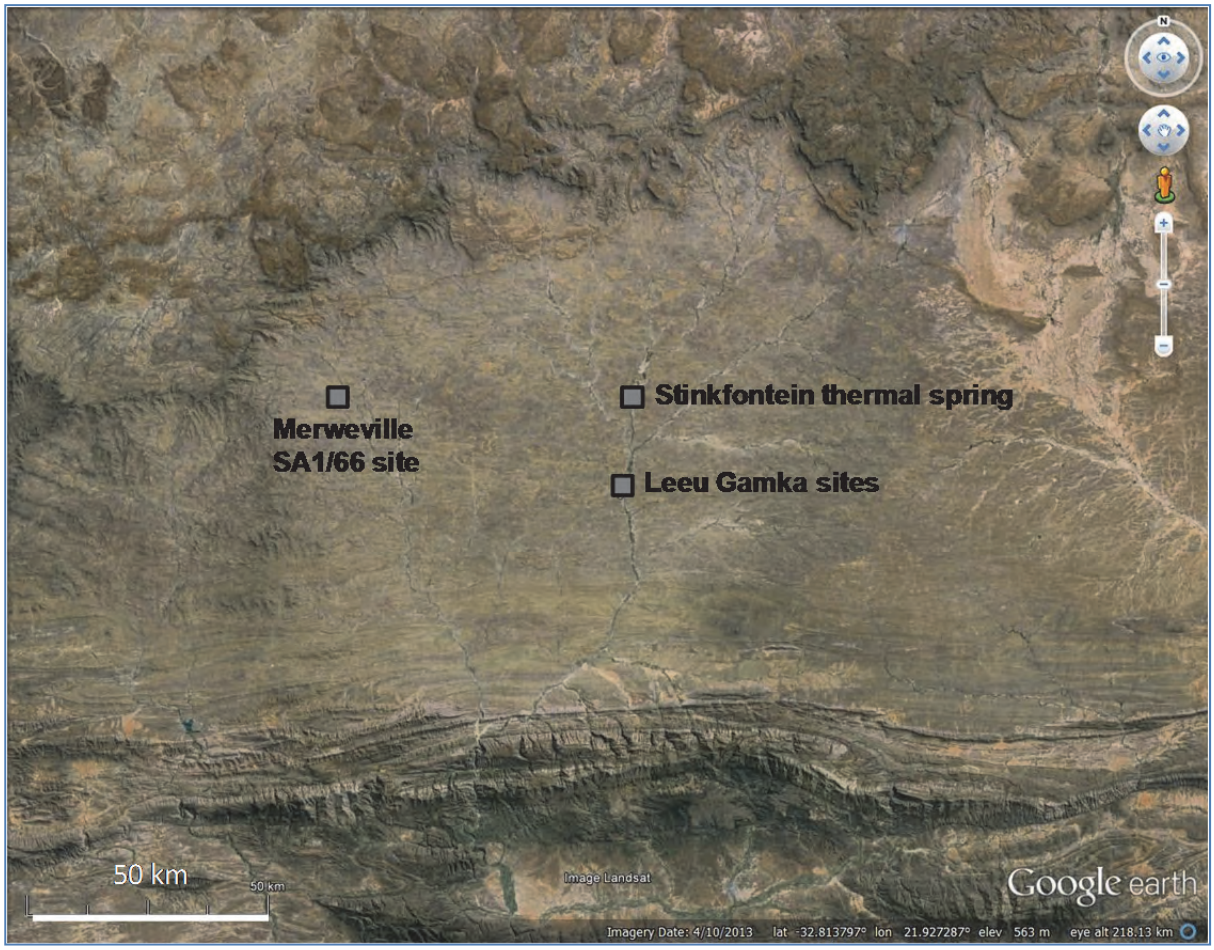

Figure 4.19. The Merweville and Leeu Gamka sites showing the Cape Fold Belt to the south, the Karoo's great escarpment to the north, and the location of the Stinkfontein warm spring.

In 1965 Soekor along with the Geological Survey of South Africa drilled a number of deep exploration wells in the Karoo. The aim of the drilling project was to prove or disprove the existence of economic accumulations of oil or gas in South Africa (Rowsell & De Swardt 1976). The boreholes were sealed with cement, however, the seal must have failed in borehole SA1/66 and it was finally sampled by Prof. Van Tonder in 2012 when he opened it nearly half a century after it was drilled. The total depth of the borehole is 4169 m and water was struck within the Dwyka Group at 3206 m (Rowsell & De Swardt, 1976). The original drilling/geological log describes the water as artesian with a temperature of 46°C, a TDS of 8745 ppm and "a very high gas content". A summary log is presented in Appendix 3.

Due to a lack of artesian flow during this project's field trips in 2014 the borehole was not re-sampled, and Prof. Van Tonder and his doctoral student, Mr Fanie de Lange of the Institute for Groundwater Studies at the University of the Free State kindly gave permission to use

samples and data they collected from the borehole in 2012 and 2013 prior to the drop in artesian pressure. It is not known exactly how the samples were collected, but during the 13 hours of data logger deployment on the day of the 2013 sampling, the temperature and TDS did not continuously rise as would be expected if water was rising from great depths; rather these values fluctuated mostly around 22-24^{o}C and 10000-11500 mg/L respectively (i.e. the temperature did not rise to the first measured value, but the TDS values were in the same order as those originally measured).

Both Merweville and Leeu Gamka are located on arenaceous and argillaceous sediments of the Abrahamskraal Formation which overlie the Cape Supergroup sediments at depth. The impact of the Cape Fold Belt is evident in the E-W trending shallow folds throughout this area (Figure 4.20). Photographs of borehole SA1/66 are shown in Photos 17-20.

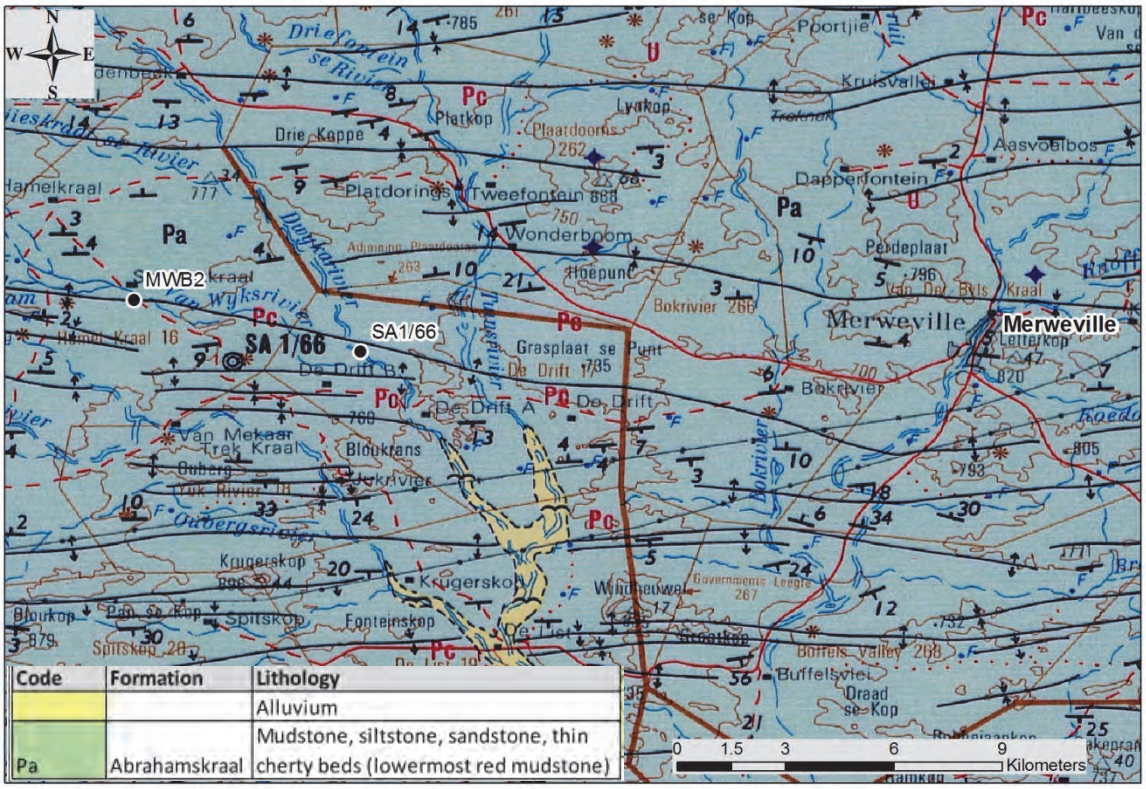

Figure 4.20. Geological map (1:250 000) of Merweville including the final sampling sites

Photos 17 & 18. Borehole SA1/66 and Prof. Van Tonder at the discharge point after opening the flow valve in 2012

Photos 19 & 20. Burning gas at the outlet pipe; and the new valve and pressure gauge installed by the IGS, University of the Free State

4.2.8 Leeu Gamka

Leeu Gamka is a small town situated south-west of Beaufort West along the N1 highway. Boreholes on two farms, Kruidfontein and Groot Kruidfontein, located south of Leeu Gamka were sampled for this project. The area was selected for three reasons:

1. The warm springs at Stinkfontein ~13 km north of Leeu Gamka, and at Groot Kruidfontein ~4 km south of Leeu Gamka.

2. Previously sampled boreholes that suggested deep flow (Talma and Weaver, 2003).
3. The area is seismically active.

The warm springs are shown on the Geological Survey's 1952, 125 000 map, and are mentioned in the accompanying explanation sheet (Rossouw and De Villiers, 1953). At the time, the Stinkfontein spring had a temperature of 28.8°C and the Groot Kruidfontein had a temperature of 24°C, and both carried a distinct hydrogen sulphide odour.

The location of the Stinkfontein spring was pointed out by the land owner who unfortunately had excavated a small dam over the spring and it was not suitable for sampling (Photo 21).

Photo 21. Current-day Stinkfontein warm spring site

The geology of Leeu Gamka is similar to that of Merweville (folded Abrahamskraal Formation – see the previous section) (Figure 4.21), and the source of the deep water is thought to be from recharge in the Cape Mountains to the south, and then via faults or fracture zones associated with the Cape Fold Belt.

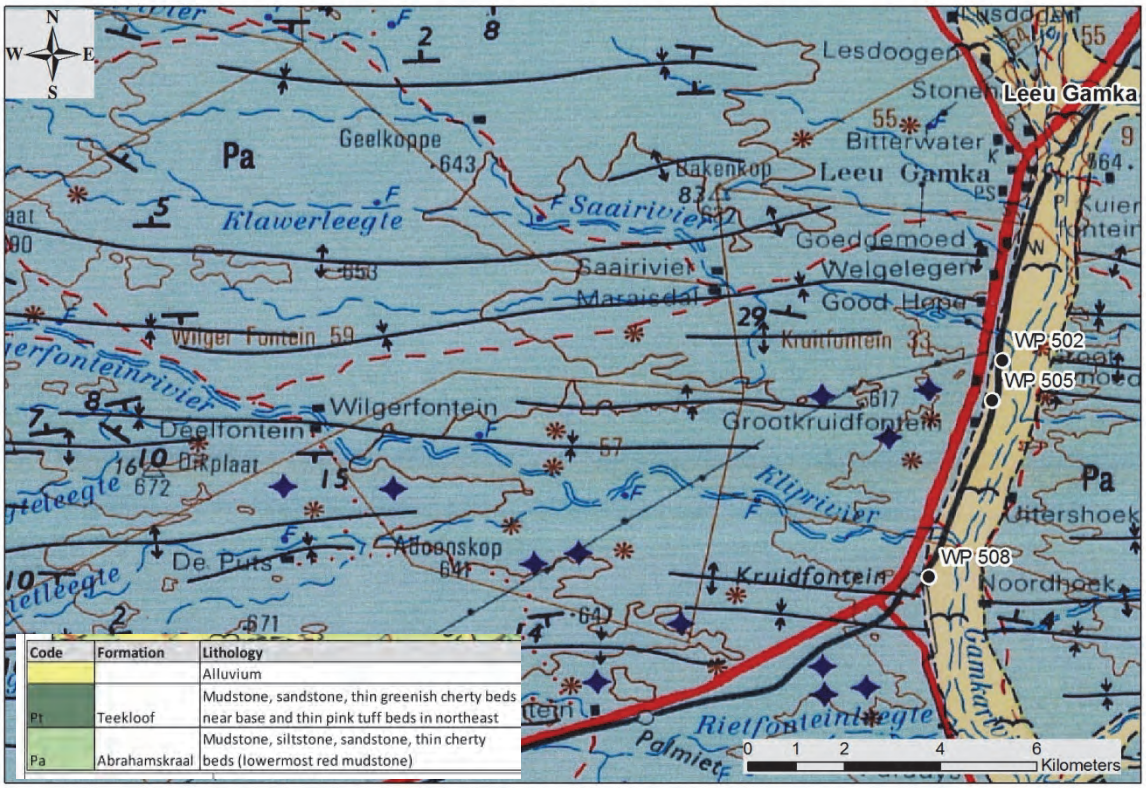

Figure 4.21. Geological map (1:250 000) of Leeu Gamka including the final sampling sites

5. PRESENTATION AND ASSESSMENT OF HYDROCHEMICAL RESULTS

After selection of the final sampling sites as outlined in Chapter 4, a second sampling run was conducted in June/July 2014 to expand the geochemical database. Samples were collected during this second sampling run for all of the parameters that had previously been analysed, with the exception of the rare earth elements as the concentrations of these elements were too low to be significant. Additionally, samples for an expanded set of parameters, including a number of different isotope systems as well as gases, were also collected and analysed. The sampling protocol and analytical methods are described in Appendix 2; the results from the first and second sampling runs are presented in Appendices 4 and 5 respectively; and the final geochemical dataset used and presented in this chapter (which comes predominantly from the second sampling run), is given in Appendix 6.

The large geochemical dataset that was collected in the course of this study was to facilitate evaluation of which geochemical parameters are best suited to differentiate deep from shallow groundwater. However, the size of the dataset makes it difficult to present without some initial assessment. All the sources selected for sampling in this phase were classified as either deep or shallow, based solely on the temperature of the water emanating from the surface at the collection point or in a couple of cases on historical information (see Appendix 3). In any particular area where climatic conditions are similar it is assumed that groundwater derived from a similar depth (i.e. hosted in the same sedimentary unit) will have similar hydrochemistry. Differences in hydrochemistry will relate either to hosting in different stratigraphy (or major dolerite intrusions) or to the age of the groundwater whereby older groundwater has interacted with the host rocks over a longer period of time. Thus deep and shallow groundwater should have different hydrochemical characteristics because they are hosted in different units and have been underground for longer times (deep equating to older). To test the validity of this initial temperature-based deep versus shallow classification, the data was put through a second assessment using standard Stiff diagrams. From these two assessments, the groundwaters were classified into three groups. These three groups were then used as a framework to present the likely deep-flow indicators identified in Section 2.3, as well as other determinands, including gases, that could be of use to differentiate between deep and shallow groundwater. Based on the information presented below, a final list of important deep groundwater indicators is discussed in Chapter 6.

With regard to terminology, many sites were considered “suspected deep” or “suspected shallow” until the process of classifying them was complete. In this chapter, the term “suspected” has mostly been dropped for ease of reading.

5.1 Characterisation of sources by hydrochemistry and temperature

In the sections that follow, for each location, classic Stiff diagrams using the cations Ca^{2+}, Mg^{2+} and $Na^{+} + K^{+}$ and the anions Cl^{-}, SO_4^{2-}, and $HCO_3^{-} + CO_3^{2-}$ are constructed for each site. The anions PO_4^{3-}, Br^{-}, F^{-} and NO_3^{-} are not considered. In conjunction with temperature, the Stiff diagrams showed two fairly consistent shapes defining deep and shallow groundwater, and an ambiguous shape defining a mixed group.

5.1.1 Florisbad

The deep water site at this location is the Florisbad Spa, FLS1, which contains elevated concentrations of Na^{+}, K^{+} and Cl^{-} and negligible concentrations of Ca^{2+}, HCO_3^{-}, Mg^{2+} and SO_4^{2-} (Figure 5.1). In contrast, the groundwater collected from the shallow borehole, FLB5, contains higher concentrations of Na^{+}, K^{+}, Cl^{-}, Ca^{2+}, HCO_3^{-}, Mg^{2+} and SO_4^{2-} (Figure 5.1).

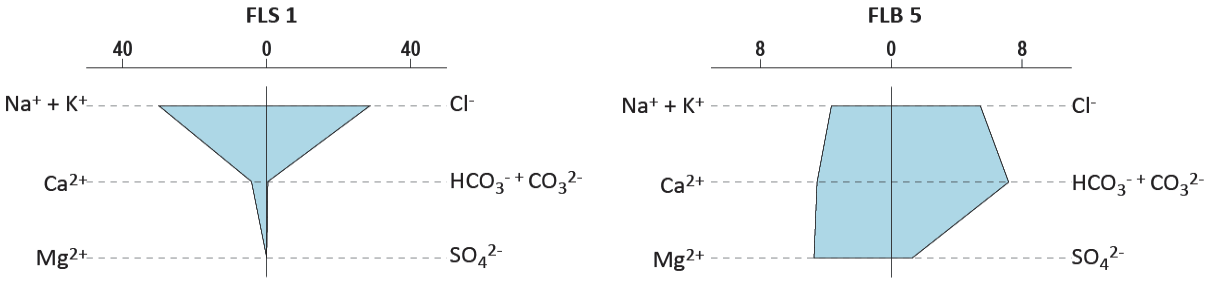

Figure 5.1. Stiff diagrams of the Florisbad samples (units meq/L)

The groundwater temperature of the deep site (FLS1) recorded during the first sampling (March 2014) was 28.7°C, and during the second sampling (June 2014) was 20°C. Previous sampling over many years has consistently shown the temperature of this spring as 28-30°C. For this reason, the temperature from the first sampling run (28.7°C) has been used in the final data compilation (Appendix 6). The temperature of the shallow borehole, FLB5, is cool at 19.2°C. Therefore FLS1 was classified as deep and FLB5 shallow.

5.1.2 Trompsburg

The deep water source is the 1.5 km deep, warm, artesian flowing borehole in Trompsburg, VFB1, which has a similar Stiff diagram to Florisbad’s warm spring (Figure 5.2). The

dominant ions are Na^+ and Cl^-, however, minor amounts of Ca^{2+} and SO_4^{2-} and negligible concentrations of HCO_3^- and Mg^{2+} occur. The shallow borehole, VFB2, also shows a similar shape to the shallow borehole sampled in Florisbad (Figure 5.2). The groundwater is dominant in HCO_3^- and Ca^{2+}, and also has relatively high concentrations of Mg^{2+} and Na^+. The temperature of the deep source, VFB1, is warm at 29.5°C and the temperature of the groundwater sampled from the shallow borehole, VFB2, is cool at 18.2°C. Although there is a slight difference in the shape of the Stiff diagram for VFB1 in comparison to FLS1, the high temperature means this source was classified as deep, whilst VFB2 was classified as shallow.

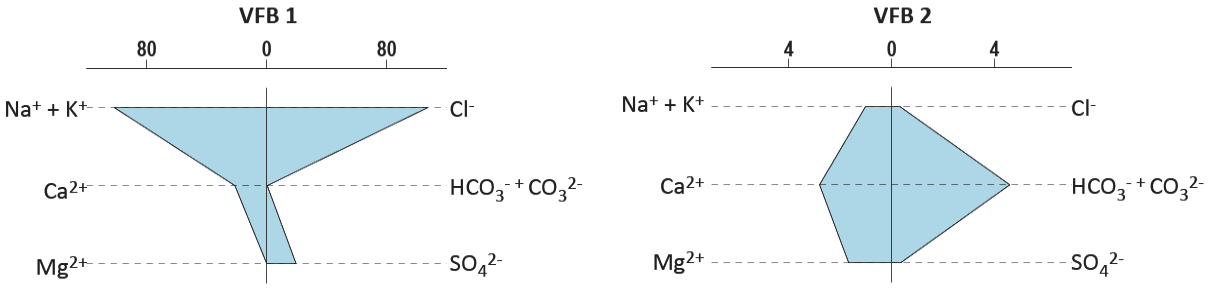

Figure 5.2. Stiff diagrams of the Trompsburg samples (units in meq/L)

5.1.3 Venterstad

Two suspected deep- and shallow sites were sampled in the vicinity of Venterstad. The first deep borehole site, RWB1c, has a significantly different Stiff diagram shape to the previously described deep sites FLS1 and VFB1 (Figure 5.3). This source is considered to be deep because it has a slightly elevated temperature (25.7°C) and lies adjacent to the old Rooiwal warm spring which no longer flows. The Rooiwal warm spring had an average temperature of 30.0°C (Visser, 1962). The Stiff diagram of RWB1c shows high concentrations of Na^+ as well as low concentrations of Mg^{2+}. However, elevated HCO_3^- is recorded as well as slightly higher concentrations of Ca^{2+} and SO_4^{2-}. The shallow pair of RWB1c is RWB5. It has a Stiff diagram that is an almost identical shape to the shallow site VFB2 in Trompsburg (Figure 5.3) where elevated HCO_3^-, Ca^{2+} and Mg^{2+} concentrations and depleted Cl^- and SO_4^{2-} concentrations are recorded. Its temperature is 18.1°C. RWB1c was classified as mixed because of the ambiguous Stiff diagram and only moderately elevated temperature, whilst RWB5 was classified as shallow.

The second suspected deep site in Venterstad is the shallow borehole VBB1 (Figure 5.3). By all accounts, this borehole lies within metres of the warm spring sampled by Visser in 1962. The shape of the Stiff diagram for this borehole is similar to that of the first suspected deep

borehole in Venterstad (RWB1c). However, VBB1 contains more Cl^- than RWB1c. Its temperature is a cool 18.2°C and thus is hydraulically not well-linked to the old warm spring at this site. The shallow pair for VBB1 is LRB2 (Figure 5.3). LRB2 has an almost identical Stiff diagram shape to that of RWB5 and a temperature of 17.3°C. Therefore LRB2 was classified as shallow. VBB1 was classified as mixed because of the low temperature and ambiguous Stiff diagram.

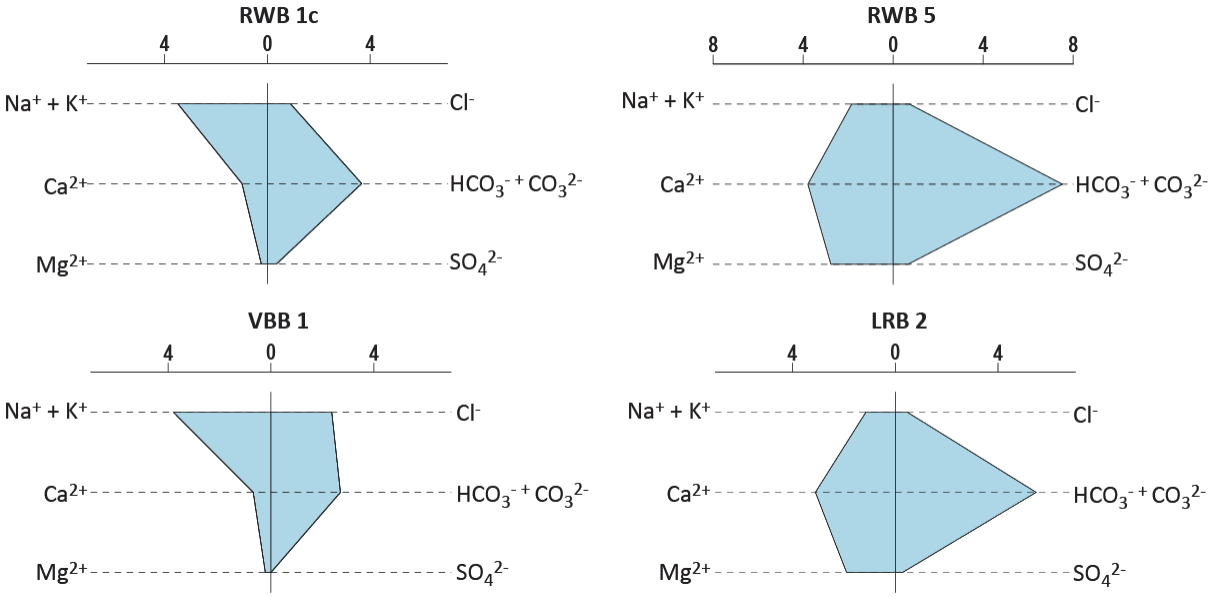

Figure 5.3. Stiff diagrams of the Venterstad samples (units in meq/L)

5.1.4 Aliwal North

The deep flow site in Aliwal North is the warm spring ANS1 which supplies the spa with 29°C water. The Stiff diagram has a similar shape to VFB1 with elevated Na^+ and Cl^- concentrations, only slightly elevated Ca^{2+} concentrations, and negligible HCO_3^-, Mg^{2+} and SO_4^{2-} concentrations (Figure 5.4). The shallow borehole is ANBH1, 1.8 km south-east of the warm spring. Its Stiff diagram is a similar shape to that of ANS1 (Figure 5.4) with elevated Na^+, K^+ and Cl^- and negligible Ca^{2+}, HCO_3^-, Mg^{2+} and SO_4^{2-}. Its temperature is 21.6°C and the hypothesis needs to be tested whether this is merely cooled water from the same source as the spa. Despite the low temperature for ANBH1, the similarity of its Stiff diagram shape has led to both ANS1 and ANBH1 being classified as deep.

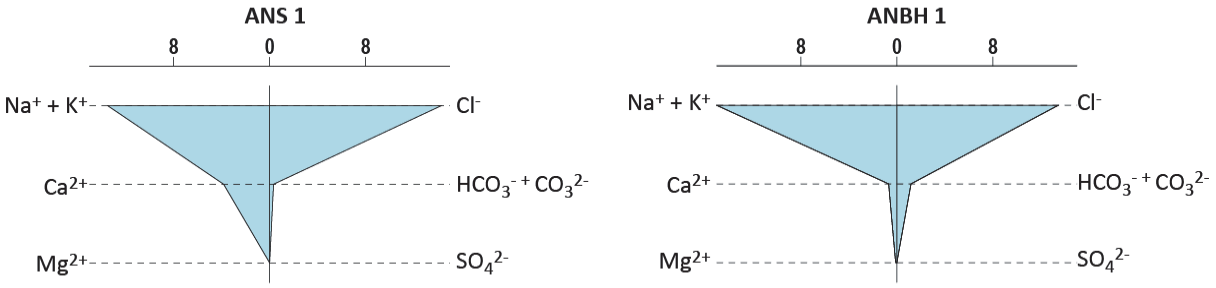

Figure 5.4. Stiff diagrams of the Aliwal North samples (units in meq/L)

5.1.5 *Cradock*

The deep site in Cradock is the warm, spring-fed spa (29.4°C), CRS1. The low concentration of Cl^- gives a different shaped Stiff diagram to the other deep sources (Figure 5.5), especially in conjunction with slightly elevated HCO_3^- concentrations. The suspected shallow source is DRB4 (Figure 5.5) with a temperature of 16.2°C. While this site records elevated HCO_3^-, consistent with previously defined shallow sites, it is also depleted in Ca^{2+} yielding a different shaped Stiff diagram to the suspected shallow boreholes elsewhere. Despite the slightly ambiguous Stiff diagrams, CRS1 is classified as deep and DRB4 as shallow because of the extremes in their temperatures. DRB4 was the lowest temperature recorded for all the sites.

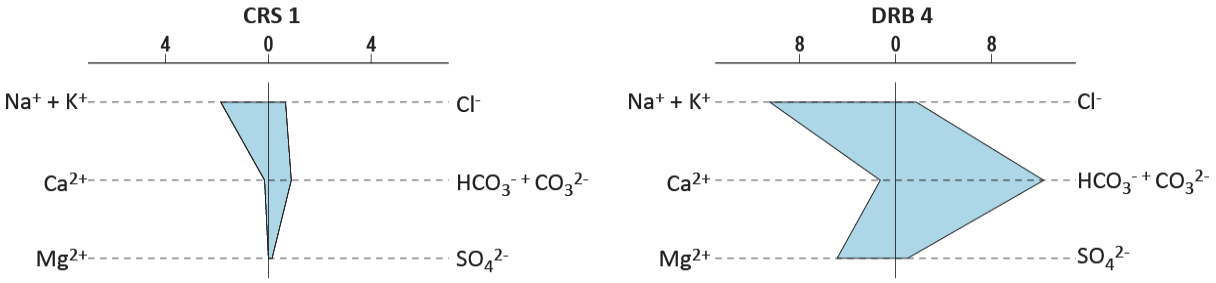

Figure 5.5. Stiff diagrams of the Cradock samples (units in meq/L)

5.1.6 *Fort Beaufort*

The deep site in Fort Beaufort is the borehole BFB1 (23.5°C) about 30 m from the disused warm baths (Figure 5.6). With the exception of slightly elevated HCO_3^- and SO_4^{2-} concentrations, the shape of the Stiff diagram is similar to that of the previous classified deep boreholes. The shallow site is BFB2 (Figure 5.6). The groundwater contains elevated concentrations of Na^+, K^+, Cl^- and HCO_3^-, slightly higher Ca^{2+} and Mg^{2+} and negligible concentrations of SO_4^{2-}. The water temperature was 21.2°C. A second shallow borehole site, RRB1, was sampled during the second sampling round (Figure 5.6). High concentrations of Na^+, K^+, Cl^-, HCO_3^-, Ca^{2+} and Mg^{2+} were recorded although the concentration of SO_4^{2-} is low.

The water temperature was also 21.2°C. Based on the Stiff diagram shape, BFB1 was classified as deep, BFB2 was classified as mixed and RRB1 was classified as shallow.

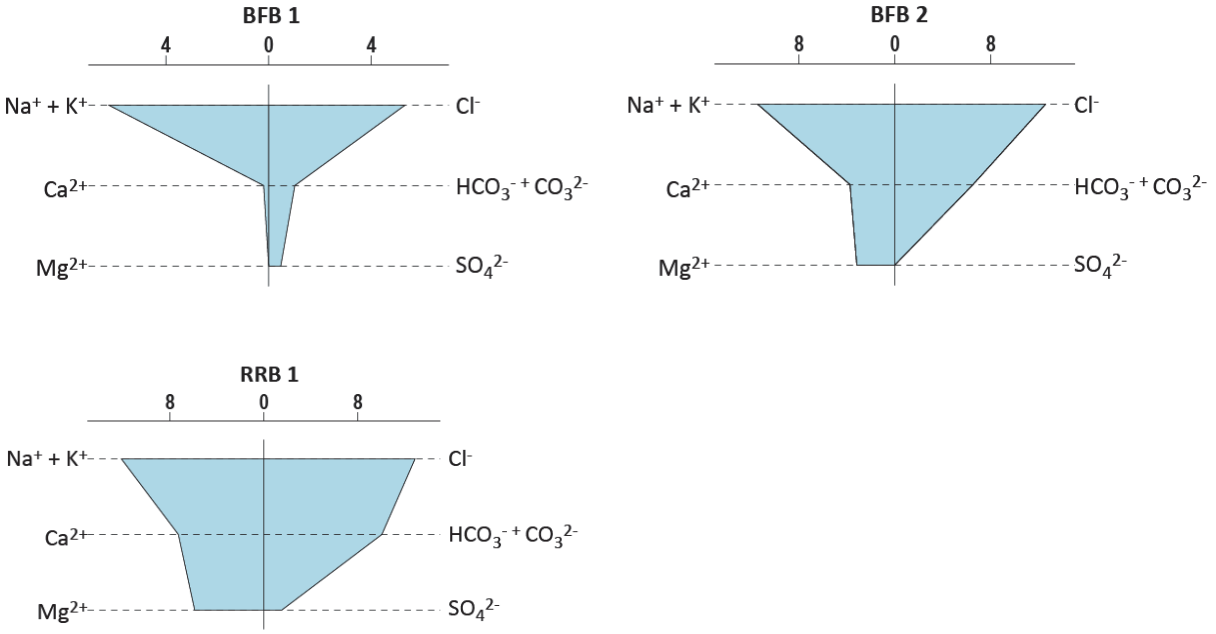

Figure 5.6. Stiff diagrams of the Fort Beaufort samples (units in meq/L)

5.1.7 Leeu Gamka

Unfortunately the eye of the Stinkfontein warm spring could not be sampled because an earth dam had been built over the spring. Two suspected deep sites were however sampled in Leeu Gamka: WP508 and WP505 (Figure 5.7) about 4 km apart. WP505 is on the farm that once had a warm spring (Rossouw, 1953). Both WP508 and WP505 are located on farms where borehole waters uncharacteristic of shallow groundwater were found in the past (Talma and Weaver, 2003). WP508 has high Na^+, K^+, and HCO_3^- concentrations, as well as moderate Ca^{2+}, Cl^- and SO_4^{2-} concentrations, while its Mg^{2+} concentration is negligible. The temperature of site WP508 was 26.5°C. The Stiff diagram for WP505 (Figure 5.7) shows elevated Na^+ and K^+ concentrations, with moderate HCO_3^- and SO_4^{2-} concentrations. The Cl^- is quite low and there is no Mg^{2+}. The temperature of site WP505 is 23.5°C. The suspected shallow site with a temperature of 20.3°C, is WP502. The Stiff diagram has a similar shape to the previous classified shallow sites (Figure 5.7). WP508 and WP505 were therefore classified as mixed because of the absence of clearly elevated temperatures and the ambiguous Stiff diagrams, and WP502 was classified as shallow on the basis of its low temperature and similar Stiff diagram shape to other classified shallow sources.

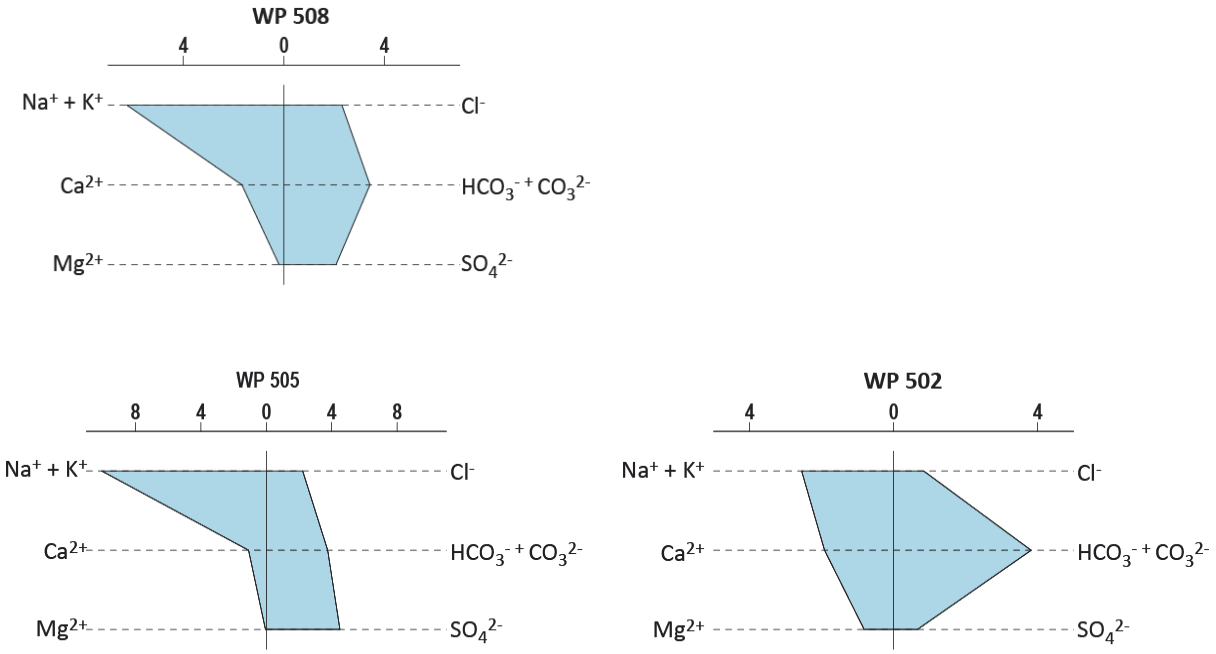

Figure 5.7. Stiff diagrams of the Leeu Gamka samples (units in meq/L)

5.1.8 Merweville

The deep flow source in Merweville is the old Soekor borehole SA1/66. This 4169 m deep artesian flowing borehole drilled in 1966, struck water in the Dwyka Group at 3206 m with a temperature of 46°C (Rowsell & De Swardt, 1976). As discussed in Chapter 4, SA1/66 could not be sampled in July 2014 due to a lack of pressure and can no longer be considered artesian. The borehole was however artesian when sampled for the first time in November 2012 by Prof van Tonder of the Institute for Groundwater Studies (IGS), University of the Free State. It was re-sampled by Mr Fanie de Lange (IGS) in September 2013, and the chemistry and temperature (22°C) used in this project are those obtained from the September 2013 analysis.

The shape of the Stiff diagram is similar to the previous deep boreholes, with high concentrations of Na^+ and Cl^-, as well as negligible concentrations of Ca^{2+}, HCO_3^-, Mg^{2+} and SO_4^{2-} (Figure 5.8). Unfortunately little is known about the current status of this borehole and specifically if the sampled water actually came from the tillites where water was originally struck. It is possible, and maybe probable that the sample has been affected in some way by the ~1 km thick layers of shales (Ecca Group) and ~1 km thick layers of mudstones/sandstones (Beaufort Group) that overlie the tillites. The suspected shallow source at this location is MWB2 (Figure 5.8) which has a temperature of 21.5°C. The shape

of the Stiff diagram is also similar to previously classified shallow boreholes. SA1/66 was thus classified as deep whilst MWB2 was classified as shallow.

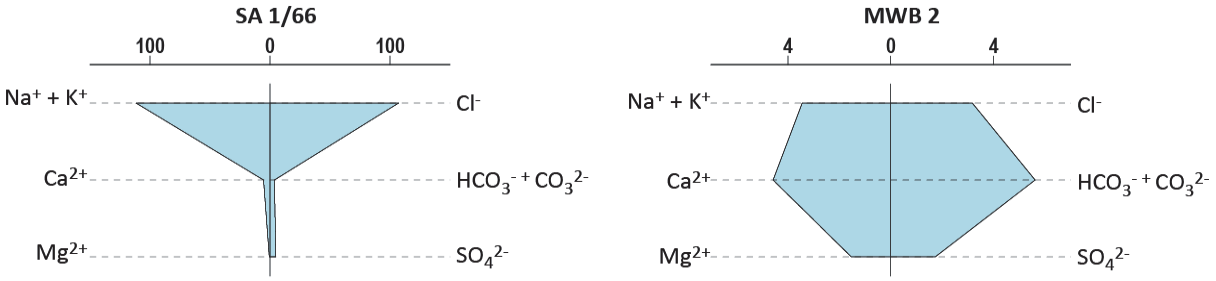

Figure 5.8. Stiff diagrams Merweville samples (units in meq/L)

5.1.9 *Evaluation and interpretation of Stiff diagrams and temperature*

In order to more easily compare and contrast the shape of the Stiff diagrams they were grouped together in Figure 5.9. The diagrams on the left hand side are from sources classified as deep and those on the right hand side are presumed to be from shallow sources. Because of significant differences in the concentrations of the total cations and anions in the different samples, the Stiff diagrams are not all on the same scale and this should be borne in mind when interpreting these figures.

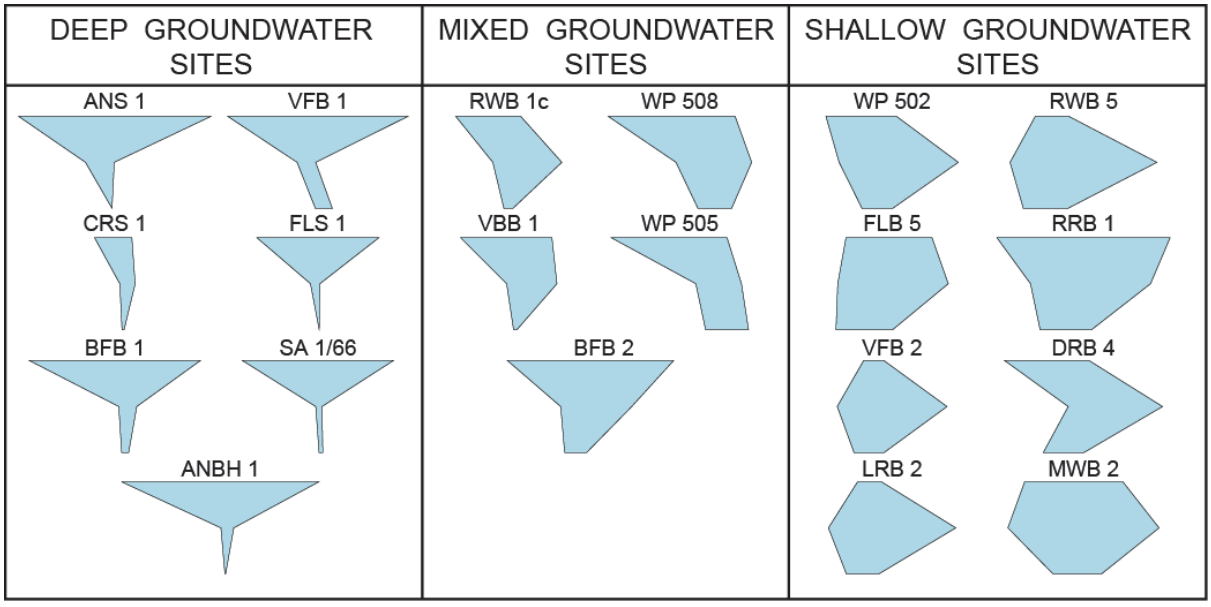

Figure 5.9. Presentation of all Stiff diagrams

Figure 5.10 presents the temperatures of all of the boreholes and springs sampled during this project. In this diagram the source groups are shown as they have been classified based

on the hydrochemical data as summarised in Figure 5.9. While historic data revealed higher temperatures at some sites, the temperatures used in the final analysis and presentation in this report are those taken at the time of sampling with the exception of FLS1 where the historical temperature is taken as more accurate, since the measured temperature (20°C) was demonstrably lower than all historical readings (28-30°C) and indeed lower than the measurement taken during the first sampling run (28.7 °C).

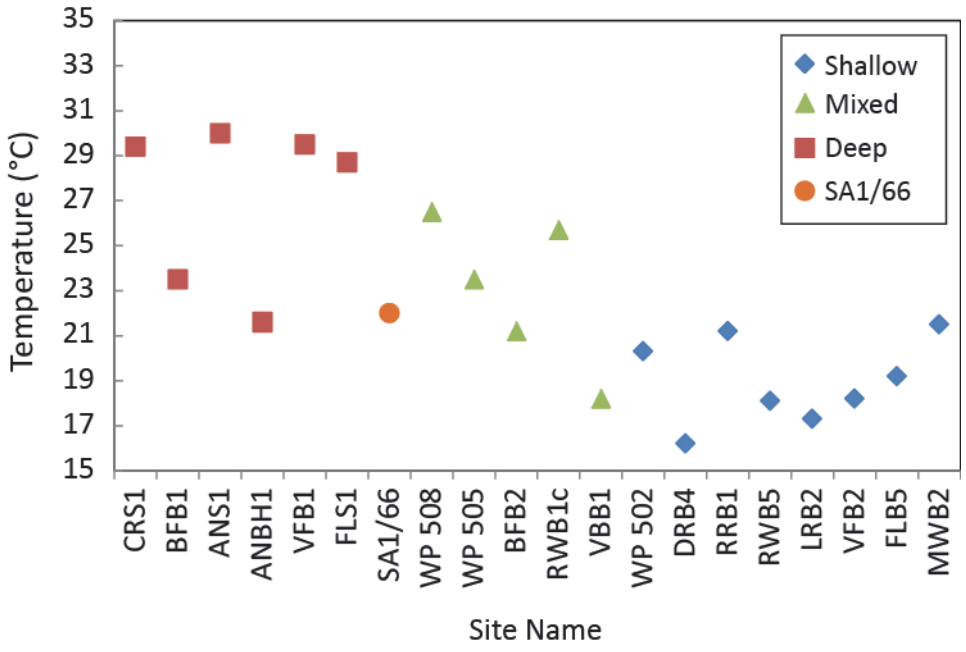

Figure 5.10. Groundwater temperatures

Six out of ten sites that were sampled as suspected deep sites (FLS1, VFB1, ANS1, CRS1, BFB1 and SA1/66) have similar Y-shaped Stiff diagrams. CRS1 (Cradock) is slightly different in shape owing either to low Cl^- or elevated alkalinity which distorts the Y-shape, but it does have one of the highest temperatures recorded in this study. These six sites also either have a temperature of above 25°C or, according to historical data, the temperatures used to be above 25°C. The ionic chemistry and temperature of these six sites are interpreted to represent a similar groundwater type, which because of the generally elevated temperature, is taken to be a deep groundwater. Borehole ANBH1 (temperature 21.6°C) has similar hydrochemistry and produces a very similar Y-shaped Stiff diagram (Figure 5.4) to the Aliwal North warm spring (ANS1), and is therefore thought to represent a deep flow path where cooling takes place through slow upward movement from depth.

Six out of the ten sites that were sampled as suspected shallow sites (FLB5, VFB2, RWB5, LRB2, WP502 and MWB2) display a hexagon shape on the Stiff diagrams that is quite distinct from the deep groundwater type above. All of these sites have temperatures

below 22°C. The ionic chemistry and temperature of these sites are also interpreted to represent similar groundwater types, which because of the low temperature, is taken to be a shallow groundwater.

Two sites sampled as suspected shallow boreholes have slightly ambiguous Stiff diagrams. They are RRB1 near Fort Beaufort and DRB4 near Cradock. Both appear to have lower calcium concentrations and RRB1 also has an elevated chloride level compared to the other shallow sites. However, DRB4 has the lowest temperature recorded during sampling, and RRB1, on the basis of other parameters, also looks to be consistently shallow in nature. These two samples RRB1 and DRB4 are therefore also classified as shallow groundwater types.

The remaining sites (BFB2, RWB1c, VBB1, WP508, WP505, MWB2) have ambiguous characteristics and have been grouped together as mixed samples. BFB2 was sampled as a shallow site due to its cool temperature of 21.2°C but produces an ambiguously shaped Stiff diagram with some characteristics similar to the deep groundwater diagrams (Figure 5.9). RWB1c, VBB1, WP508 and WP505 were sampled as suspected deep sites but all produced ambiguously shaped Stiff diagrams and only two of the sites (RWB1c and WP508) have temperatures indicative of deep groundwater above 25°C.

To summarise, deep groundwater is characterised by “Y” shaped Stiff diagram shapes and/or elevated temperature; shallow groundwater is characterised by hexagon shaped Stiff diagrams and/or low temperatures; and mixed groundwater typically has an ambiguous Stiff diagram shape and/or inconsistent temperature information. Table 5.1 summarises the classification of each site and this is used (including colour coding) for the rest of the data presentation.

Table 5.1. Classification of groundwater depth groups

Group	Town/Location	Site	Sample No.
Deep [red group on plots]	Cradock	Cradock Spa	CRS1
	Fort Beaufort	Sulphur Baths	BFB1
	Aliwal North	Aliwal North Spa	ANS1
	Aliwal North	Aliwal North Farm	ANBH1
	Trompsburg	Vlakfontein	VFB1
	Florisbad	Florisbad Spa	FLS1
	Merweville	Soekor borehole	SA1/66
Mixed [green group on plots]	Leeu Gamka	Kruidfontein	WP 508
	Leeu Gamka	Groot Kruidfontein	WP 505
	Fort Beaufort	Sulphur Baths	BFB2
	Venterstad	Rooiwal	RWB1c
	Venterstad	Vaalbank	VBB1
Shallow [blue group on plots]	Leeu Gamka	Groot Kruidfontein	WP 502
	Cradock	Waaikraal Farm	DRB4
	Fort Beaufort	Rocky Ridge	RRB1
	Venterstad	Rooiwal	RWB5
	Venterstad	La Rochelle	LRB2
	Trompsburg	Vlakfontein	VFB2
	Florisbad	Farm	FLB5
	Merweville	Farm	MWB2

5.2 Assessment of potential deep groundwater indicators

The groundwater groups identified above in Table 5.1 were evaluated against the parameters listed in Section 2.3 and other determinands to assess the validity of this depth grouping. In all the graphs in the following sections, the same colour coding has been used for the three depth groups: (1) red squares = deep sites; (2) blue diamonds = shallow sites; and (3) green triangles = ambiguous sites grouped as mixed. While SA1/66 has been classified as deep on the basis of temperature, it is represented uniquely (as an orange circle) because it was not sampled during this project and the sampling method and depth of origin of the sampling in 2013 are not known.

5.2.1 *Radiocarbon (^{14}C)*

Due to budget and logistical constraints, ^{14}C was unfortunately not determined for all samples. Where available, the ^{14}C values show, as expected, that the samples from the deep group have a lower ^{14}C than the samples from the shallow group, and that the samples from the mixed group fall between these two classes (Figure 5.11). In general there is a good relationship between temperature and the ^{14}C value of the samples (Figure 5.12). The shallow group has the coldest temperatures (16-22°C) and highest ^{14}C values (74-94 pmC), indicative of shallow and young groundwater. The temperature of the deep group ranges between 20-30°C and they have the lowest ^{14}C values (20-53 pmC). The low temperature of BFB1 is discussed elsewhere. The mixed group plots in between the deep and shallow group with moderate to high ^{14}C values that slightly overlap with the other two groups (50-74 pmC) and moderate to warm temperatures.

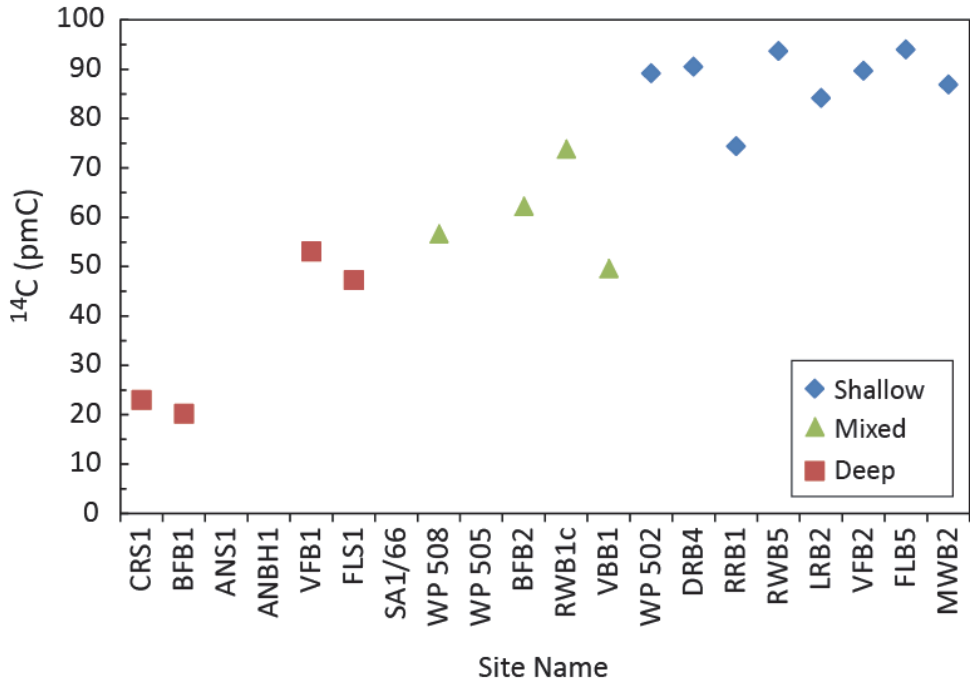

Figure 5.11. ^{14}C values in groundwater depth groups

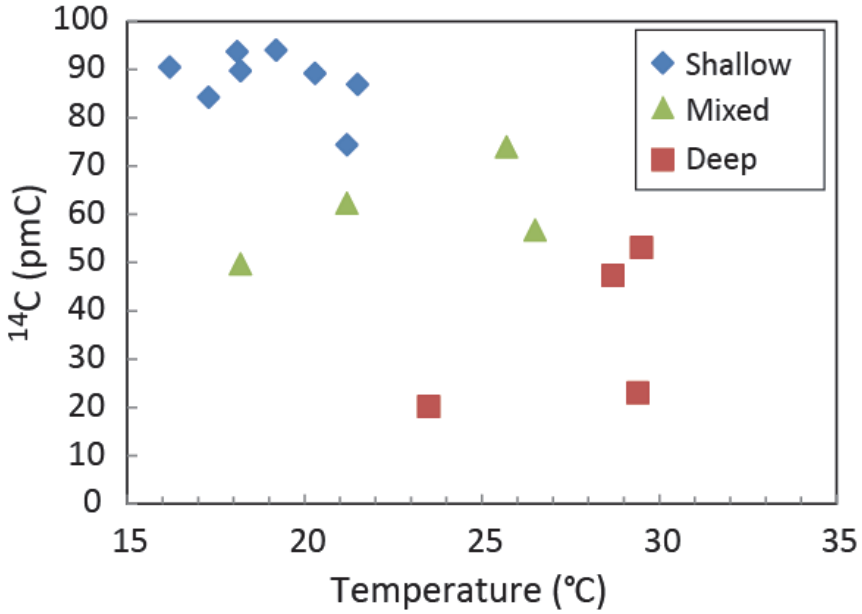

Figure 5.12. Plot of ^{14}C versus temperature for the three groups of sources

5.2.2 *Tritium (^{3}H)*

Figure 5.13 shows ^{3}H along with the depth classification of each site. The deep sites generally have low ^{3}H values (0-0.5 TU), the shallow sites have a range of ^{3}H values from moderately low to moderately high (0.5-3.1 TU), while the mixed sites have ^{3}H values that fall in between and overlap with both these groups (0.1-0.9 TU). Analysis of the relationship between ^{3}H and ^{14}C (Figure 5.14) shows a good correlation, with shallow sites having both higher ^{3}H and ^{14}C in comparison to deep sites with low ^{3}H and ^{14}C. There are however a couple of outliers to this general trend and the relationship between ^{3}H and ^{14}C values is not unique. Figure 5.14 shows a mixing line derived from an exponential mixing model that is widely used for the evaluation of time related tracers (Zuber and Maloszewski, 2001). The good fit of the study data to this exponential mixing line indicates that the samples are likely to be well-mixed groundwaters of various residence times (Talma and Weaver, 2003; Butler and Verhagen, 2013). The deep site in Florisbad, FLS1, is an outlier on this trend due to a moderate ^{3}H value of 1.6 TU combined with a moderately low ^{14}C content of 47 pmC and probably reflects two-component mixing between a young and an old water. The deep site at Trompsburg, VFB1, and the Aliwal North spring, ANS1, are exceptions to the dashed-line model of Figure 5.14. This is probably due to similar two-component mixing between deep and shallow water or an analytical error (± 0.2 TU for tritium).

Groundwater with low to negligible ^{3}H and low ^{14}C are indicative of deep, and therefore older, groundwater. The mixed group have moderate to high ^{3}H and ^{14}C values, supporting the idea that these sites deliver a mixture of both deep and shallow groundwater.

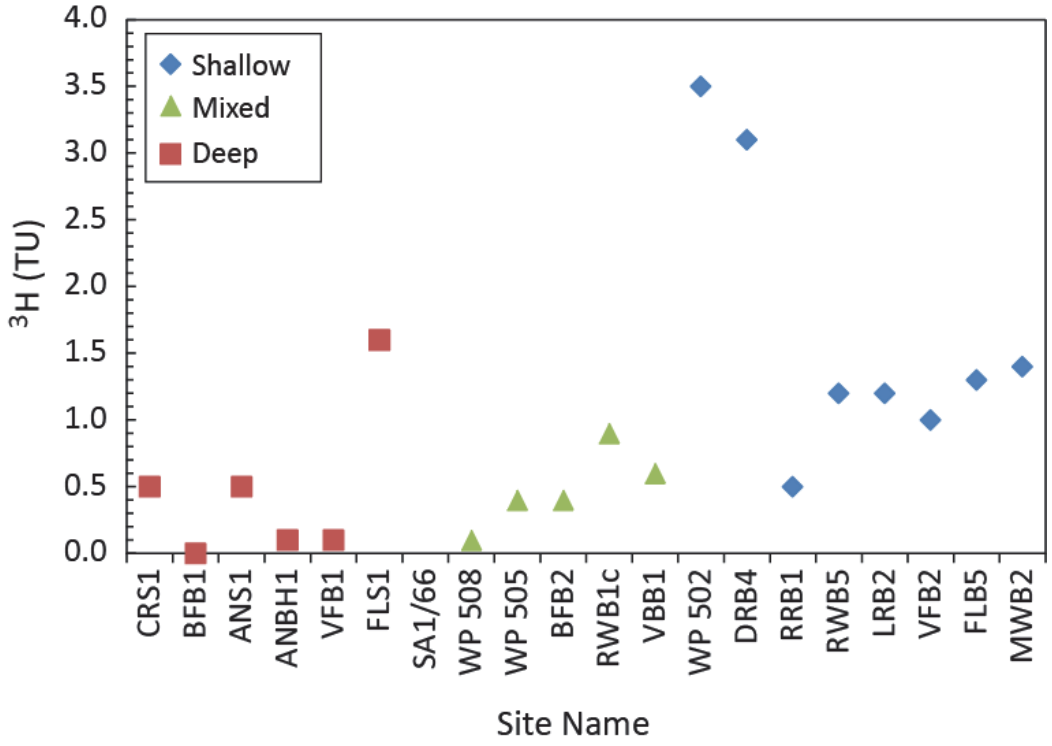

Figure 5.13. Tritium values in groundwater depth groups

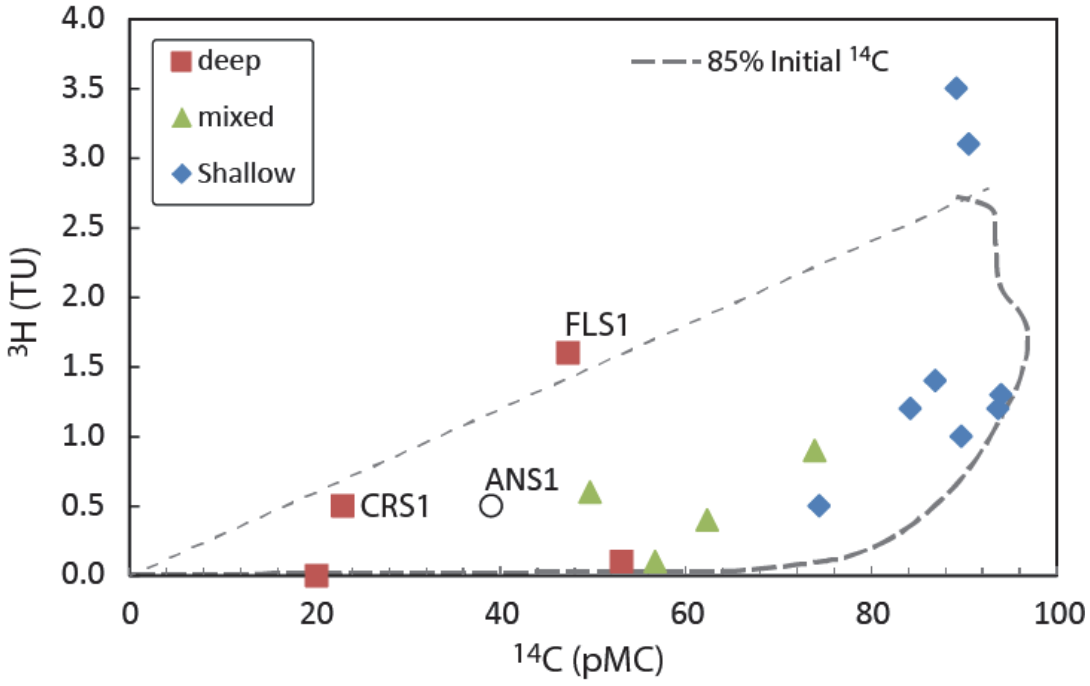

Figure 5.14. ^{3}H as function of ^{14}C for the three groups of samples. The heavy dashed line represents a typical plot of groundwater mixing using an exponential mixing model, calculated from MRT software (Talma and Weaver, 2003). The light dashed line shows one possible mixing line to illustrate how the "anomalous" high ^{3}H can be modeled as two-component mixing of young and old water.

5.2.3 *The stable isotopes of oxygen and hydrogen ($\delta^{18}O$ and $\delta^{2}H$)*

$\delta^{18}O$ values show a good distinction between deep and shallow sites, with some overlap with the mixed group and the shallow group (Fig 5.15). The shallow group with lower temperatures has higher $\delta^{18}O$ content (-4.9 to +0.4 ‰). In contrast, the deep group has lower $\delta^{18}O$ values of between -6.7 and -7.7 ‰. Even ANBH1 and BFB1, with anomalously low temperatures, fall within the low ^{18}O group. The mixed group samples have $\delta^{18}O$ values within a narrow range from -4.9 to -5.7 ‰ which is distinct from the deep group and only very slightly overlaps with the shallow group. One mixed sample, WP502, is an outlier in this case, with the only positive stable isotope ratios of +2.8‰ for $\delta^{2}H$ and +0.4‰ for $\delta^{18}O$.

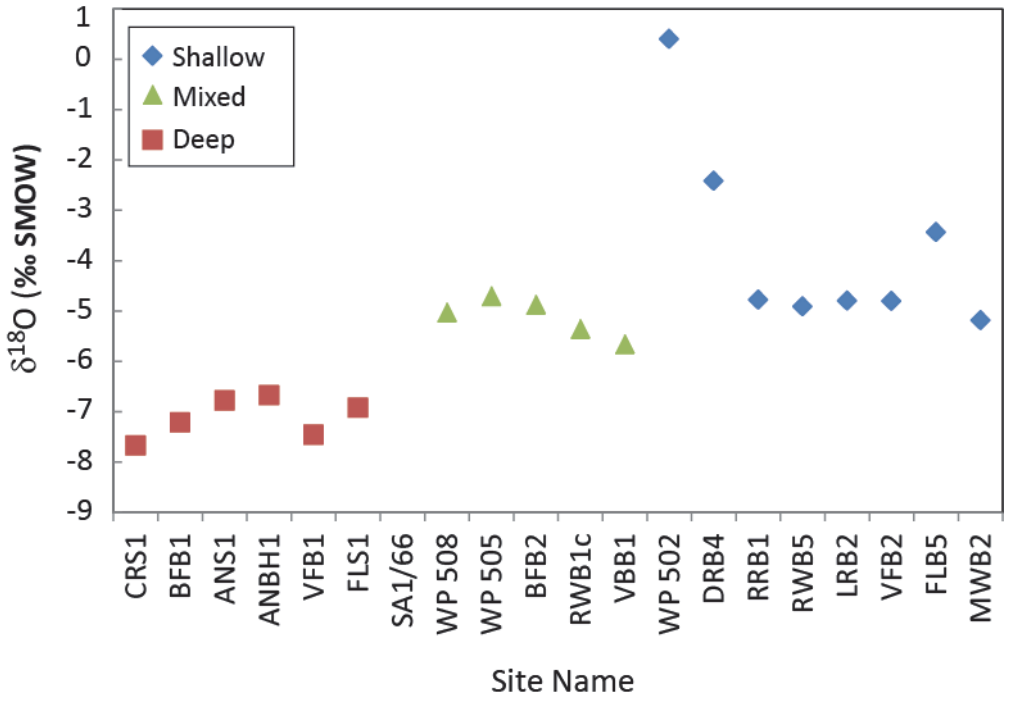

Figure 5.15. $\delta^{18}O$ for the different water type groups

Figure 5.16 presents the relation between $\delta^{2}H$ and $\delta^{18}O$ in all of the groundwater samples. The deep group is depleted in the heavy isotopes with $\delta^{2}H$ and $\delta^{18}O$ around -39 and -7.7‰ respectively. This is characteristic of deep groundwater, as generally heavy rainfall events will result in the infiltration of precipitation depleted in the heavier isotope. The shallow group plots higher up the global meteoric water line (GMWL) with higher $\delta^{2}H$ and $\delta^{18}O$ values: near 0‰ for both isotopes (Figure 5.16). The mixed group plots in between the deep and shallow groups. The relational slope of all the samples (the local meteoric water line: LMWL) is 5.2, compared to the 8 of GMWL, the worldwide reference line). This is quite common for groundwater in southern Africa (van Wyk, 2010; Talma and van Wyk, 2013).

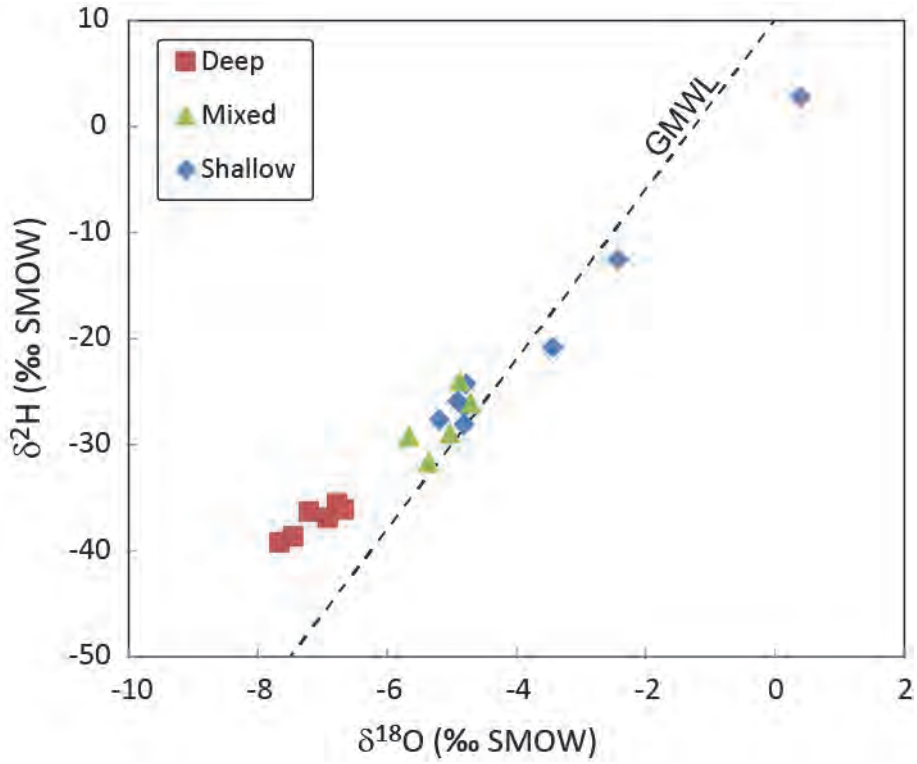

Figure 5.16. $\delta^{18}O$ versus $\delta^{2}H$. The global meteoric water line is plotted on the graph as reference

Similar to the relationship with temperature, there are distinct differences in the different groundwater depth groups between ^{14}C and $\delta^{18}O$ showing a good separation between the three groups (Figure 5.17). The most distinct feature is that the deep groundwater group is clearly differentiated such that the oldest groundwater samples have the lowest $\delta^{18}O$ values. Although not shown here, the relationship between tritium and $\delta^{18}O$ values shows a similar pattern. One sample FLS1 though has an anomalously high tritium value of 1.5 TU and this is possibly due to mixing as indicated in Figure 5.14.

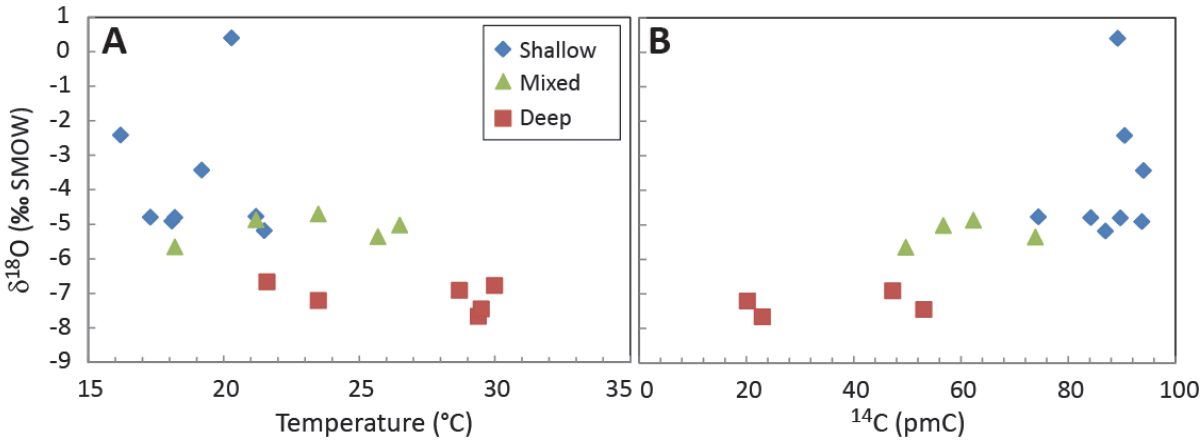

Figure 5.17. $\delta^{18}O$ versus (a) temperature and (b) ^{14}C

5.2.4 *Nitrate (NO_3^-)*

Figure 5.18 presents the nitrate values in the depth groups. Only four of the samples contain any appreciable NO_3^-, all of which are from the shallow group. This is not unexpected as NO_3^- is often elevated in shallow groundwater as a result of anthropogenic factors although natural factors also play a role (Tredoux & Talma, 2006). In older water there is either no nitrogen source or the nitrate has already been removed by bacterial reduction (Heaton et al., 1983). Only half of the samples from the shallow group contain NO_3^-. The other half that do not contain any NO_3^- are WP502, DRB4, RWB5 and MWB2 (although DRB4 did have 1.1 mg NO_3^-/L in the first sampling run). While these sites are situated on farms, these specific boreholes (except for DRB4) are distant from farming and human activities, and this may be the reason for the lack of NO_3^- at these sites.

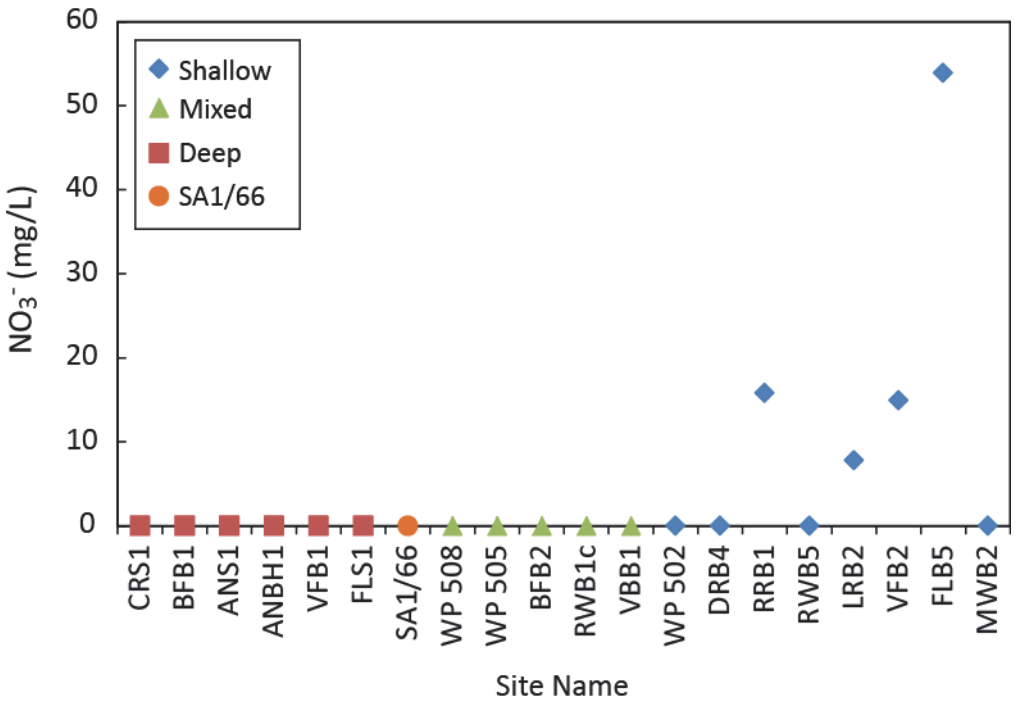

Figure 5.18. Nitrate concentrations in groundwater depth groups

Figure 5.19A presents NO_3^- concentrations versus the temperature of the groundwater, and show that the warmer groundwaters do not contain NO_3^-. Similarly, comparison of NO_3^- concentrations with ^{14}C values indicates that NO_3^- is only present in younger groundwaters with higher ^{14}C content (Figure 5.19B). The disappearance of nitrate from deeper circulating water can only be ascribed to denitrification under reducing conditions in deeper aquifers.

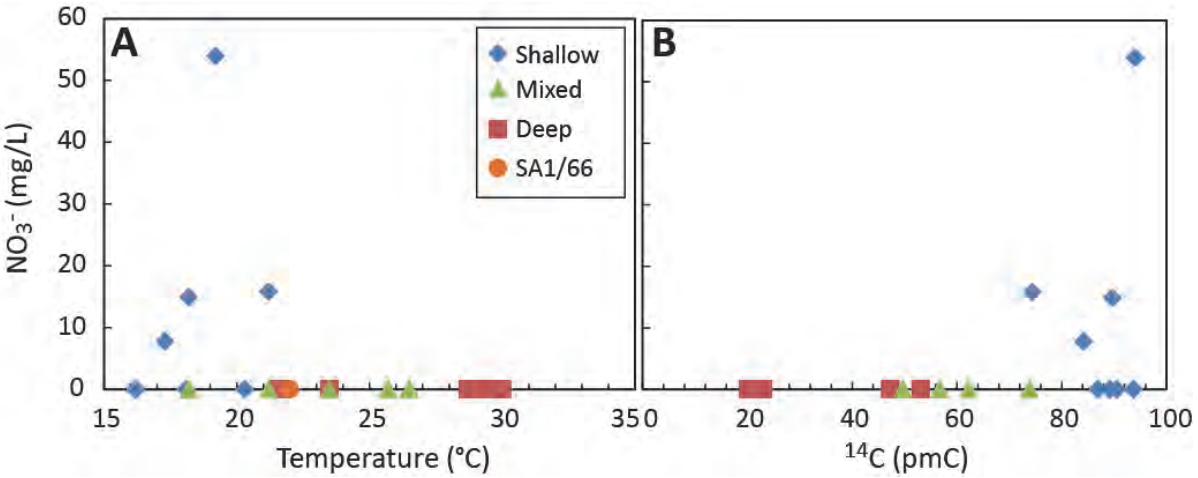

Figure 5.19. NO_3 versus (a) temperature and (b) radiocarbon (^{14}C)

5.2.5 *Fluoride (F^-)*

Deep groundwaters have higher fluoride levels than shallow groundwaters (Figure 5.20). Little to negligible fluoride concentrations (<1.3 mg/L) are present in the shallow groundwater group. Moderate concentrations (2.1-3.7 mg/L) are present in the mixed groundwater group, and relatively high concentrations (3.7-16.1 mg/L) are found in the deep groundwater group.

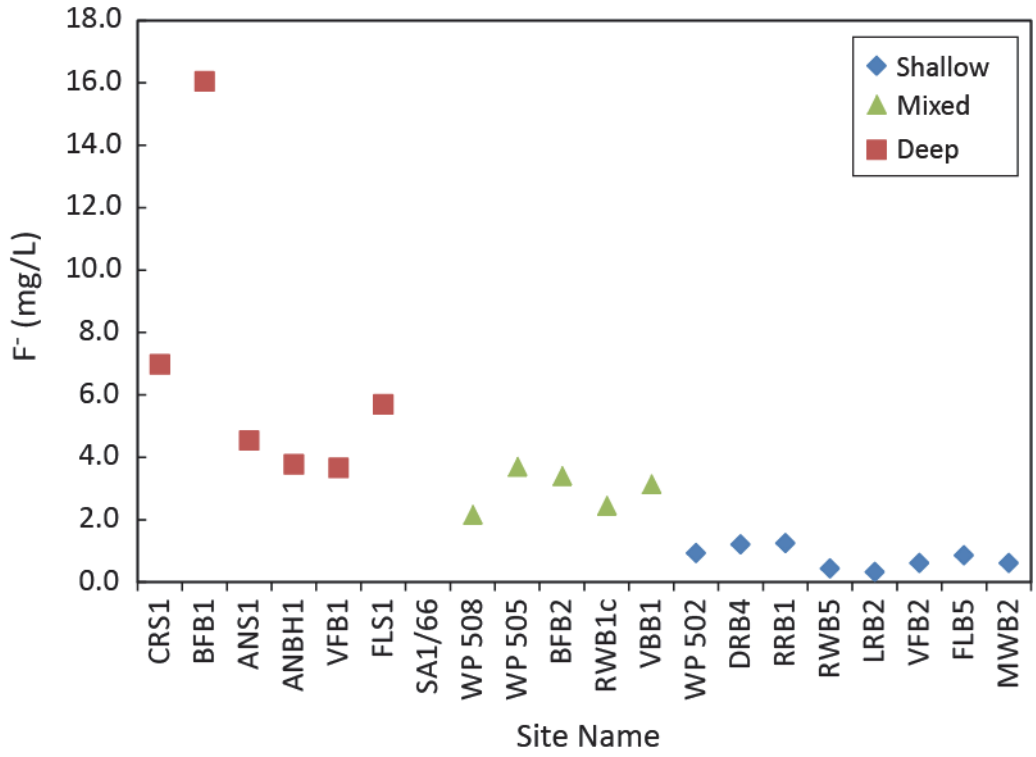

Figure 5.20. Fluoride concentrations in groundwater depth groups

The relationship between fluoride and temperature (Figure 5.21A) supports the interpretation that all low fluoride concentrations are in the cooler (shallow) groundwaters and the higher fluoride concentrations are in the warmer (deep) and mixed groups. Fluoride versus ^{14}C (Figure 5.21B) presents a more consistent trend from high-F/low-^{14}C to low-F/high-^{14}C.

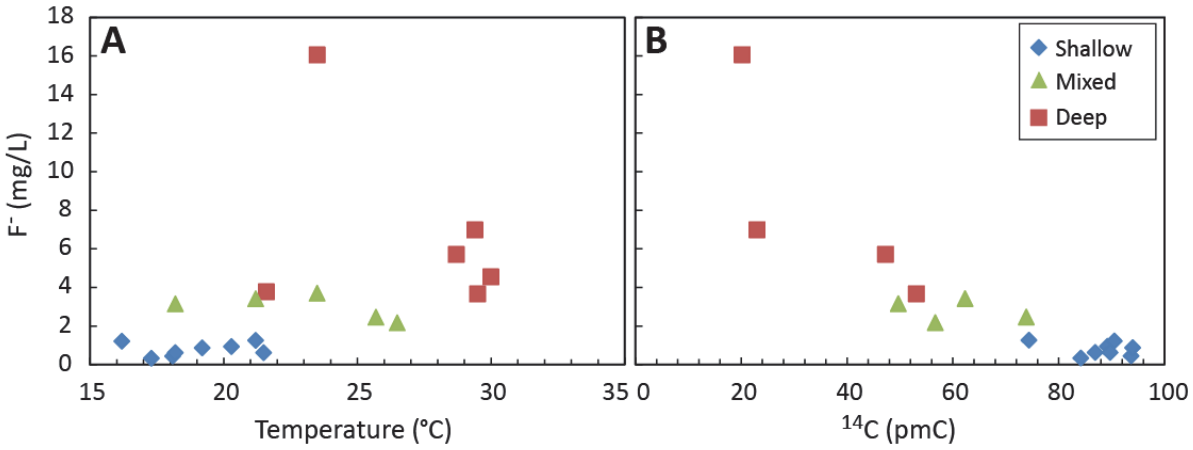

Figure 5.21. Fluoride versus (a) temperature and (b) radiocarbon (^{14}C)

5.2.6 *Lithium (Li^+)*

Figure 5.22 presents lithium (on a log scale) grouped into the three depth categories. A fair correlation exists between low Li in shallow cold groundwater and high Li in deep warm groundwater. However, there is an overlap between the groups and differentiation of deep and shallow groundwater based on Li concentrations alone does not appear to be possible.

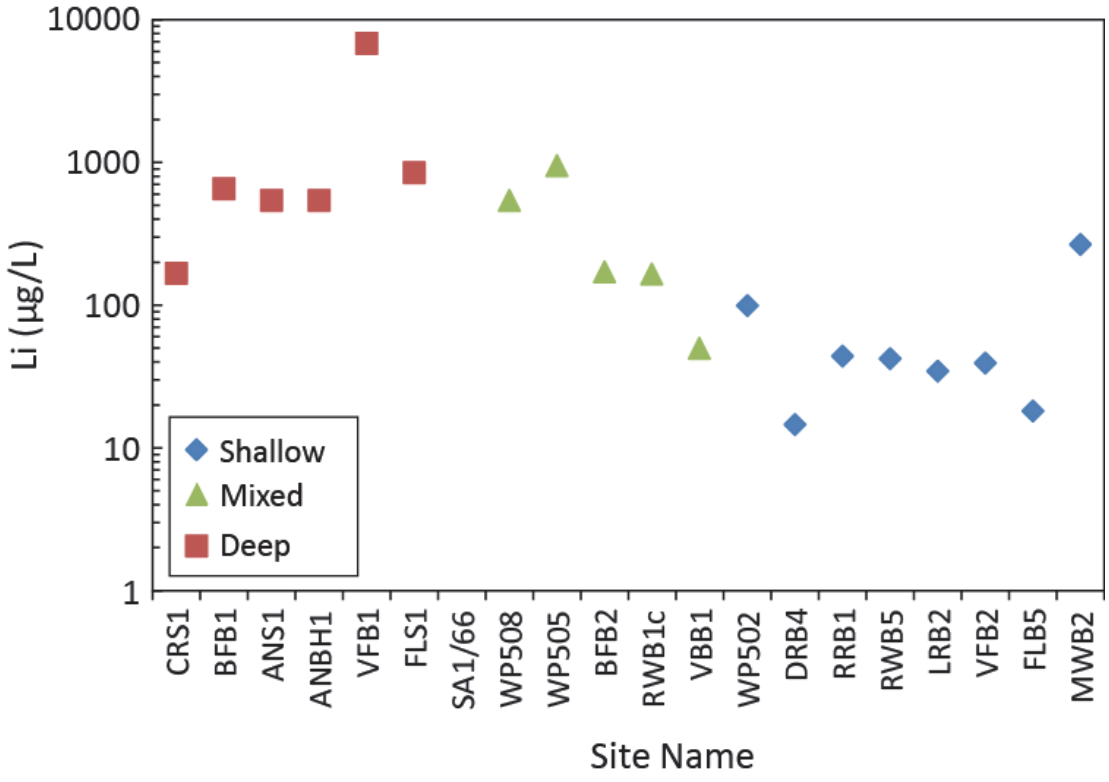

Figure 5.22. Lithium concentrations in the groundwater depth groups

The relationship between lithium and temperature (Figure 5.23A) also supports the interpretation that most low lithium samples belong to the cooler (shallow) groundwaters and the higher lithium concentrations are in the warmer (deep) and mixed groups. Lithium versus ^{14}C (Figure 5.23B) suggests a similar pattern although this is only based on a few samples and with one exception. The young waters appear to distinguish themselves from the deep and mixed samples by having low (< 300 µg/L) lithium levels (although the sample size is very limited).

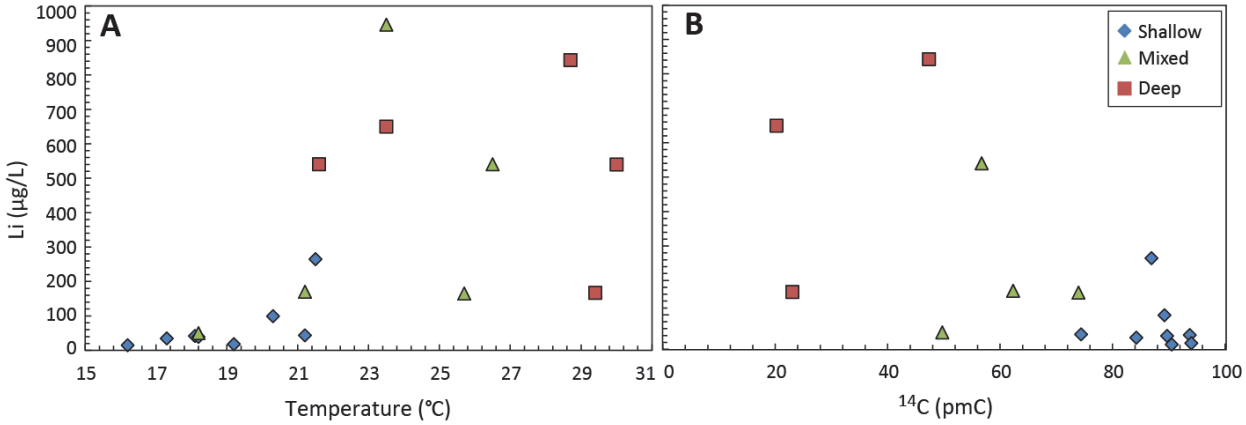

Figure 5.23. Lithium versus (a) temperature and (b) radiocarbon (^{14}C). The Trompsburg sample (VFB1) with high Li content (6583µg/L) is not shown

5.2.7 Sodium (Na^+)

As discussed in Chapter 2, there are good reasons to expect that deeper circulating groundwater should have higher sodium concentrations than shallow water. This appears to be the case for the samples of this study (Figure 5.24A). While the mixed and shallow groups have Na levels below 300 mg/L, the deep group has sodium levels that range between 43 and 2584 mg/l which includes the ranges of the mixed and shallow waters. Trompsburg deep (VFB1) and Merweville deep (SA1/66) have exceptionally high sodium levels (Fig 5.24A).

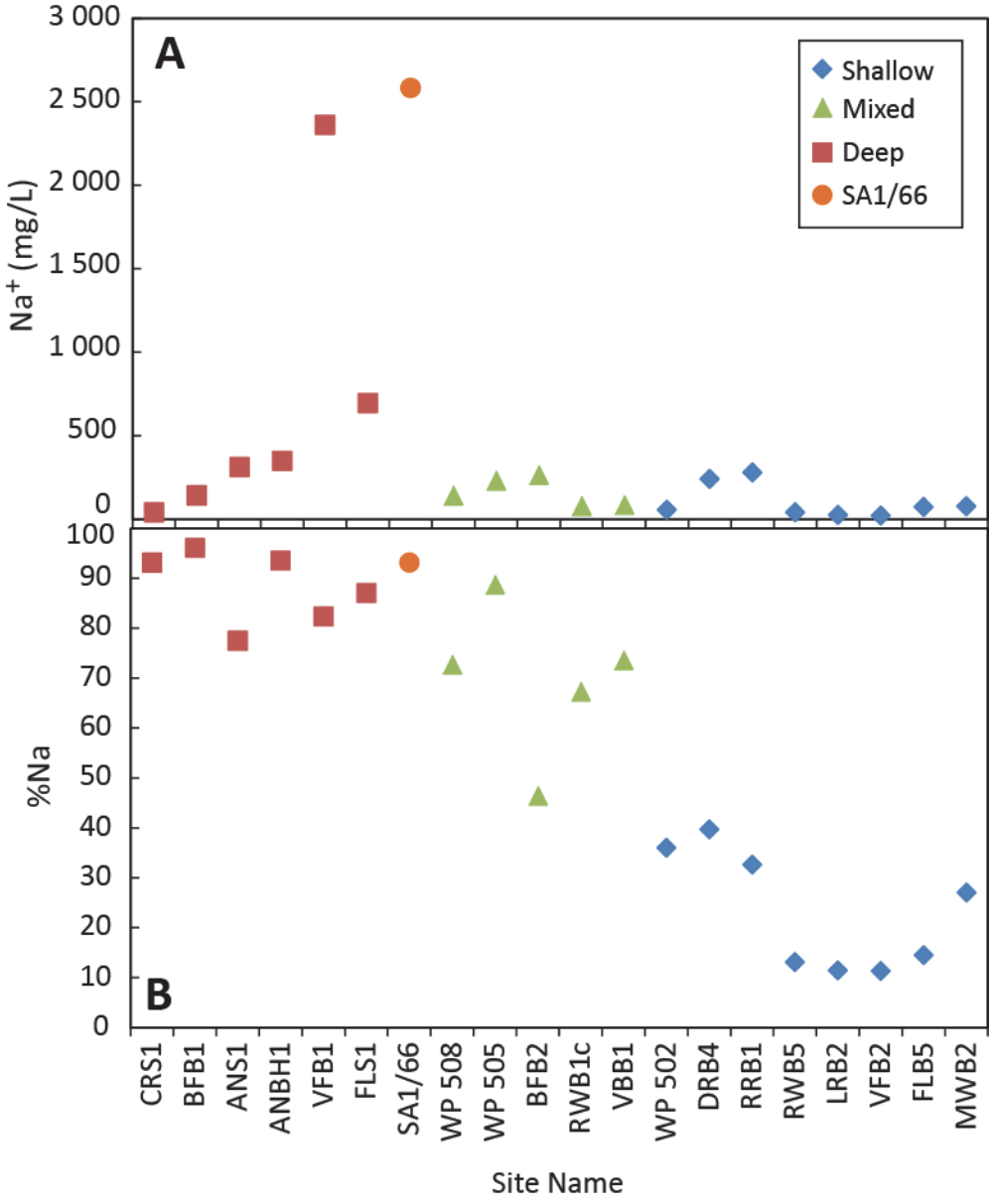

Figure 5.24. Sodium (Na) in the groundwater depth groups; expressed as (A) concentration in mg/L, and (B) %Na (of the total cations).

A plot of **relative** sodium concentration (by meq/L) provides a better way of expressing the chemical evolution of groundwater with time (Tredoux and Kirchner, 1981). %Na (+K) is one of the axes of the diamond-shaped field in a Piper plot and is frequently used as an indicator of residence time (see examples in Appendix 3). Figure 5.24B presents sodium as percentage of the cation total (in meq/L). Using %Na there is a clear separation between the different water types with the shallow group having low %Na and the deep group having high %Na. There is nevertheless still some overlap between the groups. The relationship between

%Na and the other depth indicators temperature and ^{14}C shows similar patterns (Figures 5.25 A & B). While the trend is as expected, there are nevertheless some overlaps between the deep and mixed groups.

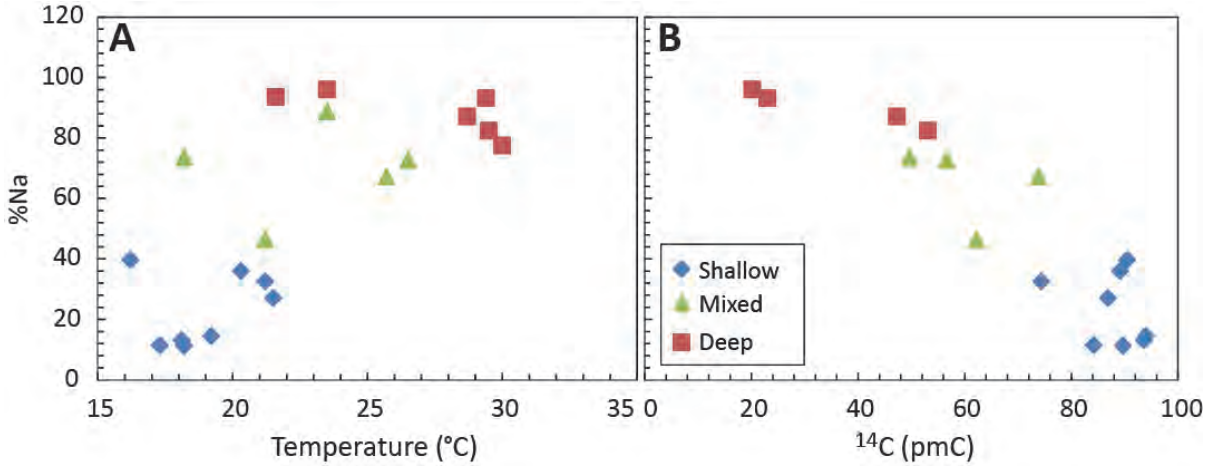

Figure 5.25. %Na with (a) temperature and (b) ^{14}C

The origin of sodium in the water is sufficiently explained by the correlation of the Na/Cl ratio (mol/mol) in the samples (Figure 5.26). At low salinities there is an excess Na over Cl. Increased chloride leads to Na/Cl ratios closer to 1 indicating that NaCl dissolution is the principal process affecting these two parameters. Sodium increase due to ion exchange of Ca^{2+} and Mg^{2+} with aquifer material does not appear to be important. Seawater as a NaCl source can be excluded since that would produce a lower Na/Cl ratio (0.85: Weaver et al., 1999).

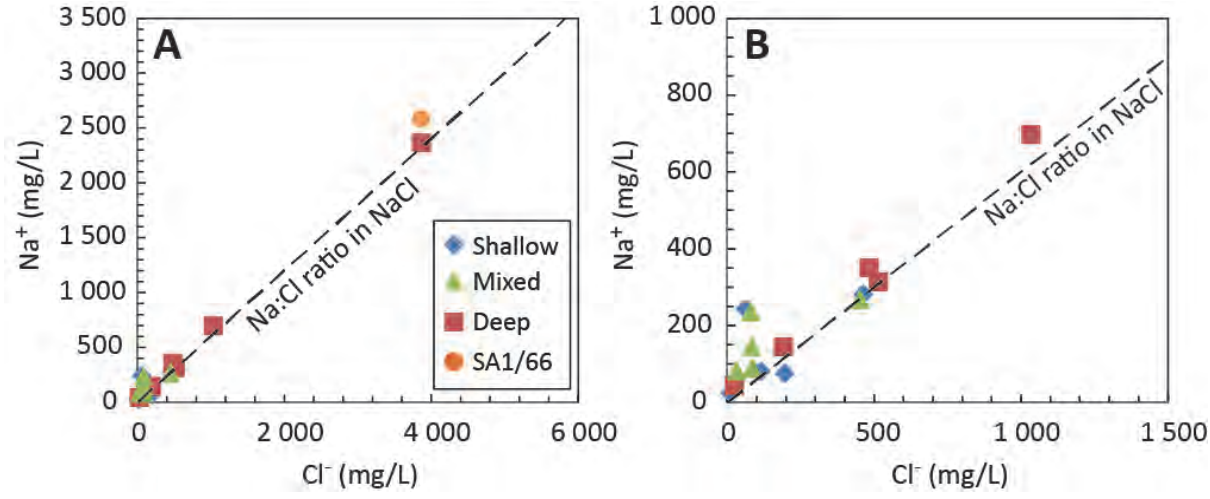

Figure 5.26. Relationship between Na and Cl; note the difference in scale between A and B

5.2.8 *Magnesium (Mg^{2+})*

Magnesium concentrations, grouped into the depth categories, are shown in Figure 5.27A and against ^{14}C in Figure 5.27B. Both plots show that Mg concentrations are negligible for the deep groundwater sites, whereas both the mixed and shallow groundwater sites have variable higher Mg concentrations. However, the spread in Mg concentrations for the shallow group (10.1-72.6 mg/L), is so wide however, that the data tends to suggest even a fairly low concentration of Mg (e.g. 10 mg/L) is sufficiently indicative of deep groundwater. The only deep site that has a slightly higher Mg concentration is the deep Soekor borehole at Merweville (SA1/66) with of 7.5 mg/L magnesium. The rest are all zero or below 1.3 mg/L. The mixed samples also show low magnesium. BFB2 is the exception here with low ^{14}C, but high Mg.

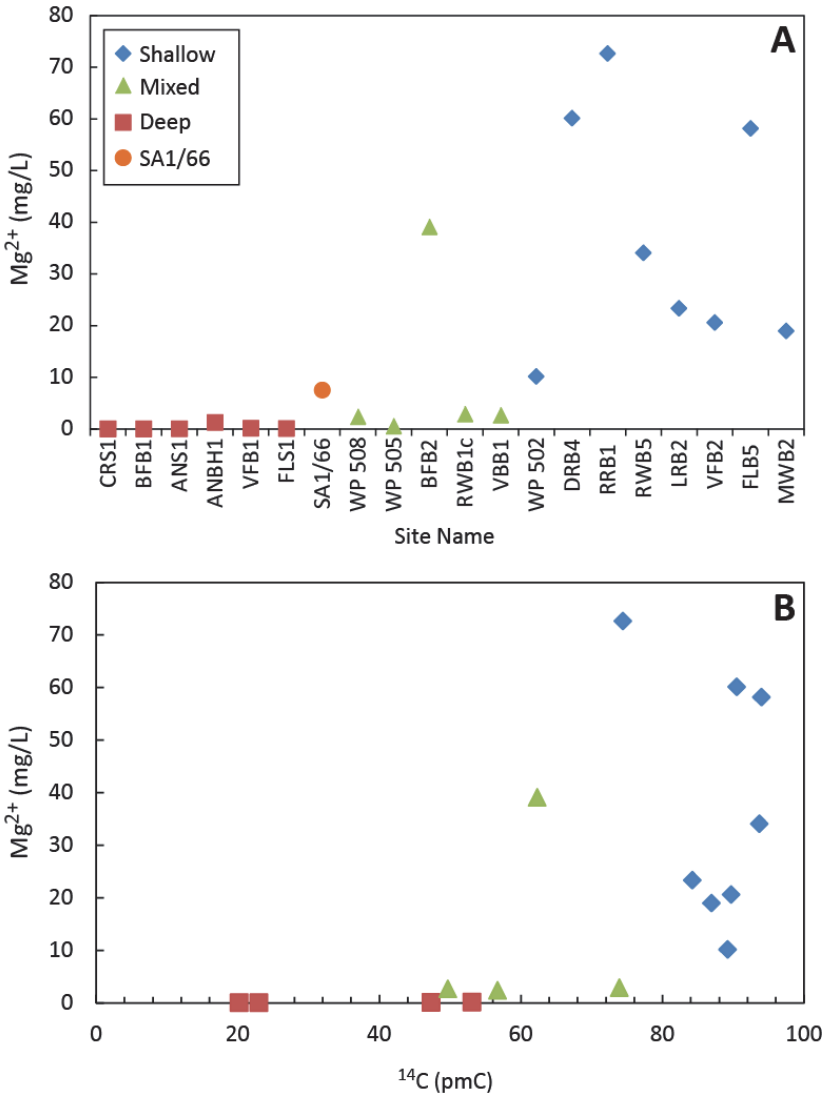

Figure 5.27. (A) Magnesium concentrations plotted in groundwater depth groups; and (B) against ^{14}C

5.2.9 Chloride and its isotopes

The distribution of chloride in the three depth groups is rather scattered (Fig 5.28A). While the highest chloride levels are found in the deep water (up to nearly 4000 mg/L), there are an equal number of samples having Cl within the range of shallow and mixed water types. The ^{36}Cl concentrations show, with the exception of the Tromspburg deep borehole (VFB1), a general pattern of low values for deep groundwater and slightly higher values for shallow groundwater (Figure 5.28B). This is consistent with the model that ^{36}Cl concentrations are high in shallow water and decay to lower levels in deep water. However, significant overlap exists between these groups and the mixed groundwater group cannot be distinguished from either the shallow or the deep group. When however, ^{36}Cl is expressed as the ratio of $^{36}Cl/Cl$, a clear differentiation of the deep group from the other groups emerges (Fig 3.28C). Deep water has low ratios (20-126 $x10^{-15}$), and the shallow group has considerably higher and more variable ratios (112-2294 $x10^{-15}$). The mixed group is in between, and while there is some overlap between the mixed and shallow groups, there is a good distinction between the deep group and the shallow/mixed groups (Fig 5.28C). RRB1 is anomalous in this pattern in that it is a shallow sample but has a very low $^{36}Cl/Cl$ ratio of 113 ($x10^{-15}$) more consistent with the deep group ratios.

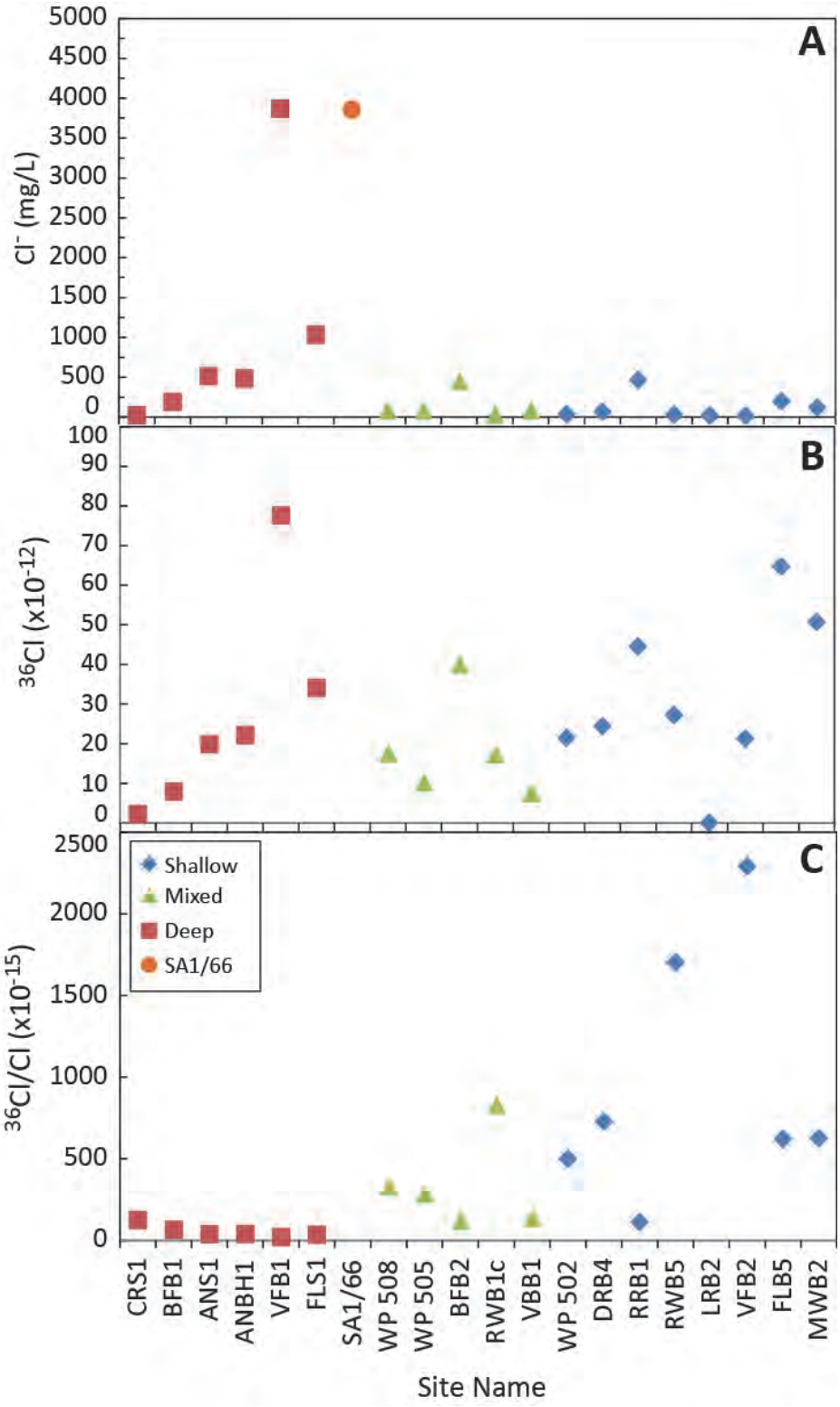

Figure 5.28. (a) ^{36}Cl values, (b) stable chloride (Cl) and (c) $^{36}Cl/Cl$ ratios for the different groundwater depth groups

The robustness of the $^{36}Cl/Cl$ ratio as a means of differentiating the deep group from the shallow group is further emphasized by plotting this ratio against temperature (Fig 5.29A) and ^{14}C (Figure 5.29B). In both these plots, the deep groundwater group is distinct from both the mixed and the shallow groups. What is interesting from Figure 5.29A is how clearly the potential problems associated with temperature stand out. The two boreholes (BFB1 and ANBH1) grouped as deep groundwater in spite of their low temperatures (23.5°C and 21.6°C respectively), clearly look to belong to the deep group (Figure 5.29B).

One further aspect that must be addressed with the ^{36}Cl isotope system is the reason for expressing it as a $^{36}Cl/Cl^-$ ratio. This is to account for increasing Cl^- with "aging" of groundwater. Figure 5.30 shows the $^{36}Cl/Cl^-$ ratio versus Cl^- (mg/L) and indicates that there is a strong negative relationship between these parameters. This is expected since Cl^- is likely added to groundwater at a rate that is considerably faster than the decay of ^{36}Cl (half-life of 301 000 yrs). Although the mixed group is not so clearly defined, the shallow and the deep groups define two well constrained arrays with very similar slopes but different intercepts. This pattern suggests that the data are robust and not easily reset or disturbed and that the two arrays define two different water compositions as is being postulated. However, there is almost no other $^{36}Cl/Cl^-$ data in South Africa against which any comparisons could be made and further work needs to be done to fully understand this part of the dataset.

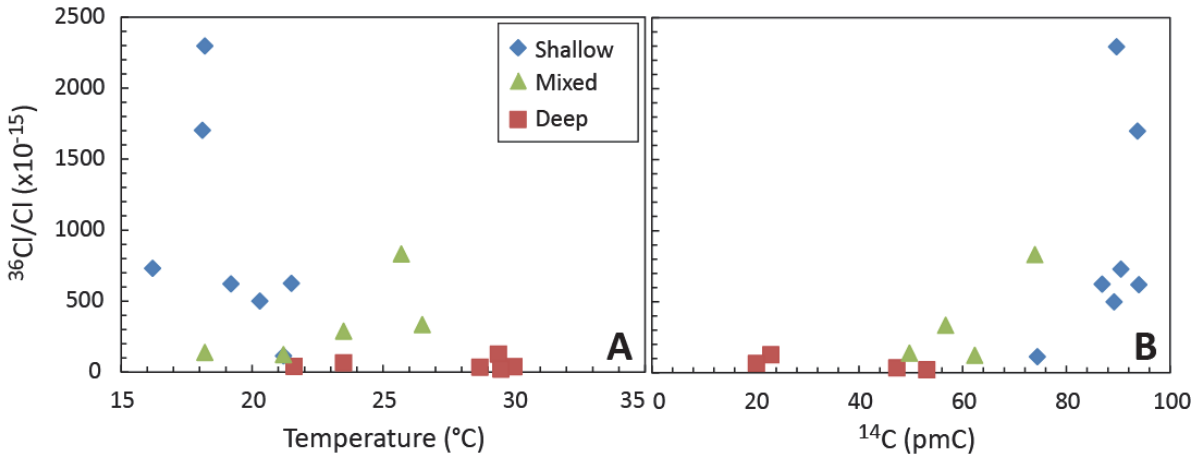

Figure 5.29. $^{36}Cl/Cl$- versus (a) temperature and (b) ^{14}C

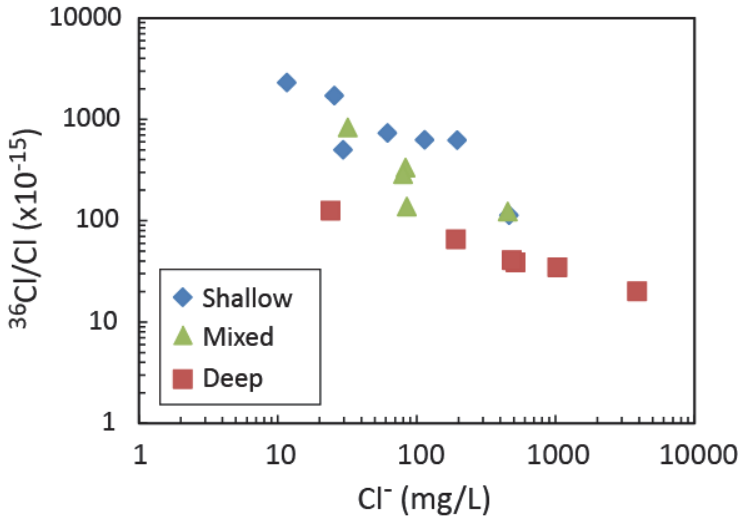

Figure 5.30. $^{36}Cl/Cl$ ratio versus Cl^-

5.2.10 *Strontium Isotopes*

$^{87}Sr/^{86}Sr$ ratios for all the groundwater samples are fairly consistent varying between 0.70887 and 0.71206 with two radiogenic outliers at 0.77719 (VFB1) and 0.75392 (FLS1). These outliers are the two northern-most sites in the study area (Florisbad and Trompsburg), where the base of the Karoo Basin shallows to the north (these two sites are west of the Drakensberg Mountains/Lesotho in Figures 3.1 and 3.2). While this confirms that the water from the deep Trompsburg borehole VFB1 originates, at least partly, from the basement gneisses where water was struck. it also suggests that at Florisbad, the spring water may have a very deep flow path and be in contact with basement rocks. The similarity in $^{87}Sr/^{86}Sr$ ratios for the bulk of the samples suggests that this determinand may not be a good depth indicator for much of the Karoo Basin. It may however, be of value for assessing where boreholes are intersecting groundwater that has interacted with basement rocks.

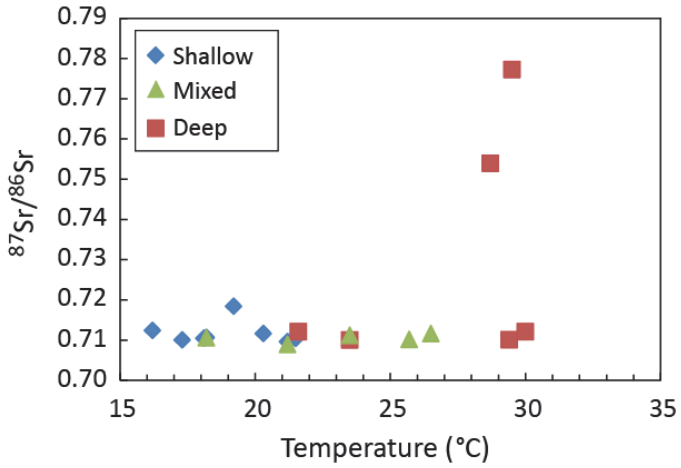

Figure 5.31. $^{87}Sr/^{86}Sr$ versus temperature

5.2.11 Boron and its isotopes

Boron concentrations and $\delta^{11}B$ isotope ratios appear to be differentiated between the deep and shallow sites in different ways. There is significant overlap between the three classified water types (Figure 5.32). The deep group has a wide spread in boron concentration from 473 to >3 000 µg/L. The shallow group contains the lowest B concentrations of between 42-753 µg/L. The mixed group more or less coincides with the shallow group (333-760 µg/L). Both shallow and mixed groups overlap with the deep group. The two deep boreholes (Trompsburg's VFB1 and Merweville's SA1/66) have the highest values, both being >3 000 µg/L).

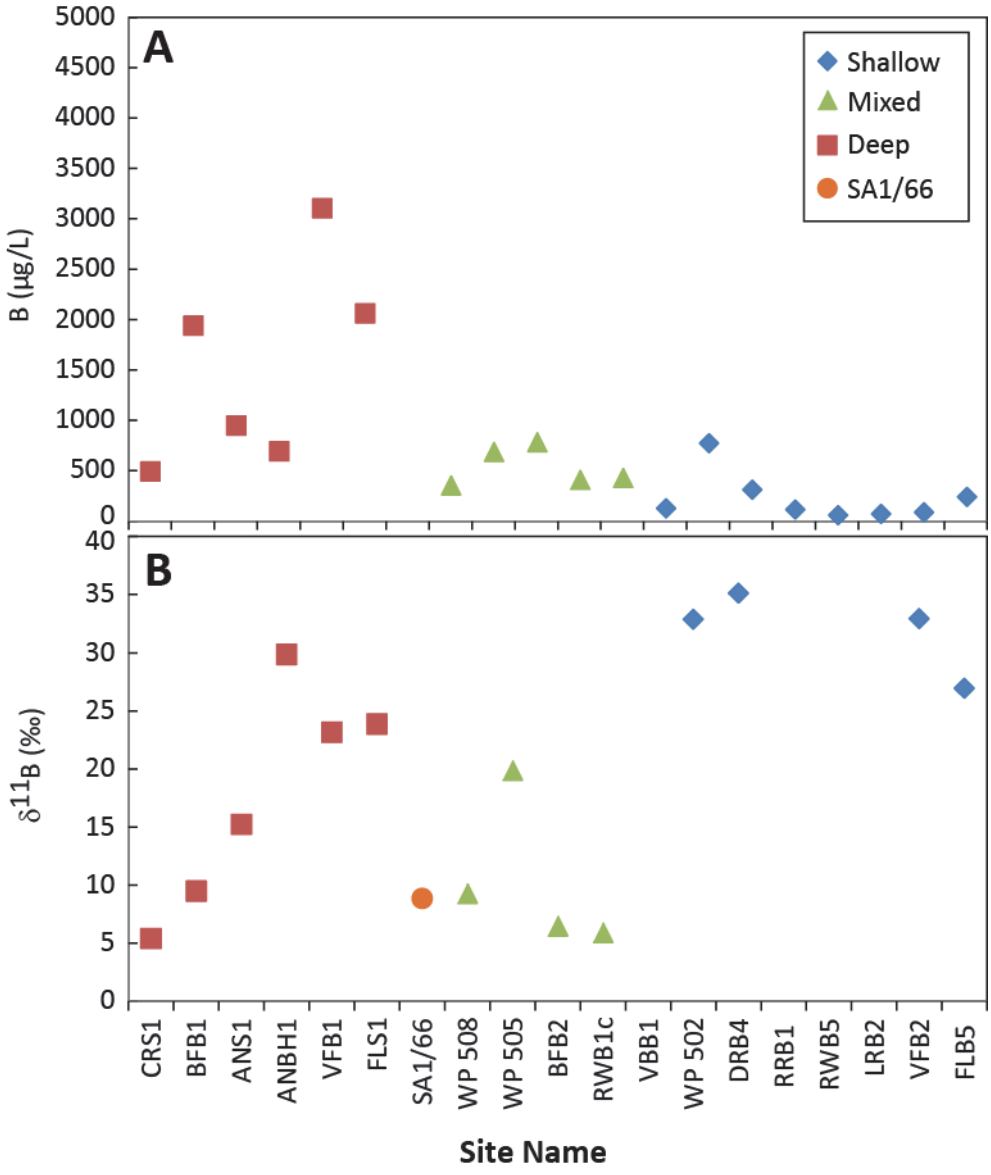

Figure 5.32. Boron concentrations (a) and $\delta^{11}B$ ratios (b) in groundwater depth groups. The boron value of >5 000 µg/L for the Soekor borehole water (SA1/66) is not shown.

$\delta^{11}B$ ratios show a different pattern to that of boron (Figure 5.32B). The shallow sites have high $\delta^{11}B$ ratios between +27 and +35 ‰, whereas the deep and mixed sites are both between +5 and +30 ‰. Figure 5.33 shows boron concentration and $\delta^{11}B$ ratios against temperature and ^{14}C. Although the correlation between $\delta^{11}B$ ratios and temperature is poor (Figure 5.33 A & C) there is a weak correlation between B concentration and temperature (Figure 5.33 B & D) consistent with boron being higher in the deep sites. This is supported by correlations with ^{14}C values, where high B concentrations and low $\delta^{11}B$ ratios are correlated with low ^{14}C values although again the mixed group overlaps significantly with the deep group.

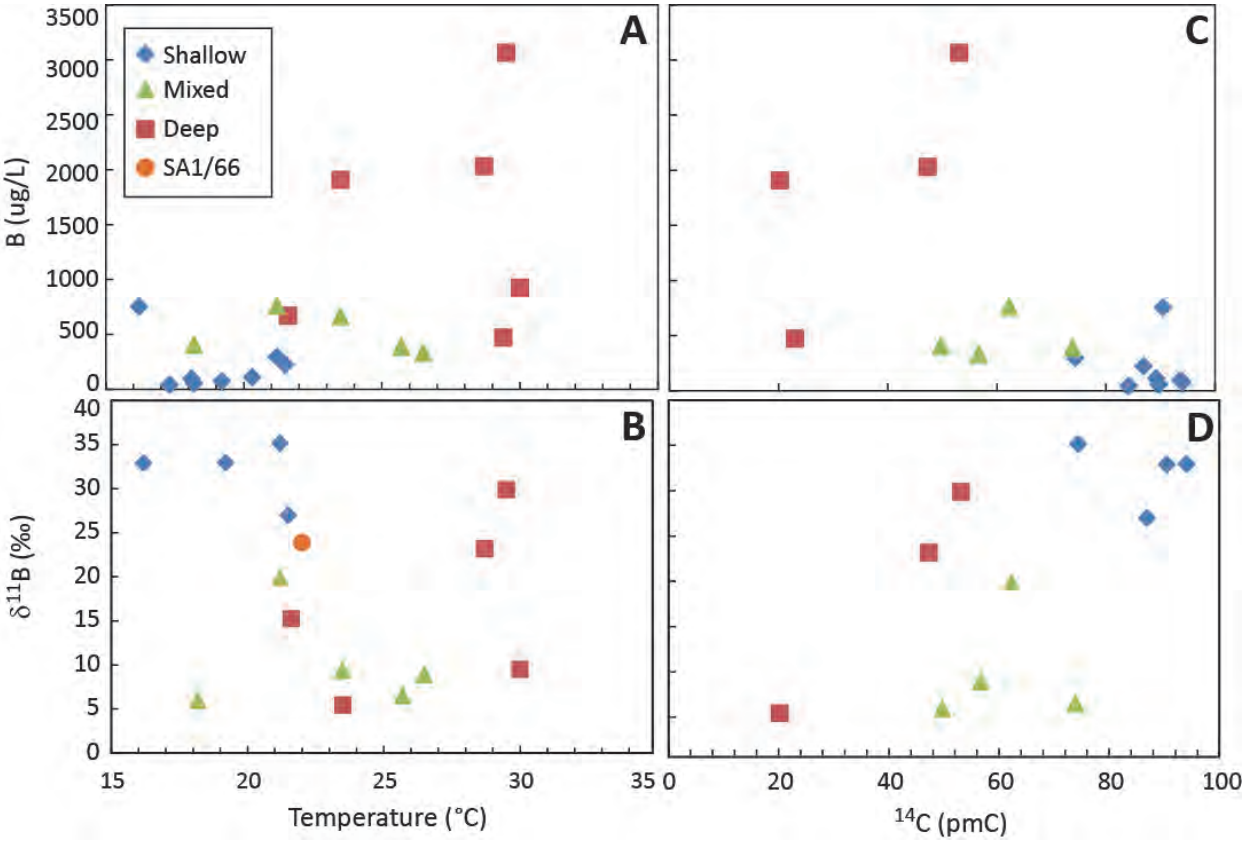

Figure 5.33. (A): Boron concentration vs temperature; (B) $\delta^{11}B$ vs temperature; (C) boron vs ^{14}C and (D) $\delta^{11}B$ ratio vs ^{14}C.

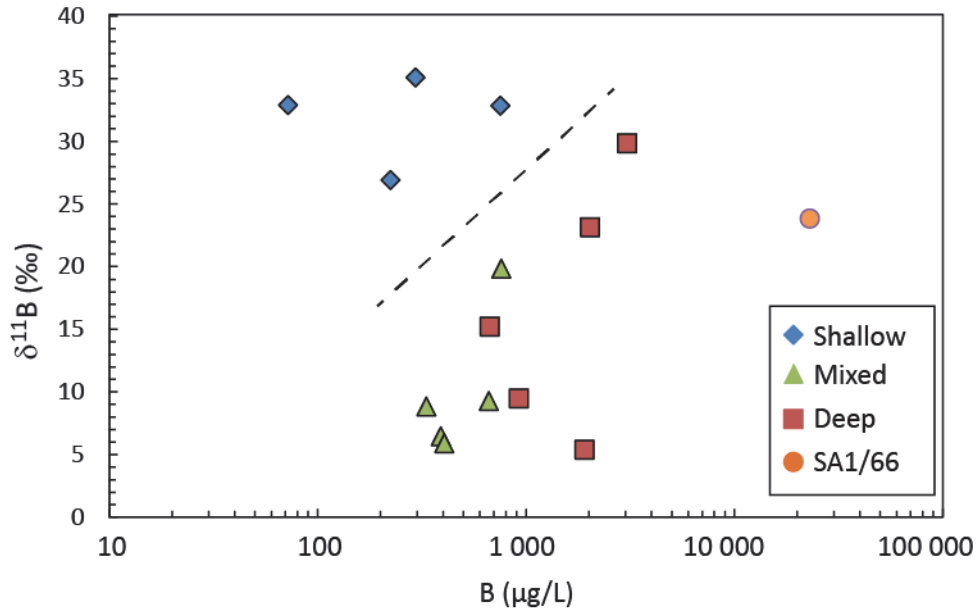

Figure 5.34. $\delta^{11}B$ versus boron concentration

Plotting $\delta^{11}B$ ratios vs B concentrations significantly improves the definition of shallow water sites from the other sites (Figure 5.34). The four shallow groundwater sites plot at high $\delta^{11}B$ ratios and low B concentrations and are distinct from the mixed and deep groundwater groups which plot at low $\delta^{11}B$ ratios and high B concentrations.

5.2.12 Carbon-13 ($\delta^{13}C$)

Carbon isotope ratios for the total inorganic carbon content are expressed as $\delta^{13}C_{\text{-TIC}}$ values. For the groundwater samples examined in this study, the shallow and mixed samples had a relatively narrow range of values (Figure 5.35). The mixed sites had the narrowest range between -15 and -11 ‰, while the shallow sites range between -14 to -5 ‰. These ranges showed little variation with temperature but a slight decrease, when plotted against ^{14}C, from the shallow to the mixed (Figure 5.35). However, the deep sites recorded a significant variation in $\delta^{13}C_{\text{-TIC}}$ values from -26.0 to +5 ‰ making correlation with temperature and ^{14}C impossible. The significant variation in the $\delta^{13}C_{\text{-TIC}}$ values could imply that they represent different aquifer systems with different $\delta^{13}C_{\text{-TIC}}$ ratios. Earlier work in the Venterstad area yielded a much smaller range of $\delta^{13}C_{\text{-TIC}}$ values (-17 – 5 ‰) from 25 samples including a number of deep samples with ^{14}C as low as 47 pmC (Vogel et al., 1980).

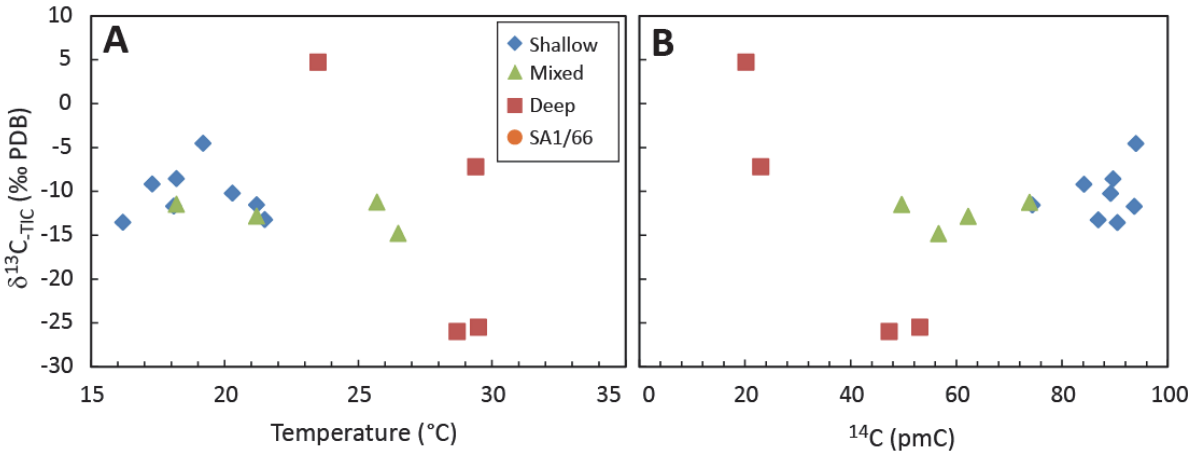

Figure 5.35. $\delta^{13}C$ values for the total inorganic carbon (TIC) in the groundwater samples expressed as a function of (a) temperature and (b) radiocarbon (^{14}C)

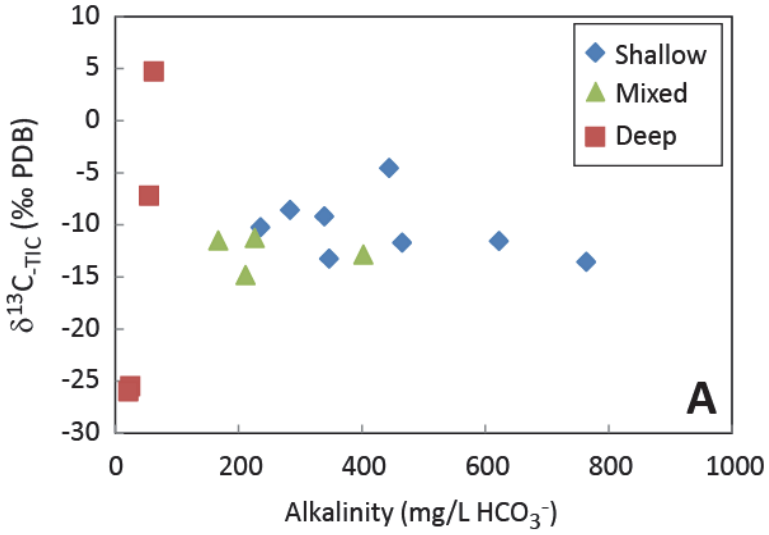

Figure 5.36. A plot of $\delta^{13}C_{-TIC}$ against alkalinity (in mg HCO_3^-/L)

5.2.13 Vanadium

Vanadium is present in significantly higher concentrations in the shallow group when compared with the intermediate and deep groups (Figure 5.37). The shallow group has vanadium concentrations of between 0.6-93 µg/L, while the mixed and deep groups contain negligible vanadium concentrations (<0.5 µg/L). In all cases except three, the shallow low-vanadium waters are at least an order of magnitude greater than the mixed or deep group values. From this data it appears as if vanadium is a good indicator of shallow groundwater while the deep and mixed waters are not differentiated (Figures 5.37 and 5.38). The two outliers in each group are Merweville's shallow sample MWB2 (0.6 µg/L) and Cradock's deep sample CRS1 (0.5 µg/L).

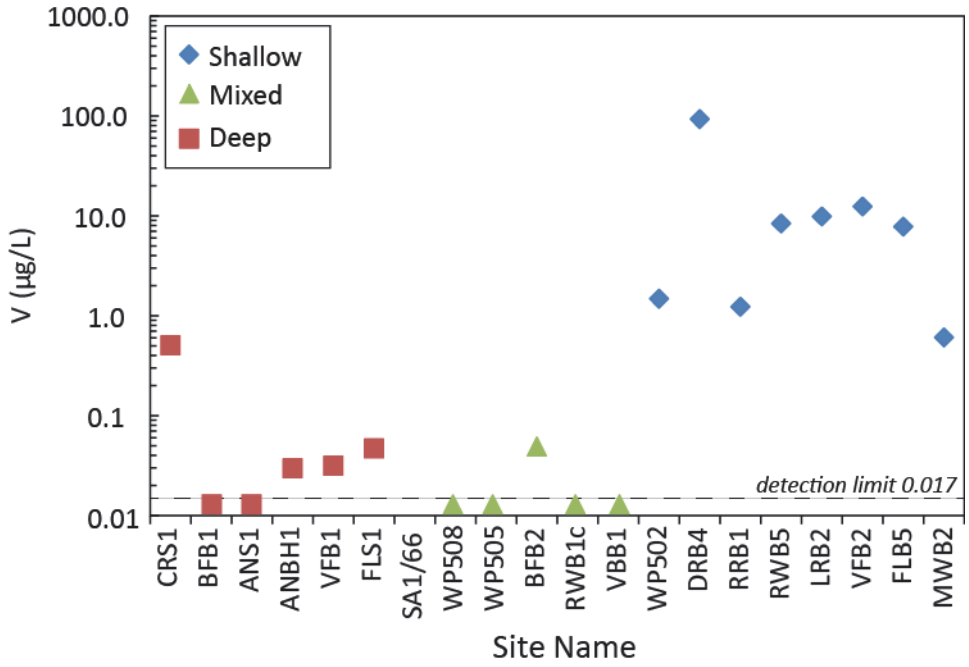

Figure 5.37. Vanadium concentrations in the groundwater depth groups (values below detection limits have been included)

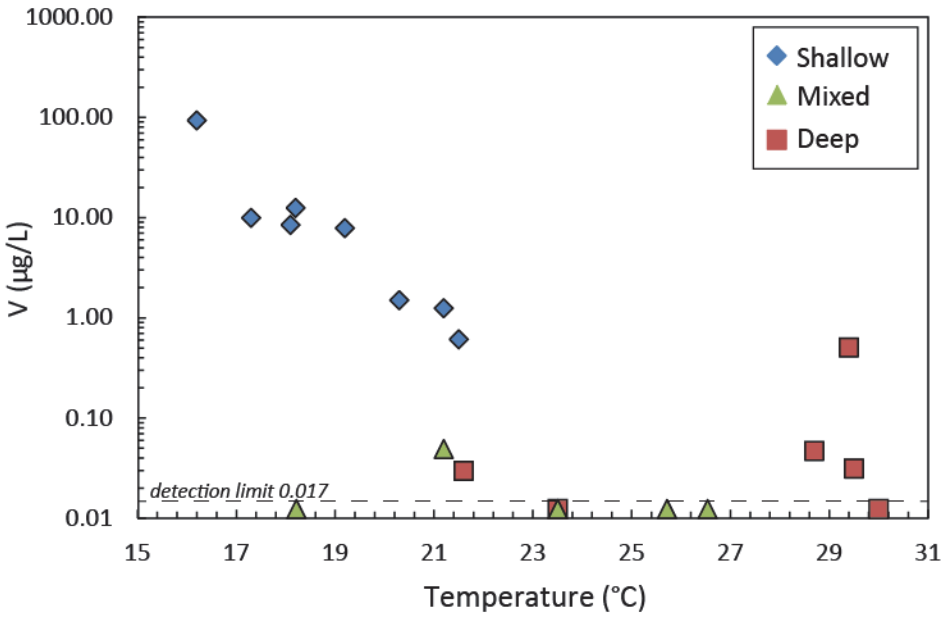

Figure 5.38. Plot of vanadium versus temperature (values below detection limits have been included)

5.2.14 Uranium

Like vanadium, uranium is present in significantly higher concentrations in the shallow group when compared with the mixed and deep group (Figure 5.39). Uranium concentrations for

the shallow group range between 2 and 41 µg/L, while the deep and mixed groups contain less than 1.4 µg/L uranium. This suggests that the presence of uranium is also a good indicator of shallow groundwater but does not distinguish between the deep and mixed water groups. Uranium is less soluble in reduced water with low carbonate content and high pH (Fröhlich, 2013) and therefore uranium levels in old (anoxic) groundwater are expected to be low., In this study, the uranium content of groundwater is positively correlated with alkalinity and ^{14}C, consistent with this premise (Figure 5.40).

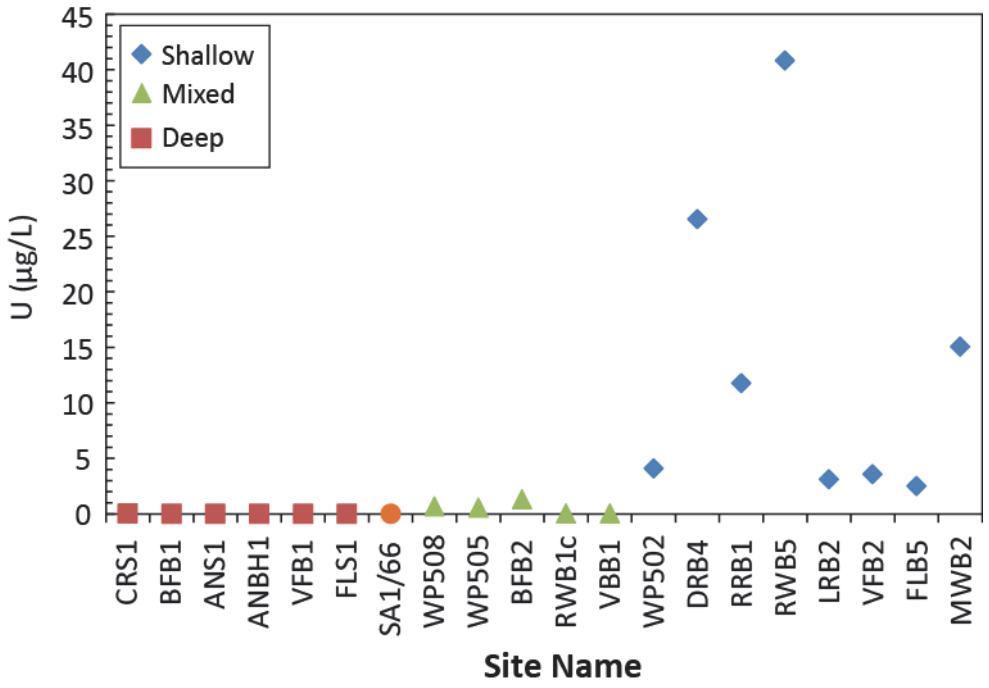

Figure 5.39. Uranium concentrations in the groundwater depth groups

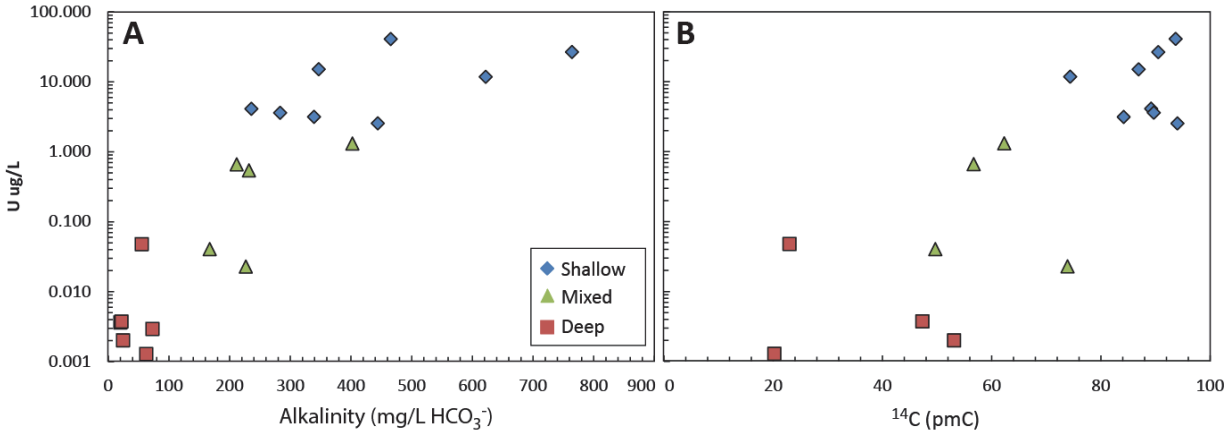

Figure 5.40. Uranium concentration as a function of (A) alkalinity and (B) radiocarbon (^{14}C). Note that in figure A the two deep sites ANS1 & FLS1 appear as one red square as their values are almost identical (~0.004 µg/L U & ~20 mg/L HCO_3-).

5.2.15 Radon (^{222}Rn)

Figure 5.41 shows a general pattern of low radon levels for deep and some of the mixed samples, and high values for shallow samples. Samples from the deep group have low ^{222}Rn activities (1.3-58 Bq/L), the mixed group have moderate values (1-21 Bq/L), and the shallow group generally has the highest values (14-163 Bq/L). The anomalous high Rn value from what is presumed to be a deep groundwater source at the Aliwal North Farm borehole (ANBH1), 1.8 km from the Aliwal North spa (ANS1), can be explained as spring water that found its way to this borehole, in the process picking up radon from the aquifer, losing H_2S and lowering pH. No ^{14}C is available from this borehole.

The remaining samples show a fairly good correlation between radon and ^{14}C (Figure 5.42). Due to the short half-life of radon (3.8 days), it can be expected that radon will only be present in water that has recently been in contact with its mother isotope (radium) (Hobbs et al., 2010) and therefore only exist in shallow and possibly mixed groundwater. Assuming the deep groundwater is old, the Rn will have decayed sufficiently resulting in very low levels.

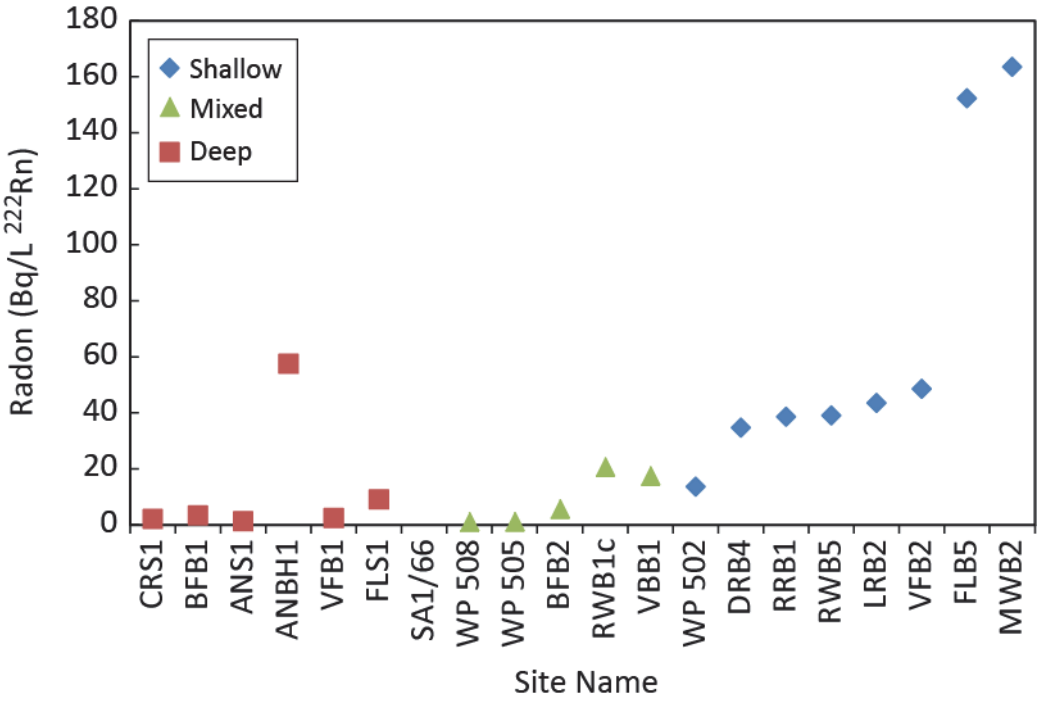

Figure 5.41. Radon (^{222}Rn) activities in the groundwater depth groups

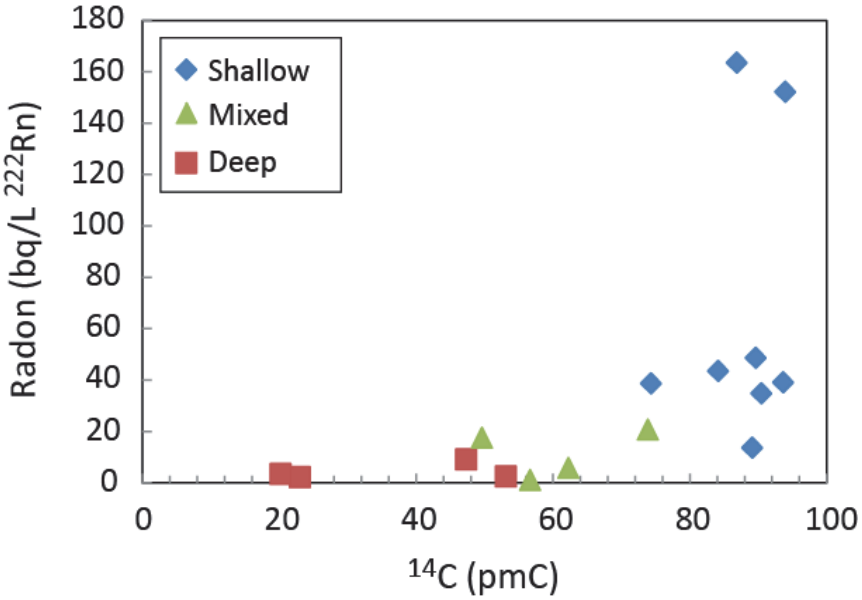

Figure 5.42. Radon (^{222}Rn) versus radiocarbon (^{14}C)

5.2.16 Alkalinity

The alkalinity values show clear differences between the shallow, mixed and deep groups (Figure 5.43). The shallow groundwater sites have the highest alkalinities of between 236-764 mg/L HCO_3^-, whereas the deep groundwater sites have substantially lower alkalinities of between 20-228 mg/L HCO_3^-. The mixed samples have moderate alkalinities of between 167-403 mg/L HCO_3^- and overlaps with the shallow group. The mixed group is distinct from the deep group (apart from the deep Soekor borehole SA1/66 at Merweville).

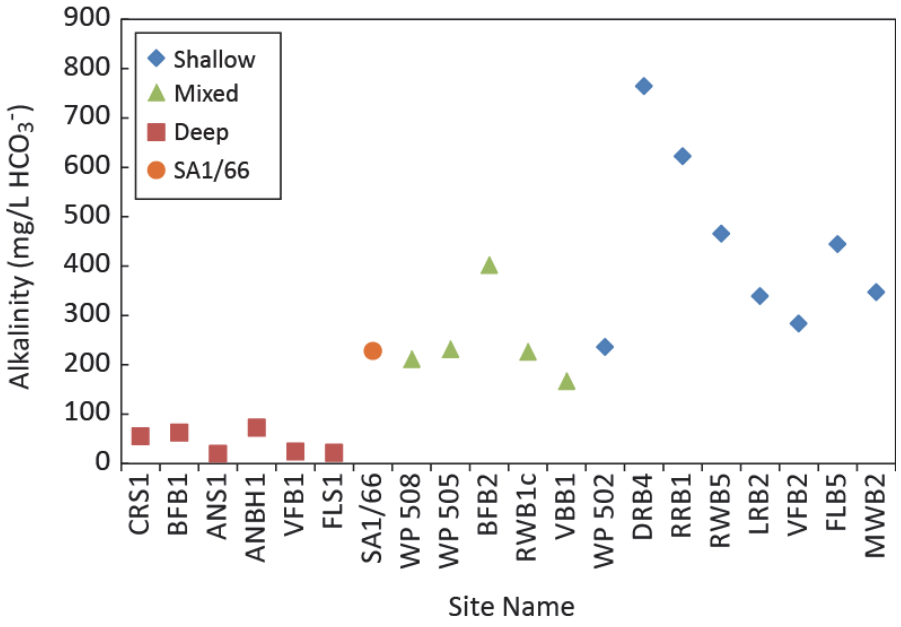

Figure 5.43. Alkalinity of the different groundwater depth groups

Comparison of the alkalinity with temperature shows, not unexpectedly, that there is a fair negative trend between temperature and alkalinity, where warmer groundwaters have lower alkalinities and cooler groundwaters have higher alkalinities (Figure 5.44). A possible mechanism for the removal of carbonate is the precipitation of calcium carbonate at the high pH that generally develops in deep groundwater.

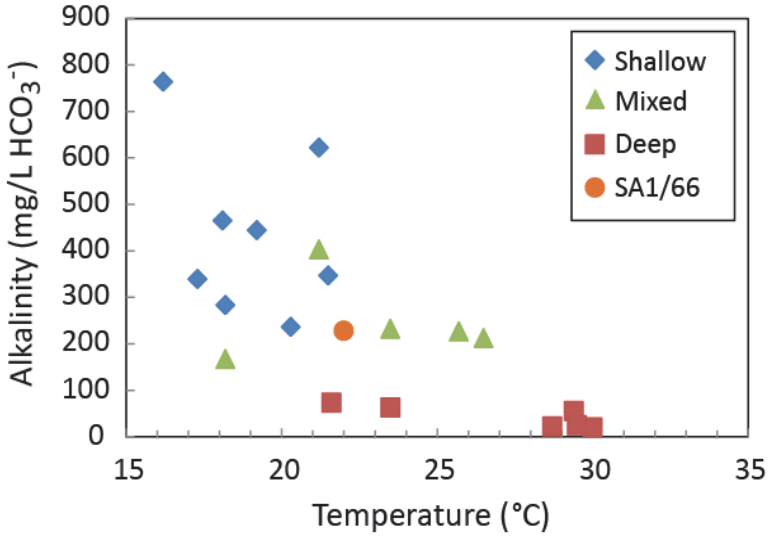

Figure 5.44. Alkalinity versus temperature

5.2.17 pH

pH in this sample set behave opposite to alkalinity (Figure 5.45) with deep water pH in the 9-10 range. A discernible trend from the shallow group to the deep group can be seen in the pH versus temperature plot (Figure 5.46A). The shallow group has the lowest pH values of between 7.1-7.9, while the deep group has the highest pH values of between 7.5 and 10. The mixed group, with moderate pH values between 7.4 and 8.4, overlaps both these other groups. Figure 5.46B depicts alkalinity versus pH. A good trend supports the graphs described above with the same determinands. The exception to the general trend is ANBH1 (deep water with pH = 7.5). It is believed to be warm water from the Aliwal North spa source (ANS1) that has undergone some changes towards the borehole (loss of H_2S, decrease of pH, increase of radon).

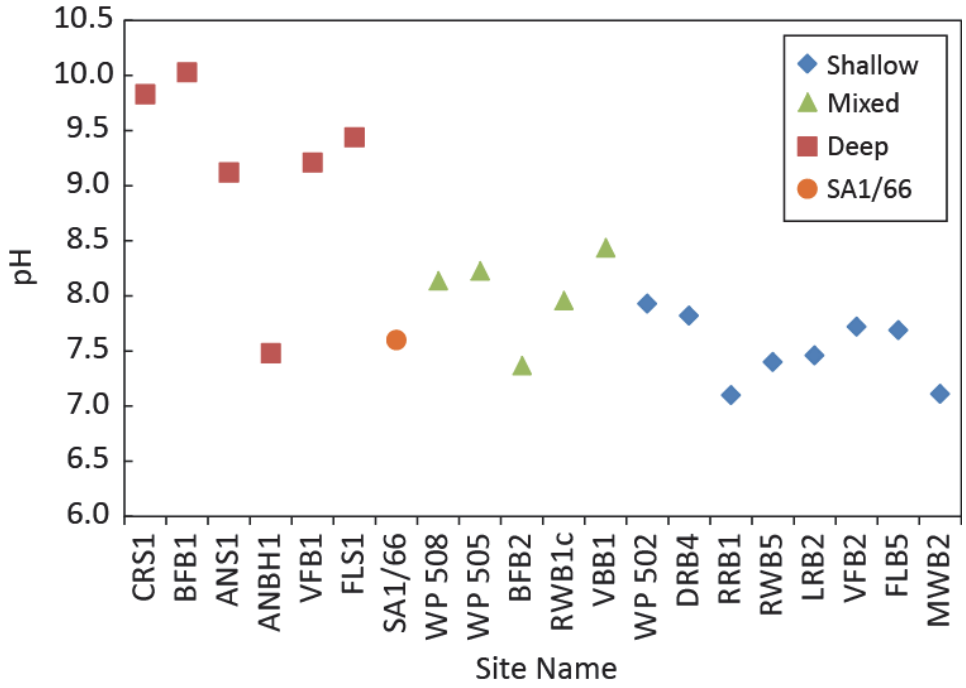

Figure 5.45. pH values in groundwater depth groups

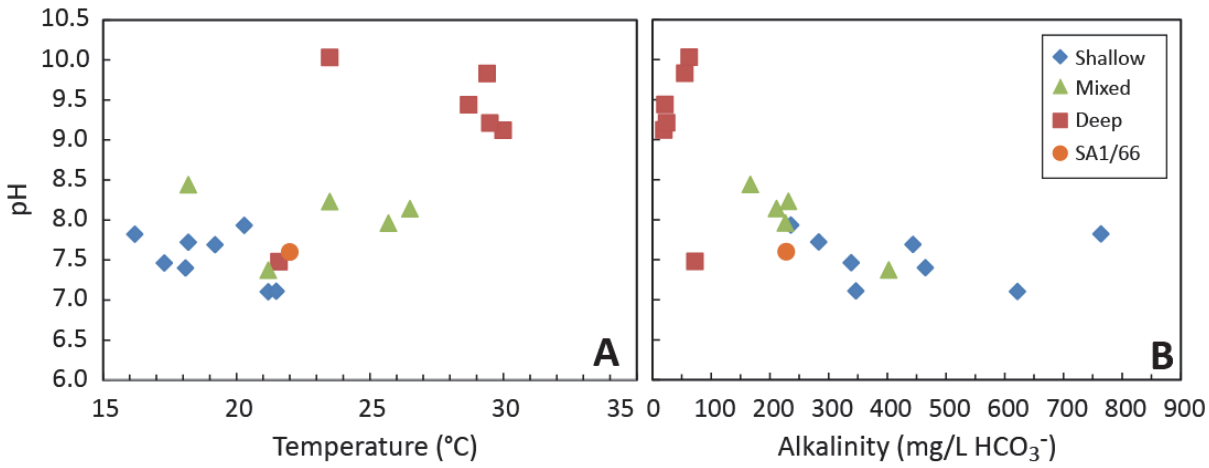

Figure 5.46. (a) pH versus temperature; and (b) pH versus alkalinity

5.2.18 Helium and its isotopes

^{4}He, as the most abundant isotope of helium, shows only parts of the distribution expected for helium as a cumulative dating tool. The distribution of ^{4}He for the different sampling sites (Figure 5.47A) shows that for waters defined as shallow, the ^{4}He content is low. Deep water has the expected high ^{4}He content caused by gradual accumulation of ^{4}He due to increased underground residence time. The exceptions are CRS1 (Cradock spa), BFB1 (Fort Beaufort sulphur springs) and, less so, VFB1 (Trompsburg). The ^{3}He/^{4}He distribution follows the same sort of pattern (Figure 5.47B) in that the different ratios of the mixed and deep waters are consistent except for the low R/R_0 ratio of CRS1 (Cradock spa) and BFB1 (Fort Beaufort Sulphur Springs).

Taken together (Figure 5.48), the helium isotopes follow the predictable pattern reasonably well. As discussed in Chapter 2, the helium growth model implies that $R/R_0 = 1$ for low ^{4}He and this drops to near zero as the ^{4}He content increases with increasing contact with the aquifer. This is the text book example of dating with ^{3}He/^{4}He described in Chapter 2 (IAEA, 2013; Darrah et al., 2014). The exceptions CRS1 (Cradock spa) and BFB1 (Fort Beaufort sulphur springs) fit in well with the general pattern of Figure 5.48 and appear to be young water. In most of the other parameters they are classified as old/deep water.

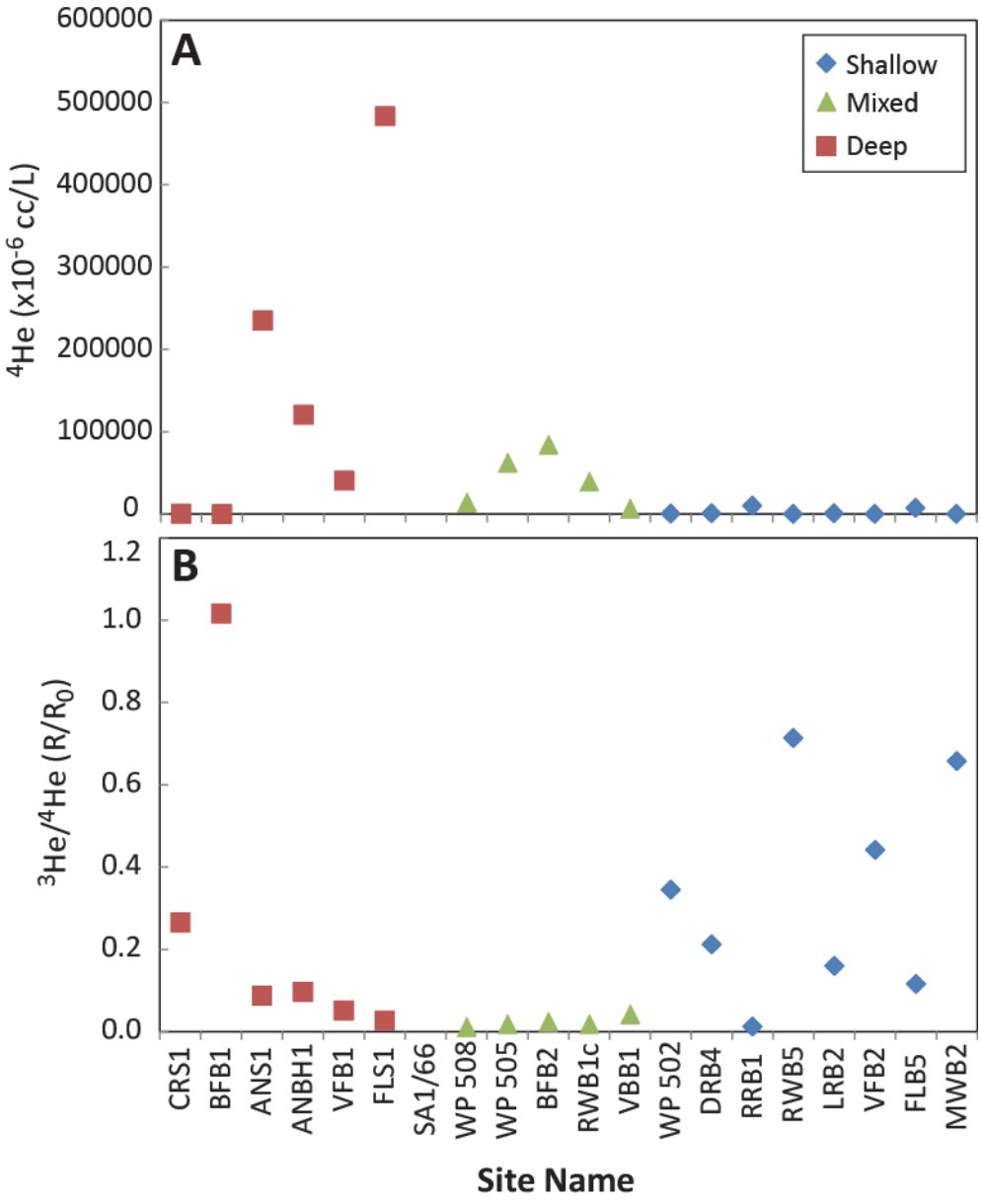

Figure 5.47. Distribution of (a) ^{4}He and (b) ^{3}He/^{4}He ratios as a function of groundwater depth groups

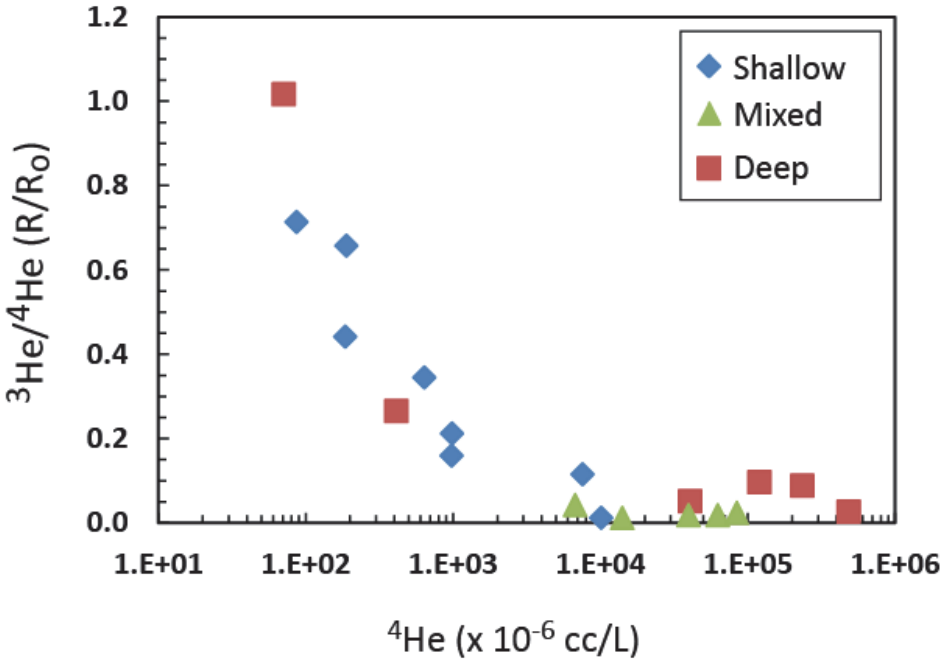

Figure 5.48. Plot of the $^{3}He/^{4}He$ ratio (as R/R_0) against ^{4}He

5.2.19 Methane and its isotopes

Methane (CH_4) is a natural constituent in many Karoo borehole waters (Talma & Esterhuyse, 2015). During the present study, methane concentrations above 1 cc/kg appear in 14 of the 19 samples that were analysed (Fig 5.49). Even the shallow sample group only showed one out of 8 samples with less than 1 cc/kg methane. The overall methane distribution in all the groundwaters sampled here, form two groups:

- Low CH_4 (<5cc/kg): 15 samples;
- High CH_4 (>10cc/kg): 4 samples.

As is the case with the helium isotopes, there is not a rigid separation of methane concentrations according to the earlier deep/shallow classification (Figure 5.49). Of the deep waters, three sources have low methane levels and three are high. The shallow waters all have methane levels less than 4 cc/kg. The mixed waters have low and high methane levels (Figure 5.49).

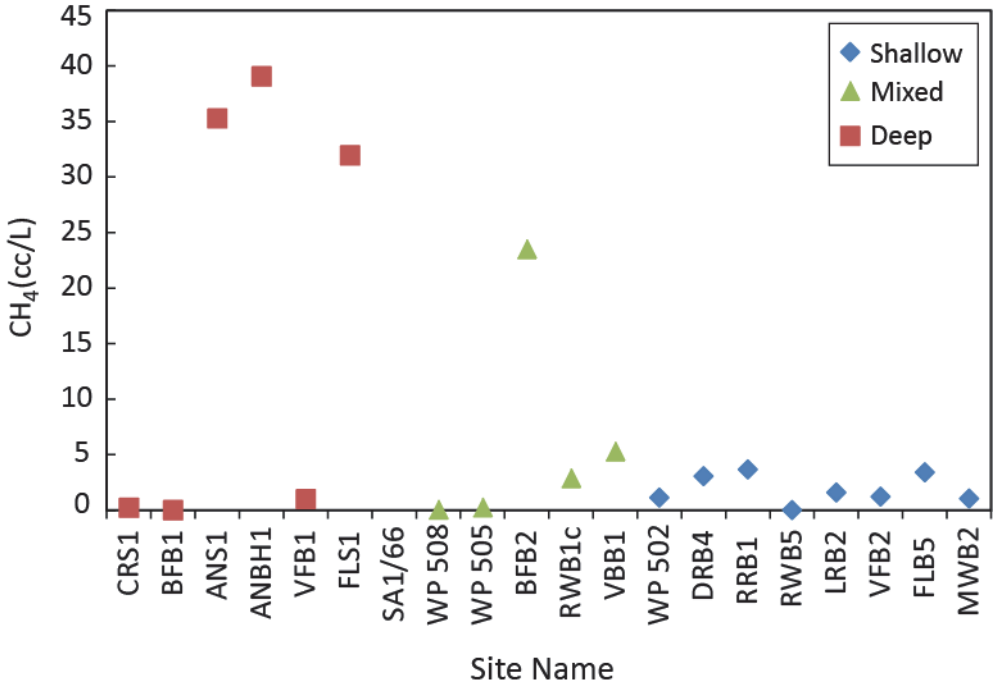

Figure 5.49. Methane concentrations in groundwater depth groups

This lack of distinction can also been seen in the CH_4-temperature plot (Figure 5.50A). While the shallow boreholes with their low temperatures all have low methane levels, the deep and mixed type have both low and high methane levels. ^{14}C as a depth indicator shows a similar pattern (Figure 5.50B). Using helium as a possible water depth indicator improves the consistencies slightly (Figure 5.51) in the sense that there is better correlation (on a semi-log scale) between ^{4}He and CH_4.

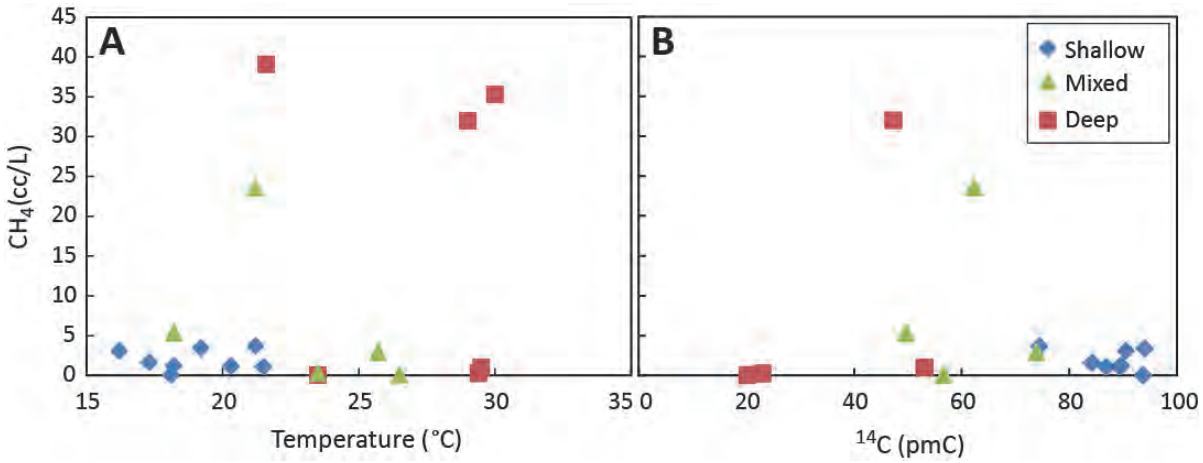

Figure 5.50. (a) Methane-temperature plot; and (b) Methane-radiocarbon plot

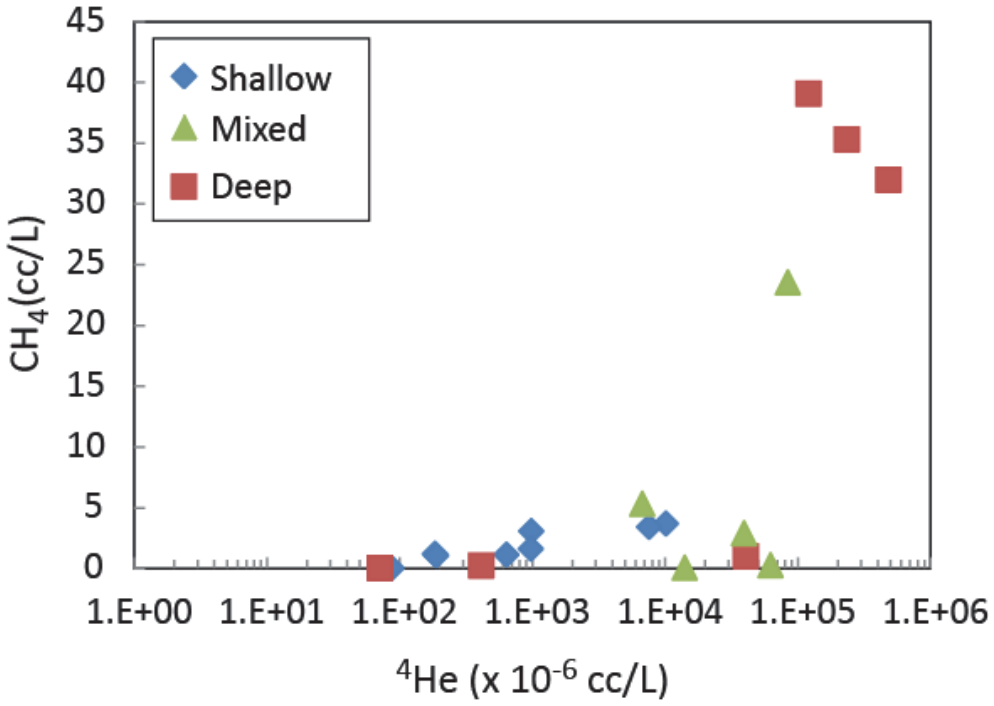

Figure 5.51. Relationship between methane and ^{4}He

The ^{13}C content of the methane ($\delta^{13}C_{-CH4}$) samples shows a wide variation from -75 to -50 ‰ (Figure 5.52) and there does not appear to be much correlation with the deep vs shallow classification that is used in this report. Using the $^{3}He/^{4}He$ ratio as a relative dating parameter (Figure 5.53B) indicates that young water (high R) contains low ^{13}C in methane typical of that originating from bacterial (i.e. local) sources. $\delta^{13}C_{-CH4}$ of older water trends towards the high values that are typical of thermogenic methane as is found in some shale gases (Molofsky et al., 2013). Talma and Esterhuyse (2015) reported a number of ^{13}C analyses in methane as high as -28‰ in parts of the Karoo. These values are typical of thermogenic methane. The relation between ($\delta^{13}C_{-CH4}$) and the C_1/C_{2+} ratio in methane from these waters bears some relation to the origin of the methane (Figure 5.53A). The upper left hand corner of Figure 5.53A represents a methane origin of bacterial source and the lower right corner approaches the levels for thermogenic methane (Schoell, 1980; Whiticar, 1996) as are present in most shale gas. The different methane sources are not well correlated with the classification of deep and shallow water adopted in this study. Further work in the Karoo is presently underway to provide more clarity on this aspect.

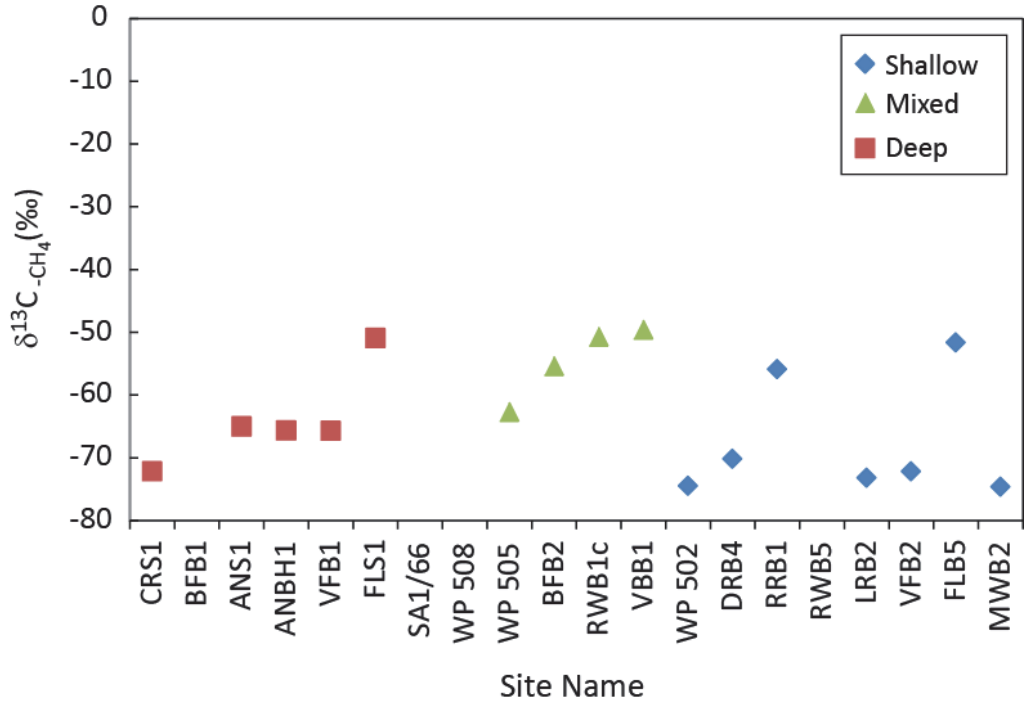

Figure 5.52. Site plot of $\delta^{13}C$ in methane

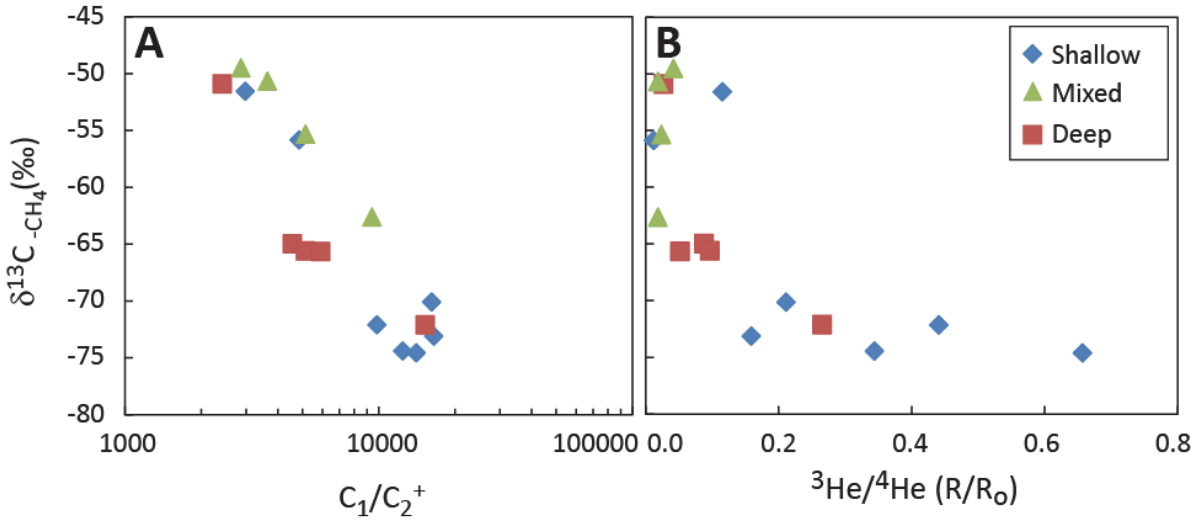

Figure 5.53. Relationship of $\delta^{13}C_{-CH4}$ ratios to (A) the C_1/C_{2+} ratio in water; and (B) to the $^3He/^4He$ ratio

5.2.20 Hydrogen sulphide (H_2S)

The smell of rotten eggs is a common feature of warm groundwater and has been commented on earlier (Kent, 1949; Whittingham, 1970; Vogel et al. 1980). There is a clear difference between the shallow samples with no H_2S on the one hand and the mixed and deep samples that contain varying quantities of H_2S (Figure 5.54A). Even when the H_2S assessment is merely based on smell, the distinction between the types is clear (Figure

5.54B). The exception is borehole ANBH1 which delivers Aliwal North Spa water after having been cooled. During the first sampling run (March 2014) this water had a distinct H_2S smell, but by June 2014 when the second sample was collected, no smell was evident. It does, however seem that during the flow process from depth to the borehole, H_2S is lost. H_2S, when present in natural, unpolluted situations is an indicator for anoxic or reducing conditions generally associated with deeper flow. The presence of H_2S will therefore serve as indicator for separating deep and mixed water from shallow. The presence of H_2S is, however, not a necessary condition for the identification of deep water.

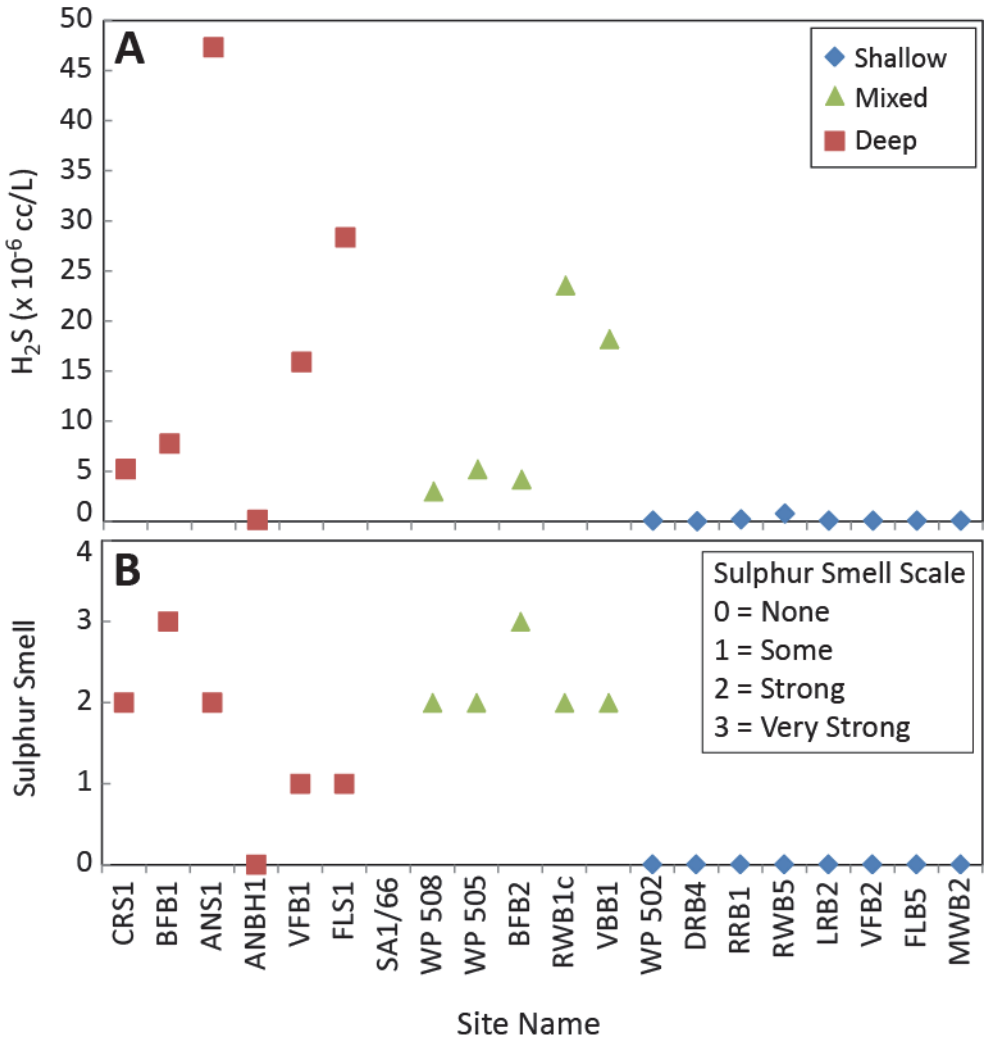

Figure 5.54. Distribution of H_2S in the groundwater depth groups based on (A) actual gas analyses; and (B) the sampler's sense of smell

6. DEEP GROUNDWATER INDICATORS

In the previous chapter all the data collected to evaluate differences between deep and shallow groundwater were individually presented and described. Relationships to temperature and age (using ^{14}C as a proxy) were explored briefly. As has been indicated previously, “deep” groundwater is now essentially defined as groundwater that either has: (a) a temperature > 25°C combined with low ^{14}C, implying that it is sourced from deep older groundwater systems; or (b) has a “Y” shaped Stiff diagram again combined with low ^{14}C implying that it is geochemically distinct from the other groundwaters sampled but again derived from an older groundwater system. In this chapter, the data are evaluated to:

- Determine how clearly deep versus shallow groundwater can be differentiated.
- Determine how internally consistent each group is (i.e. was it one compositional water type or more than one).
- Establish what the best indicators of deep and shallow groundwater are.
- Outline a statistical method for testing how robust these indicators are.
- Assess the nature of the mixed groundwater group.

Following on from this, data are taken from sites in the 1st sampling round that were not part of the 2nd sampling round and are used in the classification matrix to see whether the nature of these groundwaters can be predicted. Using these findings, an assessment is provided of what are the most important indicators of deep groundwater from several different standpoints, including scientific strength, cost, and availability. Finally, the difference between deep groundwater indicators that should be part of long term monitoring programs and the environmental tracers of fracking contamination is discussed to see where points of commonality occur.

6.1 Characterisation of Deep Groundwater

In Chapter 5, a large number of hydrochemical determinands have indicated that seven of the 22 groundwater sites sampled represent what was called deep groundwater (this includes the Soekor borehole SA1/66), eight sites suggest shallow groundwater and five sites are what was called mixed groundwater in that they are neither clearly deep nor clearly shallow. In order to assess the character of deep groundwater in a general sense, all the geochemical parameters analysed and presented in Chapter 5 are discussed below by grouping them into common themes.

6.1.1 Temperature

Temperature is certainly a key indicator of deep groundwater. This is based on the assumption that warmer water must come from deeper crustal levels. This reasoning was what led to the targeting of warm springs as potential sources of deep groundwater in the Karoo. However, now that all other hydrochemical parameters have been assessed, it would appear that low temperature is not a sufficient condition to classify a source as shallow. Two sites (ANBH1 from Aliwal North Farm and BFB1 from the Fort Beaufort Sulphur Baths) have temperatures below 25^{o}C while the other deep water indicators are positive (Figure 5.10). The most likely explanation for this would be cooling of the groundwaters during their migration to the surface. In fact this could be extremely variable depending on the specific nature of the migration path at each site and further supports the contention that although high temperatures are a clear indicator of deep groundwater, a low temperature does not preclude the possibility that the groundwater has circulated at depth. Therefore high temperature (in the present case >25^{o}C) is a sufficient, but not a necessary, condition to identify deep water.

6.1.2 Major Ion Chemistry

The chemical parameters that are most distinctive in their characterisation of deep water were found to be pH, alkalinity, magnesium, sodium and fluoride. To some extent this is the result of the use of Stiff diagrams to identify deep and shallow water, as described in section 5.1. There are however sufficient clues to indicate its general application.

The deep and shallow groundwater sites could be fairly clearly distinguished based on pH (Figure 5.45). The deep groundwater sites had high pH values, generally >9, while the shallow groundwater sites all had pH values <8 (median 7.6). The mixed sites were in between with four of the five being between 8.0 and 8.4. Alkalinity showed the opposite pattern (Figure 5.43). The highest alkalinity for the deep water was 73 mg/L HCO_3^-, (median 40 mg/L). In comparison, the lowest alkalinity for the shallow groundwater group was 236 mg/L HCO_3^- (median 396 mg/L). Based on this, alkalinity is the best field indicator of groundwater depth with a boundary set at <100 mg/L HCO_3^- likely to indicate deep groundwater. For pH a boundary set at >9 would correctly classify all but one site as deep.

Sodium concentrations in the groundwater samples turned out not to be a good depth indicator as defined in this report. Sodium concentrations in the deep groundwaters spanned a considerable range between 43 and 2584 mg/L Na with a median value of 332 mg/L Na. The shallow groundwater sites all had sodium concentrations below 300 mg/L Na but so too

did two of the deep groundwater sites (Figure 5.24). This variation in sodium concentration can also be seen in the sodium distribution map of the country (Figure 6.1). For the Karoo area there is a gradual increase of sodium towards the western part of the Karoo. A better indicator of deep water was obtained by using sodium as percentage of the total cations (Na/(Ca+K+Mg+Na) in equivalents). Expressing sodium in this way shows a much clearer separation between deep (%Na >77%) and shallow (%Na <62%) groundwater sites (Figure 5.5.24). Furthermore, sodium is well correlated with chloride (Figure 5.26) indicating that variations of both Na and Cl are due to variations in the contribution of NaCl to the water mix. The correlation between Na and Cl (1:1) is such that it excludes a contribution from seawater, which has a lower Na/Cl ratio (0.85).

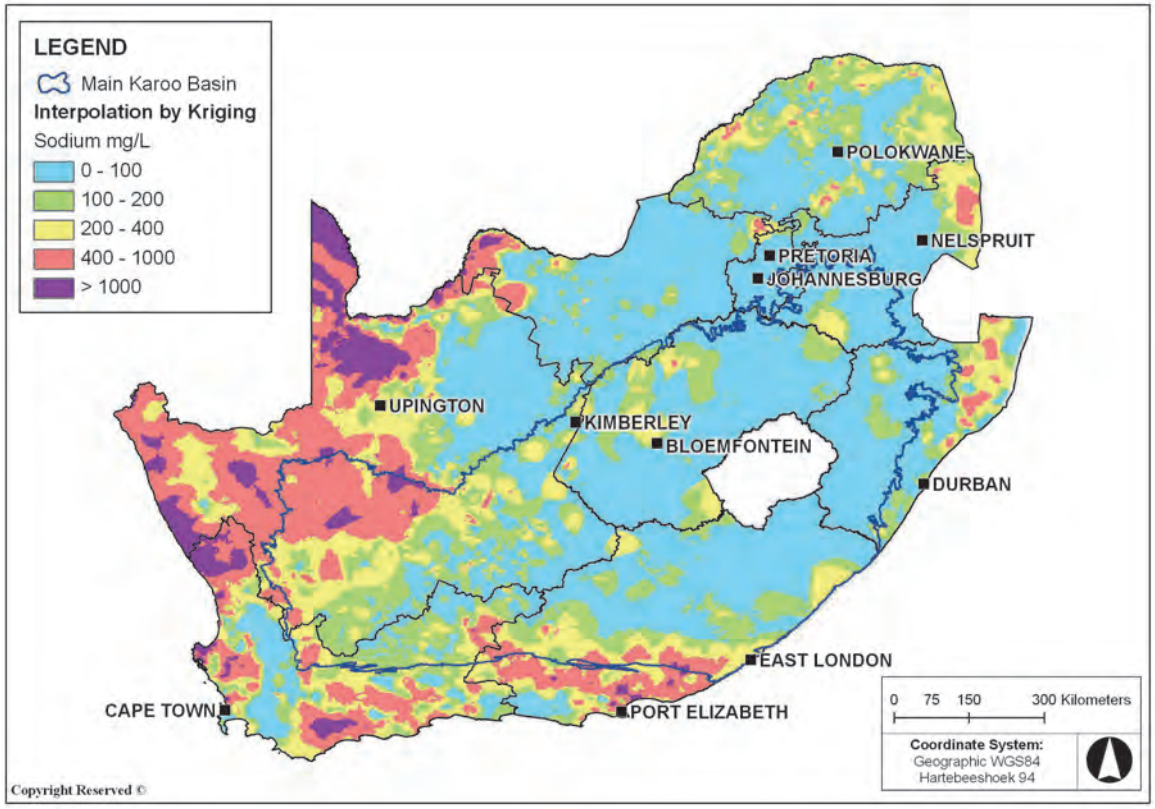

Figure 6.1. Distribution of sodium in groundwater throughout South Africa (Murray et al., 2012). The blue lines indicate the extent of the Main Karoo Basin.

Calcium in the groundwater samples is unrelated to water source (deep water 3-432 mg/L; shallow water 26-148 mg/L). Magnesium, on the other hand, is present in very low concentrations in the deep groundwaters (<1.3 mg/L) (Figure 5.27). Shallow water magnesium values range from 10 to 73 mg/L. This was also observed in Venterstad (Vogel et al., 1980) and could be attributed to loss of magnesium by ion exchange involving Ca substitution.

As expected, fluoride is a good indicator of deep groundwater (Figure 5.20) with F^- >3.7 mg/L, while the fluoride concentration in shallow water in this study is consistently <1.3 mg/L. The high values of deep groundwater fluoride stand out against a background of fluoride in Karoo water of less than 3.5 mg/L (Figure 6.2) (Note that point sources of high fluoride, such as the warm Karoo springs are not significant at the resolution of the Kriged map). The most obvious source of fluoride in water would be from the mineral fluorite (CaF_2). This mineral dissolves slowly and may explain why high residence time underground is required to build up significant fluoride levels in deeper water.

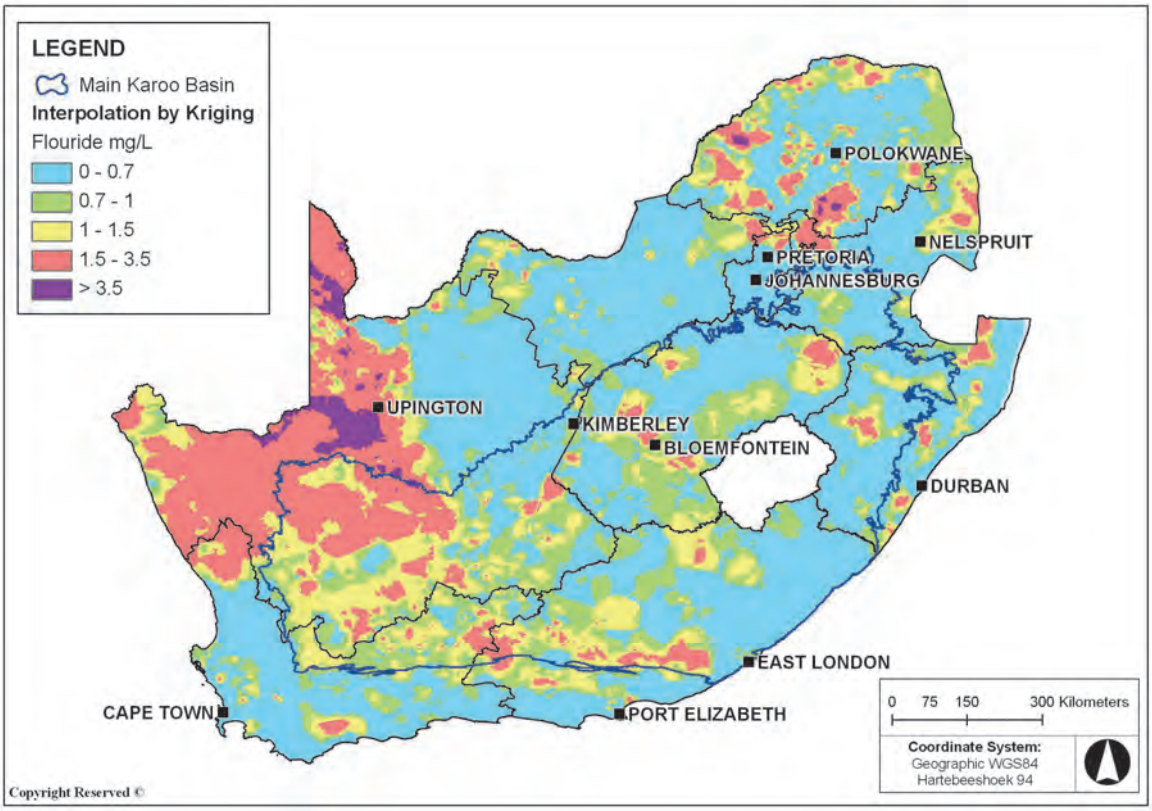

Figure 6.2. Distribution of fluoride in groundwater throughout South Africa (Murray et al., 2012). The blue lines indicate the extent of the Main Karoo Basin.

Nitrate concentrations from the deep and mixed groundwater sites are below the detection limit of nitrate for this study (<1 mg/L NO_3^-) (Figure 5.18). For the shallow water sites there are an equal number of samples with nitrate concentrations <1 mg/L NO_3^- as there are high ones (8-54 mg/L). Figure 6.3 shows that the levels of nitrate in Karoo groundwater are generally low, compared to those in the rest of the country. However, individual farm boreholes may be polluted but these would not show up on the Kriged map. In the northwest there are regions of the Karoo Basin with nitrate levels above 26 mg/L NO_3^- (6 mg/L N) which is higher than the levels found in the shallow water of the present project samples. Natural

nitrate is produced by nitrogen fixing bacteria that are prolific among the roots of the Acacia tree and shrubs and certain grasses (Tredoux and Talma, 2006). These are not very common in the general Karoo environment but become more abundant towards the west where Kalahari vegetation cover increases. The other source of nitrate is contamination from animal and human waste and this usually shows up in boreholes close to human and animal habitation. This is probably the case for all of the high nitrate boreholes in the present study.

Whatever the source of nitrate may be, once the water leaves the vadose zone, dissolved oxygen (DO) will be consumed and once DO is low enough, denitrification will set in (Heaton et al., 1983). Reducing waters therefore seldom contain any nitrate. This is evidently the case with the deep and the mixed groundwaters sampled in this project.

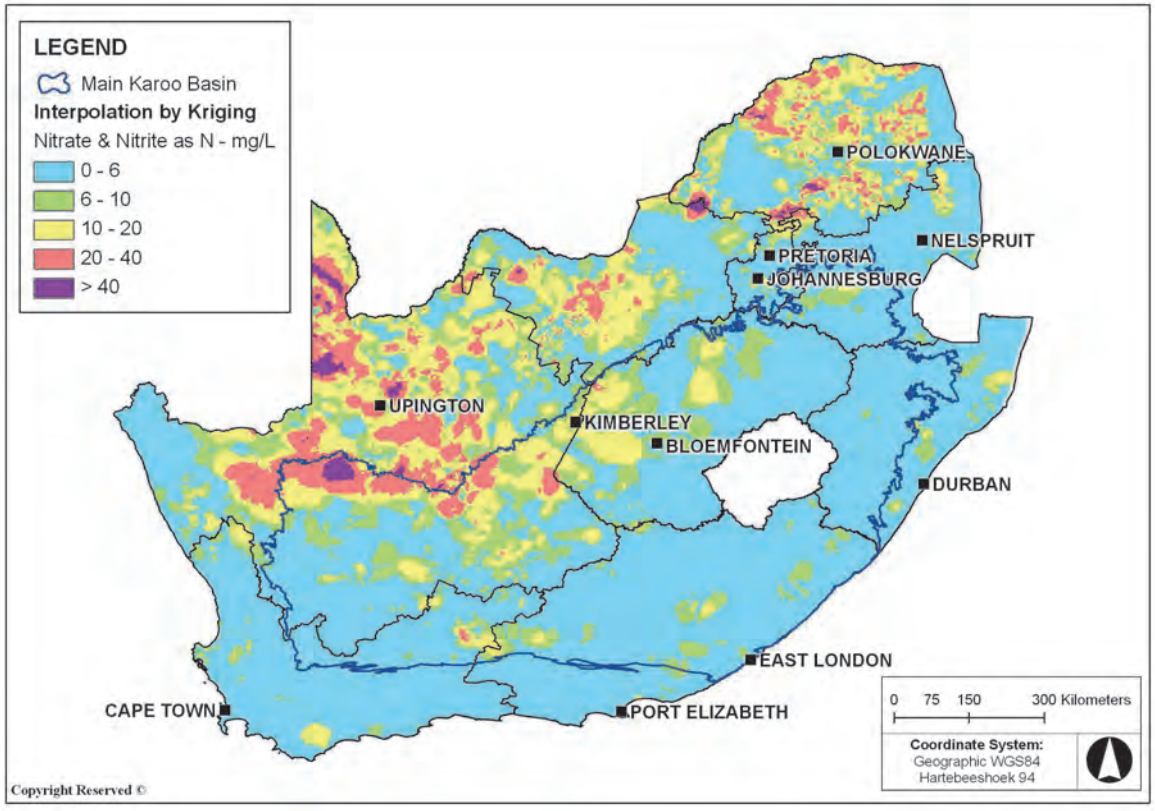

Figure 6.3. Distribution of nitrate in groundwater throughout South Africa (Murray et al., 2012). The blue lines indicate the extent of the Main Karoo Basin. Note that the nitrate levels in this figure are presented as mg/L N. To convert to the mg/L NO_3^- as is used in the present report, multiply by 4.4.

A characteristic feature of the deep water is its hydrogen sulphide (H_2S) content. Warm springs in the Karoo are invariably smelly (Kent, 1949). Attempts to quantify this "smelly" characteristic have included analysis of total sulphide (S^{2-}) dissolved in the water (Vogel et al., 1980) and analysis of H_2S as dissolved gas in the present project (Figure 5.54). Both of these measurements involve challenging analytical procedures. A less accurate method is

the use of H_2S indicator strips. The most probable origin of sulphide is the reduction of sulphate in water or organic matter, by bacteria when the groundwater is in the reduced state. For groundwater this will occur when the water has been underground sufficiently long for bacterial action and other processes to remove all the dissolved oxygen. H_2S is therefore more characteristic of the older deep groundwaters, although it can also be produced in near-surface anoxic water.

The picture that emerges of the chemical development of groundwater from the shallow group to the deep group consists of well-oxidised $Ca.Mg.HCO_3$ water that is moving underground and there subjected to:

- Temperature increase during downward movement and decrease (to some extent) during upward movement.
- Addition of NaCl.
- Removal of dissolved oxygen.
- Reduction of nitrate to nitrogen gas.
- Reduction of sulphate and/or organics to H_2S.
- Loss of magnesium.
- Loss of HCO_3^-, probably in conjunction with calcium loss.
- Increase of fluoride by fluorite dissolution.

The samples that were obtained from what has been identified as “deep” water in this report show the result of these different reactions occurring to varying degrees in each case. The extent of these reactions requires quantitative modelling in each separate case, which is beyond the scope of the present project. Some of these reactions are already evident from Figure 6.4 which shows the deep, shallow and mixed samples on a Piper diagram. Note the special positions of the deep water and the wider chemical variation of the shallow water group.

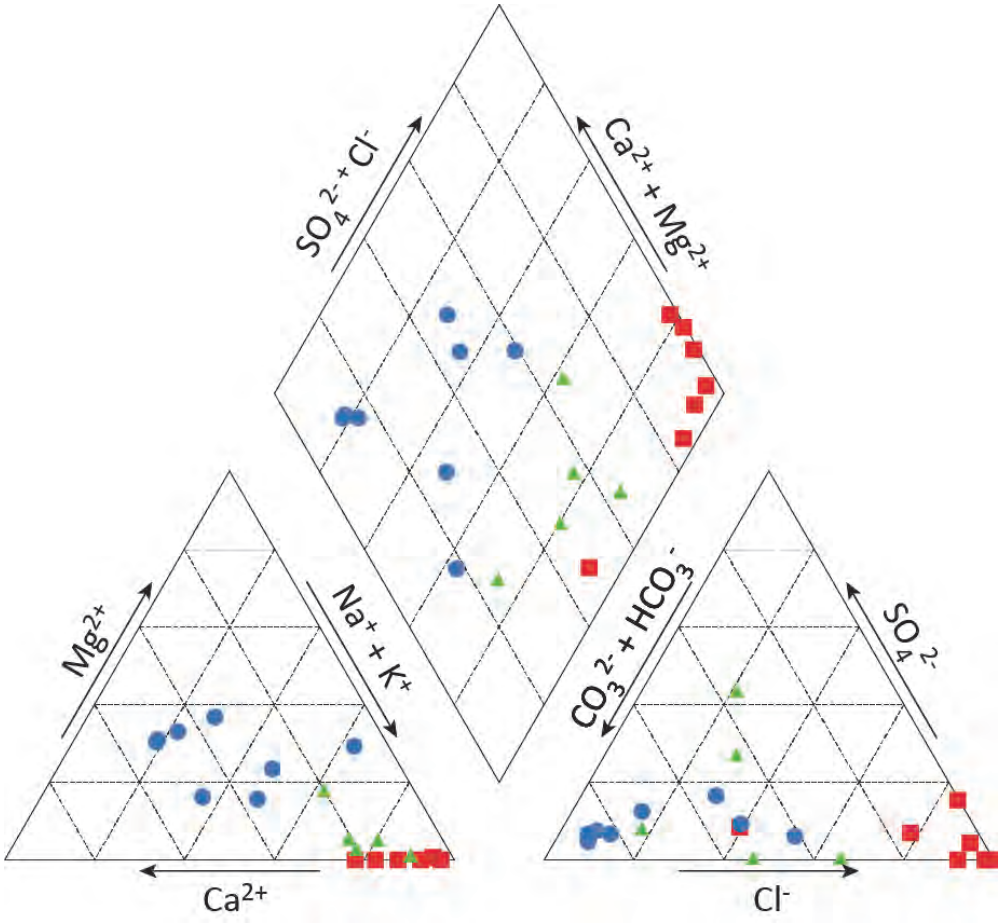

Figure 6.4. Position of deep, shallow and mixed groundwaters on a Piper diagram

6.1.3 Trace elements

In the course of this study, a full suite of trace elements, including transitional metals and rare earth elements were collected (data presented in Appendices 4 and 5). Most of these turned out to not be particularly useful in differentiating deep from shallow groundwater. Rare earth elements, as has been mentioned previously, were present in such low concentrations, approaching, or at, the detection limit of the mass spectrometer, that they were not considered useful for differentiation of groundwater types. It is possible that different collection and analysis techniques might yield better results but the sample collection procedures might be too onerous for routine use (Weaver et al., 2007). Of the trace elements analysed and examined four stood out in differentiating deep from shallow groundwaters: Uranium, boron, vanadium and lithium. The data for each of these elements is summarised in Appendix 6 and discussed in Chapter 5. U is particularly interesting because of the mineable uranium deposits in the Karoo Basin around Beaufort West (D Cole, Council for Geoscience, pers. comm.). Boron is interesting due to the potential importance of $\delta^{11}B$

isotope ratios for tracing contamination of fracking fluids in the United States (Warner et al., 2014).

Uranium and vanadium show similar trends with low concentrations present in the deep groundwater group and higher concentrations in the shallow groundwater group. The uranium concentration in the deep groundwater was always less than 0.05 µg/L, while for the shallow groundwater group the uranium concentrations are above 2.5 µg/L (Figure 5.39). The mixed sites are generally also low in uranium with a median of 0.5 µg/L uranium from five sites. Uranium solubility is enhanced by the presence of bicarbonate and oxygen (Stumm and Morgan, 1981). The geochemistry of the deep groundwater samples is therefore not conducive to the presence of dissolved uranium, because of the high pH, low alkalinity, anoxic environment found in these waters. The virtual absence of uranium is therefore the consequence of the specific environment into which groundwater develops at depth. The high uranium deposits found in the so-called Karoo Uranium Province are a surface phenomenon associated, amongst others, with calcrete deposits (D Cole, Council for Geocsience, pers. comm.) and impact only on the shallow groundwater system.

Vanadium shows a similar pattern to uranium, with all deep groundwater sites but one having vanadium concentrations of less than 0.05 µg/L (the outlier is CRS1 with 0.5 µg/L V), whilst the shallow sites have greater than 1 µg/L vanadium with one outlier (MWB2: 0.61 µg/L) (Figure 5.37). Similar to uranium, the mixed water sites also have low vanadium contents (<0.05 µg/L V). The chemistry of vanadium is similar to that of uranium. The literature shows frequent associations between vanadium and uranium (Garrels & Christ, 1965) in natural water and this explains the similar pattern found in the deep water sites of the present project.

In contrast to uranium and vanadium, boron and lithium record low concentrations in the shallow groundwater sites and high concentrations in the deep groundwater sites. Boron concentrations range from 42-753 µg/L in the shallow groundwater, and from 473->3065 µg/L in the deep sites with one outlier of 23 057 µg/L for the Soekor SA1/66 site (Figure 5.32). Boron is derived from various minerals and is known to be present in significant quantities in warm water where it is speculated to develop due to slow dissolution rates, enhanced by higher temperatures (Murray, 1996; Ozgurd, 2001). Boron therefore might be a very good indicator of very deep water, especially in view of the extremely high value found in the deep SA1/66 borehole. The isotopic composition of boron is discussed in section 5.2.11. The distribution of lithium follows the same pattern as boron with low values in shallow water (<100 µg/L, with MWB2 being an outlier with 265 µg/L Li) and higher values in

the deep water (167-843 µg/L with VFB1 being an outlier with 6814 µg/L Li) (Figure 5.22). Lithium is frequently found in association with sodium and its isotopes have been suggested as tracers for fracking fluids (Warner et al., 2014).

When taken together, these four trace elements vary in their ability to differentiate deep from shallow groundwater but in all cases a boundary concentration could be defined. Boundaries set at < 0.05 µg/L uranium, < 1µg/L vanadium, > 100 µg/L lithium and > 300 µg/L boron for the current dataset would classify all the deep groundwater sites successfully with no outliers.

6.1.4 Stable isotopes

The stable isotopes ratios analysed in this study were $\delta^{18}O$, $\delta^{2}H$, $\delta^{11}B$ $\delta^{13}C_{\text{-TIC}}$ in water and $\delta^{13}C_{\text{-CH4}}$ in dissolved gas. The $\delta^{13}C_{\text{-TIC}}$ ratios were not useful for differentiating deep from shallow groundwater as outlined in section 5.2.12. The values in the deep groundwater varied considerably while those for the shallow groundwater were within narrower bounds (Figure 5.35). $\delta^{13}C_{\text{-CH4}}$ values were also not particularly useful for differentiating deep from shallow groundwater because of the overlap in the data (Figure 5.52) such that no clear boundary could be defined between values for deep groundwater and values for shallow groundwater. In fact the highest $\delta^{13}C_{\text{-CH4}}$ found during the present project (-50‰) is considerably lower than the highest value of -28‰ measured forty years ago in the similar area and water (see summary in Talma and Esterhuyse, 2015). Further work is needed to understand the differences between these two studies.

$\delta^{18}O$ and $\delta^{2}H$ ratios show a regular pattern of higher values in shallow groundwater and lower values in deep groundwater (Figure 5.15). In the deep groundwater samples the median $\delta^{18}O$ and $\delta^{2}H$ ratios are -7.1 and -37 ‰ respectively. In the shallow groundwater samples the median $\delta^{18}O$ and $\delta^{2}H$ ratios are -4.8 and -25 ‰ respectively. This gives a $\delta^{18}O$ and $\delta^{2}H$ shift of -2.3 and -12 ‰ respectively from the shallow groundwater to the deep groundwater and is a function of the age of recharge. This is a well-known phenomenon documented in most textbooks dealing with stable isotopes of O and H and has also been documented in the South African context. The studies of Heaton et al. (1986) on the Uitenhage aquifer in the TMG and Kulongoski, et al., (2004) on the Botswana Kalahari dealt with groundwater characterised by regular flow in artesian-like aquifers. The $\delta^{18}O$ isotope shifts at the Pleistocene/Holocene boundary of these well-dated waters (10-15 ka) were in the order of -1‰ reflecting lower recharge temperatures in the past. The dry cool environment before 15 ka is a sufficient explanation for the isotope differences found in these aquifers.

Radiocarbon and ^{36}Cl data of the deep groundwaters found during the present project indicate similar ages of water, and therefore the same interpretation can probably be applied.

The $\delta^{18}O$ and $\delta^{2}H$ levels in any groundwater are the final products of many fractionation processes along the hydrological cycle, from evaporating sea water via local precipitation to eventual groundwater recharge (Mook, 2006). Once water is below the groundwater table, the behaviour of these isotopes is more or less stable and $\delta^{18}O$ and $\delta^{2}H$ behave as conservative tracers. The fractionation processes are influenced by factors as temperature, rainfall seasonal pattern and continental position (e.g. Mook, 2006; Aggarwal et al., 2005) and produce variations in $\delta^{18}O$ and $\delta^{2}H$ of groundwater in different localities. The map of the country with $\delta^{18}O$ derived from a network of groundwater sampling (Figure 6.5) indicates that within the boundaries of the Karoo Basin, there are variations in the order of 1-3 ‰ in $\delta^{18}O$ in, mostly, shallow waters. Nevertheless, the shallow and the deep samples from this project have, apart from a few obvious outliers, produced fairly homogenous clusters of $\delta^{18}O$ and $\delta^{2}H$ values (Figure 5.16).

Based on the data presented in Chapter 5, a boundary of < -6 ‰ for $\delta^{18}O$ and < -35 ‰ for $\delta^{2}H$ could be set for differentiating deep from shallow groundwater and would successfully classify all the deep groundwater sites and exclude any shallow or mixed sites. The trouble with setting this limit though is that, particularly for the shallow sites, variations in climate (such as rainfall amount and intensity as well as ambient temperature) can lead to local changes that have to be considered (van Wyk, 2013). Therefore whilst in this study $\delta^{18}O$ and $\delta^{2}H$ values can be used to differentiate deep and shallow groundwater, the application of the boundary values set in this study to other areas and sites should be undertaken with caution.

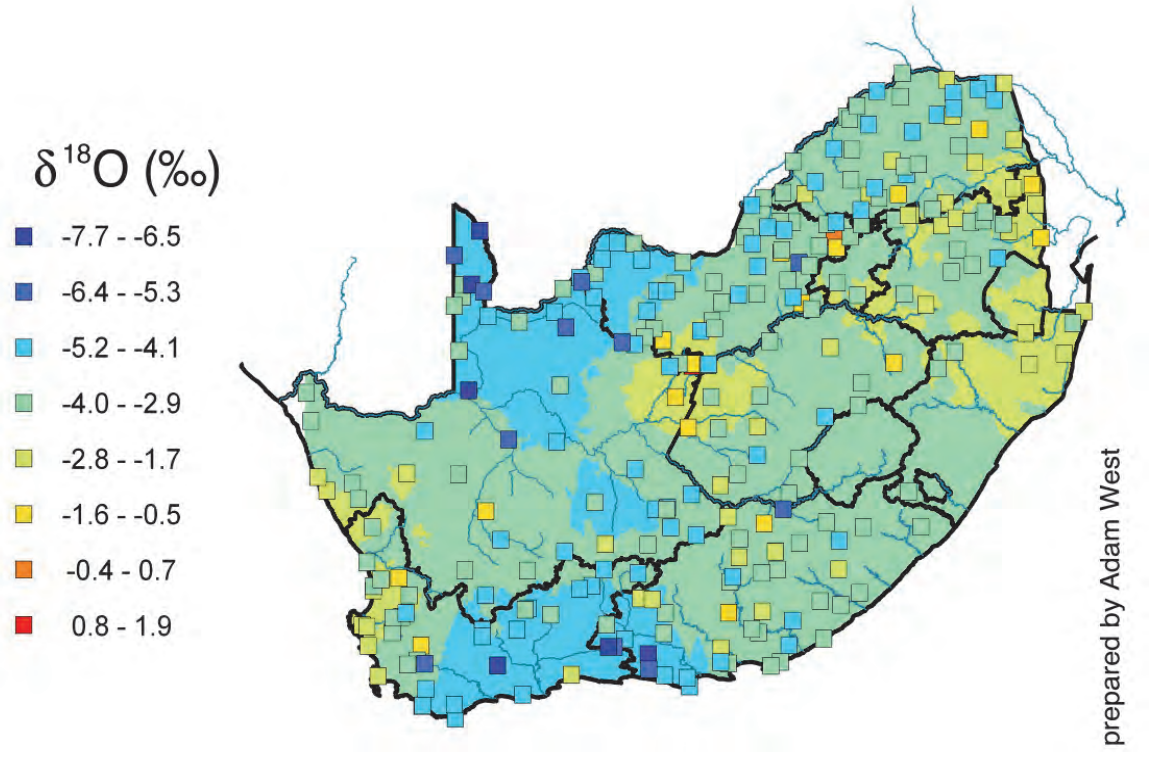

Figure 6.5. Distribution of $\delta^{18}O$ in samples from a DWA groundwater national survey (Talma and van Wyk 2013). The data points are indicated as blocks. The map colours were produced by Kriging the data

The boron isotope ratios show a wide variation in groundwater sampled in this project, with $\delta^{11}B$ in deep water ranging from +5 up to +30 ‰ and shallow water >+33 ‰ (Figure 5.32). These reflect the range of $\delta^{11}B$ found in nature; from +40 ‰ in the marine environment (Vengosh et al., 1994), towards negative values in continental sediments. Another source of isotope fractionation is preferential absorption of ^{10}B during interaction with clays (Warner et al., 2014). This will tend to increase $\delta^{11}B$ during increased contact with clays underground. Whatever the process or source in action here, there is a clear separation of shallow water from mixed and deep water based on the combination of high $\delta^{11}B$ and low boron content (Figure 5.34). Future work would have to be done with this isotope pair because of its potential use as tracer of fracking fluid (Warner et al., 2014).

6.1.5 Radiogenic isotopes

The radiogenic isotopes that were analysed in this study were strontium ($^{87}Sr/^{86}Sr$), radon (^{222}Rn) and radium (^{228}Ra and ^{226}Ra). The $^{87}Sr/^{86}Sr$ ratios obtained are internally very consistent and average 0.7112. There are two outliers within the deep groundwater samples, Trompsburg VFB1 and Florisbad FLS1, which have higher ratios: $^{87}Sr/^{86}Sr$ ratios of 0.77719

and 0.75392 respectively. Whether these two deep sites in the northern part of the study area signify a change to a different geological environment is not clear at this stage. Because of the lack of clear differentiation between the deep and shallow groups (Figure 31), $^{87}Sr/^{86}Sr$ does not appear to be a useful determinand of water type.

In contrast, radon (as ^{222}Rn) is a good separator of water type with deep water having <10 Bq/L Rn and shallow water 14-163 Bq/L Rn (Figure 5.41). Radium as (^{228}Ra and ^{226}Ra), on the other hand, has activities less than 0.02 Bq/L with no distinction between deep and shallow (Appendix 6). Note that only six samples were analysed for radium because of the extremely low concentrations that were found in the first samples. Although the data are very limited, there is no indication that spring water transports any radioactivity from deep levels. The large difference between ^{222}Rn and its mother isotope, ^{226}Ra (ratio 200-30 000) indicates that all of the radon is unsupported by radium in the water, and that radon in the deep groundwater samples originate instead from radium precipitated on the aquifer material close to the sampling point. Evidently there is very little radium available there, since most of its parent isotope, uranium, has been deposited much earlier along the flow path when the water became anoxic.

6.1.6 Radioactive isotopes

The levels of the radioactive isotopes analysed in this study all pointed to the deep groundwater group being older, with low tritium, low ^{14}C and low $^{36}Cl/Cl$. In terms of ability to differentiate, the most successful was the $^{36}Cl/Cl$ ratio (Figure 5.21). All the deep sites had $^{36}Cl/Cl$ ratios less than 100 ($x10^{-15}$) with the exception of site CRS1 from the Cradock Spa which had a ratio of 126 ($x10^{-15}$). However, all the shallow and mixed sites had $^{36}Cl/Cl$ ratios above 100 ($x10^{-15}$). In comparison, ^{14}C values for the four deep sites that were analysed were less than 60 pmC while the shallow sites were all above 70 pmC. However, the mixed sites were both above and below these values. Setting a boundary value of 60 pmC would successfully classify all the deep sites and the shallow sites but the mixed sites would be ambiguous. Tritium (^{3}H) values were harder to define in terms of deep versus shallow and a single tritium value to identify deep water cannot be defined (Figure 5.47). Using a boundary value of 0.7 TU (to include the highest 0.5 ± 0.2 TU) would exclude all of the shallow sites except the Venterstad site RRB1. It would however, also include all but one site from the mixed group.

These “discrepancies” between the different time-related indicators could well be related to the choice of flow model used to interpret them (Talma & Weaver, 2003). The simplest model is that a sample represents water all with the same travel time, which can then justly be

called the “age” of the sample. The dating concept is implicit in most of the discussion on water flow because it is the easiest to conceptualise. This has been shown to be valid in certain confined aquifers and in primary aquifers where depth-defined samples could be taken. The next level is a two-component mixing of a “young” water and an “older” water which is more applicable in some hard-rock aquifers. In the case of conservative tracers, the mixing components would simply plot on a straight line between the two end members. If the mixing components are tracers that are not conservative, as in radioactive isotopes and reactive trace elements, then more complex modelling is required. A widely applied general mixing model is the exponential model where a mixture consists of contributions of water from all ages (Zuber, 1994; Mook, 2006). It is also called a box model (having constant in- and outflow). This is a popular model to use in our hard-rock aquifers (Talma et al., 2000; Talma and Weaver, 2002; Butler & Verhagen, 2013). It provides the opportunity to accommodate the presence of a small amount of a young parameter mixed in an old water. The example of tritium and ^{14}C from this project’s data reflects this model (Figure 5.14).

6.1.7 Dissolved gases

The distinctive dissolved gases in these samples appear to be ^{4}He, ^{3}He and CH_4 (see section 5.2.18 and 5.2.19). Nitrogen, argon, oxygen and carbon dioxide were also analysed as part of this run (Appendix 6), but the data were not deemed to be useful within the aims of the current project. ^{4}He showed high values in the deep samples and low in the shallow ones (Figure 5.47A). ^{3}He (expressed as the ratio R/R_0) decreases from 1 to near-zero in deep water (Figure 5.47). Methane increases from low to high values going from shallow to deep water (Figure 5.49) and is well correlated with helium (Figures 5.51 and 6.6). This fits in with the model that increasing residence times underground increase the opportunity for helium and methane (from whatever source) to be added to groundwater. The results of four gas samples (FLB5, RRB1, CRS1 and BFB1) do not fit this classification scheme. Figure 6.7 includes data from early work in the Venterstad area (Vogel et al., 1980) where a similar correlation between ^{4}He, CH_4, ^{14}C and groundwater chemistry was found.

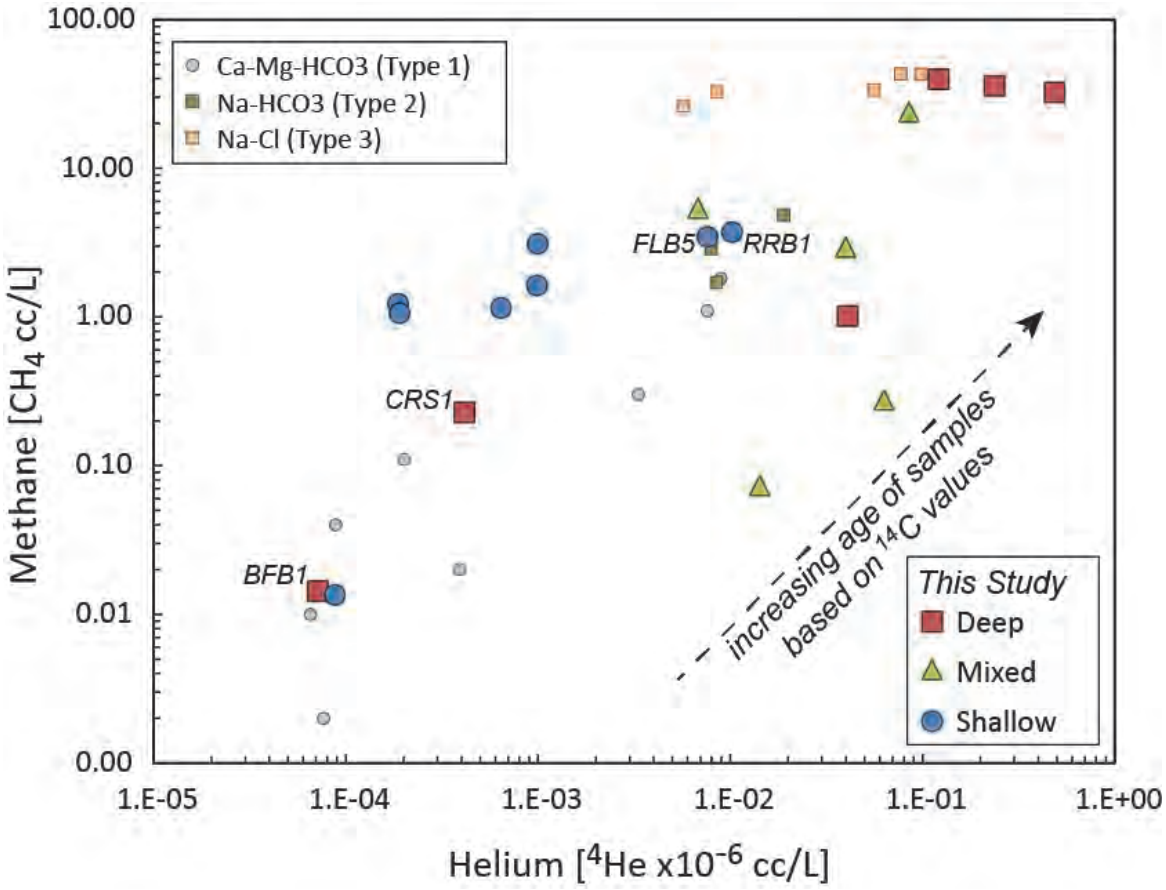

Figure 6.6. Plot of methane against ^{4}Helium for data in the present project. The small markers show data from an early study near Venterstad where water was classified according to chemical type (Vogel et al., 1980).

6.2 Development of a Classification Matrix

From the above discussion of the data produced during this project, it is evident that the deep water indicators that were employed are reasonably successful although the specific characterisation of each water source may differ. However, dealing with a wide spectrum of parameters, from the mundane to the exotic, made a simple statistical approach impossible. An attempt was therefore made to demonstrate the effectiveness of each of the determinands presented in Chapter 5 and discussed above to identify deep water. Table 6.1 lists 22 determinands analysed in this study and assigns a criterion for each determinand that would successfully classify as many deep sites as possible while excluding shallow sites and mixed sites. Because of the good correlation between $\delta^{18}O$ and $\delta^{2}H$, either could be used in this classification. In this report $\delta^{18}O$ has been used.

The classification of deep, shallow and mixed sites is the same as outlined in Chapter 5, Section 5.1 using temperature, Stiff diagram shape and ^{14}C and resulted in the identification of 7 deep groundwater sites, 8 shallow groundwater sites and 5 mixed groundwater sites. For each of the deep and shallow groundwater sites three columns are presented. The first two columns are the same for deep and shallow groundwater sites and are: (1) the number of samples that conform to the criteria (#conform), and (2) the number of samples which don't conform to the criteria (#except). The third column (ID) gives the confidence of classification expressed as a ratio of the number of samples that conform to the criteria. For the deep groundwater sites the value of this ratio should ideally be 1 meaning that all the sites conform to the criteria. For the shallow sites, the ratio is the number of samples that don't conform to the deep groundwater criteria. If the value is also 1 for the shallow groundwater sites, it implies that that particularly criterion is effective at separating the shallow from the deep groundwater sites. The fourth column gives the exception sources, i.e. the sites that do not conform to the deep groundwater criterion for a specific determinand. The last two columns show the number of sites in the mixed group that do, or do not, conform to the deep water criterion. As expected these numbers show an inconsistent pattern. $\delta^{13}C$ for TIC and CH_4, $^{87}Sr/^{86}Sr$ ratios and ^{36}Cl (as concentration) do not appear in the classification system because the values found in this project do not differ significantly between the different classes.

Table 6.1. Separation matrix using 22 determinands identified in this study as possible indicators of deep groundwater. See the above text for an explanation of this table.

		DEEP GROUNDWATER SITES				SHALLOW GROUNDWATER SITES				MIXED GROUND-WATER SITES	
Determinands	**Deep groundwater criteria**	**#conform**	**#except**	**ID**	**exception sources**	**#conform**	**#except**	**ID**	**exception sources**	**#conform**	**#except**
^{14}C (pmC)	<60	5	0	1		0	8	1		2	2
$\delta^{18}O$ (‰ SMOW)	<-6	6	0	1		0	8	1		0	5
F^- (mg/L)	>3	6	0	1		0	8	1		3	2
$\%Na^+$	>70	7	0	1		0	8	1		4	1
Mg^{2+} (mg/L)	<10	7	0	1		0	8	1		5	0
U (µg/L)	<0.05	7	0	1		0	8	1		2	3
Alkalinity (HCO_3- mg/L)	<100	6	0	1		0	8	1		0	5
B (µg/L)	>300	7	0	1		1	7	0.88	DRB4	5	0
V (µg/L)	<1	6	0	1		1	7	0.88	MWB2	5	0
Li (µg/L)	>100	6	0	1		1	7	0.88	MWB2	4	1
$\delta^{11}B$ (‰)	<+30	6	0	1		1	3	0.75	MWB2	5	0
NO_3^- (mg/L)	<1	6	0	1		4	4	0.5	WP502 DRB4 RWB5 MWB2	5	0
$^{36}Cl/Cl$ ($x10^{-15}$)	<100	5	1	0.83	CRS1	0	7	1		0	5
^{222}Rn (Bq/L)	<10	5	1	0.83	ANBH1	0	8	1		3	2
H_2S ($x10^{-6}$ cc/L)	>1	5	1	0.83	ANBH1	0	8	1		5	0
^3H (TU)	<1	5	1	0.83	FLS1	1	7	0.88	RRB1	5	0
Na^+ (mg/L)	>300	5	2	0.71	CRS1 BFB1	0	8	1		0	5
pH	>9	5	2	0.71	ANBH1 SA1/66	0	8	1		0	5
^4He ($x10^{-6}$ cc/L)	>30 000	4	2	0.67	CRS1 BFB1	0	8	1		3	2
$^3He/^4He$ (R/R_0)	<0.1	4	2	0.67	CRS1 BFB1	1	7	0.88	RRB1	5	0
Temp. (°C)	>25	4	3	0.57	BFB1 ANBH1 SA1/66	0	8	1		2	3
CH_4 (cc/L)	>10	3	3	0.5	CRS1 BFB1 VFB1	0	8	1		1	4

From Table 6.1 it is clear that there are seven determinands that successfully classified both all the deep sites as deep and all the shallow sites as shallow, assuming we accept that the deep and shallow classification based on temperature, Stiff diagram and ^{14}C is correct. Note that this can be considered correct in the sense that the deep and shallow sites represent two different groundwater types. These seven determinands are ^{14}C, $\delta^{18}O$, F^-, %Na, Mg^{2+}, U, and alkalinity. Of these ^{14}C, $\delta^{18}O$, F^-, and Mg^{2+} were identified as possible indicators of deep groundwater in Section 2.3. Sodium was highlighted as a possible indicator of deep groundwater but we concluded that %Na is more useful than Na^+ concentration *per se* (see Figure 5.24).

A further seven determinands had only one exception in either the classification of the deep sites or the shallow sites. These determinands are B, V, Li, $^{36}Cl/Cl$ ratio, radon, H_2S and $\delta^{11}B$. Of these only Li and the $^{36}Cl/Cl$ ratio were identified in Section 2.3 as possible indicators of deep groundwater. The remaining possible indicators highlighted in Section 2.3 were temperature, He, NO_3^-, and tritium. Of these tritium and ^4He classified two sites incorrectly, whereas temperature and NO_3^- classified 3 or more sites incorrectly.

From this we can see that U and alkalinity are important indicators of possible deep groundwater that were not identified as such at the start of this study. In both cases, the anoxic reducing conditions of deep groundwater serve to remove U and alkalinity from groundwater and differentiate them from shallow groundwaters. B and V concentrations, radon levels, H_2S concentrations and $\delta^{11}B$ ratios have also proved to be effective at differentiating deep from shallow groundwater, with only one exception each.

The less-performing indicators in Table 6.1 need to be looked at with care, since they may provide essential information. While not all deep water reaches the surface as warm water, an abnormally high temperature is a sufficient reason to classify a site as deep. Inversely, nitrate is absent in all deep water but only in some shallow water. Therefore low (<1 mg/L NO_3) nitrate is a necessary condition for identifying deep water, but not sufficient. At the same time the identities of the non-conforming sources can reveal something useful. ANBH1 is a borehole close to Aliwal North Spa (ANS1). It has most of the characteristics of the spa water, except for loss of H_2S, pH and temperature while gaining magnesium and radon. These are all explainable as the opposite of the processes that caused the original values of these parameters. The Soekor borehole SA1/66 is a deep borehole that used to be artesian, but has now stopped flowing thereby acquiring the temperature of its surroundings. The explanations for the other outliers (BFB1, CRS1, FLS1) are not clear yet.

6.3 Classification of Mixed Samples

As shown in Table 5.1, five of the sites selected for detailed analysis in the second sampling round could not be classified as either deep or shallow on the basis of temperature, Stiff diagram shape and ^{14}C value. These sites were labelled “mixed” and this label has been used throughout Chapter 5 and 6. There are three possible origins for these samples: (1) the samples are either deep or shallow samples that have been wrongly identified; (2) the samples represent genuine mixtures of deep and shallow groundwater; or (3) they could be a completely different groundwater type with a different origin altogether. To test which of these is the more likely explanation, the mixed samples were assessed against how many of the deep groundwater indicators they conformed with. Table 6.2 shows the results for the mixed groundwater sites. The third column labelled “ID” is the ratio of the number of sites that conformed to the deep water criteria to the total number of mixed sites. Again a value of 1 indicates that all the mixed sites conformed to that particular criterion. To clarify which sites met which criteria, a “D” indicates that the site conformed to that particular criterion whereas a blank indicates that it did not. All the sites identified as mixed sites conformed to 14 out of 22 deep water indicators, giving a net conformation ratio of 0.64. This would suggest that in fact the mixed sites are true mixtures and not actually mislabelled deep or shallow sites.

There are a large number of deep groundwater indicators for which all five mixed sites conformed to deep water criteria. However, what is interesting is that only one of these, magnesium, is one of the seven determinands identified in section 6.2 that successfully classified all the deep and all the shallow sites. Many of the determinands that suggest the mixed sites are deep, were actually poor at classifying the actual deep sites as deep. Conversely, many of the deep groundwater indicators that were successful at classifying the deep sites did not classify the mixed sites as deep. This leads to the conclusion that many of the mixed sites are actually deep groundwater that has mixed with shallow or that are transient waters moving from shallow aquifer systems to deeper aquifer systems. Some determinands strongly suggest the influence of mixing such as the relationship between tritium, ^{14}C and $^{36}Cl/Cl$ (see Figures 5.12, 5.14 and 5.48). Quantification of such mixtures is difficult, since pre- or post-mixing chemical changes may change the patterns. None of the “mixed” class of samples has enough positive ID’s to be classed as either deep or shallow. The identification of samples in Section 6.1 therefore appears robust.

Table 6.2. Separation matrix using 22 determinands identified in this study to examine the nature of the mixed sites.

Determinands	Deep water criteria	ID	Mixed samples: DEEP?				
			WP508	WP505	BFB2	RWB1C	VBB1
Mg (mg/L)	<10	1	D	D	D	D	D
B (µg/L)	>300	1	D	D	D	D	D
V (µg/L)	<1	1	D	D	D	D	D
$\delta^{11}B$ (‰)	<+30	1	D	D	D	D	D
NO_3^- (mg/L)	<1	1	D	D	D	D	D
H_2S ($x10^{-6}$ cc/L)	>1	1	D	D	D	D	D
^3H (TU)	<1	1	D	D	D	D	D
$^3He/^4He$ (R/R_0)	<0.1	1	D	D	D	D	D
%Na	>70%	0.8	D	D		D	D
Li (µg/L)	>100	0.8	D	D	D	D	
F^- (mg/L)	>3	0.6		D	D		D
^{222}Rn (Bq/L)	<10	0.6	D	D	D		
^4He ($x10^{-6}$ cc/L)	>30 000	0.6		D	D	D	
^{14}C (pmC)	<60	0.5	D				D
U (µg/L)	<0.05	0.4				D	D
Temp. (°C)	>25	0.4	D			D	
CH_4 (cc/L)	>10	0.2			D		
$\delta^{18}O$ (‰ SMOW)	<-6	0					
Alkalinity (HCO_3- mg/L)	<100	0					
$^{36}Cl/Cl$ ($x10^{-15}$)	<100	0					
Na (mg/L)	>300	1	D	D	D	D	D
pH	>9	0					
Total of deep water IDs			14/22	14/22	14/22	14/22	14/22

D = deep

6.4 Statistical strength of the matrix

The matrix developed above is based on 22 determinands and 20 sampling sites grouped into three categories. The sample size is not sufficiently large to test statistically how robust this matrix is. In addition, whilst the three groups, deep, shallow and mixed, can in many cases be distinguished from each other, the variation within each group is large enough to make calculation of any statistical analysis of each group meaningless. To illustrate this Figure 6.7 shows the range and median for the deep, shallow and mixed samples for each of the seven determinands that successfully classified both the deep and shallow sites. It is

clear that whilst the median is distinct for the deep, shallow and mixed samples, the total range in values for each determinand in many cases overlaps and somewhat reduces the potential effectiveness of the classification scheme. However, much of the overlap lies within the mixed samples and the deep and shallow samples are usually distinct from one another. There is only one exception to this and that is with fluoride where the highest value for the shallow samples and the lowest value for the deep samples overlap slightly. It is important to note that the ranges defined here are based on a very limited number of samples (at most 8). Given the overall success of the classification scheme for differentiating deep versus shallow groundwaters, ongoing work that would increase the population of the dataset would likely further refine and delineate these ranges. This would make the classification scheme more robust and more applicable to ongoing groundwater monitoring studies.

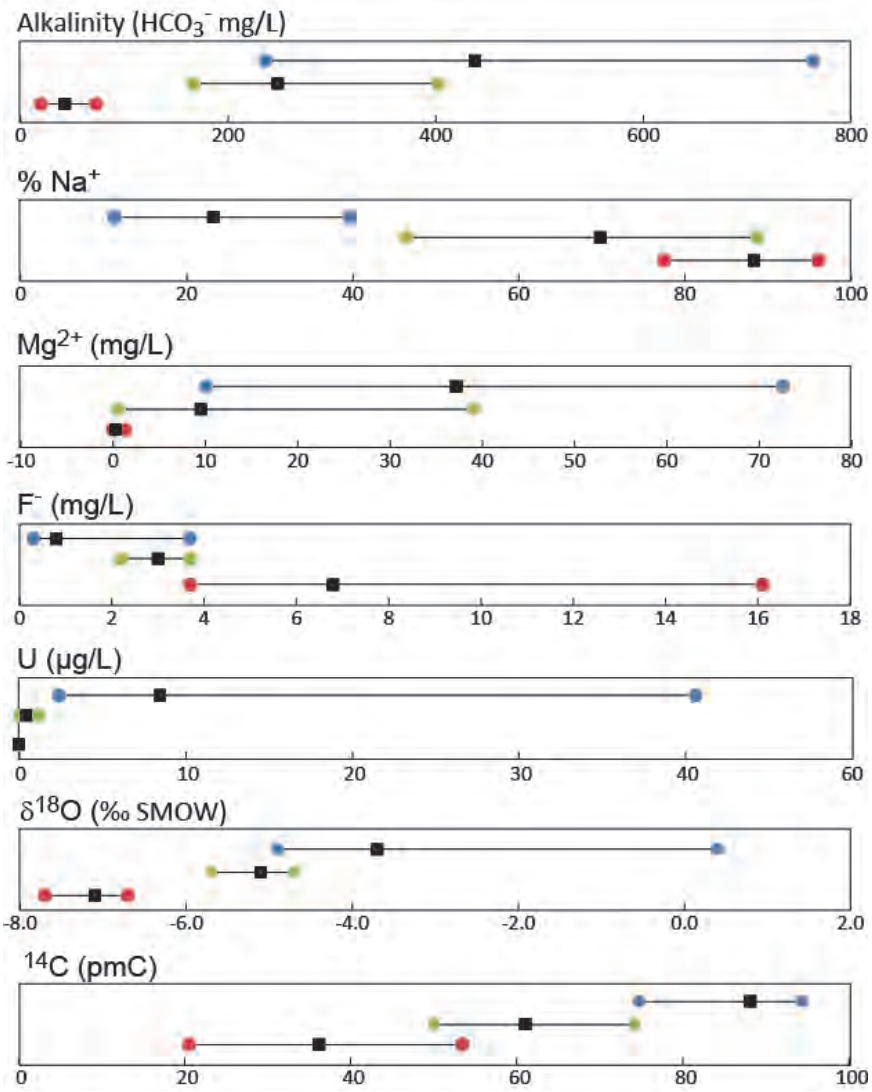

Figure 6.7. Diagrams indicating the ranges and medians of the seven parameters that are most successful to identify deep as well as shallow water

6.5 Testing matrix against other data

The data presented in Chapter 5 and discussed in Chapter 6 above are all from the 19 sites that were sampled during the more detailed (winter) sampling run in June/July 2014 when more parameters were employed. The 18 sites that had been sampled only in March 2014 (Appendix 4), but not in June/July, represent a number of analyses worth investigating. This geochemical dataset, although not as complete in terms of all the determinands analysed, provides a means of testing the classification matrix that has been developed. Table 6.3 shows the geochemical determinands that were collected for the first sampling round along with the deep groundwater criteria that was established in Section 6.2 (Table 6.1). The table shows the number of samples that conform or not to the parameter limits used and the success rate. The last column lists the sites that conform to the deep groundwater criteria. If the classification scheme works successfully, then the more often a site is listed in this last column, the more likely the site represents deep groundwater.

A quick inspection of the conforming sites indicates that FLB4 and DRB2 seem to meet most of the deep groundwater criteria, with success rates of 11/13 and 8/13 respectively. The Stiff diagrams for these two samples (Figure 6.8) indicate the characteristic “Y” shape thereby confirming that they can likely be classified as deep, even with the limited parameter list employed during the first sampling trip. Conversely, for a site that does not meet the deep groundwater criteria (for example MWB1: not listed in the column of conforming sites), the Stiff diagram is the characteristic hexagonal shape of a shallow sample. It therefore seems reasonable to conclude that the classification matrix employed to classify deep and shallow sites is fairly robust.

Table 6.3. Classification matrix for sites sampled only during the first (summer) sampling round

	Deep water criteria	#conform	#except	ID	Conforming sites
Temp. (°C)	>25	2	16	0.11	ANS2, FLB4
$\delta^{18}O$ (‰ SMOW)	<-6	1	17	0.06	DRB4
%Na	>70%	5	13	0.28	WP507, DRB2, DRB1, ANS2, FLB4
Mg^{2+} (mg/L)	<10	6	12	0.33	WP507, WP506, DRB2, DRB1, ANS2, FLB4
U (µg/L)	<0.05	4	14	0.22	DRB2, DRB1, ANS2, FLB4
Alkalinity (mg HCO_3/L)	<100	4	14	0.22	DRB2, DRB1, ANS2, FLB4
B (µg/L)	>300	8	10	0.44	WP507, WP497, WP496, DRB2, DRB1, ANS2, WVB3, FLB4
V (µg/L)	<1	11	7	0.61	WP497, WP496, DB11a, WVB1, WVB3, VBB2, LRB2, VFB3, VFB4
Li (µg/L)	>100	10	8	0.56	WP507, WP506, WP497, WP496, DRB2, DRB1, ANS2, WVB3, FLB4, MWB1
NO_3 (mg/L)$^-$	<1	6	12	0.33	WP507, WP506, DRB2, DRB1, ANS2, FLB4
^{222}Rn (Bq/L)	<10	5	11	0.31	WP 507, ANS2, LRB1, FLB4, MWB1
Na^+ (mg/L)	>300	4	14	0.22	WP497, WP496, ANS2, FLB4
pH	>9	4	14	0.22	DRB2, DRB1, ANS2, FLB4

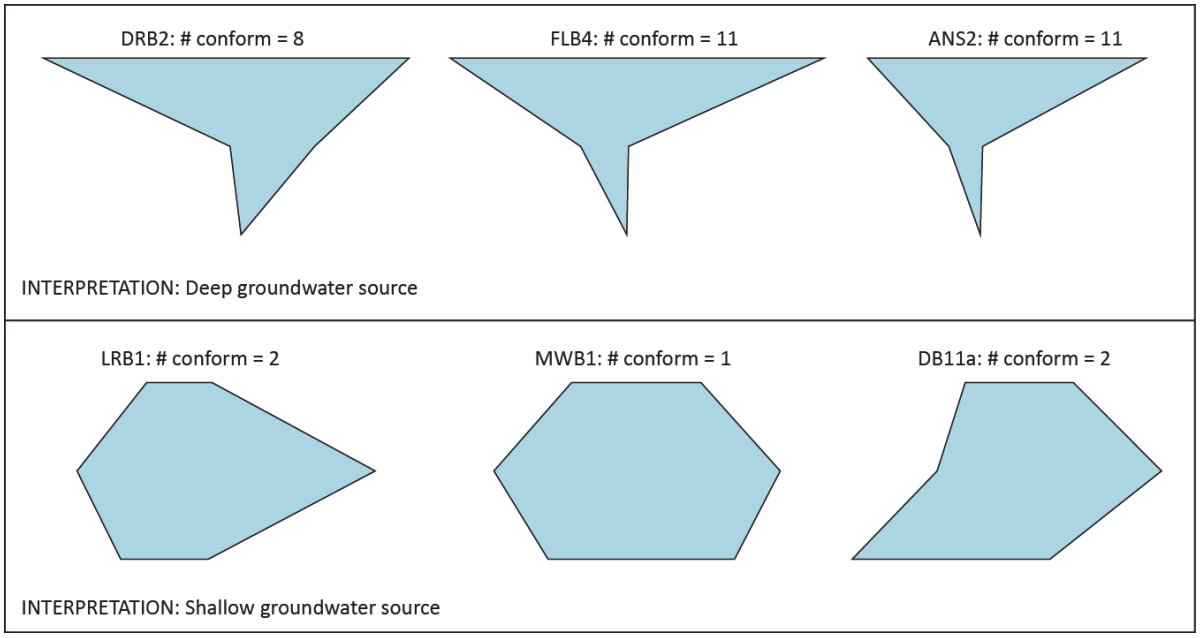

Figure 6.8. Stiff diagrams for some of the additional sites shown in Table 6.3

6.6 Best Indicators of Deep Groundwater

For operational and exploratory purposes, there are a number of other factors besides scientific strength that come into play when determining which parameters are the most useful and practical indicators of deep groundwater. The most important of these are: (1) cost per analysis; (2) sampling difficulty; (3) the time needed for analysis; and (4) the availability of suitable analytical laboratories in South Africa. Table 6.4 is an attempt to produce a score card weighting these different factors. It provides an evaluation of these individual factors by giving them a (subjective) weight, based on the experience of the authors.

Table 6.4. Ranking of all determinands in the classification matrix for prioritisation in long term monitoring of deep groundwater in the Karoo (lower scores are more favourable)

	Success at differentiating deep (total no. of exceptions + 1)	Cost	Sampling Difficulty	Time for analysis	Availability in South Africa	SUM – lower score is better
F^-	1	1	1	2	1	6
%Na	1	1	1	2	1	6
Alkalinity	1	1	2	1	1	6
H_2S*	2	1	1	1	1	6
Mg^{2+}	1	2	1	2	1	7
U	1	2	1	2	1	7
pH	3	1	1	1	1	7
B	2	2	1	2	1	8
V	2	2	1	2	1	8
Li	2	2	1	2	1	8
Temp	4	1	1	1	1	8
$\delta^{18}O$	1	2	1	2	2	8
NO_3^-	4	1	1	2	1	9
^{222}Rn	2	2	3	1	1	9
Na^+	4	1	1	2	1	9
^3H	3	4	1	4	3	15
^{14}C	1	4	4	5	3	17
$\delta^{11}B$	2	4	2	4	5	17
$^{36}Cl/Cl$	2	5	2	4	5	17
^{36}Cl	5	5	1	4	5	20
^4He	3	4	5	5	5	22
$^3He/^4He$	4	4	5	5	5	23
CH^4	4	4	5	5	5	23

** Indicating paper strips can be used for H_2S analysis*

7. CONCLUSIONS AND RECOMMENDATIONS

The central objective of this project was to characterise the chemical composition of deep groundwater in an area considered for shale-gas exploration in the Main Karoo Basin. However, there are no suitable deep boreholes from which deep groundwater can currently be sampled in South Africa. The only two open boreholes that could be located which access the required depths, are the originally 4169 m deep, Soekor borehole SA1/66 near Merweville, and the 1425 m deep borehole VFB1 near Trompsburg, neither of which are ideally suited to represent the geochemistry of the Ecca Group shales.

Direct information on the nature of the groundwater within the (probably methane bearing) deep shales is therefore lacking. The approach taken during this project was to target warm springs on the assumption that they are likely to give an indication of the type of water to be found at greater depths. Leaving this assumption aside, what has been shown are the parameters that develop in mostly warm waters which have been underground for extensive periods. At the current level of groundwater research, these parameters can be considered the best indicators of deep groundwater flow. In the course of the project, some novel (for South Africa) analytical techniques were employed that have proved useful.

The three objectives articulated at the onset of the project, namely i) to characterise deep and shallow groundwaters; ii) to identify determinands that can be used to distinguish these waters; and iii) to list the determinands to be analysed in shale gas development areas, have been addressed and are summarised in the sections below. The reader is however reminded that all the conclusions pertain to a relatively small sample number of water and gas samples derived from sources of unknown depths, and that what is presented here is an attempt to distinguish waters that clearly have significantly different depth flow paths. Nevertheless the data show fairly consistent patterns throughout the vast area of the Main Karoo Basin.

7.1 Basic definition of deep and shallow groundwater

The data and interpretations presented in this report suggest that for the Main Karoo Basin it is possible to define a “deep” or warm groundwater, which is distinct from a “shallow” or cold groundwater. For the purposes of this report, deep and shallow groundwaters were defined as follows:

- Deep Groundwater:
    - ”Y” shaped Stiff diagram
    - Low ^{14}C value
    - Temperature > 25°C (but not always the case)

- Shallow Groundwater:
    - Hexagonal shaped Stiff diagram
    - High ^{14}C value
    - Cold temperature < 25°C

7.2 Characterisation of deep and shallow groundwater in the Main Karoo Basin

To fully characterise the deep groundwater, warm springs and boreholes were sampled and analysed using a wide suite of hydrochemistry, isotopes and gases. Cold boreholes in the vicinity of the warm springs and boreholes were sampled as examples of shallow groundwaters. Of the 20 sites selected for detailed analysis, seven could be confidently classified as deep or warm groundwater and eight could be confidently classified as shallow or cold groundwater.

Deep groundwater can be characterised as:

- An anaerobic NaCl water type that may be warm (>25°C) but does not have to be.
- An older water characterised by low tritium and ^{14}C and by low $^{36}Cl/Cl$ and $^{3}He/^{4}He$ ratios.
- Very low nitrate as a result of denitrification.
- Low magnesium, probably due to ion exchange reactions with the aquifer matrix.
- Lower $\delta^{18}O$ and $\delta^{2}H$ than those in shallow groundwater.
- Low alkalinity possibly due to precipitation of $CaCO_3$ at higher pH.
- Low uranium and vanadium (and maybe other metals) as a result of anoxic conditions.
- Very low radon and radium as a result of low uranium concentrations in deep groundwater.
- Relatively high fluoride, possibly as a result of long term dissolution of fluorite and concomitant partial removal of calcium.
- Relatively high methane and helium gas concentrations.
- Relatively high boron levels.

Shallow groundwater can be characterised as:

- An aerobic $Ca.Mg.HCO_3$ water type that is <25°C.
- A young water characterised by moderate tritium, high ^{14}C, and higher $^{36}Cl/Cl$ and $^{3}He/^{4}He$ ratios.

- Variable nitrate levels that may be due either to anthropogenic factors or natural nitrification.
- Relatively higher $\delta^{18}O$ and $\delta^{2}H$ ratios due to recent recharge.
- Elevated alkalinity with higher uranium concentrations leading to elevated radon.
- Relatively low fluoride and bromide concentrations.
- Relatively low methane and helium gas concentrations.

Not all of these characteristics need be present in each sample, but the majority should comply.

7.3 Origin of Mixed Samples

Five groundwater sites could not be classified as either deep or shallow and were labelled as mixed. Of the 22 determinands assessed for their ability to assist in the classification of deep groundwater, these mixed sites each met 14 boundary criteria set for classification of deep groundwater but these criteria were not always the same 14. The conclusion drawn from this was that these samples represent true mixtures, with different proportions of shallow and deep groundwater, although other explanations including completely different groundwaters cannot be excluded. Relationships between many determinands, particularly radioactive isotopes, suggest mixing between different chemical components. These processes could possibly be modelled to determine whether these groundwaters are true mixtures of the two end members and what the relative proportions of each end member is. This is also supported by the intermediate position of the mixing samples on the Piper diagram shown in Figure 6.4. Because of the concerns regarding contamination of shallow groundwater by either deep groundwater of poorer quality or by fracking fluids, understanding the formation of these mixed groundwaters and their significance to deep flow systems is of paramount importance. This however, is beyond the scope of this project.

7.4 Deep groundwater indicators

At the beginning of this study, twelve determinands were identified as likely indicators of deep groundwater. These determinands along with additional determinands were analysed and their ability to differentiate deep from shallow groundwater assessed. As could be expected, not only the warm waters proved to be derived from deep or mixed sources, but some cool waters were also found to contain indicators of deep flow. Elevated temperatures certainly indicate deeper flow paths, but cool temperatures do not preclude deep circulation.

While temperature changes are reversible, chemical changes are not necessarily so, and water that reaches the surface from deep still retains most of its chemical character.

Of the original twelve "indicator" determinands, ^{14}C, $\delta^{18}O$, fluoride, percentage sodium (but not mg/L sodium) and magnesium were very successful at differentiating deep from shallow groundwater. However, uranium concentrations and alkalinity, which were not identified in the original list of potential determinands, had the same success rate. The remaining determinands that were analysed had variable success rates. The ability of individual determinands to differentiate deep from shallow groundwater (using the method outlined in Section 6.2) can be grouped based on success rate and these groups are shown in Table 7.1. Groups 1 to 3 would be the first choice in any groundwater monitoring program in the Main Karoo Basin where shale-gas exploration is being considered, with Group 1 being the highest priority. Group 4, whilst not being particularly useful in this study may provide further information on contamination processes after shale-gas development and hence will have their place in future monitoring programs.

Table 7.1. Success rate of different determinands in identifying deep groundwater.

Group	Success Rate	Specific Determinands
Group 1	100% success rate	^{14}C, $\delta^{18}O$ (or $\delta^{2}H$), fluoride, %sodium, magnesium, uranium, alkalinity
Group 2	>75% success rate	Boron, vanadium, lithium, $\delta^{11}B$, $^{36}Cl/Cl$, ^{222}Radon, H_2S
Group 3	50-75% success rate	Sodium, pH, tritium, nitrate, temperature, ^{4}He, $^{3}He/^{4}He$, CH_4
Group 4	< 50% success rate	$^{87}Sr/^{86}Sr$, $\delta^{13}C$, rare earth elements, other trace elements

7.5 Monitoring Recommendations

Taking into account the success rates presented in Table 7.1, cost, availability and ease of analysis, the geochemical parameters were grouped into four sampling categories:

1. **Easy to obtain, cost effective and available in South Africa**
    a. Major cations and anions including nitrate, fluoride and boron
    b. $\delta^{18}O$ and $\delta^{2}H$
    c. Uranium
    d. Alkalinity and pH
    e. Temperature
2. **Relatively easy to obtain and available in South Africa but less useful than the above determinands**
    a. ^{222}Radon
    b. Vanadium and lithium
    c. H_2S
3. **More difficult to analyse, time consuming and higher cost**
    a. ^{14}C and tritium
    b. $^{87}Sr/^{86}Sr$
    c. Rare earth elements
4. **Not currently available in South Africa**
    a. $\delta^{11}B$
    b. $^{36}Cl/Cl$
    c. ^{4}He
    d. $^{3}He/^{4}He$
    e. CH_4.

Since this project used a very limited sample size, it is recommended that all of the above determinands be assessed when aiming to identify deep groundwater sources in the Main Karoo Basin. This will enable the results of this study to be improved upon, and with time, assist in the development of a more comprehensive understanding of the nature of deep Karoo groundwaters.

7.6 Deep water indicators versus tracers of shale gas development

This study focussed on identifying natural constituents of groundwater which can successfully differentiate deep from shallow flow paths and includes most of the

determinands listed in Table 7.1. However, it is important to note that some geochemical parameters that were not found to be useful in differentiating deep from shallow groundwater during this project, such as $^{87}Sr/^{86}Sr$ ratio, Br/Cl ratio $\delta^{13}C$ and $\delta^{7}Li$, might become relevant once the properties of water from the shale bearing formations becomes known. Likewise other determinands including trace elements may prove to be useful once the geochemistry of the deep-seated shales has been developed.

7.7 Future Work

This study makes a few specific points regarding future work:

i. Knowledge of possible deep groundwater flow systems would be vastly improved by drilling deep boreholes to the methane-bearing formations and obtaining and analysing good-quality water and gas samples from all levels.
ii. Small diameter exploration core boreholes that may not be suitable for water sampling should be used to obtain as much hydrogeochemical information as possible. For example, samples from selected depths should be used for leaching tests.
iii. Review and clarification of the sampling and analysis methods to be used in future long-term monitoring programs is advised so that subtle changes in concentrations can be identified and not be lost in analytical noise. As new analytical techniques are introduced to South Africa, quality control of the laboratories will become essential.
iv. The mixed waters presented several anomalous characteristics to both the deep and shallow waters and to some extent do not conform to concepts employed to distinguish shallow and deep water in this project. This may indicate that each situation could be more complex and advanced modelling of chemical and other processes is recommended to understand the groundwater systems.
v. Many of the most interesting determinands for identifying deep groundwater are isotope tracers including tritium, ^{14}C, $\delta^{11}B$ and $^{36}Cl/Cl$. However, South Africa is very limited in its ability to measure some of these isotope systems. Investment in analytical infrastructure is a necessary step in order to be able to effectively undertake long term groundwater monitoring.

8. REFERENCES

Abiye, T. (2013). The use of isotope hydrology to characterise and assess water resources in Southern Africa. Water Resource Commission Report No. TT 570/13.

Aeschbach-Hertig, W., & Solomon, D. (2012). *Noble gas thermometry in groundwater hydrology.* Heidelberg, Germany: Springer.

Aggarwal, P. K., Gat, J. R. and Fröhlich, K. F. O. (2005). Isotopes in the water cycle: Past, present and future of a developing science. Springer, Netherlands, 381 p.

Allen, D. M., Gasby, S. E., & Voormeij, D. A. (2006). Determining the circulation depth of thermal springs in the southern Rocky Mountain Trench, south-eastern British Columbia, Canada using geothermometry and borehole temperature logs. *Hydrogeology Journal*, 159-172.

ANON. (1980). Florisbad wetenskaplike vindplek by uitnemendheid. *Navorsinge van die Nasionale Museum, Bloemfontein, 19*(1), 1-13.

Ballentine, C.J., Burgess, R., Marty, B. (2002). Tracing fluid origin, transport and interaction in the crust. In: Porcelli, D., Ballentine, C.J., Wieler, R. (Eds.). *Noble Gases in Geochemistry and Cosmochemistry. Reviews in Mineralogy & Geochemistry*, pp. 539-614.

Bond, G. W. (1946). A geochemical survey of the underground water supplies of the Union of South Africa. *Memoir Geological Survery South Africa, 41*(1), 216.

Branch, T., Ritter, O., Weckmann, U., Sachsenhofer, R. F., & Schilling, F. (2007). The Whitehill Formation – a high conductivity marker horizon in the Karoo Basin. *South African Journal of Geology*, 465-476.

Cecil, L.D. and Green, J.R. (2000). Radon-222. In: PG Cook & AL Herczeg (eds), Environmental Tracers in Subsurface Hydrology, p 175-194, Kluwer, Boston, 529p

Chevallier, L., Goedhart, M., & Woodford, A. C. (2001). *The influence of dolerite sill and ring complexes on the occurrence of groundwater in Karoo fractured aquifers: a morpho-tectonic approach.* Water Research Commission Report No. 937/1/01.

Clark, I., & Fritz, P. (1997). *Environmental Isotopes in Hydrogeology.* New York: Lewis Publishers.

Cooley, H., & Donnelly, K. (2012). *Hydraulic fracturing and water resources: separating the frack from the fiction.* California, USA: Pacific Institute.

Davis, S., Moysey, S., Cecil, L., & Zreda, M. (2003). Chlorine-36 in groundwater of the United States: empirical data. *Hydrogeological Journal*, 217-227.

Darrah T.H., Vengosh, A., Jackson, R.B., Warner, N.R., Poreda, R.J. (2014). HYPERLINK "http://www.pnas.org/content/111/39/14076.short" \t "_blank" Noble gases identify the mechanisms of fugitive gas contamination in drinking-water wells overlying the Marcellus and Barnett Shales . *Proceedings of the National Academy of Sciences* 111(39) 14076-14081.

Darrah, T.H., Jackson, R.B., Vengosh, A., Warner, N.R., Poreda, R.J. (2015). Noble gas as a geochemical tracer for fugitive gas investigations. *Groundwater* 53(1) 24-28.

Day, J. A. (1993). The major ion chemistry of some southern African saline systems. *Hydrobiologia*(267), 37-59.

Dept. Water Affairs and Forestry (1998). *Quality of Domestic Supplies. Volume 1: Assessment Guide*. Water Research Commission No TT 101/98.

Douglas, R. (2001). The quality of the Florisbad spring-water in relation to the quality of the groundwater and the effects of rainwater. *Water SA, 27*(1), 39-48.

Douglas, R. (2009). *A new perspective on the geohydrological and surface processes controlling the depositional environment at the Florisbad archaeozoological site.* Bloemfontein: Departments of Geology and Geography, University of the Freestate.

Dreyer, T. F. (1938). The archeology of the Florisbad deposits. *Argeologie, Navorsinge van die Nasionale Museum Bloemfontein, 1*(1), 65-77.

Eglington, B.M., Meyer, R. & Talma, A.S. (2001). *Assessment of the effectiveness of Isotope Chemistry for quantifying Acid Rock Drainage contributions from different sources to ground and surface water.* WRC Research Report 647/1/01. Water Research Commission, Pretoria, 72p.

Fröhlich, K. (2013). Dating of old groundwater using uranium isotopes. In: IAEA, Isotope Methods for Dating Old Groundwater. p153-178. International Atomic Energy Agency, Vienna, 356p. Available on the internet.

Garrels, RM, and Christ CM. 1965. Solutions, Minerals and Equilibria. Harper & Row, New York. 480p.

Geel, C., Schulz, H.-M., Booth, P., De Wit, M., & Horsfield, B. (2013). Shale gas characteristics of Permian black shales in South Africa: results from recent drilling in the Ecca Group (Eastern Cape). *Energy Procedia*, 256-265.

Gorody, A., Baldwin, D., & Scott, C. (2005). *Dissolved methane in groundwater, San Juan Basin, La Plata County Colorado.* Integrated Petroleum Environmental Consortium.

Grobler, N., & Loock, J. (1988). The Florisbad mineral spring: Its charactristics and genesis. *Navorsinge van die Nasionale Museum Bloemfontein, 5*(1), 474-485.

Han, D. M., Liang, X., Jin, M. G., Currell, M. J., Song, X. F., & Liu, C. M. (2009). Evaluation of groundwater hydrochemical characteristics and mixing behaviour in the Daving and Qicun geothermal systems, Xinzhou Basin. *Journal of Volcanology and Geothermal Research, 189*(1), 92-104.

Harder, H, 1970. Boron content of sediments as a tool in facies analysis. *Sediment. Geol.*, 4, 153-175.

Healy, D. (2012). *Hydraulic fracturing or "fracking": A short summary of current knowledge and potential environmental impacts.* Ireland: Environmental Protection Agency.

Healy, R. (2010). *Estimating Groundwater Recharge*. Cambridge University Press.

Heaton, T. H. E. and Vogel, J. C. (1979). Gas concentrations and ages of groundwaters in Beaufort Group sediments, South Africa. *Water, SA, 5*(4), 160-170.

Heaton, T.H.E. and Vogel, J.C. (1980). Rate of oxygen removal in some South African groundwaters. Hydrol Sci Bull 25(4):373-377, 1980.

Heaton, T.H.E. (1984). *Rates and sources of ^{4}He accumulation in groundwater*. Hydrol Sci J 29:29-47, 1984.

Heaton, T.H.E., Talma, A.S. and Vogel, J.C. (1983). Origin and History of Nitrate in confined groundwater in the Western Kalahari. J Hydrol 62:243-262, 1983.

Heaton, T. H.E., Talma, A. S. and Vogel, J. C. (1986). Dissolved gas palaeotemperatures and 0-18 variations derived from groundwater near Uitenhage, South Africa. *Quaternary Research, 25*(1), 79-88.

Hobbs, P. J., Lindsay, R., Maherry, A., Matsaya, M., Newman, R. T. & Talha S.A. (2010). *The Use of ^{222}Rn as a Hydrological Tracer in Natural and Polluted Environments.* WRC Research Report 1685/1/10. Water Research Commission, Pretoria, 95p.

Hoffmann, J. R. (1979). *Die chemiese samestelling van warmwaterbronne in Suid- en Suidwes-Afrika.* Pretoria: CSIR Report No. WAT 56A.

Hunt, A.G., Darrah, T.H., Poreda, R.J., (2012). Determining the source and genetic fingerprint of natural gases using noble gas geochemistry: A northern Appalachian Basin case study. AAPG Bulletin, 96(10): 1785-1811.

IAEA (2013). *Isotope methods for Dating Old Groundwater.* International Atomic agency, Vienna, 356p

Johnson, T.M. and De Paolo, D.J. (1994). Interpretation of isotopic data in groundwater-rock systems: model development and application to Sr isotope data from Yucca Mountain. *Water Resources Research* 30, 1571-1587.

Kent, L. E. (1949). The thermal waters of the Union of South Africa and South West Africa . *Transactions of Geological Society fo South Africa, 52*(1), 231-264.

Kent, L. E. (1969). *The thermal waters in the Republic of South Africa, In: Proc. Of Symposium II on mineral and thermal waters of the world, B-overseas countries.* Prague: Report of the 23rd session of the International Geological Conference.

Kent, L. E., Groeneveld, D., & Temperley, B. N. (1966). Thermal springs and groundwaterwater of the Badfontein Valley, Eastern Transvaal. *Annals of the Geological Survey, 5*(1), 129-151.

Knowles, R. (1982). Denitrification. *Microbial Reviews, 46*(1), 43-70.

Kok, T. S. (1992). *Recharge of springs in South Africa, Technical Report.* Pretoria: Department of Water Affairs.

Kulongoski, J. T., Hilton, D. R., & Selaolo, E. T. (2004). Climate variability in the Botswana Kalahari from the late Pleistocene to the present day. *Geophysical Research Letters, 31*(10).

La Moreaux, P. E., & Tanner, J. T. (2001). Springs and bottled waters of the world. Ancient history, source, occurrence, quality and use. *Hydrogeology*, 315.

Loock, J. C., & Grobler, N. J. (1988). The regional geology of Florisbad. *Navorsinge van die Nasionale Museum Bloemfontein*, 489-497.

Lupton, J.E., Craig, H., (1976). Primordial helium in oceanic basalts. *Transactions-American Geophysical Union*, 57(5): 408-408.

Mazor, E. (1991). *Applied Chemical and Isotopic Groundwater Hydrogeology.* NY: Hastled Press New York.

Mazor, E., & Verhagen, B. T. (1983). Dissolved ions, stable and radioactive isotopes and noble gases in thermal waters of South Africa. *Journal of Hydrology, 63*, 315-329.

Mook, W. G. (2006). *Introduction to Isotope Hydrology.* London: Taylor & Francis Group.

Mulovhedzi, A., & Tshishonge, V. (2013). *Water Research Commission Project Monitoring Points.* Department of Water Affairs.

Murray, K.S. 1996. Hydrology and geochemistry of thermal waters in the upper Napa Valley, California. *Ground Water* 34(6), 1115-1124.

Murray, R., & Baker, K. (2011). *Groundwater exploration and yield assessment for Matatiele.* Confidential report to Maluti (Pty) Ltd.

Murray, R., Baker, K., Ravenscroft, P., Musekiwa, C., & Dennis , R. (2012). *A groundwater planning toolkit for the Main Karoo Basin: Identifying and quantifying groundwater development options incorporating the concept of wellfeld yields and aquifer firm yields.* Water Research Commission No. 1763/1/11.

Olivier, J., Jonker, C. Z., & Yibas, B. (2012). Characteristics of South African Thermal Springs: Benefits and Risks. Cape Town: South African Geographic Society Conference.

Olivier, J., Van Niekerk, H. J., & Van der Walt, I. J. (2008). Physical and chemical characteristics of thermal springs in the Waterberg Area in Limpopo Province, South Africa. *Water SA, 34*(1), 163-174.

Ozgur N, 2001. Origin of high boron contents of the thermal waters of Kizildere and vicinity, western Anatolia, Turkey. *International Geology Review* 43(10), 910-920.

Phillips, F., & Castro, M. (2003). Groundwater dating and residence-time measurements. *Treatise on Geochemistry, 5*(1), 451-497.

Rossouw, P. J., & De Villiers, J. (1953). *The Geology of the Merweville Area, Cape Province, An Explanation of Sheet 198 (Merweville).* Pretoria: Geological Survey, Department of Mines.

Rowsell, D.M., & De Swardt, A. M. J. (1976). Diagenesis in Cape and Karoo Sediments, South Africa, and its bearing on their hydrocarbon potential. *Transactions of Geological Society of South Africa,* 79, 1, 81-145.

Ryan, J G, and Langmuir, C H, 1993. The systematics of boron abundances in young volcanic rocks. *Geochimica et Cosmochimica Acta*, 57, 1489-1498.

Scanlon, B. (1992). Evaluation of liquid and vapor water flows in desert soils based on Chlorine 36 and Tritium tracers and non-isothermal flow simulations. *Water Resources Research*, 28(1), 285-297.

Sharma, S., Mulder, M. L., Sack, A., Schroeder, K., & Hammack, R. (2014). Isotope approach to assess hydrologic connections during Marcellus Shale drilling. *Groundwater, 52*(3), 424-433.

Schoell, M., 1984. Recent advances in petroleum isotope geochemistry. *Organic Geochemistry*, 6, 645-663.

Schoell, M., 1980. The hydrogen and carbon isotopic composition of methane from natural gases of various origins. *Geochimica et Cosmochimica Acta*, 44(5), 649-661.

Solomon, D.K., Poreda, R.J., Cook, P.G., Hunt, A. (1995). Site characterization using H-3/He-3 groundwater ages, Cape Cod, MA. *Ground Water*, 33(6): 988-996.

Solomon, D.K., Hunt, A., Poreda, R.J. (1996). Source of radiogenic helium 4 in shallow aquifers: Implications for dating young groundwater. *Water Resources Research*, 32(6): 1805-1813.

Stumm, W, Morgan, JJ. 1981. *Aquatic Chemistry*. Wiley-Interscience New York, 780p.

Swistock, B., Sharpe, W., & Robillard, P. (2001). *Hydrogen sulphide (rotten egg odour) in Pennsylvania groundwater wells.* Pennstate Collage of Agricultural Sciences.

Talma, A.S., 1981. Chemical changes in groundwater and their reaction rates. *Transactions of the Geological Society of South Africa*, 84, 99-105.

Talma, A.S. and Esterhuyse, C. (2015). Natural Methane in the Karoo: its occurrence and isotopic clues to its origin. *South African Journal of Geology*, 118(1), 45-54.

Talma, A.S. and Van Wyk, E. (2013). Rainfall and Groundwater Isotope Atlas. In: T Abiye (editor). *The use of Isotope Hydrology to characterize and assess Water Resources in southern Africa*, 83-110. Report TT570/13, Water Research Commission, Pretoria

Talma, A. S. & Weaver, J. (2003). *Evaluation of groundwater flow patterns in fractured rock aquifers using CFCs and isotopes.* WRC Report No 1009/1/03. Water Research Commission, Pretoria.

Tredoux, G. (2009). *Nitrate in groundwater: Why is it a hazard and how to control it?* Stellenbosch: Water Research Commission Report No. TT 410/09. Water Research Commission, Pretoria.

Tredoux G and Kirchner, J (1981). The evolution of the chemical composition of artesian water in the Auob sandstone (Namibia/South Africa). *Transaction of the Geological Society of South Africa,* 84, 169-175.

Tredoux, G and Talma, A. S. (2006). Nitrate pollution of groundwater in southern Africa. In: Xu, Y & Usher, B (Eds), *Groundwater pollution in Africa*, Taylor & Francis/Balkema, Leiden, The Netherlands, pp 15-36, ISBN 10: 0-415-41167-X.

Van Tonder, G., De Lange, F., Steyl, G., & Vermeulen, D. (2013). Potential impacts of fracking on groundwater in the Karoo Basin of South Africa. *Proceedings of the 13th Biennial Conference of the Groundwater Division of the Geological Society of South Africa.* Durban.

van Wyk, E. (2010). *Estimation of episodic groundwater recharge in semi-arid fractured hard rock aquifers.* Ph D thesis, University of the Free State. 272p.

van Wyk, E. (2013). Southern African Pre-Cretaceous Deep Groundwater Flow Regimes: Evidence and Drivers. *Proceedings of the 13th Biennial Conference of the Groundwater Division of the Geological Society of South Africa.* Durban.

Veevers, J. J., Cole, D. I., & Cowan, E. J. (1994). Southern Africa: Karoo Basin and Cape Fold Belt. *Memoir Geological Society of America, 184*(1), 223-279.

Vengosh, A., Heumann, K. G., Juraske, S., & Kasher, R. (1994). Boron Isotope Application for Tracing Sources of Contamination in Groundwater. *Environmental Science and Technology, 28*, 1968-1974.

Vengosh, A., Jackson, R., Warner, N., Darrah, T., & Kondash, A. (2014). A Critical Review of the Risks to Water Resources from Unconventional Shale Gas Development and Hydraulic Fracturing in the United States. *Environmental Science and Technology* , A-O.

Vengosh, A., Warner, N., Jackson, R., & Darrah, T. (2013). The effects of shale gas exploration and hydraulic fracturing on the quality of water resources in the United States. *Procedia Earth and Planetary Science*, 863-866.

Venter, J. S., & Van Wyk, N. A. (2008). *Field report for the Limpopo Field Trip: Hot springs of southern Africa.* Pretoria: Council for Geoscience.

Vermeulen, D. (2013). Unconventional gas- a local and international perspective. Cape Town: Water Research Commission Water Indaba.

Visser, D. J. (1962). Warmbronne in die Omgewing van Venterstad, Kaapprovinsie. *Annals of the Geological Survey*.

Vogel, J. C., Talma, A. S., & Heaton, T. H. (1980). *The isotopic, chemical and dissolved gas concentrations in groundwater near Venterstad, Cape Province.* Pretoria: CSIR Research Report 391.

Vogel, J. C., Talma, A. S., & Heaton, T. H. E., (1980). *The isotopic, chemical and dissolved gas concentrations in groundwater near Beaufort West.* Pretoria: CSIR Research Report 392.

Warner, N., Darrah, T., Jackson, R., Millot, R., Kloppmann, W., & Vengosh, A. (2014). New tracers identify hydraulic fracturing fluids and accidental releases from oil and gas operations. *Environmental Science and Technology*, A-I.

Weaver, J. M., Talma, A. S., & Cave, L. (1999). *Geochemistry and Isotopes for Resource Evaluation in the Fractured Rock Aquifers of the Table Mountain Group.* Water Research Commission Report No 481/1/99.

Weaver, J. M., Talma, A. S., & Cave, L. (2007). *Groundwater Sampling (Second Edition).* Water Research Commission Report No TT 303/07.

Whiticar, M.J., 1996. *Stable isotope geochemistry of coals, humic kerogens and related natural gases.* International Journal of Coal Geology, 32(1), 191-215.

Whittingham, J. K. (1970). *Report on the geohydrological investigations along the route of the Orange Fish River tunnel.* Pretoria: Department of Water Affairs and Forestry. Technical Report GH1545.

Wood, R., Gilbert, P., Sharmina, M., Anderson, K., Footitt, A., Glynn, S., et al. (2011). *Shale gas: a provisional assessment of climate change and environmental impacts.* Manchester, UK: Tyndall Centre.

Woodford, A. C., & Chevallier, L. (2002). *Hydrogeology of the Main Karoo Basin: Current knowledge and future needs.* Pretoria: Water Research Commission No TT 179/02.

Yeatts, D. S. (2006). *Characteristics of thermal springs and the shallow groundwater system at Hot Springs National Park, Arkansas.* US Geological Survey Scientific Investigation Report 2006-5001.

Zuber A., 1994. On calibration and validation of mathematical models for the interpretation of environmental isotope tracer data. In: *Mathematical Models and their Applications to Isotope Studies in Groundwater Hydrology*, IAEA-TECDOC-777, IAEA, Vienna, 11-41. Available on the internet

Zuber A. and Maloszewski P. 2001. Lumped parameter models. In: Yurtsever Y (Ed) . *Environmental Isotopes in the Hydrological Cycle, Volume 6: Modelling*. 5-35, IHP-V, UNESCO, Paris. Available on the internet.

Appendix 1. Soekor Boreholes

Source (excluding coordinates): Rowsell and De Swart (1976)

Borehole	Coordinates*	Elevation (m)	Depth (m)	Groups analysed	Depths analysed (m)	C_{org} range (%)	C_{org} average (%)
KL 1/65#	-32.616879° 20.453519°	729	3 459.5	U. Ecca	131, 1070	0.22-1.25	0.6
QU 1/65	-31.826622° 21.438272°	1 261	2 530.8	Beaufort Ecca Dwyka	564 835-1 495 1 798-1 859	0.16 0.24-0.44 0.92-2.34	0.2 0.4 1.6
AB 1/65#	-31.801610° 22.617491°	1 415	At least 1 745.4	Beaufort Ecca (undifferentiated)	342-557 766-1 490	0.02-0.04 0.08-0.40	0.03 0.3
KA 1/66	-32.013543° 23.425864°	1 036	2 600.6	-	-	-	-
SA 1/66	-32.669644° 21.328557°	741	4 169.4	Beaufort U.& L. Ecca Dwyka	222-1 264 1 617-2 751 2 862-2 898	0.17-0.49 0.34-1.08 0.30-0.42	0.3 0.6 0.4
WE 1/66	-30.898039° 26.839877°	1 532	3 746.3	Beaufort Ecca	1 875-2 242 2 853-3 143	0.04-0.13 0.08-0.33	0.07 0.2
SC 3/67#	-32.773788° 24.299516°	792	5 559.6	U.& L. Ecca	2 439-3 964	0.40-0.71	0.5
KW 1/67	-32.984344° 22.336106°	969	5 554.7	U.& L. Ecca Dwyka	3 142-4 082 4 368	0.70-1.34 4.15	1.0 4.2
VR 1/66	-32.224414° 24.212808°	875	3 947.5	U.& L. Ecca Dwyka	1 341-2 655 2 704	0.12-1.06 3.11	0.6 3.1
CR 1/68#	-32.485465° 25.008708°	793	4 658.0	Ecca (undifferentiated)	2 149-3 645	0.27-1.40	0.6
TU 1/50*	Unknown	Unknown	At least 1 326.2	Beaufort Ecca (undifferentiated)	14 106-884	0.21 0.15-0.45	0.2 0.3

Borehole	Coordinates*	Elevation (m)	Depth (m)	Groups analysed	Depths analysed (m)	C_{org} range (%)	C_{org} average (%)
SW 1/67#	-30.154469° 29.266353°	1 678	1 420.4	U. Ecca	1 372-1 410	0.30-0.42	0.4
GL 1/67	-28.952575° 26.333767°	1 292	2 946.5	-	-	-	-
SP 1/69#	-33.004325° 27.762976°	237	4 557.1	Ecca Dwyka	2 267-3 689 3 704-4 253	0.51-8.57 0.21-1.39	2.4 0.7
LA 1/68	-29.085640° 27.480469°	1 614	Unknown	Beaufort	1 014-1 683	0.02-0.20	0.1
FI 1/72	-28.893711° 27.847709°	1 572	Unknown	U. M. & L. Ecca	1 085-1 590	0.29-18.39	4.0
WI 1/72	-28.708719° 27.688538°	1 695	Unknown	-	-	-	-
MA 1/69*	Unknown	Unknown	1 892.2	Molteno Beaufort U. Ecca	145-327 388-1 376 1 536-1 640	0.31-0.90 0.05-0.54 0.05-0.11	0.6 0.1 0.1
OL 1/69	-32.000244° 19.860426°	Unknown	At least 1 058.2	Ecca Dwyka	7-241 245-363	0.25-9.26 0.26-3.02	4.2 0.8
BE 1/67	-28.677067° 29.386933°	1 151	Unknown	Beaufort U. M. & L. Ecca	20-283 329-1 034	0.68-2.32 0.20-18.83	1.5 2.2
UMG 1 &Ifafa*	Unknown	Unknown	Unknown	L. Ecca and Dwyka	9-224	0.24-3.09	1.7
B10*	Unknown	Unknown	Unknown	U. Ecca	26-81	0.44-0.62	0.5
B11*	Unknown	Unknown	Unknown	U. Ecca	42-102	0.31-0.63	0.5
G9*	Unknown	Unknown	Unknown	L. Ecca	57-73	0.49-0.58	0.5
KC 1/70*	Unknown	Unknown	At least 1 382.3	L. Ecca Dwyka	1 166-1 169 1 362	2.28-2.50 0.48	2.4 0.5
KD 1/71 outcrop*	Unknown	Unknown	Unknown	Ecca	353-1 168	0.20-2.18	0.9
DE 12 Calvinia outcrop*	Unknown	Unknown	N/A	L. Ecca	Surface	0.08-1.18	0.7
Laingsburg*	Unknown	Unknown	N/A	L. Ecca	Surface	0.60	0.6

*exact locations unknown; #boreholes analysed for vitrinite reflectance; U. = Upper; M. = Middle; L. = Lower

Appendix 2. Sampling and analytical procedures

1. SAMPLING PROCEDURES

Sampling was carried out in two field seasons. The first was in March 2014 for two weeks during which eleven locations were visited and 25 borehole and eight spring sites were sampled. After analysing and processing these samples, the number of locations was reduced to eight, and the number of sampling sites reduced to thirteen boreholes and six springs. The eight locations were chosen because of known or suspected deep groundwater flow, and within a few kilometres of these sites, one or two shallow boreholes were selected to represent shallow groundwater in the area. The second sampling session ran over two weeks in June-July 2014. All of the water samples were collected in the same manner, with the exception of the radiocarbon, radon and noble gasses. The collection methods are described in their respective analysis sections.

All boreholes were pumped for at least 30 minutes prior to sampling in order to remove any stagnant water and to ensure that “fresh” groundwater was sampled. The EC was monitored whilst pumping took place and the sample was collected once the EC had stabilized. Once the EC stabilized, pH and temperature were measured using an Extech EC500, ORP was measured using an Extech RE300 probe, and DO was measured using an Extech DO600 probe. All the probes were calibrated on a daily basis. Field alkalinity was determined using a Hach Digital Titrator with Green-Methyl Red and Phenolphthalein indicators. Samples were titrated to a pH of 4.5 using 1.6M sulphuric acid. In all samples total alkalinity was equal to the bicarbonate alkalinity.

Samples for different geochemical purposes were collected directly from the pump discharge. Tritium (^{3}H), ^{14}C and ^{36}Cl samples were collected in HDPE acid washed bottles, whilst cations and anions, Sr, O and H isotopes were collected in PP acid washed conical tubes. With the exception of the ^{3}H and ^{36}Cl samples, all water samples were filtered on site with 0.45µm cellulose acetate filters. ^{36}Cl samples were filtered in the laboratory during processing and tritium samples were not filtered because the samples were distilled. Cation samples were acidified to a pH less than 2 using ultrapure concentrated nitric acid. All samples were kept at less than 4°C in the field and transferred to fridges in the laboratory.

2 ANALYTICAL PROCEDURES

The groundwater samples collected were sent to various laboratories. The analytical procedures, calibration processes and the instruments and standards used for each parameter that was measured are described in their respective sections below.

2.1 Anions and Cations

Major cation and trace element analysis on field acidified samples were performed in the ICP-MS/AES Laboratory of the Central Analytical Facility at Stellenbosch University using an Agilent 7700 ICP-AES and 7700 ICP-MS respectively. Calibration was done according to NIST traceable standards. Anion analysis was performed using a Waters IC-Pak 717 Autosample-conductivity detector-Agillent 1120 pump in the Mass Spectrometry laboratory also of the Central Analytical Facility at Stellenbosch University. Samples were run either as undiluted, diluted x10 or diluted x100 depending on the EC to bring the anion concentration to within range of the standards. Calibration was done using Spectrascan SS-028555 standards and analytical errors did not exceed 10%.

2.2 Stable Isotopes

Stable isotopes of O and H from the first field trip were analysed using a Los Gatos Research (LGR) DT-100 Liquid Water Isotope Laser Analyser in the Centre for Water Resources Research at the University of KwaZulu-Natal. The standard deviation for was less than 0.77‰ for δ^2H and less than 0.2‰ for $\delta^{18}O$. Stable isotopes of O and H from the second field trip were analysed using a Finnigan GasBench II at iThemba LABS at Witwatersrand University in Johannesburg. The standards used are in-house standards which have been calibrated using the international standards SMOW, SLAP and GISP. 200µL of each water sample was placed in 10ml vials along with a platinum catalyst. δ^2H is determined by flushing the samples with 2% H_2 in He, to remove residual air in the vials, and equilibrating the samples with the H_2 gas for forty minutes. After δ^2H is determined, the vials are then flushed with 0.3% CO_2 in He, allowed to equilibrate for 20 hours, and then the $\delta^{18}O$ value is measured. Each sample is measured in duplicate with 10 cycles per analysis. The precision of the instrument is < 1‰ for δ^2H and < 0.06‰ for $\delta^{18}O$ and the standard deviation is 0.2‰ for O and 0.8‰ for H.

2.3 Strontium Isotopes

Strontium isotope ratios were measured on a NuPlasma HR MC-ICP-MS in the Department of Geological Sciences at the University of Cape Town, South Africa. Depending on the Sr concentration, between 1 and 5ml of the sample water was pipetted into a Teflon beaker and dried down at 140°C. Once dry, 2ml of 65% 2B HNO_3 was added to the samples and the samples were again dried down at 140°C. This process was repeated twice after which 1.5ml of 2M HNO_3 was added to each sample. Sr was separated from other elements in cation exchange columns (4mm in diameter and 2.5cm in length) using TRU.Spec resin and washed with 2M 2B HNO_3. The resultant Sr solution is analysed as a 200ppb 0.2% HNO3 solution using the NIST SRM987 standard with the $^{87}Sr/^{86}Sr$ ratio normalized to a value of 0.710255. The data has been corrected for Rb interference using the measured signal for 85Rb and the natural $^{85}Rb/^{87}Rb$ ratio as well as the instrumental mass fractionation using the exponential law and an $^{87}Sr/^{86}Sr$ value of 0.1194.

2.4 Boron Isotopes

Boron isotopes were analysed by thermal ionization mass spectrometer (TIMS) on a Thermo Fisher Triton at the TIMS laboratory at Duke University. $^{11}B/^{10}B$ ratios were collected in negative mode with a signal between 50-900 mV at an ionization temperature between 870°C and 920°C. The average B^{11}/B^{10} of NIST SRM-951 during this study was 4.0055 +/- 0.0015. The long-term standard deviation of $\delta^{11}B$ in the standard through replicate measurements was 0.5‰.

2.5 Radium Isotopes

Radium was extracted from 25 to 50L of sample volume through Mn-oxide fibres and stored in sealed cans. The sealed cans were incubated for at least 3 weeks (to allow Ra^{226} to reach secular equilibrium with its Bi^{214} granddaughter) and each sample was counted in a Canberra DSA2000 broad energy germanium (BEGe) gamma detector in the LEARN facility at Duke University to measure nuclides from the U-Th series. Ra^{226} activities were obtained through the 609keV energy line of its radioactive decay product, Bi^{214} assuming secular equilibrium. Ra^{228} activities were obtained through the 911keV energy line energy line of its radioactive decay product, Ac^{228}. The activities of all these nuclides were calibrated using CCRMP U-Th ore standard DL-1a and Canberra Multi-Gamma ray standard MGS-5C, measured under physical conditions identical to the samples (e.g., can size, grain size).

2.6 Tritium

Tritium concentrations were analysed at iThemba LABS at Witwatersrand University in Johannesburg. The 1000ml samples collected in the field were distilled into round glass container to collect 500 ml of the sample water after which 4g of sodium peroxide was added. The solution is then weighed and then introduced into an electrolytic cell made up of two concentric cells, one inside the other and which are insulated from each other. A direct current of 10-15 ampere at 12V is passed through the cell which is cooled continuously due to heat generation within the cell. After several days the volume is reduced to 20ml, a reduction of 25 times. This reduction corresponds to a tritium enrichment of a factor of about 20. Standards of known tritium concentration are used to confirm the enrichment factor. The 20ml sample goes through a vacuum distillation using a gas flame to heat the sample. The sample is reduced to 10ml and added to 11ml of Ultima Gold LLT LSC cocktail in a counting vial. The final sample is placed into a Packard Tri-Carb 2770TR/SL which is a low level liquid scintillation analyser. The samples are counted for at least 3 cycles of 4 hours to improve analysis accuracy and to eliminate outliers. The results are expressed as tritium units (TU).

2.7 Radiocarbon

For ^{14}C analysis, the volume of water to be processed was determined from the alkalinity such that at least 2 g of C could be collected per sample. For most samples this involved the collection of either 25L or 50L of water. Directly on collection of the water sample 250g of $BaCl_2$, 200ml of 400g/L NaOH solution and 10ml of phenolphthalein indicator were added to each sample. This resulted in the precipitation of $BaCO_3$ which was allowed to settle for 2 hours after which the supernatant was allowed to drain away and the resultant $BaCO_3$ slurry was collected in 1L HDPE bottles. Radiocarbon was analysed via Liquid Scintillation Counting (LSC) at iThemba LABS at Witwatersrand University in Johannesburg. Orthophosphoric acid is added to the $BaCO_3$ slurry collected in the field under vacuum in order to release the C as CO_2 from the $BaCO_3$. Water is removed from the CO_2 using dry ice traps and the resultant "dry" CO_2 is collected in a liquid N_2 (LN_2) trap. The CO_2 was allowed to thaw and expand into the vacuum line. One part of the line is connected to two 10ml ampoules. After the CO_2 expands into these ampoules this part of the line is isolated from the vacuum and the 10ml ampoules are sealed and used for determination of the $\delta^{13}C$ ratio. The other part of the line is connected to a one litre round bottomed flask into which the CO_2 has also expanded. This flask is then isolated from the vacuum and the remaining CO_2 in the line is pumped away. At the same time an LSC glass vial containing 10ml of Carbo-Sorb is attached to the vacuum via a Y connection that is also attached to a 10ml ampoule. Once

vacuum has been reached, the 1L round bottomed flask is then opened and the CO_2 transferred to the 10ml ampoule using a LN_2 trap. When the vacuum has been regained (ie all CO_2 is transferred to the 10ml ampoule) the Y connector is isolated from the vacuum line and the LN_2 trap removed. This allows the CO_2 to thaw and move over to the Carbo-Sorb container. The glass vial containing the Carbo-Sorb is placed in water to cool while it absorbs the CO_2 in an exothermic reaction. The glass vial is also shaken to allow for the full absorption of the CO_2. The glass vial can then be removed and 10ml of Permafluor is added. The sample needs to stand for 2 to 3 weeks before LSC to allow for the full decay of the radon.

Five of the radiocarbon samples were analysed by Accelerator Mass Spectrometer (AMS) at Beta Analytic in Miami, Florida. There are two parts in the process of radiocarbon dating through AMS. The first part involves accelerating the ions to extremely high kinetic energies and the second part involves mass analysis of the atoms. Beta Analytic uses a tandem electrostatic accelerator as opposed to a cyclotron. Once the samples arrived they are prepared for the AMS by converting them into a solid graphite form. This is done by conversion to carbon dioxide with subsequent graphitization in the presence of a metal catalyst. Other elements, such as nitrogen 14, are introduced into the samples when burning the samples in order to convert them to graphite. When the samples have been converted to a few milligrams of solid graphite, they are pressed onto a metal disc. These metal discs are then mounted on a target wheel so they can be analyzed in sequence. At this stage, other negatively charged atoms are unstable and cannot reach the detector. The negatively charged carbon atoms, however, move on to the stripper (a gas or a metal foil) where they lose the electrons and emerge as the triple, positively charged carbon atoms. At this stage, molecules that may be present are eliminated because they cannot exist in this triple charged state. The carbon atoms with triple positive charge further accelerate away from the positive terminal and pass through another set of focusing devices where mass analysis occurs. In mass analysis, a magnetic field is applied to these moving charged particles, which causes the particles to deflect from the path they are travelling. If the charged particles have the same velocity but different masses, as in the case of the carbon isotopes, the heavier particles are deflected least. Detectors at different angles of deflection then count the particles. At the end of an AMS run, data gathered is not only the number of carbon 14 atoms in the sample but also the quantity of carbon 12 and carbon 13. From these data, concentration ratio of the isotopes can be known to allow evaluation of the level of fractionation.

2.8 Chlorine 36

Depending on the Cl concentration, between 45 and 90ml of the sample water was acidified with 2ml of concentrated ultrapure nitric acid and 1ml of a 50mg/ml solution of silver nitrate ($AgNO_3$) was added. The resultant silver chloride (AgCl) precipitate was left to settle inside a cupboard in a dark room due to the light sensitivity of AgCl. After 30 minutes the sample was centrifuged at 3000 rpm for 3 minutes, rinsed with 10ml of milli Q water and centrifuged again at 3000 rpm for 3 minutes. The AgCl precipitate was left to dry overnight in a 60°C oven. Once dry the precipitate was sealed in PP containers and wrapped in foil to exclude light. The concentration of the Cl^{36} isotope was measured via accelerator mass spectrometry at the Australian National University in Canberra Australia in order to differentiate between S^{36} and Cl^{36}, S being one of the major contaminants in water samples Cl^{36} concentrations are expressed as the ratio $^{36}Cl/Cl$. The samples were analysed using accelerated mass spectrometry. This is because sulfur is usually an important components of water and only large accelerators have high enough energies to differentiate between S^{36} and Cl^{36} at very low concentrations (typically 10^{-10} to 10^{-13} ppm).The results are given as a ratio of $^{36}Cl/Cl$, where Cl^{36} is the radioactive isotope and Cl is the total concentration of Cl.

2.9 Radon

Samples were collected from the closest take off point from the borehole or spring once the flow rate had stabilised and laminar flow was dominant. The samples were collected in two 250ml glass flasks that were rinsed with the sample water and then filled to overflowing before capping to minimize trapped air. The concentration of radon in the water samples was measured using Durridge RAD-7 alpha-spectroscopy detectors. Three detectors, two on each sampling trip, were used in the course of this study to provide quality control on each analysis and to independently assess the operation of the detectors. The RAD-7 detectors were prepared for each measurement by purging the system (open and closed) and lowering the relative humidity to below 5%. Radon concentrations were measured using the WAT-250 protocol involving a 5 minute closed loop aeration step, a 5 minute extraction step and then a 5 to 10 minute radon concentration counting step. A 5 minute radon concentration counting step was used in the first sampling trip whilst a 10 minute radon concentration counting step was used in the second sampling trip. For both sampling trips the radon counting step was repeated in 4 cycles giving a total radon concentration count time of 20 minutes for the first sampling trip and 40 minutes for the second sampling trip. All measurements are performed within 4 to 6 hours of sampling and therefore decay corrections are not applicable.

2.10 Noble Gases

The samples were collected directly from the springs or wellheads, or as close to the wellhead as possible. Before attaching the sampling line to the wellhead, the Swagelok fittings are securely tightened and the NPT fitting is wrapped with HOPE/Teflon tape. Once the sampling line is secure, the NPT fitting is tightened to the pressure-release valve and attach the sampling line. The sample cylinder and regulator are set to open positions as the pressure release valve is slowly opened to allow the water to start flowing. The flow of the sample water is increased to ~40 psi (front pressure) for a few minutes. The front line pressure did not exceed 70 psi. The valve on the exiting side of the sampling line is then closed in order for the line to pressurize. This is repeated five times in order to flush the static dead-volume leaks from the sampling valves. After the line has been pressurized, each of the valves in the sampling line are slightly opened and closed five times (known as exercising the valves) starting with the pressure-release valve on the wellhead and moving toward the water discharge exit. Once the valves have been exercised the outermost valve on the stainless steel cylinder is closed, immediately followed by the other valve on the cylinder. After both valves are securely tightened the pressure-release valve is opened to eliminate any pressure that may have built up. After the line has equilibrated with atmospheric pressure, the valves on the cylinder are secured using electrical tape and end caps are attached.

The samples were analysed at Ohio State University, USA under the guidance of Dr T Darrah. The concentrations of N_2, O_2 and Ar were measured from the headspace using a Shimadzu 15A gas chromatograph (GC) equipped with a 10-m-long 5A molecular sieve column and a thermal conductivity detector (TCD). Hydrocarbons, including CH_4, were analyzed using a Shimadzu 14A GC equipped with a 10-m-long stainless steel column (Φ, 2 mm) packed with a Chromosorb PAW 80/100 mesh coated with a 23% SP 1700, and a flame ionization detector (FID). The carbon dioxide (CO_2) composition is determined by separating the alkaline solution from the solid precipitate by centrifugation to determine: 1) CO_2 as CO_3^{2-} by titration (Metrohm Basic Titrino) with a 0.5 N HCl solution; and 2) H_2S by first oxidizing CdS to SO_4^{2-} with H_2O_2 and then using ion chromatography (Tedesco, 1994; Montegrossi et al., 2001; Tassi et al., 2010, 2011). The analytical uncertainty for all reported data was b5%. The carbon isotopic composition ($^{13}C/^{12}C$) of CO_2 (hereafter expressed as $\delta^{13}C–CO_2$ ‰ (per mil) V-PDB) was determined by adding ~5 mL anhydrous phosphoric acid to 2 mL of the soda solution under vacuum and allowing the emanated CO_2 to equilibrate at 25±0.1°C in a thermal bath overnight. The extracted CO_2 was then purified using liquid N_2 and N_2-trichloroethylene cryogenic traps, and analyzed using a Finnigan Delta S mass spectrometer.

We used internal (Carrara and San Vincenzo marbles) and international 18 (NBS18, limestone, and NBS19, carbonate) standards to estimate the external precision. The analytical precision and reproducibility were ±0.05‰ and 0.1‰, respectively (Capaccioni et al., 2011; Aguilera et al., 2012). The isotopic composition of N_2 was determined on the residual gases by coupling a GC (Agilent Technologies 6890 N) with the Finnigan Delta S MS. The GC is equipped with a molecular sieve column (MS 5 Å capillary, 30 m×0.53 mm×50 μm; He carrier gas), TCD detector and a post column switching device (Denswitch), which is able to split the column gas flow to the TCD detector and to the MS. The ion beam focuses masses 28, 29 and 30 on the three cups using a jump calibration procedure taking into account any hysteresis of the magnet. The analytical procedure allows simultaneous determination of ^{36}Ar, ^{40}Ar, O_2, N_2, CH_4 and $\delta^{15}N$ (Chiodini et al., 2012). Noble gas elemental and isotopic compositions were analyzed at the University of Rochester Rare Gas Facility. Prior to gas analysis, a 77 μcm^3 air standard at STP was used to tune mass calibrations, minimize formation of doubly charged species (e.g. $^{40}Ar^{2+}$ and CO_2^{2+}), and quantify isobaric interferences on neon isotopes as b3%. Ne isotopic composition was corrected by measuring [$^{40}Ar^+$] and [CO_2^+] and subtracting the quantified production ratio for each doubly charged species by methods reported previously (Poreda and Farley, 1992; Darrah and Poreda, in press). Other potential interferences, including HF and H_2O were similarly monitored for and corrected. The elemental and isotopic analyses of helium (He), neon (Ne), argon (Ar), and krypton (Kr) gases were carried out on a VG 5400 mass spectrometer by methods described previously (Poreda and Farley, 1992; Darrah and Poreda, in press; Hunt et al., in press). For noble gas isotope analysis, the gas samples were purified in a high vacuum line constructed of stainless steel and Corning-1724 glass to minimize helium diffusion. Water vapour and CO_2 were cryogenically trapped at −90°C and −195°C, respectively. Bulk gases (N_2 and O_2) were purified by consecutive exposure to a Zr–Al getter (SAES ST-707) held at 450°C and a SAES SORB-AC cartridge held at 250°C then cooled to 25°C in an activated charcoal cold finger. This was followed by the sequential trapping of Ar into an activated charcoal finger at liquid nitrogen temperatures and He and Ne into an activated charcoal cold finger at 12K. The helium was released from the cryogenic finger at 31K and expanded into the spectrometer and measured, followed by Ne and Ar analyses (e.g. Poreda and Farley, 1992; Darrah and Poreda, in press). He, Ne, Ar, and Kr concentrations were determined by comparison to an air standard of known volume (0.77 cm^3 of air at STP) to an accuracy of ±3%. Average blank levels were 1×10−10 cm^3 for 4 He, 2×10^{-16} cm^3 for 3 He, and 1×10^{-11} cm^3 for ^{22}Ne. Sample errors were propagated quadratically (square root of the sum of individual errors squared) and include sample standard deviation, mass estimation, and external precision. The 1σ variation on standards of comparable concentration was 1.5% for

^{4}He and 4.5% for ^{3}He on average, respectively. The helium (^{3}He/ ^{4}He) isotope ratios (hereafter expressed as R/Ra ratios, where R is the ^{3} He/^{4}He measured ratio and Ra is the ^{3}He/^{4}He ratio of the air: 1.39 $\times 10^{-6}$) (Clarke et al., 1969) were normalized to Yellowstone Park standard (MM) with ^{3}He/^{4}He =16.5±0.1 times the air ratio (as measured in five noble gas laboratories) using a Yellowstone Park standard (RMM/RA= [^{3}He/^{4}He MM]/[^{3}He/^{4}He air]) (Poreda and Farley, 1992). SAES-ST-101 getters reduced the HD+ background to ~1000 ions/s. The VG 5400 noble gas mass spectrometer is fitted with a Johnston electron multiplier with pulse counting electronics on the axial collector (Poreda and Farley, 1992). Mass resolution of 550 (m/Δm) enabled complete baseline separation of the ^{3}He^{+} and HD+ peaks. The measured ^{3}He/^{4}He ratios were corrected for the addition of air (monitoring ^{4}He/^{22}Ne), by assuming that the fumarolic Ne is low and of atmospheric origin (Craig and Lupton, 1976; Sano and Wakita, 1988; Sano et al., 1988). Analytical error for the R/Ra determination was ≤0.3%. Sensitivity for the Ar concentrations was about 4 × 10^{-4} A/Torr on the Faraday cup (resolution 200 (m/Δm)), while precision for the ^{40}Ar/^{36}Ar ratios averaged at 0.3%.

Bibliography

Aguilera, F., Tassi, F., Darrah, T., Moune, S., & Vaselli, O. (2012). Geochemical model of a magmatic-hydrothermal system at the Lastarria volcanom northern Chile. Bulletin of Volcanology, 74(1), 119-134.

Capaccioni, B., Aguilera, F., Tassi, F., Darrah, T., Poreda, R. J., & Vaselli, O. (2011). Geochemical and isotopic evidences of magmatic inputs in the hydrothermal reservoir feeding the fumarolic discharges of Tacora volcano (northern Chile). Journal of Volcanology and Geothermal Research, 208(3-4), 77-85.

Chiodini, G., Caliro, S., Lowenstern, J., Evans, W., Bergfeld, D., Tassi, F., & Tedesco, D. (2012). Insights from fumarole gas geochemistry on the origin of hydrothermal fluids on the Yellowstone Plateau. Geochemica et Cosmochimca Acta, 89(1), 265-278.

Clarke, W. B., Beg, M. A., & Craig, H. (1969). . Excess 3He in the sea: evidence for terrestrial primordial helium. Earth and Planetary Science Letters, 6(1), 213-220.

Craig, H., & Lupton, J. E. (1976). Primordial neon, helium, and hydrogen in oceanic basalts. Earth and Planetary Science Letters, 31(3), 369-385.

Darrah, T. H., & Poreda, R. J. (In Press). Evaluating the accretion of meteoric debris and interplanetary dust particles in the GPC-3 sediment core using noble gas and mineralogical tracers. Geochemica et Cosmochimica Acta, 84(1), 329-352.

Hunt, A. G., Darrah, T. H., & Poreda, R. J. (In Press). Determining the source of genetic fingerprint of natural gases using noble gas geochemistry: A northern Appalachian Basin case study. American Association of petroluem Geologists, 96(10), 1785-1811.

Montegrossi, G., Tassi, F., Vaselli, O., Buccianti, A., & Garofalo, K. (2001). Sulfur species in volcanic gases. Analytical Chemistry, 73(15), 3709-3715.

Poreda, R. J., & Farley, K. A. (1992). Rare gases in Samoan xenoliths. Earth and Planetary Science Letters, 113(1-2), 129-144.

Sano, Y., & Wakita, H. (1988). Precise measurement of helium-isotopes in terrestrial gases. Bulletin of the Chemical Society of Japan, 61(4), 1153-1157.

Sano, Y., Wakita, H., & Xu, S. (1988). Atmospheric helium isotope ratio. Geochemical Journal, 22(4), 177-181.

Tassi, F., Aguilera, F., Darrah, T., Vaselli, O., Capaccioni, B., Poreda, R. J., & Delgado, A. (2010). Fluid geochemistry of hydrothermal systems in the Arica-Parinacota, Tarapaca and Antofagasta regions (northern Chile). Journal of Volcanology and Geothermal Research, 192(1-2), 1-15.

Tassi, F., Aguilera, F., Vaselli, O., Darrah, T., & Medina, E. (2011). Gas discharges from four remote volcanoes in northern Chile (Putana, Olca, Irruputuncu and Alitar): a geochemical survey. Annals of Geophysics, 54(2), 121-136.

Tedesco, D. (1994). Chemical and isotopic gas emissions at Campi Flegrei—evidence for an aborted period of unrest. Journal of Geophysical Research-Solid Earth (B8), 15623-15631.

Appendix 3. Location Characterisation and Final Site Selection

1. INTRODUCTION

The following sections outline the specific characteristics of each study location. The hydrogeological setting, historical water quality assessments, a description of the location as well as the processes of selecting the specific sampling sites within the locations are discussed. The field data (temperature, electrical conductivity, pH, alkalinity and the presence of H_2S gas identified by a strong or weak smell of sulphur) and major ion chemistry, including B, Sr and Li, collected during the first round of sampling are presented in tables and piper diagrams. The number of sites sampled during the second sampling round was reduced from the first sampling round. Therefore, using the preliminary data, the decisions on which sites to sample during the second sampling round were made.

Six of the 8 sampling sites selected for research in this project were previously assessed by Kent (1949) when he sampled 25 thermal boreholes and springs across South Africa. The remaining two sampling sites were previously assessed by Mazor and Verhagen (1983) after sampling 16 thermal springs throughout South Africa in 1971. $\delta^{18}O$ and $\delta^{2}H$, tritium, radiocarbon, as well as dissolved ionic species were analysed in this study.

2. FLORISBAD

The Florisbad site, about 50km north-west of Bloemfontein, is diverse in archaeology, palaeontology and geology, and hosts the Florisbad Quaternary Research Department of the National Museum. The site is registered on the Department of Water Affairs' (DWA) Water Management System (WMS) database, WMS 171921. A considerable amount of research is being conducted on the fossil remains on the site, and over the years a few studies have been made on the water quality. The main land use in the area is agricultural, with wheat, maize and sunflower being the predominant crops.

The site sits at the boundary of the C52G and C52H quaternary catchments which have a mean annual precipitation (MAP) of 481 and 455 mm/a respectively. The spring actually consists of several eyes which appear to occur in a structurally controlled east-west orientation.

Figure 1: Florisbad spring pool and ~10cm diameter pipes at the base of the pool from which the spring flow discharges into the pool.

2.1 Hydrogeological setting

At the surface are Quaternary aeolian sand deposits and calcretes which are underlain by Beaufort and Ecca Group sediments (predominantly shales, siltstones and sandstones). Within 5 km of the springs numerous dolerite sills and dykes outcrop, and these would also be prominent at depth throughout this area. At the spring site Grobler and Loock (1988) located a north-west plunging dolerite sill, and in 1938 Dreyer (1338) uncovered a dyke in an excavation. It appears as if the location of the springs and reason for the up-welling of the water is due to presence of these dolerite intrusions. The basement rocks of the area are the lavas of the Ventersdorp Supergroup, and these overly older granites and gneisses (Loock and Grobler (1988). The Ecca Group shales mentioned above overly these basement rocks.

The location of the recharge area that feeds the Florisbad spring is not known. Grobler and Loock (1988) suggested that the recharge area may be some 30 km north of Florisbad at Basberg where Beaufort Group sandstones outcrop 150 m above Florisbad. However, they also considered that intake area may be south-east of Florisbad, in the hills north of Bloemfontein. While it is uncertain where the spring flow originates, rainfall is likely to enter Karoo sedimentary rocks some distance from Florisbad (at higher elevation), migrate several hundred meters into the subsurface and flow towards the lower-lying area around the springs. The flow is quite likely along preferential pathways which are governed by the location and orientation of the dolerite intrusive. At some point below the springs the groundwater is blocked by either an impermeable dolerite sill or dyke, or by impermeable sedimentary rocks adjacent to a dolerite intrusion, and the water flows to the surface.

The recorded flows from the springs vary considerably with Kent (1948) measuring 44 L/s and Grobler and Loock (1988) measuring 5.2 L/s. It has been suggested that seismic activity has played a role in the flow rate of the spring over time, as well as in the migration of spring

eyes. During the September 1912 earthquake at Fauresmith, apparently a new spring eye appeared at Florisbad and the flow was said to have increased, and that gas, sand, artefacts and fossils were expelled from the new eye (Anon, 1980). This observation suggests that the increased secondary permeability associated with the springs may not only be a result of dolerite intrusions, but is likely to also be linked to localised seismic activity with associated geologic reactivation.

The Florisbad Quaternary Research Station was established at this site due to its archaeological significance. Numerous research papers and reports have been written on this site, and the most recent comprehensive study is the PhD thesis of Douglas (2009), to which the reader is referred, and from which some of the information above has been drawn.

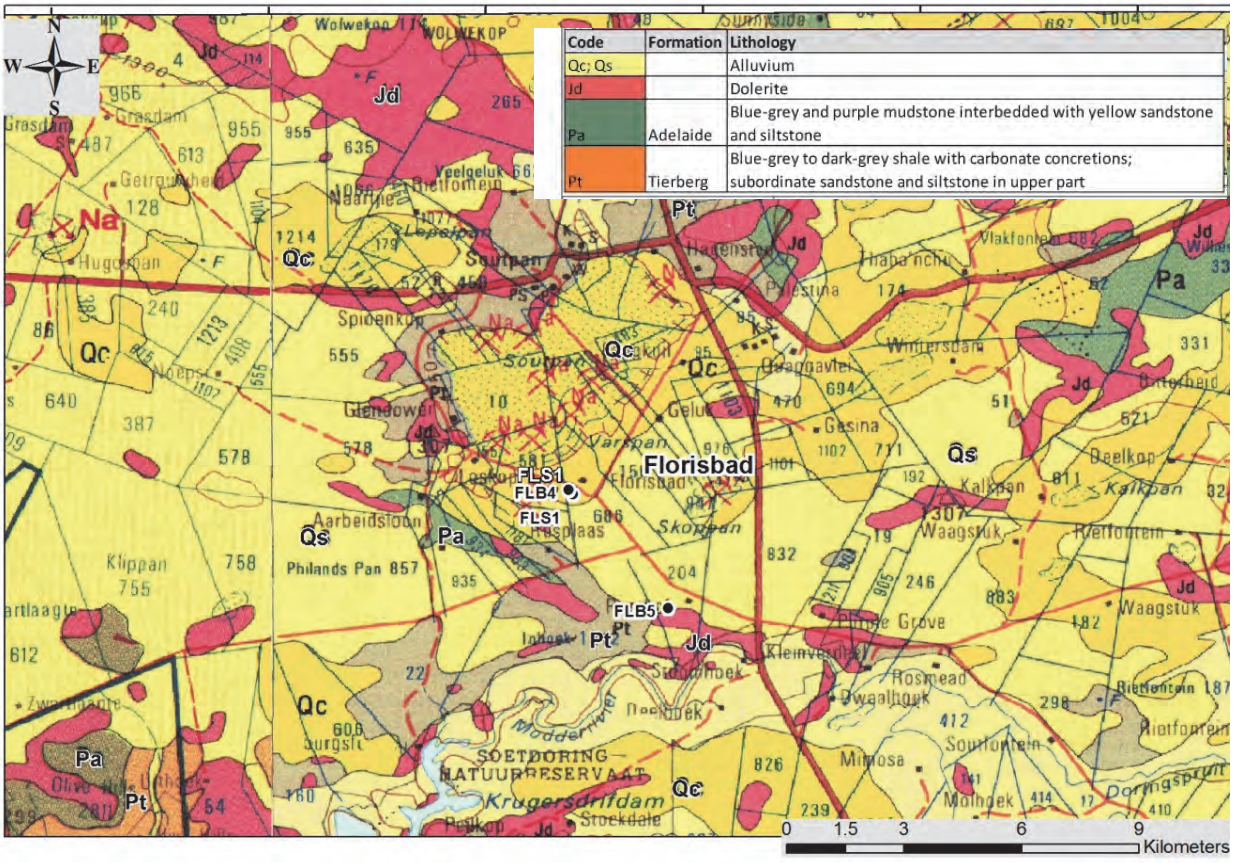

Figure 2: Geological map (1:250 000) of Florisbad including the sampling sites from first and second rounds of sampling.

2.2 Historical water quality assessments

Douglas (2001) studied the spring-water, the groundwater in four surrounding excavation pits and the rainfall in the area. Despite the excavation pits and the spring being only metres apart, the chemistry of the water varied extensively. It was concluded that the spring water was affected slightly through long-term rainfall, and not affected through short-term rainfall (Douglas, 2001). Douglas also measured the variations in the quality of the spring-water over a ten year period from 1988 to 1999. The following parameters were monitored: pH, alkalinity, EC, salinity and major anions and cations. It was noted that the quality of the water was relatively stable during this period (Douglas, 2001).

Historical data from the spring over an 84 year period has been collected by Douglas (2001) as well as Grobler and Loock (1988). The first samples were collected by Rindl in 1916, Fourie in 1970 and Mazor and Verhagen in 1971. It was concluded that the quality of the spring water has remained constant throughout this period (Douglas, 2001). Determinands such as temperature, pH, alkalinity, EC, salinity, major ionic species, trace elements, gases and stable and radioactive isotopes were measured. The results are shown in Table 1.

Table 1: Previous water quality data of the spring in Florisbad. Only a few of the measured parameters are shown in this table.

Source	T	EC	pH	Alk	$\delta^{18}O$	$\delta^{2}H$	^{3}H	^{14}C	Cl	SO_4	Ca	Na	Sr	Li	B
	°C	mS/m		mg/L	‰		TU	pMC	mg/L						
1	29.05														
2	28.88		8.3												
3	29				-6.8	-36.5	0.3								
4		398	9.43												
5	29	388	8.91												
6	26	359	8.6	23					1213.2	173.8	91.8	672.3	2.7	0.9	0.5
7	30	392	8.8	31.2					1375.1	5.4	104.1	777.7			

Sources: *1) Rindl, 1915; 2) Fourie, 1970; 3) Mazor & Verhagen, 1983; 4) Douglas, 2001 (1988); 5) Douglas, 2001 (1999); 6) Olivier, 2012; 7) WMS*

2.3 Location description

Florisbad is located near a large salt pan, Soutpan (Fig. 2). The land is flat with a few small hills. The elevation range between sites is 22m. Two sites were sampled in Florisbad during the first round of sampling: the main spring from the Florisbad pool (FLS1) as the suspected deep site, and a borehole located at the Florisbad Resort adjacent to the spring grounds

(FLB4), as the suspected shallow site (Fig. 2). The field data and major ions, including B, Sr and Li, are shown in Tables 2 and 3 respectively, and the sites are plotted on a piper diagram (Fig. 3).

2.4 Selection of sampling sites

All preliminary results suggest that the groundwater collected from the two sites originate from the same source. The field data as well as the major ion chemistry and the groundwater facies as indicated by the piper diagram (Fig. 3) are almost identical. Both the spring (FLS1) and the borehole water (FLB4) were warm with temperatures of 28.7 and 24.5°C respectively. Therefore, a different source of cold groundwater was collected during the second round of sampling in order to obtain a distinct pair of potential deep and shallow groundwater sources. Firstly, boreholes in the area were located using GIS and secondly the site was identified as cold based on the field measurements. The site that was finally selected was the borehole FLB5 (Figure 2) which has a distinctly different chemistry to the spring (FLS1). Its chemistry is presented in Chapter 5.

Table 2: Field data of the two sites sampled in Florisbad during the first round of sampling.

Sample	Latitude	Longitude	Temp	EC	pH	Alk	H_2S smell
	°S	°E	°C	mS/m		mg/L	
FLS1	28.76819	26.06972	28.7	362	9.5	21.3	N/A
FLB4	28.76718	26.06870	24.5	358	9.5	19.4	weak

Table 3: Major ion plus B, Sr and Li results of the two sites sampled in Florisbad during the first sampling round

Sample	Cl	NO_3	SO_4	Ca	K	Mg	Na	B	Sr	Li
	mg/L							µg/L		
FLS1	1462.7			102.1	9.1	0.1	790.8	2	4.3	0.6
FLB4	1336.6			95.4	5.5	0.1	815.5	2.1	3.7	0.6

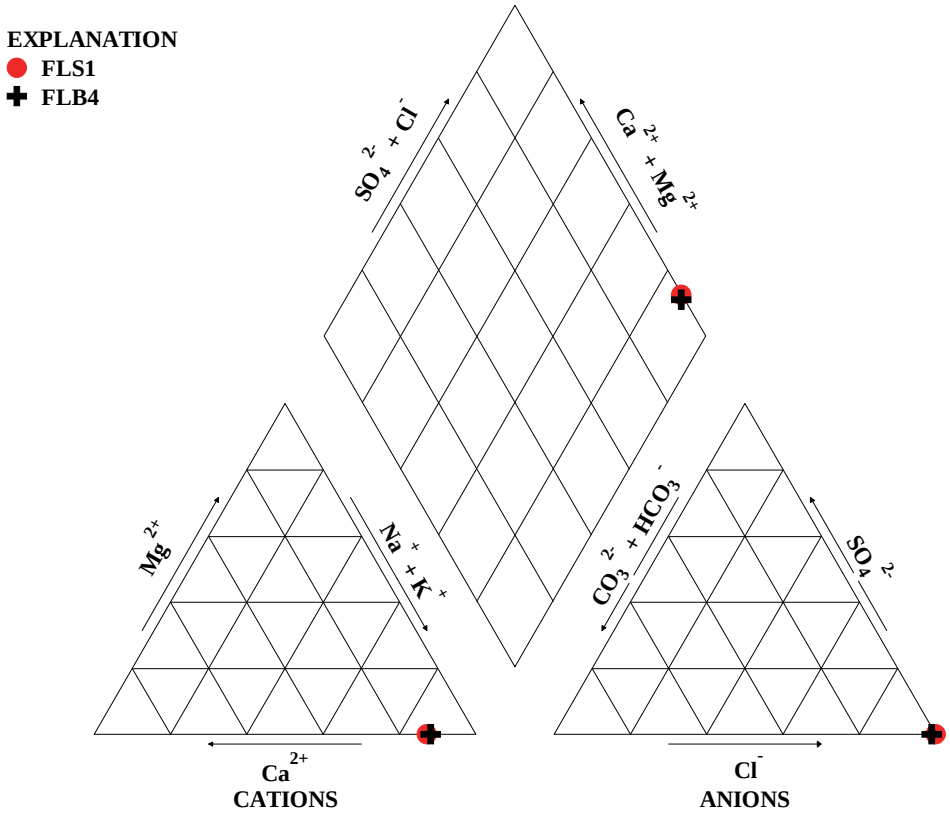

Figure 3: Piper diagram of major ions collected in Florisbad during the first round of sampling.

3. TROMPSBURG

Trompsburg is small agricultural town situated on the N1 between Colesberg and Bloemfontein in the Free State Province. The farm at which the samples were collected is located about 20km north-west of the town.

Figure 4: The Trompsburg artesian borehole (located to the left of the beacon), and discharging into a brick reservoir.

3.1 Hydrogeological setting

In the late 1940s seven core boreholes were drilled in this area (Ortlepp, 1959), one of which is the borehole that was sampled during this project. The drilling records show that the area is underlain by Adelaide Formation sandstones (interbedded with mudstones) of the Beaufort Group to a depth of about 150m; then Ecca Group shales to about 700m; and then a thin lens of Dwyka Formation tillites (<25m thick). These Karoo-age rocks lie unconformably on intrusive gabbro-anorthosite basement rocks which in places have a layer of marble in between. The area has also been intruded by the relatively young Karoo dolerites, dykes, sills and ring structures which are all evident at the surface.

The specific borehole that was sampled during this project is TG1 which was renamed VFB1 for this project (unfortunately the correlation to TG1 was only made near the end of the project). Its position on the geological map is shown in Figure 5 and its lithological log is shown in Figure 6. Water was struck in the mafic basement rocks at a depth of about 1425 m

and it gave an artesian yield of 2.4 L/s. While this site does not strictly represent deep Karoo water, it is only the 2nd very deep borehole that penetrates Karoo rocks and was retained as a study site for the project. Whether the current artesian flow is purely from the mafic basement rocks or whether it contains a portion of deep Karoo water is not known.

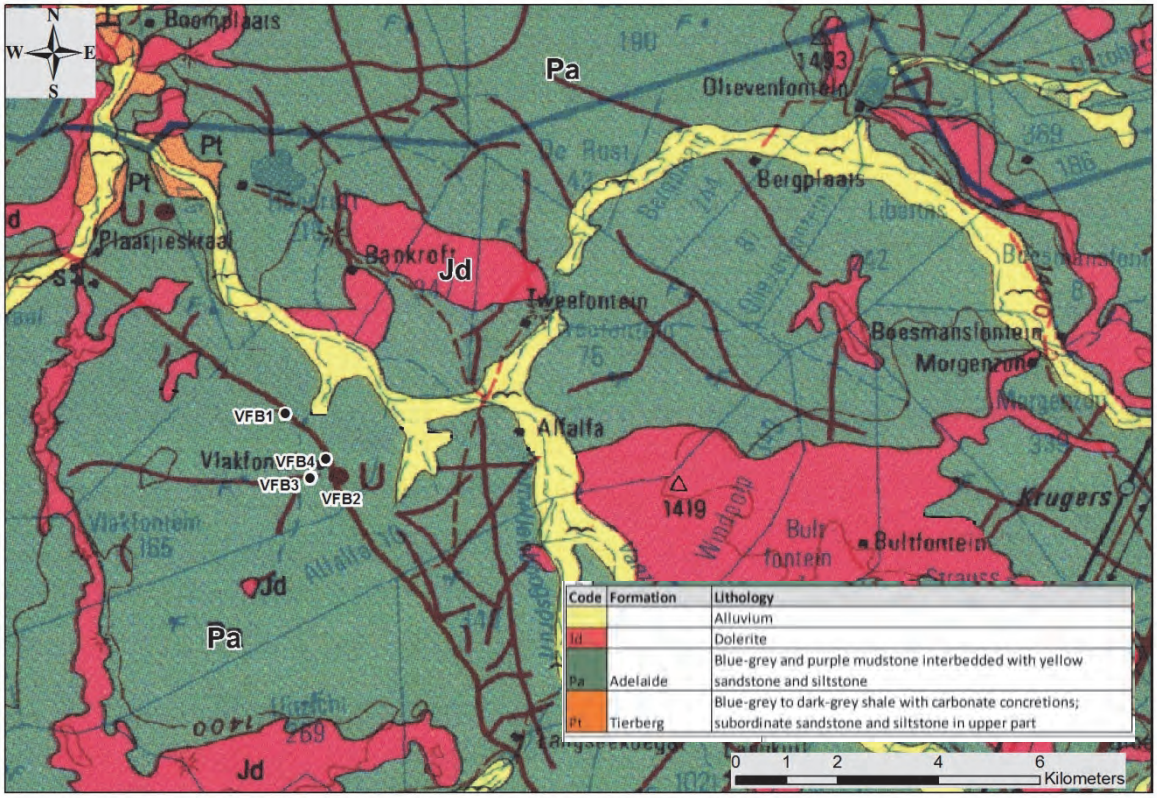

Figure 5: Geological map (1:250 000) of Trompsburg including the sample sites from the first and second rounds of sampling.

Figure 6: Lithological log of the Trompsburg deep artesian borehole VFB1 (originally called TG1).

3.2 Historical water quality assessments

The artesian borehole in Trompsburg was one of the boreholes sampled by Kent (1949). This borehole is situated on a private farm and has only been previously sampled twice before. Kent sampled the borehole in 1948 and the owner of the farm had the borehole analysed in 1981 by Karoostreek.

The groundwater collected in Trompsburg was classified as type 3 at 37.2°C (Kent, 1949). The samples were analysed for major ionic species and trace elements. Elevated concentrations of Li at 9ppm were measured. Table 4 shows the results of all of the analyses.

Table 4: Previous water quality data of the deep artesian borehole in Trompsburg. Only a few of the measure parameters are shown in this table.

Source	T	EC	pH	Alk	$\delta^{18}O$	$\delta^{2}H$	^{3}H	^{14}C	Cl	SO_4	Ca	Na	Sr	Li	B
	°C	mS/m		mg/L	‰		TU	pMC	mg/L						
8	37.2		9						4245.8	946.2	473.2	2665.3	7.2	9	4
9			8.5						4141.8	848.6	505.8	2679.5			

Sources: *8) Kent, 1949; 9) Karoostreek, 1981.*

3.3 Location description

Four sites were sampled on a farm in Trompsburg: an artesian borehole (VFB1) as the suspected deep site, and three shallow boreholes (VFB2, VFB3 and VFB4) each of approximately 30m depth (Fig. 5). The topography of the area is flat with a variation in elevation of about 20m. The field data and major ions, including B, Sr and Li, are shown in Tables 5 and 6 respectively, and the sites are plotted on a piper diagram (Fig. 7).

3.4 Sampling site selection

The preliminary results show that the artesian borehole, VFB1, with a temperature of 30.8°C, has significantly different field measurements and chemistry to that of the three shallow boreholes (VFB2, VFB3 and VFB4) with temperatures of 19.6°, 20.7° and 19.6°C respectively. The groundwater facies as indicated by the piper diagram (Fig. 7) also differ significantly between the suspected deep and shallow sites. Only one source of shallow groundwater was sampled during the second round of sampling. The shallow site most distinct from the deep site with the largest difference in temperature and groundwater facies

indicated by the piper diagram was selected. Therefore, the shallow borehole sampled in the second sampling round was chosen to be VFB2.

Table 5: Field data of the four sites sampled in Trompsburg during the first round of sampling.

Sample	Latitude	Longitude	Temp	EC	pH	Alk	H_2S smell
	°S	°E	°C	mS/m		mg/L	
VFB1	29.91796	25.6749	30.8	1035	9	23.2	weak
VFB2	29.92921	25.67945	19.6	53	7.5	217.2	none
VFB3	29.92939	25.67929	20.7	56	7.5	215.1	none
VFB4	29.92598	25.68213	19.6	102.5	7.1	288.5	none

Table 6: Major ion plus B, Sr and Li results of the four sites sampled in Trompsburg during the first sampling round.

Sample	Cl	NO_3	SO_4	Ca	K	Mg	Na	B	Sr	Li
	mg/L							µg/L		
VFB1	3417.2		953.0	452.6	21.0	0.2	2418.0	3.6	17.8	6.6
VFB2	56.3	12.8	23.5	73.7	2.1	23.5	29.2	0.1	0.6	0.0
VFB3	39.7	16.6	31.4	78.3	1.3	17.6	34.9	0.1	1.6	0.0
VFB4	109.1	58.4	55.3	129.8	2.7	39.7	51.3	0.1	1.2	0.0

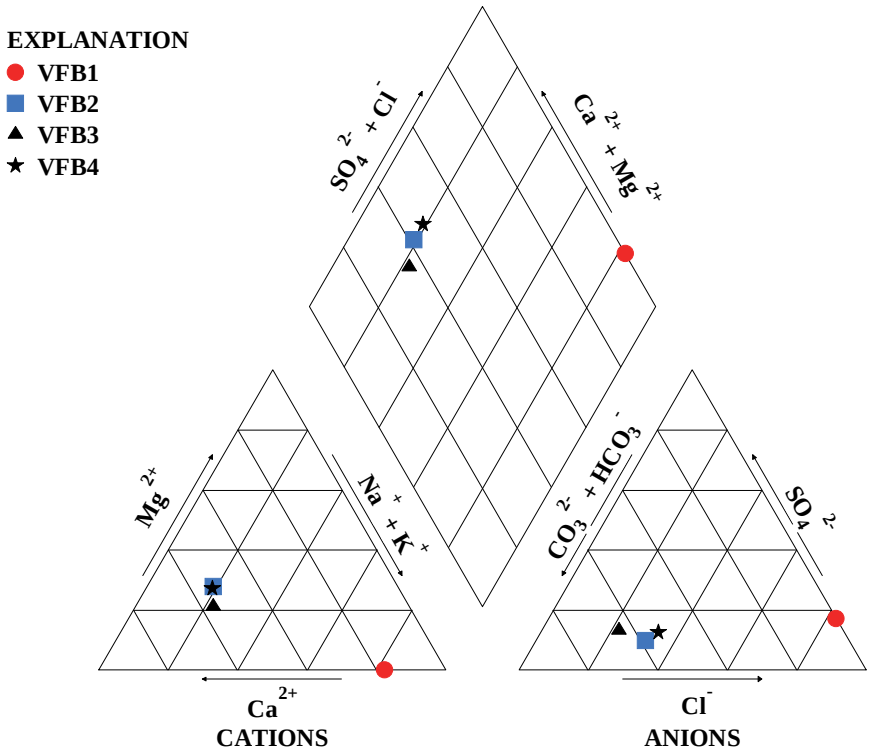

Figure 7: Piper diagram of major ions collected during the first round of sampling in Trompsburg.

4. VENTERSTAD

The small agricultural town of Venterstad is situated approximately 10km south of the Gariep Dam. Thermal springs in the neighbourhood of the town have been used by farmers for years but have now dried up due to groundwater abstraction from boreholes. The three farms on which they are specifically mentioned in the Annals of the Geological Survey (Visser, 1962) were visited during this project.

During and after the construction of the Orange-Fish River tunnel in 1969, a great deal of research was conducted in the area after tunnelling encountered a high in-flow of groundwater. The research showed very different water types, some of which were warm and old, and were considered to contain an element of deep flow (Vogel, et al, 1980). Guided by this information and the information on warm springs in the area, a number of sites within the greater Venterstad area were sampled during this project.

The two sites that were finally selected for detailed analysis are both boreholes adjacent to the old thermal springs mentioned by Visser (1962). They are on the farms Rooiwal and Vaalbank, and the Rooiwal site is listed on the WMS database (WMS 171922). The borehole that was sampled in this study, however, is not necessarily the same borehole as that listed on the WMS database as there are several around the old warm spring.

Figure 8: Possible location of the old Rooiwal warm spring; and sampling the nearby borehole RWB1c.

Figure 9: The borehole that was sampled near the old Vaalbank spring; and the adjacent old stoneworks that may indicate the location of the old, warm spring.

4.1 Hydrogeological setting

The Venterstad area sits in the Tarkastad Formation which consists of interbedded mudstones (predominantly) and sandstones. The area was intensely intruded by Karoo-age dolerites in the forms of dykes, sills and ring structures (Fig. 10). Besides the deformation resulting from the intrusive dolerites, the area may also lie in an east-west trending neotectonic zone (Woodford and Chevallier, 2002). This latter instability, coupled with the dolerites, may account for the high density of localised deep-shallow hydraulic conductivity and the consequent warm springs in this area.

The Vaalbank area, which is the site of an old warm spring (and the sampled site VBB1), sits near the inside margin of a 20km wide dolerite ring structure which is transsected by numerous major dykes. The location of the sampled borehole (which by all accounts is next to the old spring), lies 130m away from a large, north-east trending dyke. Like all other areas, it is not certain where the recharge area is, but it is probable that the location of the spring is associated to this nearby dyke.

The Wildebeest Valley site (DB11a) site also sits in an area dense with dyke intrusions. This specific site is about 800m north of a major east-west trending dyke. Unfortunately the property in which the warm Badsfountain spring occurs, some 4km south of DB11a, was not accessible. The Badsfountain spring itself lies about 2km east of the Orange-Fish River tunnel where a major fracture zone was intercepted that flooded the tunnel (at a rate of ~860

L/s!); and it was postulated that this fracture zone may represent reactivation of an eastward extension of the pre-Karoo Doornberg fault zone that is exposed near Prieska (Vogel, et al, 1980). Based on possibilities of geologic events from pre-Karoo, Karoo-age (dolerties) and neotectonics, it is evident that understanding the nature of deep groundwater flow in this area is a challenging task that would require considerable research.

The Rooiwal warm spring (and sampled borehole RW1c) lies adjacent to a major NE-SW trending dyke which crosses and merges with other dykes. The greater area has also been intruded with sills and ring structures. The spring is 19km east of the Badsfountain thermal spring and may also be the product of more than one intrusive/tectonic event.

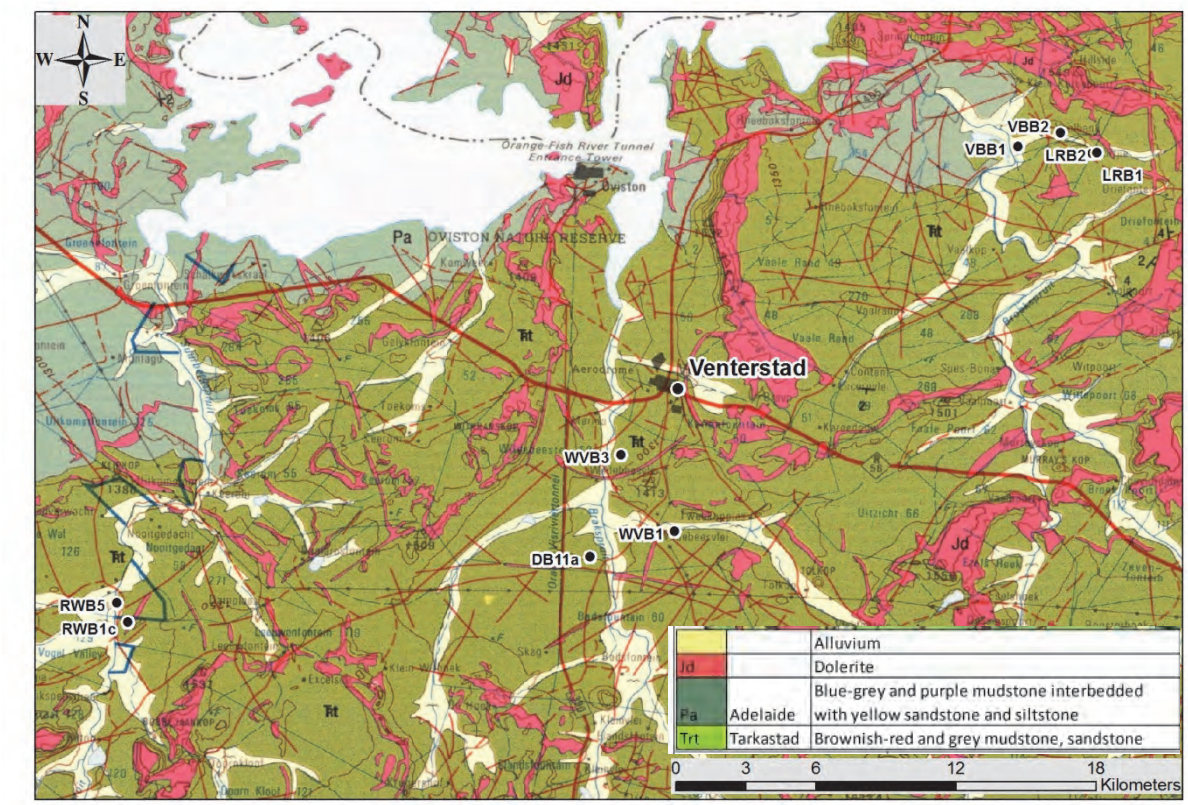

Figure 10: Geological map (1:250 000) of Venterstad including the sampling sites from first and second rounds of sampling.

4.2 Historical water quality assessments

In 1977, 27 boreholes and springs in the Venterstad area were sampled by the CSIR. The groundwater was analysed for major ionic species, ^{14}C, ^{13}C, $\delta^{18}O$, ^{3}H, ^{222}Rn,^{226}Ra and ^{4}He, as well as the dissolved gases oxygen, nitrogen, argon, methane and hydrogen sulphide. The temperature, pH and alkalinity were also monitored (Vogel et al., 1980). A journal article

based on the CSIR report was written by two of the authors (Heaton and Vogel, 1979). One of the 27 boreholes sampled by Vogel et al., (1980) had also been sampled by Kent (1949).

Vogel et al., (1980) classified the groundwater was into three types based on the dissolved ion concentrations. Type 1 is dominated by calcium/magnesium bicarbonate and is of a shallow and recent origin (<20 years). Type 2 is dominated by sodium bicarbonate and type 3 is dominated by sodium chloride. Both type 2 and 3 waters range in age from 800-7500 years and are warm, indicating that they are circulating from depth (Vogel et al., 1980). After assessing the $\delta^{18}O$ values, Vogel et al., (1980) concluded that the three water types have different origins. Heaton and Vogel (1979) noticed a correlation between the temperature and the age of the water, suggesting an increase in age with depth. Elevated He gas levels were associated with high methane concentrations along with high temperatures, suggesting the gas is derived from depth (Heaton & Vogel, 1979). The previous results are shown in Table 7.

Table 7: Previous water quality data of five boreholes in the Venterstad area. Only a few of the measured parameters are shown in this table.

Source	Site	T	EC	pH	Alk	$\delta^{18}O$	$\delta^{2}H$	^{3}H	^{14}C	Cl	SO_4	Ca	Na	Sr	Li	B
		°C	mS/m		mg/L	‰		TU	pMC	mg/L						
8	1	30														
10	2	16	66.5	7.4		-4.6		12	111.2							
10	2	18	97.5	7.8		-4.5		7	95.1							
10	2	16.8	65	7.2		-5.1		5.4	110.8							
10	1	30.2	36.5	8		-5.2		2	77							
10	3	20.2	48	7.9		-5.1		1.9	59.5							
10	DB11a	18.1	85	8.1					63	180.8	36.5	19.2	137.9			

Sources: *8) Kent, 1949; 10) Vogel et al., 1980;.*

Sites: *1) Rooiwal, 2) Wildebeest Valley 3) Vaalbank.*

4.3 Location description

Four livestock farms in three areas within the greater Venterstad area were sampled during the first sampling round (Fig. 10). One suspected deep site and two suspected shallow sites were sampled in Wildebeest Valley (DB11a, WVB1 and WVB3 respectively). One suspected deep site and one suspected shallow site were sampled in Rooiwal, RWB1c and RWB5 respectively. The suspected deep site is located at the WMS 171922 site registered on DWA's data base. One suspected deep and one suspected shallow site were sampled in

Vaalbank, VBB1 and VBB2 respectively. The suspected deep site, VBB1, is a shallow borehole drilled approximately 8m away from a warm spring. The eye of the warm spring could not be located in the marshy surrounds; therefore a sample was collected from the nearby borehole. Two suspected shallow groundwater flow sites were sampled from boreholes in La Rochelle, namely LRB1 and LRB2. In total, nine sites were sampled during the first sampling round.

The topography of the area varies from fairly extensive flat stretches to areas of hilly terrain. The range in elevation between the four sampled farms is 207m. The field data and major ions, including B, Sr and Li, are shown in Tables 8 and 9 respectively, and the sites are plotted on a piper diagram (Fig. 11).

4.4 Sampling site selection

Using temperature of above 25°C as the preliminary indicator of warm groundwater, only one site is suspected to be deep, RWB1c with a temperature of 28.1°C. Historic data indicates that DB11a and VBB1 are both of deep origin, although the water temperatures measured in the field were 20.5 and 19.9°C respectively. The two suspected deep sites chosen for the second round of sampling were based on temperature and the groundwater facies indicated by the piper diagram (Fig. 11). Therefore boreholes RWB1c and VBB1 were selected as representing deep groundwater. RWB5 was selected as the shallow pair for RWB1c and LRB2 was selected as the shallow pair for VBB1, as the chemistry from these shallow borehole sources differed the most from the suspected deep sources.

Table 8: Field data of the nine sites sampled on three farms in the Venterstad area during the first round of sampling.

Sample	Latitude	Longitude	Temp	EC	pH	Alk	H_2S smell
	°S	°E	°C	mS/m		mg/L	
DB11a	30.84099	25.76566	20.5	127.3	7.6	392	strong
WVB1	30.83115	25.79826	19.8	74.5	7.4	347.7	none
WVB3	30.80172	25.77744	21.7	103.4	7.5	241	none
RWB1c	30.86604	25.58741	28.1	64.1	7.9	216.6	strong
RWB5	30.85875	25.58318	18.4	83.5	7.2	354.4	none
VBB1	30.68329	25.93046	19.9	52.6	8.1	124.1	strong
VBB2	30.67785	25.94696	20.1	54.9	7.1	253.3	none
LRB1	30.68586	25.95916	20.5	78.1	7.2	304.8	none
LRB2	30.68546	25.96099	20.8	59.1	7.3	267.2	none

Table 9: Major ion plus B, Sr and Li results of the nine sites sampled on three farms in the Venterstad area during the first sampling round.

Sample	Cl	NO_3	SO_4	Ca	K	Mg	Na	B	Sr	Li
	mg/L							µg/L		
DB11a	108.7	3.8	27.6	53.7	4.0	17.4	192.4	1.0	1.2	0.1
WVB1	35.0	1.4	17.2	58.6	2.0	32.8	56.6	0.1	0.9	0.0
WVB3	146.9	3.4	42.4	97.4	1.8	37.6	78.2	0.2	1.3	0.1
RWB1c	68.7		42.6	32.4	0.7	4.5	102.1	0.4	1.1	0.1
RWB5	63.9		35.8	81.9	1.5	34.5	45.1	0.1	0.9	0.0
VBB1	118.3			15.0	0.6	2.7	93.6	0.4	0.3	0.0
VBB2	31.0	6.9	19.8	61.3	0.8	26.4	19.2	0.0	0.5	0.0
LRB1	51.1	14.0	27.0	89.3	1.1	31.1	33.5	0.0	0.8	0.0
LRB2	51.0	6.6	17.3	66.7	1.0	23.4	27.9	0.0	0.6	0.0

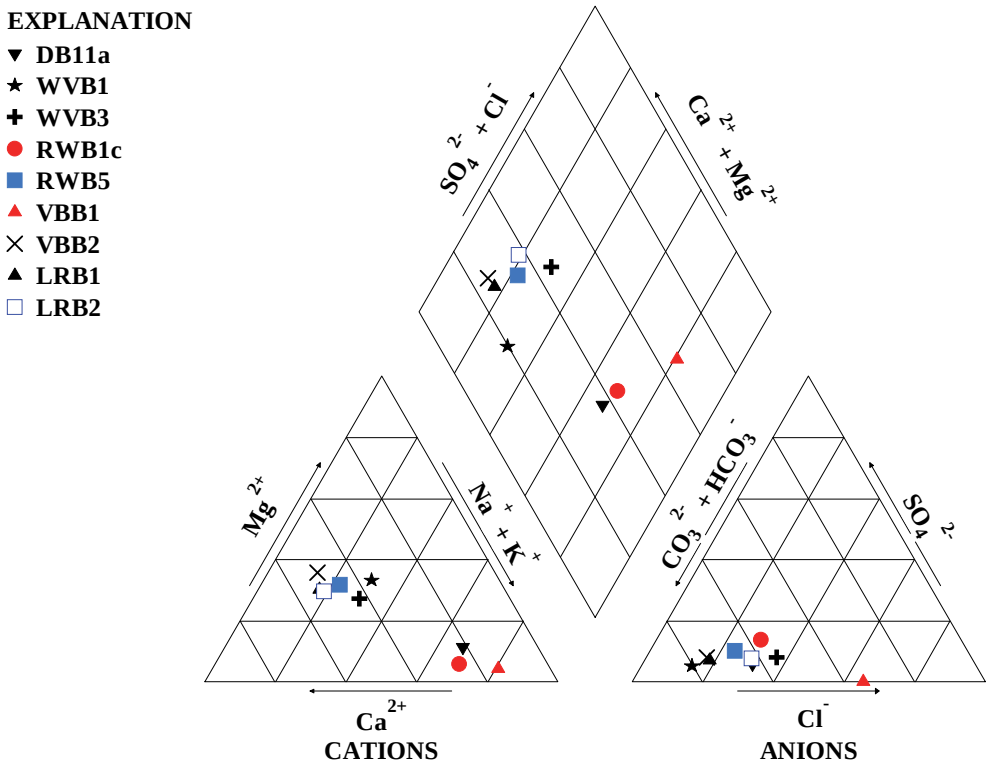

Figure 11: Piper diagram of major ions collected from three areas in Venterstad during the first round of sampling.

5. ALIWAL NORTH

The warm spring situated in Aliwal North was once a popular tourist attraction as the spring flows into indoor and outdoor pools. However, the resort has not been maintained for the last decade or so and has fallen into a shocking state of disrepair. The site is registered on the WMS database, No. 89868.

5.1 Hydrogeological setting

The Aliwal North thermal spring is located on the south-western side of a large dolerite ring structure. This structure is cut by a major north-south trending dyke which at surface, appears to have “cut-off” the south-western part of the ring structure (Fig. 12). There are also numerous other dykes and sills in the greater Aliwal North area, and it forms part of the major east-west neotectonic zone postulated by Woodford and Chevallier (2002). The sub-surface geology of this area is not straight forward, and like other ring-dyke-sill complexes, it is not possible to identify particular structures that may impede flow at depth and provide conduits for upward flow. A simplified cross section is shown in Figure 13.

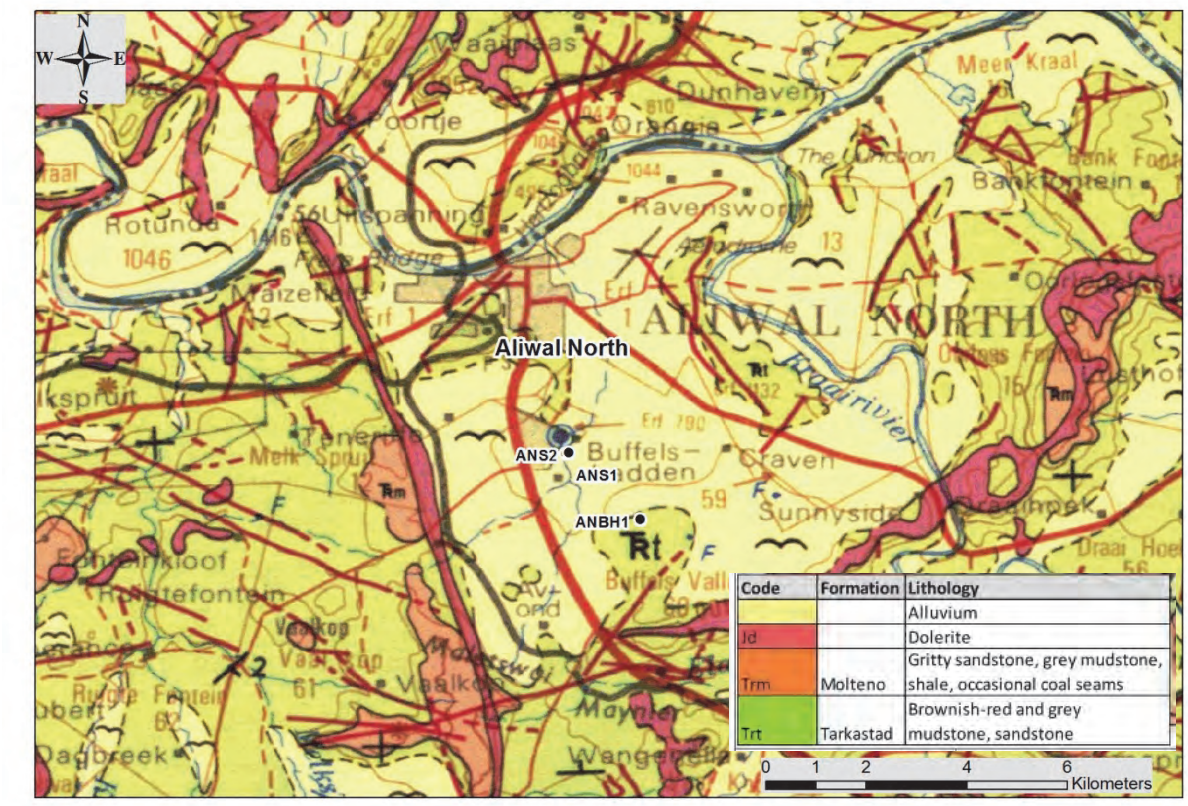

Figure 12: Geological map (1:250 000) of Aliwal North including the sampling sites from first and second rounds of sampling.

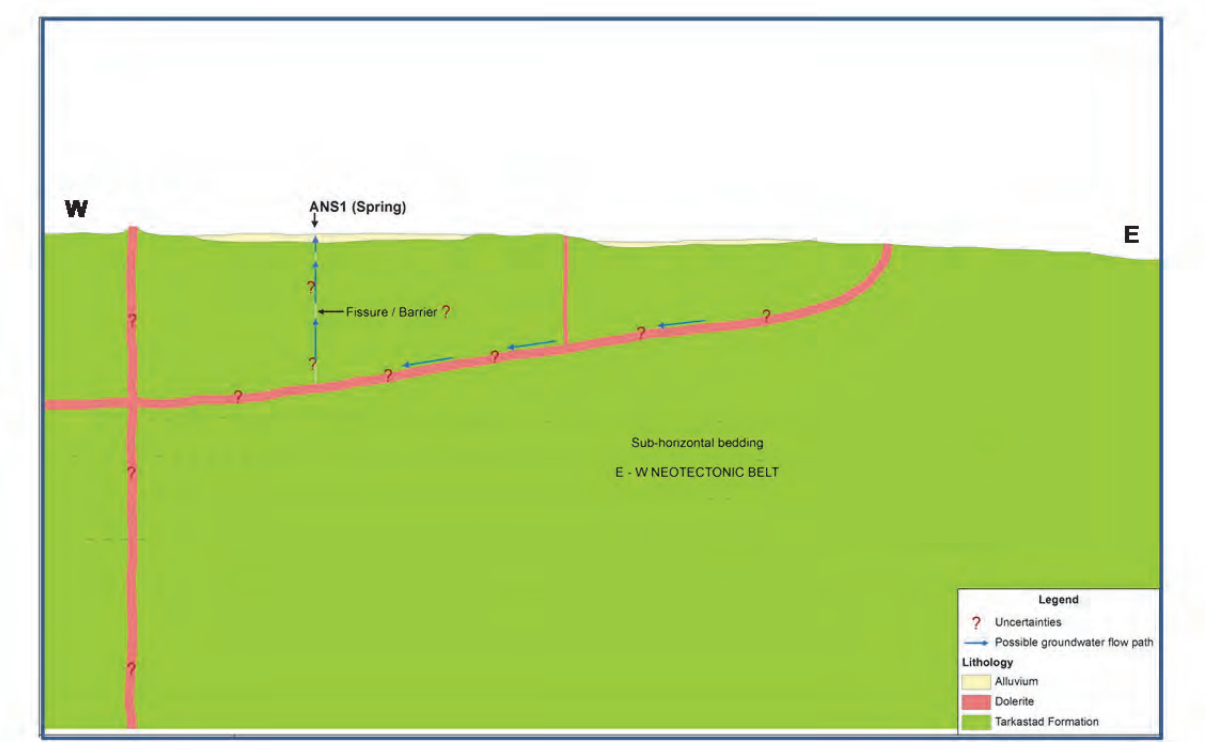

Figure 13: Simplified conceptual cross section of the Aliwal North spring area.

5.2 Historical water quality assessments

The spring was one of the 25 sampled by Kent (1949). It was classified as a warm spring with a temperature of 36.9°C (Kent, 1949). The spring in Aliwal North was identified as the second highest saline groundwater in the study with a total dissolved ion (TDI) content of 1205mg/L, and is therefore, classified as a Type 2 water (Mazor & Verhagen, 1983). The study involved the collection of river water from adjacent rivers to the springs. It was observed that the river water was enriched in $\delta^{18}O$ and $\delta^{2}H$ with respect to the thermal spring water. This suggests that the springs are recharged by direct rain infiltration (Mazor & Verhagen, 1983). Table 10 shows the data of the previous analyses and indicates that some of the water quality parameters have varied considerably over time.

Table 10: Previous water quality data of the warm spring in Aliwal North. Only a few of the measured parameters are shown in this table.

Source	T	EC	pH	Alk	$\delta^{18}O$	$\delta^{2}H$	^{3}H	^{14}C	Cl	SO_4	Ca	Na	Sr	Li	B
	°C	mS/m		mg/L	‰		TU	pMC	mg/L						
8	36.9			29.4					605.3	68.6	83.8	344.5	n.d.	2.3	
3	34			27	-5.96	-31	1		678	46	85	360			
12								38.9							
13	34	170	8.6	80					335	410	86	340	1.1		
14				1.6					333.3	408.3	86.2	340.3			
15	28	145	7.2	10					599.7	1.5	72.9	303.2	1		
16	30		8.9												

Sources: *8) Kent, 1949; 3) Mazor &Verhagen, 1983; 12) Siep Talma; 13) Hoffman, 1979; 14) Day, 1993; 15)WMS; 16) DWA, 2013.*
Notes: *n.d. = not detected*

5.3 Location description

Three sites were sampled in Aliwal North during the first round of sampling. Indoor (ANS1) and outdoor (ANS2) pools were sampled as the suspected deep sites at the once popular Aliwal North spa. A shallow borehole (ANBH1) on a private farm situated about 5km away from the spa (Fig. 20) was sampled as the suspected shallow site for the location. The topography of the area is relatively flat with an elevation range of 40m between the two sites. The field data and major ions, including B, Sr and Li, are shown in Tables 11 and 12 respectively, and the sites are plotted on a piper diagram (Fig. 14).

5.4 Sampling site selection

The preliminary chemistry and field results suggested that the two suspected deep sites, ANS1 and ANS2, originate from the same source. The field data as well as the major ion chemistry and the groundwater facies as indicated by the piper diagram (Fig. 14) are almost identical. The temperatures of the warm springs, ANS1 and ANS2 are 33.4 and 33.6°C respectively. The suspected deep site chosen for the second round of sampling was ANS1, as it is thought to be the eye of the spring. The suspected shallow source, ANBH1, has a temperature of 21.6°C, however, the field results and groundwater facies as indicated by the piper diagram (Fig. 14) suggest that the water originates from a similar source to that of ANS1 and ANS2. A different source of shallow groundwater was meant to have been located for the second round of sampling. However, due to time constraints, none was found.

Table 11: Field data of the three sites sampled in Aliwal North during the first round of sampling.

Sample	Latitude	Longitude	Temp	EC	pH	Alk	H_2S smell
	°S	°E	°C	mS/m		mg/L	
ANS1	30.7153	26.715	33.4	208	9.1	13.9	strong
ANS2	30.715268	26.715481	33.6	212	9.2	17.7	strong
ANBH1	30.72716	26.72824	21.6	187.2	8.3	50.9	strong

Table 12: Major ion plus B, Sr and Li results of the three sites sampled in Aliwal North during the first sampling round.

Sample	Cl	NO_3	SO_4	Ca	K	Mg	Na	B	Sr	Li
	mg/L							µg/L		
ANS1	671.7		1.1	79.7	2.0	0.0	325.7	0.9	1.4	0.4
ANS2	703.7		0.1	79.3	2.0	0.0	325.5	0.9	1.4	0.4
ANBH1	570.6			13.5	0.8	0.5	375.2	0.6	0.7	0.4

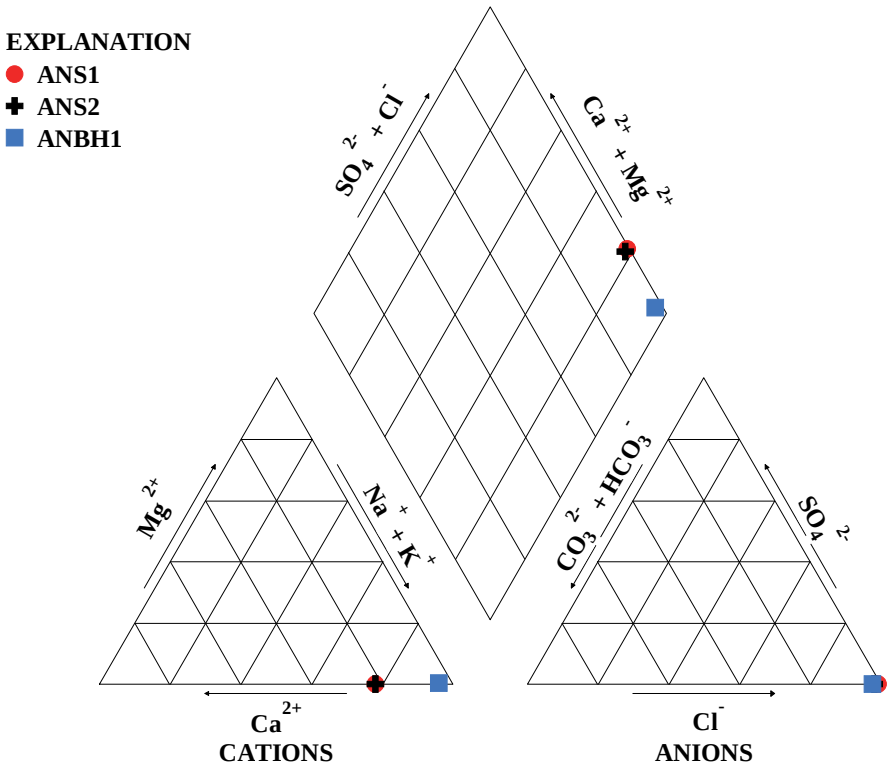

Figure 14: Piper diagram of major ions collected in Aliwal North during the first round of sampling.

6. CRADOCK

The Cradock spa is a popular resort and the pool is well maintained and suitable for sampling. This is registered on the WMS database: No. 101267. Like at Aliwal North, it appears as if the swimming pool was built over the main eye of the spring.

Figure 15: Cradock spa swimming pool in August 2013 (after being drained for cleaning), with metal grids protecting the bubbling springflow from below (photo courtesy S Mullineux, DWA, Cradock).

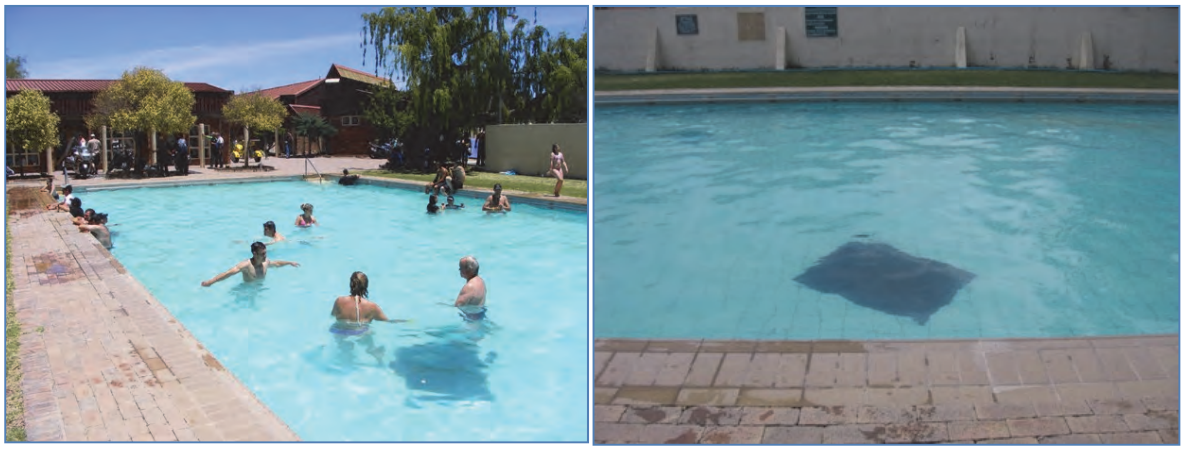

Figure 16: Left: Swimming pool in December 2012 (photo courtesy S Mullineux, DWA, Cradock). Right: Pool at the time of sampling in 2014. Sampling pipes were inserted into the grid to collect rising spring water.

6.1 Hydrogeological setting

The Cradock thermal spring daylights from the Balfour Formation which consistes mostly of mudstone with intercalated fine-grained sandstone. At the surface, a fairly dense distribution of dolerite sills and dykes can be seen, with one fairly major north-west trending dyke outcropping 1km west of the spring (Fig. 17). The spring itself appears to located outside the western edge of a complex ring structure.

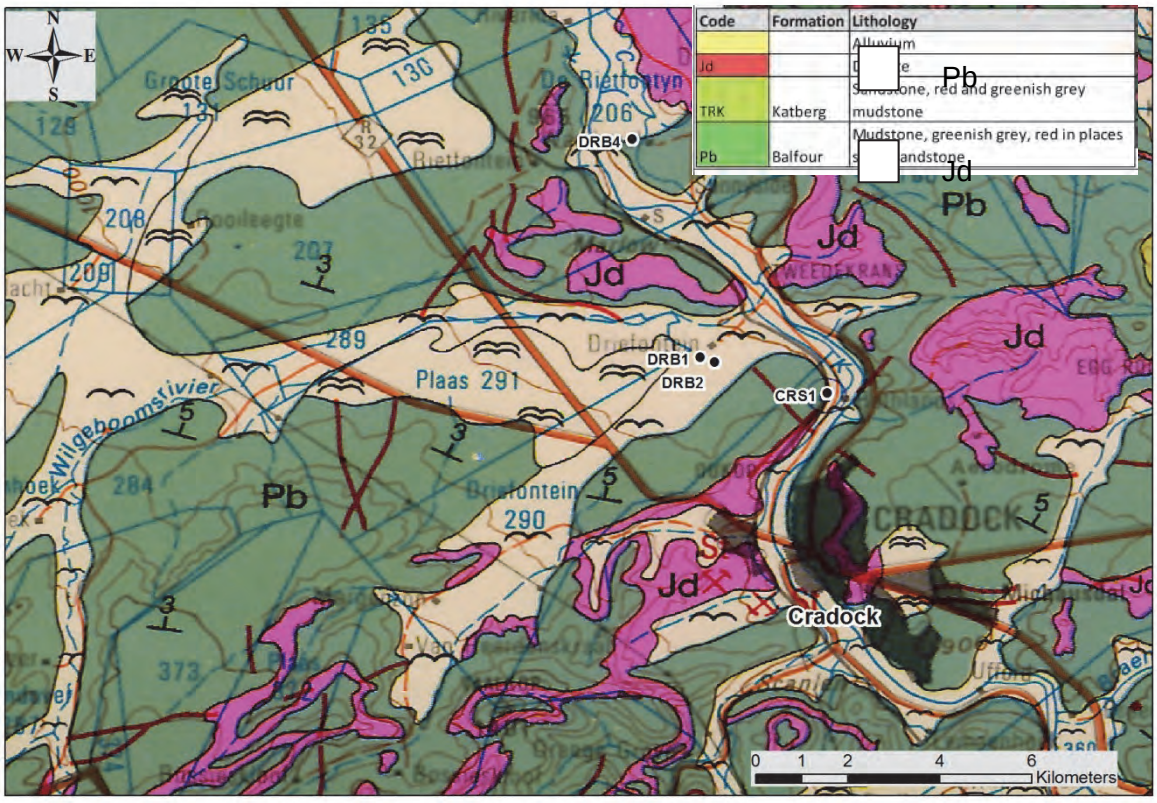

Figure 17: Geological map of Cradock including the sampling sites from first and second rounds of sampling.

6.2 Historical water quality assessments

This spring is one of the 25 sites sampled by Kent (1949). It was classified as a warm spring with a temperature of between 29-31.3°C.

Table 13: Previous water quality data of the warm spring in Cradock. Only a few of the measured parameters are shown in this table.

Source	T	EC	pH	Alk	$\delta^{18}O$	$\delta^{2}H$	^{3}H	^{14}C	Cl	SO_4	Ca	Na	Sr	Li	B
	°C	mS/m		mg/L	‰		TU	pMC	mg/L						
8	29-31.3		9.6	9.8					24.9	16.8	3	49.9	n.d.	0	
13		44	7.3	98					52	21	21	42	0.1		0.5
14				2.4					53.2	19.2	22	41.4			
17	27		6.8						54.6	16.4	9.1	40.3	0.1	1.6	0.5
15	30	20	9	48.50					18.3	13	2.6	35.3	0.1		0.6

Sources: *8) Kent, 1949, 13) Hoffman, 1979; 14) Day, 1993; 17) Venter, 2009; 15) WMS*
Notes: *n.d. = not detected*

6.3 Location description

Four sites were sampled around Cradock area during the first round of sampling (Fig. 17). The suspected deep site, CRS1, was sampled at the Cradock spa. Three suspected shallow sites were sampled. Two of the sites, DRB1 and DRB2, are situated on an agricultural school farm approximately 2km away from the spa. The third and final suspected shallow site, DRB4, is situated on a private livestock farm approximately 8km from the spa. The topography of the area is quite hilly, with an elevation difference of 165m between the spa and the private farm. The field data and major ions, including B, Sr and Li, are shown in Tables 14 and 15 respectively, and the sites are plotted on a piper diagram (Fig. 18).

6.4 Sampling site selection

The water sampled from the suspected deep site, CRS1, was warm with a temperature of 29°C. The water sampled from the two suspected shallow sites on the agricultural school farm, DRB1 and DRB2, were both cold with temperatures of 22.4 and 21.9°C respectively. The suspected shallow site sampled at the private farm, DRB4, had the coolest temperature of 21.1°C. The piper diagram (Fig. 18) indicates that the suspected deep site, CRS1, and the suspected shallow sites, DRB1 and DRB2, originate from similar sources. DRB4 has a different groundwater character to the other three sites. Therefore, based on the temperature and the groundwater facies as indicated by the piper diagram (Fig. 18), the two sites chosen for sampling during the second round of sampling were CRS1 and DRB4.

Table 14: Field data of the four sites sampled in Cradock during the first round of sampling.

Sample	Latitude	Longitude	Temp	EC	pH	Alk	H_2S smell
	°S	°E	°C	mS/m		mg/L	
CRS1	32.13552	25.62601	29	19.7	9.6	49.8	strong
DRB2	32.12957	25.60397	21.9	18.4	9.6	45.1	none
DRB1	32.12851	25.60117	22.4	20.5	9.8	47.6	strong
DRB4	32.086	25.58783	21.1	152.6	7.7	616.5	none

Table 15: Major ion plus B, Sr and Li results of the four sites sampled in Cradock during the first sampling round.

Sample	Cl	NO_3	SO_4	Ca	K	Mg	Na	B	Sr	Li
	mg/L							µg/L		
CRS1	58.2			3.3	0.4	0.4	44.2	0.4	0.1	0.1
DRB2	57.1			2.1	0.3	0.0	45.6	0.4	0.0	0.1
DRB1	58.6		3.5	2.4	0.2	0.0	45.1	0.4	0.0	0.1
DRB4	77.1	10.7	38.2	25.2	3.7	55.8	226.0	0.7	0.6	0.0

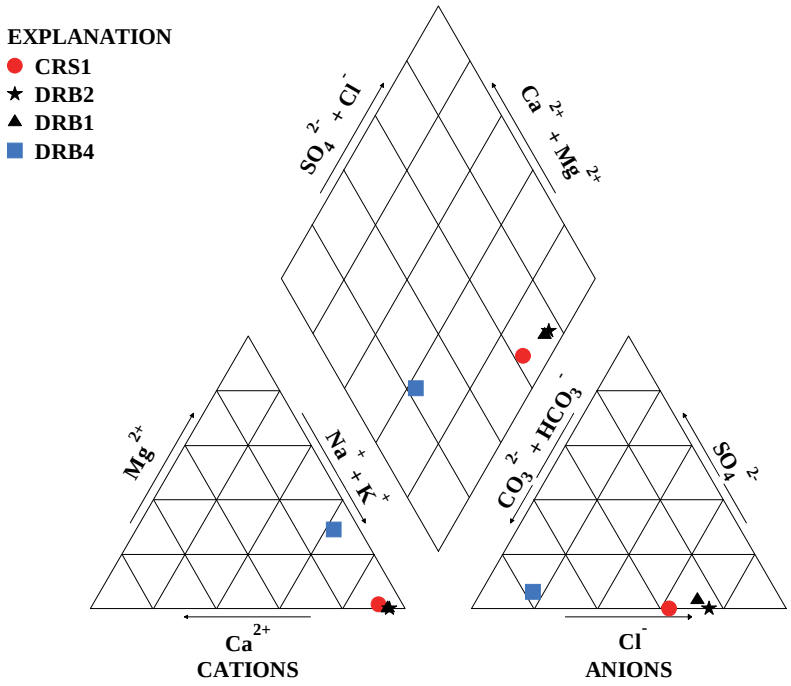

Figure 18: Piper diagram sowing major ions collected from Cradock during the first round of sampling.

7. FORT BEAUFORT

An artesian, warm spring is situated on the private citrus farm Bath Farm near Fort Beaufort. A health spa, named Sulphur Baths, used to exist at this site, but it has not been maintained and is now in a state of disrepair. An open, nearby warm-water borehole with gas bubbles rising to the surface was used to collect water from this source.

Figure 19: The main spring (old recreational pool) and the nearby gently-flowing artesian borehole from which groundwater rises and bubbles to the surface.

7.1 Hydrogeological setting

Fort Beaufort, like the remaining two sites, Leeu Gamka and Merweville, lie below/south of the great escarpment and thus outside the central Karoo Basin that is so distinctly defined by the dense network of dolerite dykes, sill and ring structures. The dolerites are still present in this area, and the spring site sits about 3km north of a >100km long dolerite sheet that runs into the Indian Ocean. The area is located in gently folded sediments of the Middleton Formation which consists of mostly mudstone with interbedded sandstone, and the spring daylights from a point between anticline and syncline axes (Figure 20).

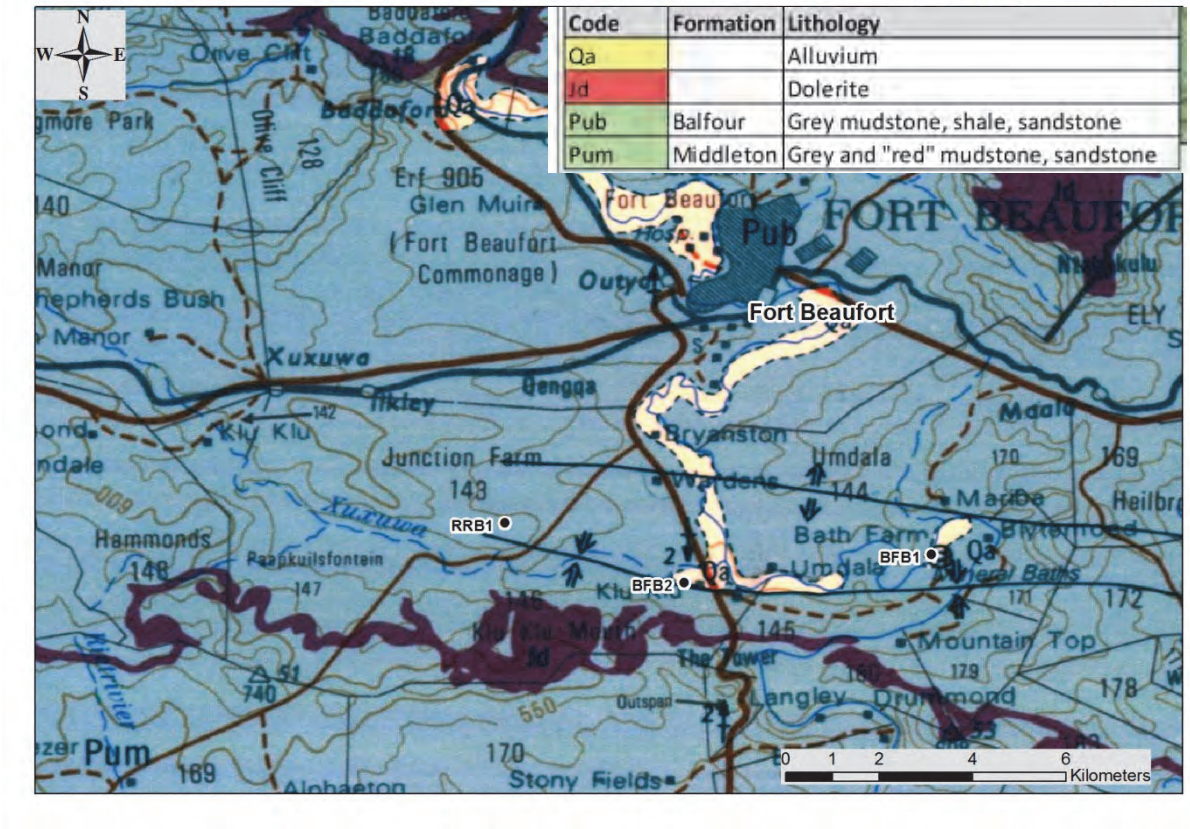

Figure 20: Geological map of Fort Beaufort including the sampling sites from first and second rounds of sampling.

7.2 Historical water quality assessments

The groundwater was sampled by Kent in 1949 and was classified as warm with a temperature of between 27-29°C. The spring contained the second highest dissolved oxygen concentration of the 25 boreholes and springs sampled by Kent, (1949). Another of these 25 boreholes and springs includes a spring situated less than a kilometre away from the Fort Beaufort spring, named the Kat Valley spring. Kent (1949) noted a significant difference in the Li and Ba content of the two springs (Fort Beaufort contained higher Li and Ba), despite their close proximity and that the springs originate from the same rocks of the Karoo Supergroup. It was suggested that the Fort Beaufort spring is of deeper origin than the Kat Valley spring (Kent, 1949). Methane has been identified as a component of the gas emanating from this spring (Talma and Esterhuyse 2015).

Table 16: Previous water quality data of the warm, artesian spring in Fort Beaufort. Only a few of the measured parameters are shown in this table.

Source	T	EC	pH	Alk	$\delta^{18}O$	$\delta^{2}H$	^{3}H	^{14}C	Cl	SO_4	Ca	Na	Sr	Li	B
	°C	mS/m		mg/L	‰		TU	pMC	mg/L						
8	29		9	39.7					190	36	11	164	n.d.	n.d.	n.d.
16	25	75	9.2												

Source: *8) Kent, 1949; 16) DWA.*

Notes: *n.d. = not detected*

7.3 Location description

Two sites were sampled on a private farm in Fort Beaufort. A suspected deep site, BFB1, and a suspected shallow site, BFB2, were sampled during the first round of sampling (Fig. 20). The topography of the Fort Beaufort area is very hilly, however, the elevation range between the two sites is only 40m. The suspected deep site, BFB1, is a warm (25.8°C), artesian borehole. The eye of the original spring is situated approximately 30m from the borehole but is not suitable for sampling because of the overgrown vegetation. The temperature of the groundwater from the borehole is slightly cooler (about 1°C) than the spring water at the surface of the pool (which appears to have been constructed over the eye of the spring). The field data and major ions, including B, Sr and Li, are shown in Tables 17 and 18 respectively, and the sites are plotted on a piper diagram (Fig. 21).

7.4 Sampling site selection

The field measurements and chemistry results suggest that the two samples are quite similar and both sites are in the same facies as indicated by the piper diagram (Fig. 21). The groundwater sampled as the suspected shallow site, BFB2, had quite warm water at 24.3°C. Therefore, a different source of cold groundwater was collected during the second round of sampling in order to obtain a distinct pair of warm and cold groundwater sources. This borehole is about 15km away from BFB1, and the site could be identified as shallow based on the field measurements.

Table 17: Field data of the two sites sampled in Fort Beaufort during the first round of sampling.

Sample	Latitude	Longitude	Temp	EC	pH	Alk	H_2S smell
	°S	°E	°C	mS/m		mg/L	
BFB1	32.8264	26.67059	25.8	82.3	9.9	49	strong
BFB2	32.83183	26.62285	24.3	201	7.3	303.3	strong

Table 18: Major ion plus B, Sr and Li results of the two sites sampled in Fort Beaufort during the first sampling round.

Sample	Cl	NO_3	SO_4	Ca	K	Mg	Na	B	Sr	Li
	mg/L							µg/L		
BFB1	196.4		7.7	4.3	2.0	0.0	153.3	1.9	0.4	0.5
BFB2	505.0		9.1	78.6	1.5	40.3	277.1	0.8	3.2	0.1

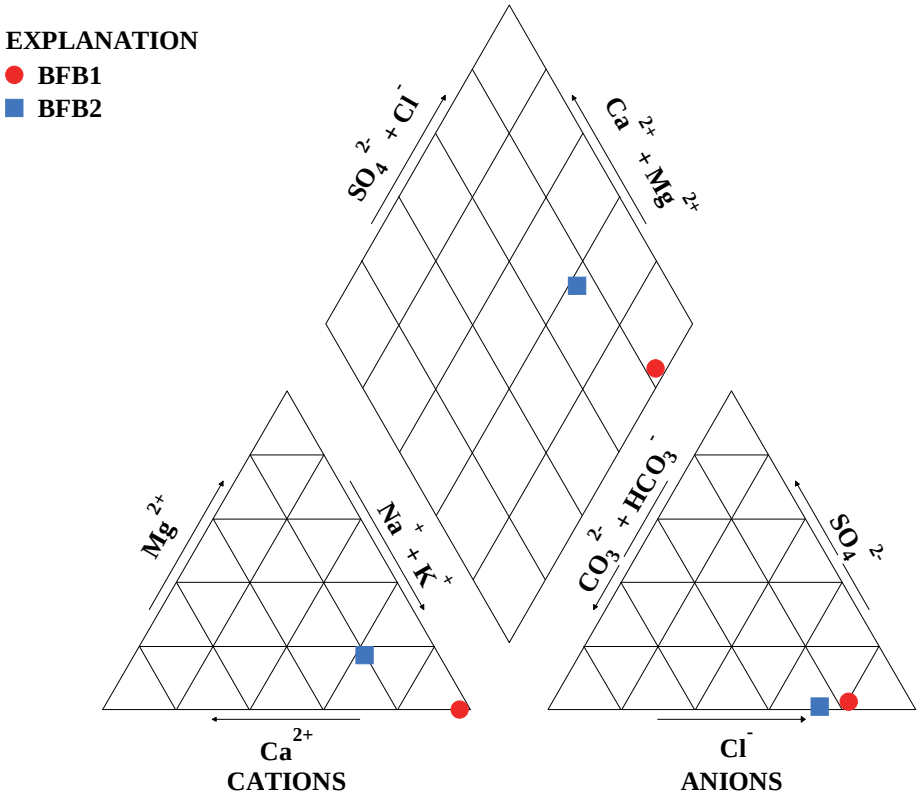

Figure 21: Piper diagram of major ions collected from Fort Beaufort during the first round of sampling.

8. LEEU GAMKA

Leeu Gamka is a small, farming town situated south-west of Beaufort West along the N1. Boreholes on two farms, Kruidfontein and Groot Kruidfontein, located south of Leeu Gamka were sampled for this project.

The area was selected for three reasons:

1) The thermal springs at Stinkfontein ~13 km north of Leeu Gamka and at Groot Kruidfontein ~4 km south of Leeu Gamka.
2) Previously sampled boreholes that suggested deep flow
3) The area is seismically active.

The warm springs are shown on the Geological Survey's 1952, 125 000 map, and are mentioned in accompanying explanation sheet (Rossouw and De Villiers, 1953). The Stinkfontein spring had a temperature of 28.8°C and the Groot Kruidfontein had a temperature of 24°C and they carried the distinct hydrogen sulphide odour.

The location of the Stinkfontein spring was pointed out by the land owner (and it matched the position on the geological map next to the old Stinkfontein farm house), but unfortunately the farmer had excavated a small dam over the spring and it was not suitable for sampling.

Figure 22: Current-day Stinkfontein thermal spring site.

Figure 23: Sites sampled at the two farms in Leeu Gamka (left to right) WP 508, WP 502, WP 496 and WP 507.

8.1 Hydrogeological setting

The Leeu Gamka area sits on arenaceous and argillaceous sediments of the Abrahamskraal Formation which overly the Cape Supergroup sediments at depth. The impact of the Cape Fold Belt is evident in the E-W trending shallow folds throughout this area (Fig. 24). The source of the deep water in this area is thought to be from recharge in the Cape Mountains to the south, and then via faults or fracture zones associated with the Cape Fold Belt.

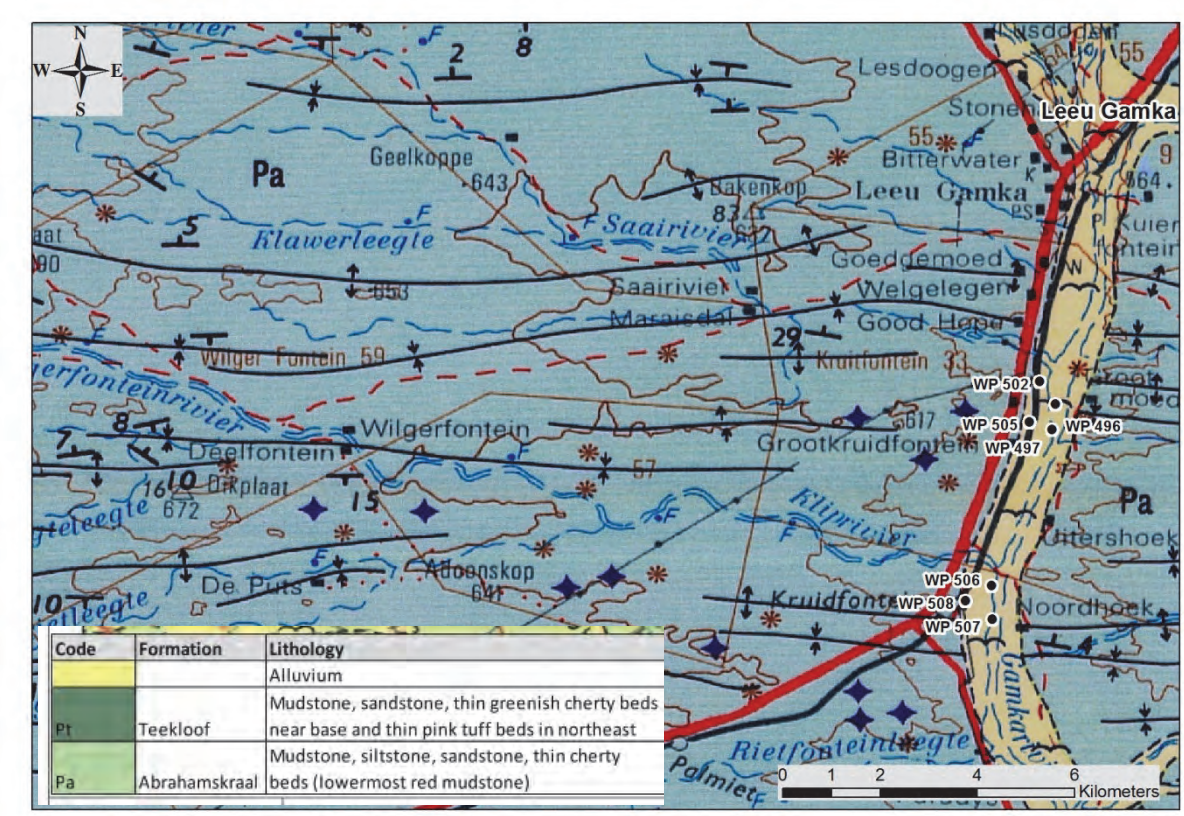

Figure 24: Geological map (1:250 000) of Leeu Gamka including the final sampling sites.

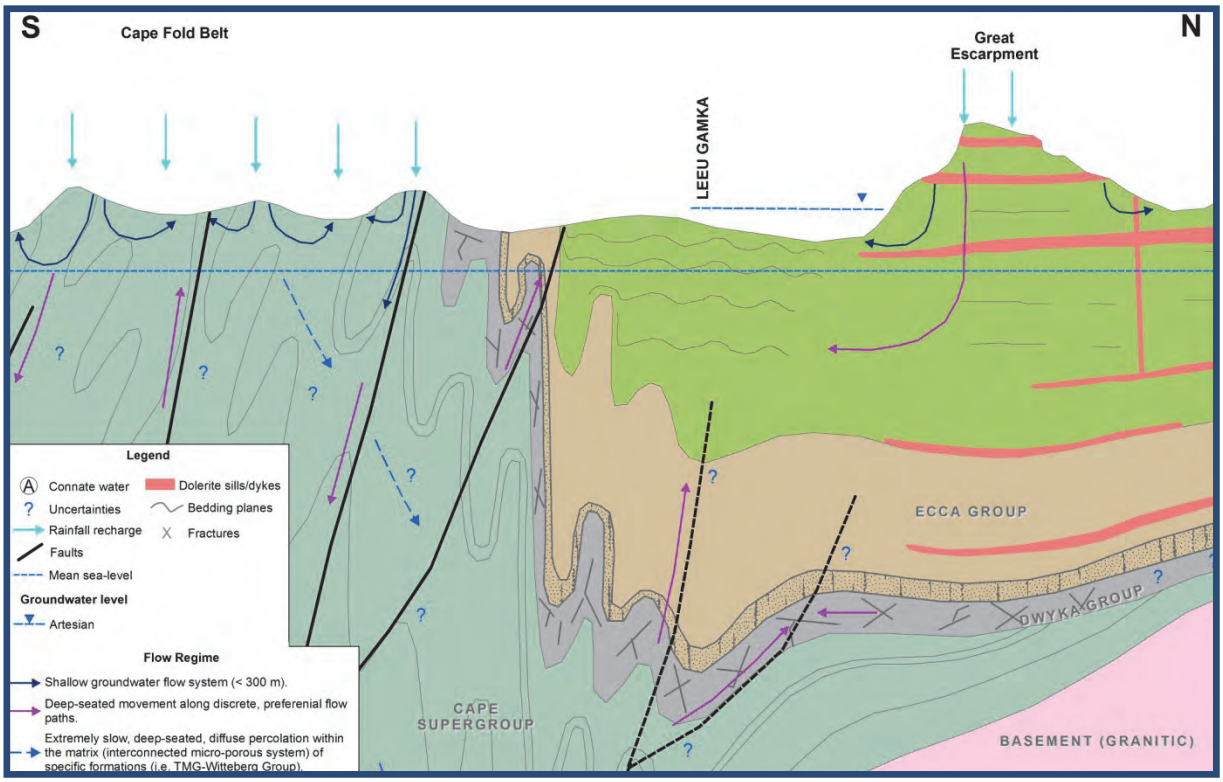

Figure 25: Schematic cross section through the Leeu Gamka area.

8.2 Historical water quality assessments

Two boreholes on the Farm Kruidfontein were sampled by Kent in 1949. One was cool and the other warm. Boreholes on the farms Kruidfontein and Groot Kruidfontein were sampled for a Water Research Commission (WRC) study in 2003. In this study chlorofluorocarbons (CFCs) as well as isotopes were analysed in the project (Talma & Weaver, 2003). Table 19 shows the results of these two studies. Interestingly, the shallow borehole at Kruidfontein was found to have a significantly higher TDS than the deep borehole.

Table 19: Previous water quality data of deep and shallow boreholes situated on two farms in Leeu Gamka. Only a few of the measured parameters are shown in this table.

Source	Site	T	EC	pH	Alk	$\delta^{18}O$	$\delta^{2}H$	^{3}H	^{14}C	Cl	SO_4	Ca	Na	Sr	Li	B
		°C	mS/m		mg/L	‰		TU	pMC	mg/L						
8	1													10	5	Tr.
8	2													8	7	3
18	3							1.1	72	63	158					
18	4							2.2	105	780	537					
18	5							2.8	112	285	291					
18	6							3.2	111	594	890					
18	7							2	83	163	533					
18	8							2.4	108	413	540					

Sources: *8) Kent, 1949; 18) Talma & Weaver, 2003.*

Sites: *1) Kruidfontein, shallow; 2) Kruidfontein, deep; 3) Kruidfontein KF1; 4)Kruidfontein KF2; 5) Kruidfontein KF3; 6) Kruidfontein KF4; 7) Groot Kruidfontein GKF1; 8) Groot Kruidfontein GFK2.*

8.3 Location description

Two farms in the greater Leeu Gamka area were visited during the first round of sampling, Kruidfontein and Groot Kruidfontein (Fig. 24). Three samples were collected from Kruidfontein: a suspected deep site, WP 508, and two suspected shallow sites, WP 506 and WP 507. Four samples were collected from Groot Kruidfontein: a suspected deep site, WP 505, and three suspected shallow sites, WP 497, WP 496 and W 502. The topography of the area is flat with an elevation range of 30m between all seven sampling sites. The field data and major ions, including B, Sr and Li, are shown in Tables 20 and 21 respectively, and the sites are plotted on a piper diagram (Fig. 26).

8.4 Sampling site selection

The preliminary chemistry results and the groundwater facies as indicated by the piper diagram (Fig. 25) suggest that three sites could potentially originate from depth: WP 507, WP 508 and WP 505. Based on temperature, WP 508 (26.9°C) and WP 505 (25.2°C) were selected as the suspected deep sites to be sampled during the second round of sampling. The most distinct suspected shallow site selected for the second round of sampling was WP 502. This was determined by temperature (22.1°C) as well as the different groundwater facies indicated by the piper diagram (Fig. 25).

Table 20: Field data of the seven sites sampled on two farms in Leeu Gamka during the first round of sampling.

Sample	Latitude	Longitude	Temp	EC	H	Alk	H_2S smell
	°S	°E	°C	mS/m		mg/L	
WP 507	32.85454	21.96143	22.6	126.3	7.8	234.3	strong
WP 506	32.84831	21.96134	23	92.3	7.3	262.8	none
WP 508	32.85104	21.95657	26.9	95.6	7.9	167	strong
WP 497	32.81943	21.97252	24.2	241	7.2	519.3	none
WP 496	32.81472	21.9732	22.5	220	6.9	519.7	none
WP 502	32.81053	21.97031	22.1	47.3	7.5	174.9	none
WP 505	32.818	21.96833	25.2	148.7	8	207.1	weak

Table 21: Major ion plus B, Sr and Li results of the seven sites sampled on two farms in Leeu Gamka during the first sampling round.

Sample	Cl	NO_3	SO_4	Ca	K	Mg	Na	B	Sr	Li
	mg/L							µg/L		
WP 507	148.1		159.2	36.0	2.7	3.4	225.1	0.6	2.7	0.7
WP 506	107.5		59.1	58.8	3.0	8.2	125.6	0.3	2.9	0.2
WP 508	117.1		125.1	37.3	3.0	2.5	155.1	0.3	2.7	0.4
WP 497	302.7	6.5	420.6	161.1	5.0	39.5	369.1	0.7	5	0.5
WP 496	256.5	8.2	396.5	129.7	4.1	33	388.4	0.8	4.3	0.6
WP 502	65.0			34.3	2.8	8.6	63.8	0.1	1.7	0.1
WP 505	138.6		260.8	27.9	2.6	0.7	271.4	0.7	3.2	0.7

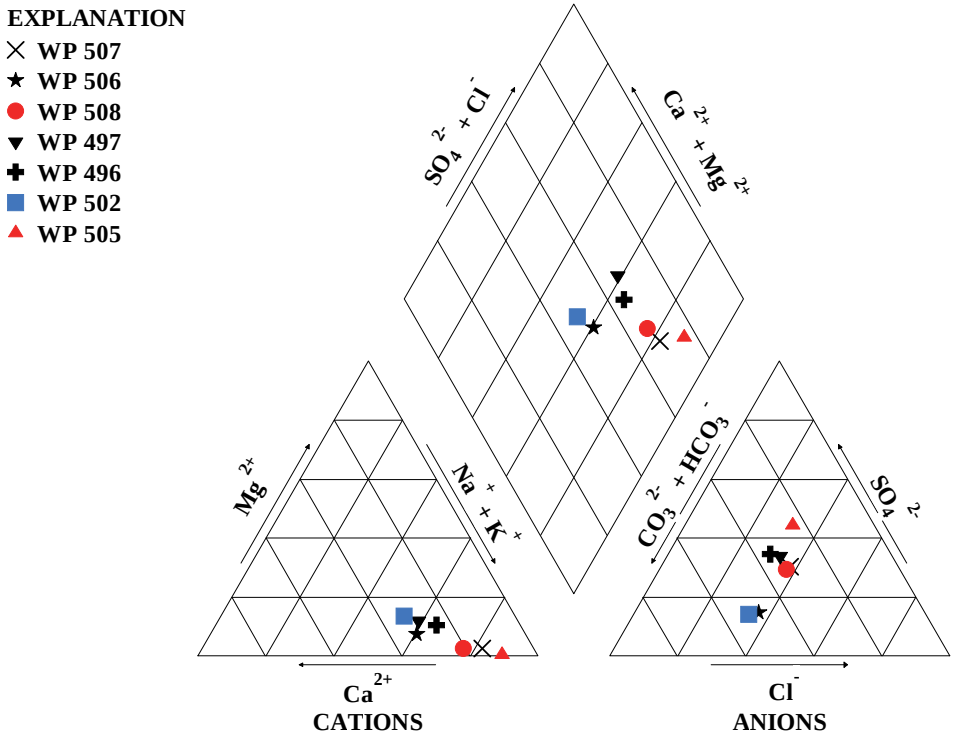

Figure 26: Piper diagram of major ions collected at two farms in Leeu Gamka during the first round of sampling.

9. MERWEVILLE

In 1965 SOEKOR (Southern Oil Exploration Corporation (Pty.) Ltd.) along with the Geological Survey of South Africa drilled a number of deep exploration wells in the Karoo. The aim of the drilling project was to prove or disprove the existence of economic accumulations of oil or gas in South Africa (Rowsell & De Swardt 1976). The boreholes were sealed with cement, however, one of the seals failed. This borehole is situated on a private farm near the town of Merweville in the Western Cape. The total depth of the borehole is 4169m and water was struck within the Dwyka Group at 3206m (Rowsell & De Swardt, 1976). The original drilling/geological log describes the water as artesian with a temperature of 46°C, a salt content of 8745 ppt and “a very high gas content”. A tap and pressure gauge was attached to the original headworks by the IGS at the University of the Free State.

Figure 27: SA1/66 being opened for the first time in about 50 years showing water and inflammable gas discharging.

9.1 Hydrogeological setting

The Merweville and Leeu Gamka sites lie in similar geological settings. The Cape Supergroup, defined by the Cape Fold Belt in the south, forms the basement for the Karoo Supergroup in this area (Fig. 28). The area is relatively low-lying when compared to the great escarpment to the north and the Cape Fold belt to the south, and like other areas sandwiched between these two prominent geologic features, is in a setting conducive to artesian pressures at depth. These are areas where the theorised Karoo artesian basin likely holds true. The site locations and their relation to fold hinges can be seen on the geological map (Fig. 29).

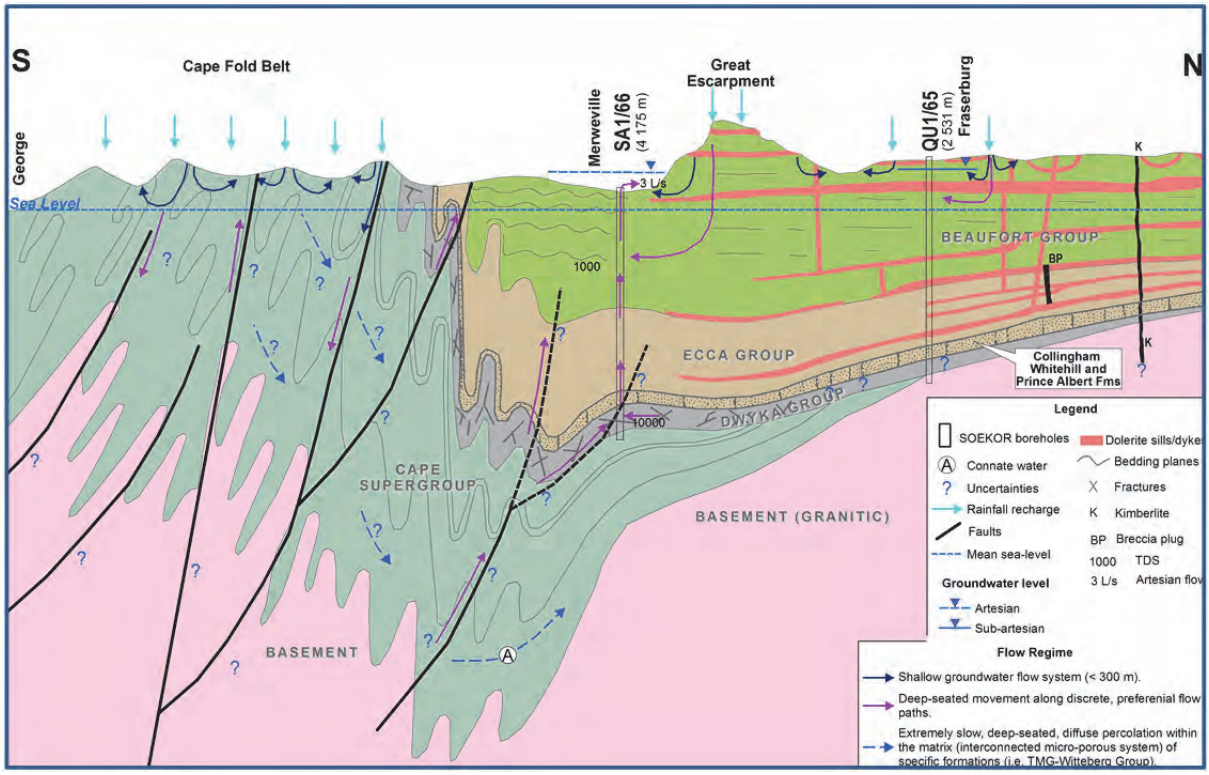

Figure 28: Schematic cross section through the Merweville area (Leeu Gamka is at a similar latitude to Merweville).

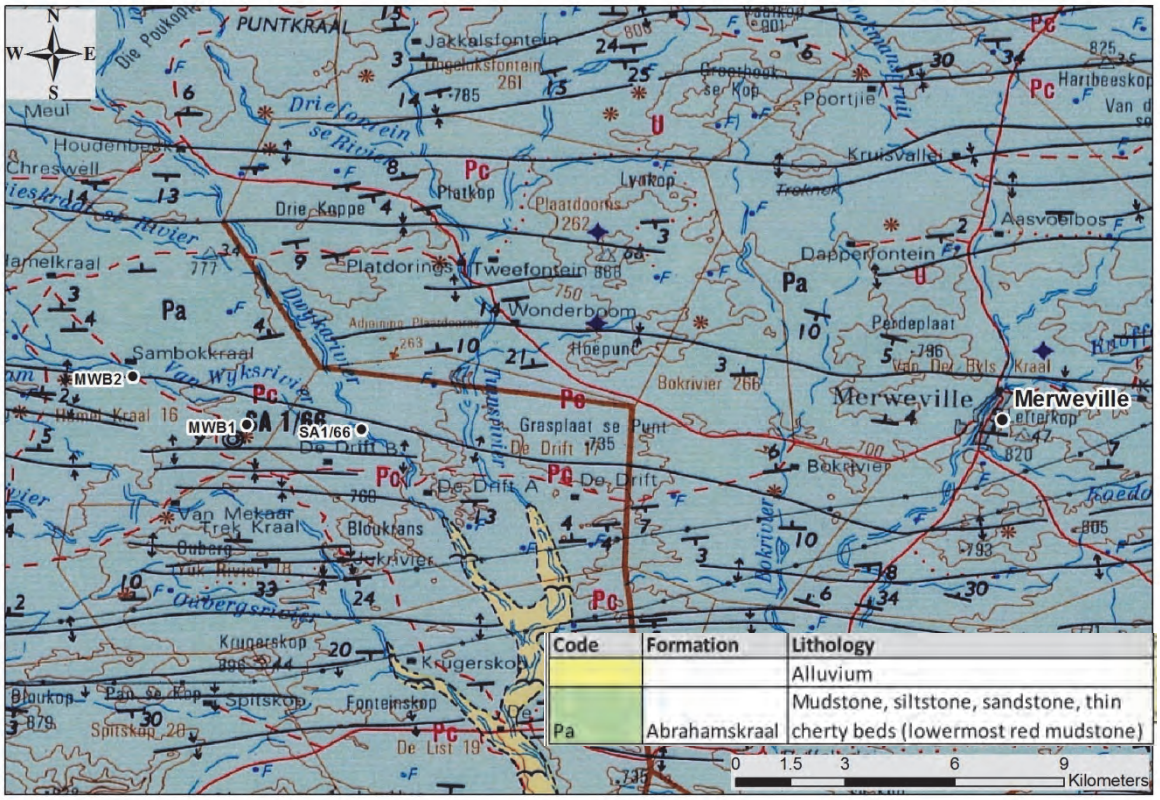

Figure 29: Geological map (1:250 000) of Merweville including the final sampling sites.

9.2 Historical water quality assessments

The borehole was opened in 2012. This was probably the first time it was opened since it was drilled in 1966 – i.e. in 46 years. Due to the high methane content, Professor Gerrit van Tonder was able to light the gas that was emanating from the hole. The methane percentage, temperature and high salinity of the groundwater were documented in a paper on the occurrence of methane in the Karoo (Talma & Esterhuyse, 2015). Besides the two samples and analyses from the 2012 and 2013 sampling by Gerrit van Tonder and Mr Fanie de Lange from IGS, University of the Free State, the only other data that was found is from the database of the CSIR isotope laboratory which shows an entry of a sample from SA1/66, collected in 1969 with a 14C content of 15.0 ± 0.25 pmC. No details of depth or sampling method are available.

Due to a lack of artesian flow, the SOEKOR borehole was not sampled on either of the field trips during this project. Prof. Van Tonder and his doctoral student, Mr Fanie de Lange of the Institute for Groundwater Studies at the University of the Free State, kindly gave permission to use samples and data they collected from the borehole in 2013 prior to the drop in artesian pressure (before the hole stopped flowing). Table 22 presents the data obtained from the IGS in 2013. Multiple samples were collected at the same time by de Lange and van Tonder.

Table 22: Previous water quality data from SA1/66, the deep SOEKOR borehole in Merweville. Only a few of the measured parameters are shown in this table. De Lange and Van Tonder collected multiple samples from this borehole on the same day.

Source	T	EC	pH	Alk	$\delta^{18}O$	$\delta^{2}H$	^{3}H	^{14}C	Cl	SO_4	Ca	Na	Sr	Li	B
	°C	µS/m		mg/L	‰		TU	pMC	mg/L						
19	46														
20		1206	7.65						3839	153	78.9	2581	13.1		22.4
20		1210	7.67						3749	202	92.9	2731	13.6		24.5
20		1203	7.49						3840	157	83.8	2593	13.7		22.8
20		1205	7.46						3969	165	84.5	2505	14.5		23.0
20		1203	7.41						3894	160	101	2796	14.4		26.1
20		1198	7.38						3914	148	89	2753	15.4		24.4
20		1217	7.38						3889	256	131.7	2674	16.8		23.3
20		1221	7.27						3937	303	166	2789	15.4		25.2
20		1224	7.42						3890	361	157.3	2617			23.1
20		1221	7.39						3927	380	173.1	2605	17.7		23.4
20		1234	7.39						3914	422	192.7	2577	16.4		22.9
20		1202	7.60						3858	237	109.5	2584	15.9		23.1

Sources: *19) Drilling logs; 20) de Lange & van Tonder, 2013*

9.3 Location description

Two sites were sampled on a private farm in Merweville during the first round of sampling, MWB1 and MWB2 (Fig. 29). Both of these sites are suspected shallow sites. The topography of the area is flat with an elevation range of 40m measured between the three sites. The field data and major ions, including B, Sr and Li, are shown in Tables 23 and 24 respectively, and the sites are plotted on a piper diagram (Fig. 30).

9.4 Sampling site selection

The field measurements, chemistry results as well as the groundwater facies shown in the piper diagram (Fig. 30), suggest that all three sites originate from different sources. SA1/66 has significantly elevated ion concentrations in comparison to MWB1 and MWB2. The original temperature of the artesian flowing water at SA1/66 (46°C) clearly puts this site apart from the others, but at the time of sampling in September 2013, the temperature was 22.9°C and did not represent water that had rapidly risen from depth. It appears as if sample collected at the surface was “stagnant” water that had risen from depth some time ago. Unfortunately a good comparison between the temperatures of the groundwater cannot be made because SA1/66 did not flow for long enough to reflect the temperature at depth. MWB2 was selected as the shallow site to be sampled again during the second round of sampling due to its low temperature of 22.3°C as well as its significantly different groundwater facies.

Table 23: Field data of the three sites sampled in Merweville during the first round of sampling.

Sample	Latitude	Longitude	Temp	EC	pH	Alk	H_2S smell
	°S	°E	°C	mS/m		mg/L	
SA1/66	32.66897	21.3589	46 / 22*	1202*	7.6*		n/a
MWB1	32.66786	21.3306	23.5	83.6	7.6	234.5	strong
MWB2	32.65599	21.30254	22.3	167	7.2	208.3	none

*46 °C is the temperature at surface measured during drilling; 22°C and 1202 mS/m are the temperature and salinity measured during the 2013 sampling by F de Lange; and the pH of 7.6 is the lab pH at IGS, UFS.

Table 24: Major ion plus B, Sr and Li results of the three sites sampled in Merweville during the first sampling round.

Sample	Cl	NO_3	SO_4	Ca	K	Mg	Na	B	Sr	Li
	mg/L							µg/L		
SA1/66*	3858.1		237	109.5	37.5	7.5	2583.6	23.1	15.9	15.9
MWB1	118.5	1.7	59.4	77	2	11.3	103.7	0.3	4.3	0.2
MWB2	161.6	3.5	599.8	260.7	2.8	29.9	142.5	0.2	7.1	0.2

* 2013 sampling by F de Lange; and the pH of 7.6 is the lab pH at IGS, UFS.

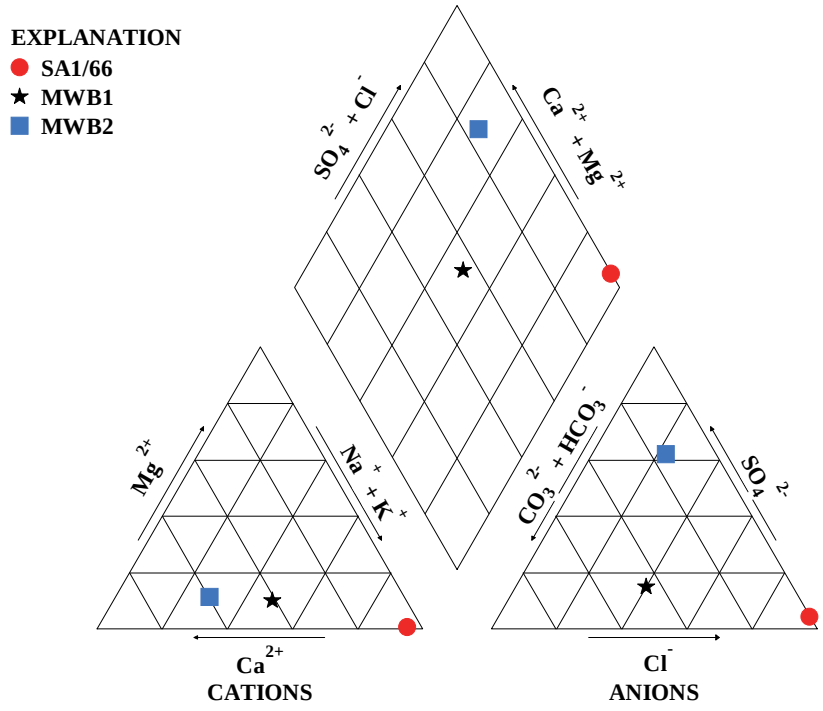

Figure 30: Piper diagram of the major ions collected in Merweville during the first round of sampling.

Appendix 4. Results of the 1st Sampling Run

				FIELD MEASUREMENTS						
Town	**Date**	**Location**	**Sample No.**	**Latitude**	**Longitude**	**Temp**	**EC**	**pH**	**ORP**	**DO**
				S (°)	**E (°)**	**°C**	**mS/m**		**mV**	**%**
Leeu Gamka	04-03-2014	Kruidfontein	WP 507	32.85454	21.96143	22.6	126	7.8	-134	42.3
	04-03-2014	Kruidfontein	WP 506	32.84831	21.96134	23.0	92	7.3	103	49.5
	04-03-2014	Kruidfontein	WP 508	32.85104	21.95657	26.9	96	7.9	-161	54.3
	04-03-2014	Groot Kruidfontein	WP 497	32.81943	21.97252	24.2	241	7.2	98	53.7
	04-03-2014	Groot Kruidfontein	WP 496	32.81472	21.97320	22.5	220	6.9	1.02	23.1
	04-03-2014	Groot Kruidfontein	WP 502	32.81053	21.97031	22.1	47	7.5	101	27.5
	04-03-2014	Groot Kruidfontein	WP 505	32.81800	21.96833	25.2	149	8.0	-169	27.6
Cradock	05-03-2014	Cradock Spa	CRS1	32.13552	25.62601	29.0	20	9.6	-143	16.8
	05-03-2014	Agri School Farm	DRB2	32.12957	25.60397	21.9	18	9.6	-152	13.5
	05-03-2014	Agri School Farm	DRB1	32.12851	25.60117	22.4	21	9.8	-156	18.1
	06-03-2014	Waaikraal Farm	DRB4	32.08600	25.58783	21.1	153	7.7	80	35.7
Fort Beaufort	06-03-2014	Sulphur Baths	BFB1	32.82640	26.67059	25.8	82	9.9	-165	34.7
	06-03-2014	Sulphur Baths	BFB2	32.83183	26.62285	24.3	201	7.3	-146	29.4
Aliwal North	07-03-2014	Aliwal North Spa (inside)	ANS1	30.71530	26.71500	33.4	208	9.1	-106	20.5
	07-03-2014	Aliwal North Spa (outside)	ANS2	30.71527	26.71548	33.6	212	9.2	-131	19.2
	07-03-2014	Aliwal North Farm	ANBH1	30.72716	26.72824	21.6	187	8.3	-58	15.8
Venterstad	08-03-2014	Wildebeest Valley	DB11a	30.84099	25.76566	20.5	127	7.6	-97	27.1
	08-03-2014	Wildebeest Valley	WVB1	30.83115	25.79826	19.8	75	7.4	78	31.1
	08-03-2014	Wildebeest Valley	WVB3	30.80172	25.77744	21.7	103	7.5	68	34.8
	08-03-2014	Rooiwaal	RWB1c	30.86604	25.58741	28.1	64	7.9	-109	20.0
	08-03-2014	Rooiwaal	RWB5	30.85875	25.58318	18.4	84	7.2	117	36.0
	09-03-2014	Vaalbank	VBB1	30.68329	25.93046	19.9	53	8.1	-106	21.7
	09-03-2014	Vaalbank	VBB2	30.67785	25.94696	20.1	55	7.1	115	49.4
	09-03-2014	La Rochelle	LRB1	30.68586	25.95916	20.5	78	7.2	132	33.9
	09-03-2014	La Rochelle	LRB2	30.68546	25.96099	20.8	59	7.3	130	40.9
Trompsburg	10-03-2014	Vlakfontein	VFB1	29.91796	25.67490	30.8	1035	9.0	-76	23.3
	10-03-2014	Vlakfontein	VFB2	29.92921	25.67945	19.6	53	7.5	80	56.2
	10-03-2014	Vlakfontein	VFB3	29.92939	25.67929	20.7	56	7.5	95	45.3
	10-03-2014	Vlakfontein	VFB4	29.92598	25.68213	19.6	103	7.1	112	36.7
Florisbad	11-03-2014	Florisbad Spa	FLS1	28.76819	26.06972	28.7	362	9.5	-53	22.2
	11-03-2014	Florisbad Resort	FLB4	28.76718	26.06870	24.5	358	9.5	-52	27.4
Merweville	13-03-2014	Soekor	SA1/66	32.66897	21.35890					
	13-03-2014	Farm	MWB1	32.66786	21.33060	23.5	84	7.6	-133	28.6
	13-03-2014	Farm	MWB2	32.65599	21.30254	22.3	167	7.2	120	42.7

continued.....

	SU	UKZN		Stellenbosch University									
Sample No.	Radon	$\delta^{18}O$	$\delta^{2}H$	Anions						Major Cations			
				Cl^-	Br^-	NO_3^{2-}	PO_4^{3-}	SO_4^{2-}	HCO_3^-	Ca^+	K^+	Mg^+	Na^+
	Bq/L	‰ SMOW		mg/L						mg/L			
WP 507	2.5	-2.9	-16.6	156.0	<1	<1	<2	164.3	234	36.0	2.7	3.4	225.1
WP 506	20.4	-2.7	-14.2	113.2	<1	<1	<2	61.0	263	58.8	3.0	8.2	125.6
WP 508	0	-3.8	-25.7	123.4	<1	<1	<2	129.1	167	37.3	3.0	2.5	155.1
WP 497	16.4	-0.4	-3.2	318.8	<1	6.7	<2	434.1	519	161.1	5.0	39.5	369.1
WP 496	29.6	-1.4	-7.3	270.1	<1	8.5	<2	409.2	520	129.7	4.1	33.0	388.4
WP 502	27.7	-0.8	-2.8	68.4	<1	<1	<2	<2	175	34.3	2.8	8.6	63.8
WP 505	3.7	-3.3	-20.4	145.9	<1	<1	<2	269.1	207	27.9	2.6	0.7	271.4
CRS1	3.3	-5.8	-32.0	61.3	<1	<1	<2	<2	50	3.3	0.4	0.4	44.2
DRB2	15.2	-3.3	-14.1	60.2	<1	<1	<2	<2	45	2.1	0.3	0.0	45.6
DRB1	31.3	-6.0	-36.1	26.0	<1	<1	<2	3.6	48	2.4	0.2	0.0	45.1
DRB4	35.4	-2.1	-5.5	41.6	<1	1.1	<2	19.2	617	25.2	3.7	55.8	226.0
BFB1	3.3	-5.9	-31.9	200.6	<1	<1	<2	7.8	49	4.3	2.0	0.0	153.3
BFB2	4.9	-3.7	-19.7	444.1	<1	<1	<2	9.4	303	78.6	1.5	40.3	277.1
ANS1	0.6	-5.0	-28.9	707.3	<1	<1	<2	<2	14	79.7	2.0	0.0	325.7
ANS2	0.9	-5.0	-29.9	741.0	<1	<1	<2	<2	18	79.3	2.0	0.0	325.5
ANBH1	55.6	-5.3	-29.3	600.9	<1	<1	<2	<2	51	13.5	0.8	0.5	375.2
DB11a	49.9	-3.2	-20.3	70.5	<1	3.5	<2	39.1	392	97.4	1.8	37.6	78.2
WVB1	81.4	-3.5	-18.5	8.6	<1	1.4	<2	17.8	348	58.6	2.0	32.8	56.6
WVB3	41.9	-3.4	-21.3	114.5	<1	4.0	<2	25.2	241	53.7	4.0	17.4	192.4
RWB1c	7.5	-3.9	-23.9	34.1	<1	<1	<2	23.1	217	32.4	0.7	4.5	102.1
RWB5	44.3	-3.5	-21.3	23.4	<1	<1	<2	29.2	354	81.9	1.5	34.5	45.1
VBB1	48.6	-4.5	-26.2	90.5	<1	<1	<2	<2	124	15.0	0.6	2.7	93.6
VBB2	86.9	-3.0	-13.8	11.5	<1	7.2	<2	20.5	253	61.3	0.8	26.4	19.2
LRB1	6.3	-3.2	-18.4	25.2	<1	6.7	<2	27.9	305	89.3	1.1	31.1	33.5
LRB2	65.1	-3.6	-20.0	12.6	<1	6.8	<2	17.9	267	66.7	1.0	23.4	27.9
VFB1	1.6	-5.9	-32.9	3598.6	14.5	<1	<2	736.4	23	452.6	21.0	0.2	2418.0
VFB2	43	-3.7	-21.6	13.9	<1	9.9	<2	24.2	217	73.7	2.1	23.5	29.2
VFB3	61.4	-3.7	-23.8	17.0	<1	2.9	<2	31.6	215	78.3	1.3	17.6	34.9
VFB4	80.8	-3.3	-19.2	57.9	<1	54.2	<2	37.1	289	129.8	2.7	39.7	51.3
FLS1	15.5	-5.2	-30.5	1540.4	2.1	<1	<2	<2	21	102.1	9.1	0.1	790.8
FLB4	4.8	-5.6	-30.4	1407.6	3.3	<1	<2	<2	19	95.4	5.5	0.1	815.5
SA1/66				3858.1				237.0		109.5	37.5	7.5	2583.6
MWB1	1.5	-3.4	-20.8	23.0	<1	1.8	<2	47.8	235	77.0	2.0	11.3	103.7
MWB2	46.8	-4.2	-25.9	90.0	<1	3.7	<2	869.4	208	260.7	2.8	29.9	142.5

SU: Stellenbosch University

UKZN: University of KwaZulu-Natal

continued....

Sample No.	Stellenbosch University Trace elements and heavy metals																										
	P	S	Si	Li	Be	B	Al	Sc	Ti	V	Cr	Mn	Fe	Co	Ni	Cu	Zn	As	Se	Sr	Y	Mo	Cd	Ba	Hg	Pb	Th	U
	mg/L			µg/L																								
WP 507	0.024	64.050	11.150	709.433	0.031	646.435	1.301	0.083	0.104	0.127	0.081	42.273	33.107	0.037	0.038	0.273	0.793	0.543	1.464	2702.276	0.037	7.986	0.011	30.890	0.012	0.027	0.006	1.323
WP 506	0.017	28.520	10.570	240.604	0.010	270.974	0.411	0.068	0.043	0.560	0.095	14.325	4.659	0.040	0.077	0.341	1.863	3.317	1.161	2909.469	0.018	23.583	0.008	42.330	<0.006	0.043	<0.001	3.660
WP 508	0.003	70.990	12.510	425.674	0.031	325.210	0.721	0.060	0.061	0.055	0.073	41.118	12.914	<0.014	0.033	0.085	0.745	0.053	4.832	2721.109	0.021	1.945	0.005	39.507	0.015	0.008	0.002	0.534
WP 497	0.051	153.300	12.880	543.684	0.031	663.193	2.220	0.078	0.829	3.882	0.862	0.855	2.049	0.114	0.493	3.194	10.874	1.381	2.465	4974.218	0.089	4.119	0.011	40.680	0.015	0.138	0.001	18.425
WP 496	0.026	147.900	11.120	594.755	0.055	826.252	1.852	0.062	0.712	2.589	0.245	118.118	2.224	0.256	0.635	5.026	12.531	2.289	1.459	4320.742	0.093	7.687	0.009	55.166	<0.006	0.063	0.002	18.392
WP 502	0.036	11.730	10.270	78.836	0.014	145.381	8.848	0.056	0.221	2.058	0.218	0.705	6.142	0.055	0.222	1.750	7.433	2.843	0.912	1689.347	0.041	8.432	0.006	33.979	<0.006	0.035	0.004	2.400
WP 505	0.016	99.450	11.020	729.475	0.020	657.374	1.207	0.047	0.074	0.068	0.092	21.617	12.102	<0.014	0.037	0.033	1.726	0.112	3.484	3195.111	0.016	4.302	0.003	40.953	0.023	<0.004	0.003	0.432
CRS1	< 0.003	34.800	19.440	122.121	0.008	435.457	30.785	0.079	0.104	0.647	0.068	0.273	3.879	<0.014	0.094	0.075	5.573	1.418	3.297	76.411	<0.003	2.057	0.002	2.150	0.033	0.010	0.004	0.037
DRB2	0.008	38.350	21.930	132.167	<0.006	428.976	5.723	0.078	0.454	0.127	0.072	0.535	225.897	0.031	0.046	0.378	29.322	2.872	2.910	29.922	<0.003	1.608	0.005	0.144	0.044	0.050	0.004	0.017
DRB1	< 0.003	55.040	21.510	123.965	0.007	432.679	3.997	0.094	0.061	0.053	0.075	0.254	0.366	0.015	<0.010	0.044	3.746	2.228	2.220	44.321	<0.003	1.040	0.000	2.470	0.033	<0.004	0.004	0.003
DRB4	0.141	16.640	22.720	10.875	<0.006	657.979	0.411	0.101	0.104	100.600	5.726	0.103	0.702	0.099	0.210	1.371	6.557	22.207	2.153	646.528	<0.003	22.008	0.002	28.724	0.015	0.006	<0.001	21.967
BFB1	< 0.003	114.000	23.890	547.808	<0.006	1899.571	5.900	0.143	0.252	0.149	0.097	0.474	6.706	<0.014	0.053	0.087	2.447	0.864	3.145	376.904	<0.003	0.621	0.001	29.700	0.063	0.025	0.019	0.006
BFB2	< 0.003	156.000	8.782	149.176	0.064	802.702	0.507	0.046	0.037	0.151	0.108	226.295	21.040	0.030	0.020	0.031	0.581	3.614	2.785	3212.473	0.064	0.160	0.004	175.580	0.040	<0.004	0.002	1.248
ANS1	0.006	16.160	11.740	446.449	<0.006	911.808	4.319	0.056	0.043	0.163	0.070	1.535	0.481	0.121	0.036	0.074	0.447	0.090	1.361	1408.137	<0.003	0.416	0.001	20.003	0.020	0.007	0.003	0.001
ANS2	< 0.003	26.270	11.750	435.794	<0.006	916.485	5.399	0.056	0.043	0.134	0.052	1.611	0.721	<0.014	<0.010	0.028	0.765	0.068	1.375	1363.066	<0.003	0.282	0.002	19.257	0.017	0.006	0.002	<0.000
ANBH1	0.002	2.789	4.950	384.233	<0.006	589.738	6.004	<0.043	0.245	0.137	0.148	50.098	8.311	<0.014	0.056	0.098	1.141	0.077	0.934	664.247	0.005	1.834	0.002	357.561	0.008	0.008	0.004	0.001
DB11a	0.052	16.150	14.330	53.622	<0.006	191.446	2.467	0.083	0.166	13.464	0.462	53.341	11.458	0.213	0.836	0.463	187.384	3.601	1.949	1317.728	0.052	1.626	0.014	90.573	0.008	0.042	<0.001	6.757
WVB1	0.023	6.827	13.310	22.661	<0.006	102.197	1.075	0.059	<0.032	17.761	0.621	0.359	0.804	0.032	0.071	0.409	2.597	3.215	1.375	899.284	0.070	1.441	0.006	66.967	<0.006	0.006	<0.001	10.134
WVB3	0.013	16.140	12.240	143.258	0.018	1028.391	0.450	0.044	0.049	41.982	0.209	50.024	496.119	0.087	0.290	0.205	34.895	6.185	1.335	1201.710	0.128	2.404	0.001	164.069	<0.006	0.012	0.002	6.985
RWB1c	< 0.003	38.740	12.310	120.558	0.008	352.820	4.031	<0.043	0.123	0.053	0.081	38.789	7.949	<0.014	<0.010	<0.023	0.138	0.040	1.593	1057.226	0.021	0.131	0.004	35.847	0.011	0.015	<0.001	0.019
RWB5	0.036	13.750	11.900	31.968	<0.006	100.653	0.083	0.060	0.043	8.933	0.323	14.594	0.508	0.023	0.217	1.758	3.218	1.007	1.441	878.331	0.080	1.510	0.008	74.273	<0.006	0.074	<0.001	35.497
VBB1	< 0.003	4.576	9.681	38.907	0.010	403.784	3.117	<0.043	0.117	0.072	0.067	6.822	12.116	<0.014	<0.010	0.039	0.283	0.071	0.908	299.547	0.003	0.053	0.000	7.192	0.006	0.007	0.001	0.026
VBB2	0.064	7.675	15.890	14.427	<0.006	33.207	0.126	0.054	0.074	16.368	0.438	0.050	0.182	0.029	0.033	3.924	4.853	5.596	1.397	472.777	0.028	1.041	0.006	15.515	<0.006	0.034	<0.001	2.678
LRB1	0.025	11.170	14.300	28.420	<0.006	46.816	<0.038	0.058	0.074	10.666	0.301	0.063	0.625	0.055	0.077	1.418	11.361	3.327	1.219	778.377	0.065	0.727	0.010	34.937	<0.006	0.070	<0.001	4.127
LRB2	0.022	6.563	14.310	26.615	0.008	45.773	0.085	0.051	0.074	10.493	0.289	0.057	0.183	0.024	0.018	0.194	1.492	3.407	1.068	604.573	0.039	1.054	0.007	29.730	<0.006	0.131	<0.001	2.601
VFB1	< 0.003	295.200	11.870	6583.303	0.006	3640.948	4.710	0.096	0.068	0.227	0.103	1.553	9.188	0.027	0.041	<0.023	0.393	0.122	1.544	17782.227	0.019	15.002	0.004	63.197	0.019	0.008	0.005	0.000
VFB2	0.025	8.904	14.700	33.732	<0.006	74.204	0.998	0.068	<0.032	14.615	0.305	0.284	2.140	0.040	0.092	0.349	73.002	3.470	1.713	602.609	0.045	1.840	0.002	108.626	<0.006	0.136	<0.001	2.596
VFB3	0.012	11.450	13.180	40.976	<0.006	89.396	0.154	0.070	0.061	9.907	0.249	0.113	1.006	0.035	0.086	0.571	6.686	3.442	2.959	1604.212	0.051	2.407	0.004	203.921	<0.006	0.015	<0.001	3.031
VFB4	0.051	20.770	14.610	36.137	<0.006	84.802	0.623	0.065	0.061	10.372	0.219	0.184	0.532	0.118	0.510	3.022	3.018	3.548	1.206	1245.183	0.166	2.417	0.004	179.089	<0.006	0.027	<0.001	10.066
FLS1	< 0.003	3.537	10.190	640.174	<0.006	1966.404	3.331	0.053	0.055	0.181	0.070	1.452	0.544	<0.014	0.012	<0.023	0.597	0.061	1.201	4276.436	<0.003	0.279	0.001	199.943	0.017	<0.004	0.002	0.002
FLB4	< 0.003	3.853	8.022	649.215	0.007	2136.616	2.152	<0.043	0.055	0.151	0.082	15.631	2.392	<0.014	<0.010	<0.023	0.600	0.079	1.161	3736.545	<0.003	0.279	0.002	995.626	0.016	<0.004	0.002	0.001
SA1/66																												
MWB1	< 0.003	60.630	10.770	155.867	<0.006	262.091	0.418	0.059	0.043	0.160	0.101	27.773	49.767	0.014	0.021	0.031	0.914	0.113	2.367	4315.813	0.144	0.390	0.002	100.365	0.006	0.016	<0.001	2.283
MWB2	0.009	201.000	9.311	207.197	0.007	220.928	7.053	0.057	0.393	0.669	0.111	75.758	11.179	0.138	0.270	7.123	41.746	0.626	1.877	7110.348	0.075	5.447	0.041	66.813	0.007	0.059	0.003	10.774

continued....

Sample No.	Stellenbosch University Rare Earth Elements													
	La	Ce	Pr	Nd	Sm	Eu	Gd	Tb	Dy	Ho	Er	Tm	Yb	Lu
	µg/L													
WP 507	0.009	0.013	0.002	0.006	<0.002	0.003	0.001	<0.004	0.002	0.000	0.002	0.000	0.001	0.001
WP 506	0.005	0.004	0.001	0.002	<0.002	0.002	0.001	<0.004	0.001	0.000	0.001	0.000	0.002	<0.000
WP 508	0.017	0.026	0.003	0.013	0.002	0.003	0.001	<0.004	0.001	0.000	0.002	0.000	<0.001	<0.000
WP 497	0.017	0.011	0.004	0.012	0.003	0.002	0.006	<0.004	0.005	0.001	0.005	0.001	0.005	0.001
WP 496	0.015	0.036	0.002	0.012	<0.002	0.004	0.006	<0.004	0.003	0.001	0.004	0.001	0.007	0.001
WP 502	0.048	0.066	0.008	0.032	0.009	0.003	0.004	<0.004	0.005	0.001	0.003	0.001	0.002	<0.000
WP 505	0.002	0.005	0.000	0.002	<0.002	0.002	0.001	<0.004	0.001	0.000	0.001	0.000	<0.001	<0.000
CRS1	0.102	0.038	0.001	<0.002	<0.002	<0.001	0.001	<0.004	0.001	<0.000	<0.001	0.000	<0.001	<0.000
DRB2	0.003	0.008	0.000	0.003	<0.002	<0.001	0.001	<0.004	0.001	<0.000	<0.001	0.000	<0.001	<0.000
DRB1	0.001	<0.001	<0.000	<0.002	<0.002	<0.001	0.001	<0.004	0.000	<0.000	<0.001	0.000	<0.001	<0.000
DRB4	0.001	0.002	0.000	<0.002	<0.002	0.002	0.001	<0.004	0.001	<0.000	<0.001	0.000	<0.001	<0.000
BFB1	0.002	0.003	0.000	<0.002	<0.002	<0.001	0.001	<0.004	0.000	<0.000	<0.001	0.000	<0.001	<0.000
BFB2	0.042	0.061	0.009	0.032	0.007	0.009	0.007	<0.004	0.007	0.001	0.005	0.000	0.004	0.001
ANS1	0.001	<0.001	<0.000	<0.002	<0.002	<0.001	0.001	<0.004	0.000	<0.000	<0.001	0.000	<0.001	<0.000
ANS2	0.000	<0.001	<0.000	<0.002	<0.002	<0.001	0.000	<0.004	0.000	<0.000	<0.001	0.000	<0.001	<0.000
ANBH1	0.005	0.007	0.001	0.004	<0.002	0.020	0.004	<0.004	0.001	0.000	0.001	0.000	<0.001	<0.000
DB11a	0.008	0.022	0.002	0.007	<0.002	0.005	0.004	<0.004	0.005	0.001	0.003	0.001	0.004	0.001
WVB1	0.007	0.001	0.001	0.006	0.002	0.005	0.004	<0.004	0.005	0.001	0.005	0.000	0.005	0.001
WVB3	0.023	0.039	0.007	0.035	0.011	0.010	0.011	<0.004	0.014	0.003	0.009	0.001	0.007	0.001
RWB1c	0.007	0.011	0.002	0.009	0.002	0.001	0.003	<0.004	0.003	0.001	0.002	0.000	0.001	<0.000
RWB5	0.005	<0.001	0.001	0.004	<0.002	0.004	0.004	<0.004	0.005	0.002	0.004	0.001	0.005	0.001
VBB1	0.005	0.007	0.001	0.002	<0.002	<0.001	0.000	<0.004	0.001	<0.000	<0.001	0.000	<0.001	<0.000
VBB2	0.011	<0.001	0.002	0.003	<0.002	0.002	0.001	<0.004	0.002	0.000	0.002	0.000	0.001	<0.000
LRB1	0.011	<0.001	0.001	0.008	<0.002	0.002	0.003	<0.004	0.003	0.001	0.003	0.001	0.003	<0.000
LRB2	0.003	<0.001	0.001	0.004	<0.002	0.002	0.002	<0.004	0.003	0.001	0.001	0.001	0.002	<0.000
VFB1	0.000	<0.001	<0.000	<0.002	<0.002	0.003	0.001	<0.004	0.000	0.000	<0.001	0.000	<0.001	<0.000
VFB2	0.008	0.001	0.001	0.008	<0.002	0.006	0.002	<0.004	0.002	0.001	0.002	0.001	0.002	<0.000
VFB3	0.021	0.001	0.003	0.013	0.004	0.013	0.004	<0.004	0.005	0.001	0.002	0.000	0.003	<0.000
VFB4	0.027	0.002	0.005	0.026	0.007	0.011	0.011	<0.004	0.012	0.002	0.009	0.001	0.007	0.001
FLS1	0.001	<0.001	<0.000	<0.002	<0.002	0.012	0.002	<0.004	0.000	<0.000	<0.001	0.000	<0.001	<0.000
FLB4	0.002	<0.001	<0.000	<0.002	<0.002	0.043	0.004	<0.004	0.000	<0.000	<0.001	0.000	<0.001	<0.000
SA1/66														
MWB1	0.064	0.099	0.013	0.058	0.010	0.005	0.014	<0.004	0.010	0.003	0.011	0.001	0.009	0.001
MWB2	0.053	0.073	0.008	0.030	0.004	0.005	0.004	<0.004	0.005	0.001	0.002	0.001	0.005	<0.000

Appendix 5. Results of the 2nd Sampling Run

Appendix 5a. Stellenbosch University Data

Town	Location	Sample No.	Latitude	Longitude	FIELD MEASUREMENTS			SU ANIONS						SU CATIONS				CB	SU FIELD Radon	
			S (°)	E (°)	Temp °C	pH	EC mS/m	Cl^- mg/L	Br^- mg/L	NO_3^{2-} mg/L	PO_4^{3-} mg/L	SO_4^{2-} mg/L	HCO_3^- mg/L	Ca^{2+} mg/L	K^+ mg/L	Mg^{2+} mg/L	Na^+ mg/L	%	Bq/L	±
Leeu Gamka	Kruidfontein	WP 508	32.85104	21.95657	26.5	8.1	93	83	<1	<1	<2	101	140	34	2.9	2.37	144	1.37	1.1	0.8
	Groot Kruidfontein	WP 502	32.81053	21.97031	20.3	7.9	53	30	<1	<1	<2	32	172	39	2.7	10.11	58	5.72	13.6	2.1
	Groot Kruidfontein	WP 505	32.81800	21.96833	23.5	8.2	133	80	<1	<1	<2	219	178	22	2.2	0.56	233	2.23	1.2	0.7
Cradock	Cradock Spa	CRS1	32.13552	25.62601	29.4	9.8	21	24	<1	<1	<2	7	28	3	0.3	0.01	43	-7.25	2.1	1.0
	Waaikraal Farm	DRB4	32.08600	25.58783	16.2	7.8	162	62	<1	<1	<2	48	612	26	3.8	60.09	242	8.05	34.7	3.5
Fort Beaufort	Sulphur Baths	BFB1	32.82640	26.67059	23.5	10.0	82	191	<1	<1	<2	23	30	4	2.0	0.01	144	3.24	3.4	1.2
	Sulphur Baths	BFB2	32.83183	26.62285	21.2	7.4	200	452	<1	<1	<2	<2	244.0	76	1.5	39.10	266	-0.16	5.7	1.4
	Rocky Ridge	RRB1	32.82032	26.58832	21.2	7.1	249	463	2.3	15.8	<2	74	418	148	5.0	72.64	280	0.65	38.6	3.5
Aliwal North	Aliwal North Spa (inside)	ANS1	30.71530	26.71500	30.0	9.1	201	515	<1	<1	<2	<2	24.0	78	1.8	0.03	314	-2.64	1.3	0.8
	Aliwal North Farm	ANBH1	30.72716	26.72824	21.6	7.5	190	484	<1	<1	<2	<2	25.0	14	1.0	1.25	350	0.41	57.6	4.4
Venterstad	Rooiwaal	RWB1c	30.86604	25.58741	25.7	8.0	49	32	<1	<1	<2	18	170	20	0.5	2.88	81	0.54	20.7	2.6
	Rooiwaal	RWB5	30.85875	25.58318	18.1	7.4	85	26	<1	<1	<2	32	280	77	1.6	34.07	42	3.28	39.1	3.6
	Vaalbank	VBB1	30.68329	25.93046	18.2	8.4	54	85	<1	<1	<2	<2	94.0	14	0.6	2.65	88	-3.04	17.5	2.4
	La Rochelle	LRB2	30.68546	25.96099	17.3	7.5	58	17	<1	7.8	<2	14	216	63	0.9	23.30	26	0.78	43.5	4.0
Trompsburg	Vlakfontein	VFB1	29.91796	25.67490	29.5	9.2	1019	3869	<1	<1	<2	956	14	432	17.2	0.14	2363	4.73	2.5	1.0
	Vlakfontein	VFB2	29.92921	25.67945	18.2	7.7	50	12	<1	14.9	<2	17	130	57	1.5	20.58	23	6.82	48.6	4.0
Florisbad	Florisbad Spa	FLS1	28.76819	26.06972	28.7	9.4	362	1034	<1	<1	<2	<2	2.0	86	7.2	0.07	696	-2.29	9.1	1.8
	Farm	FLB5	28.79426	26.09168	19.2	7.7	138	196	<1	53.9	<2	62	240	92	17.2	58.14	75	-9.7	152.3	8.0
Merweville	Soekor borehole	SA1/66	32.66897	21.35890																
	Farm	MWB2	32.65599	21.30254	21.5	7.1	107	114	<1	<1	<2	84	252	93	2.2	18.94	79	2.72	163.5	7.0

SU: Stellenbosch University

CB: Charge Balance

continued....

Town	Location	Sample No.	STELLENBOSCH UNIVERSITY																			
			Li		Be		B		Al		V		Cr		Mn		Fe		Co		Ni	
			µg/L	%RSD	µg/L	%RSD	µg/L	%RSD	µg/L	%RSD	µg/L	%RSD	µg/L	%RSD	µg/L	%RSD	µg/L	%RSD	µg/L	%RSD	µg/L	%RSD
Leeu Gamka	Kruidfontein	WP 508	540.38	1.4	0.044	15.2	333.37	2.5	1.52	3.4	< 0.017	N/A	< 0.021	31.9	42.34	2.6	11.99	0.9	0.06	3.7	0.05	26.0
	Groot Kruidfontein	WP 502	99.05	3.4	0.014	11.5	110.58	2.3	4.27	17.8	1.49	0.2	0.040	20.5	1.49	5.2	3.85	1.7	0.04	7.0	0.13	13.0
	Groot Kruidfontein	WP 505	945.82	2.4	< 0.005	35.1	664.53	1.7	2.59	3.4	< 0.017	26.7	< 0.021	330.5	23.32	1.0	11.65	1.8	0.08	11.3	0.05	22.8
Cradock	Cradock Spa	CRS1	166.90	2.1	< 0.005	62.8	473.45	2.1	27.20	1.8	0.51	7.9	< 0.021	57.1	0.21	3.8	3.12	2.6	0.04	8.3	0.08	9.1
	Waaikraal Farm	DRB4	14.52	3.8	< 0.005	113.2	753.40	1.5	0.69	6.9	93.18	2.9	5.974	2.1	0.06	1.3	0.27	13.7	0.09	4.8	0.19	2.6
Fort Beaufort	Sulphur Baths	BFB1	650.00	1.3	< 0.005	34.4	1909.28	2.9	11.68	1.9	< 0.017	67.0	0.072	9.5	0.42	6.4	8.83	1.0	0.01	27.2	0.04	21.8
	Sulphur Baths	BFB2	170.43	2.8	0.093	5.7	760.91	2.5	1.67	4.6	0.05	15.3	< 0.021	60.6	251.38	1.2	104.65	1.5	0.04	13.6	0.02	32.8
	Rocky Ridge	RRB1	43.70	2.1	0.028	2.8	295.14	0.7	0.49	8.0	1.24	2.3	0.056	17.1	0.29	14.0	0.47	3.2	0.17	4.1	0.16	8.1
Aliwal North	Aliwal North Spa (inside)	ANS1	539.58	2.2	< 0.005	56.7	924.62	1.3	14.26	2.9	< 0.017	39.0	0.128	4.9	1.69	4.4	5.64	3.1	0.01	26.0	0.06	35.1
	Aliwal North Farm	ANBH1	540.46	2.2	< 0.005	77.1	670.06	2.8	6.26	3.6	0.03	16.6	< 0.021	24.4	56.83	2.2	4.97	1.5	0.02	29.2	0.06	13.2
Venterstad	Rooiwaal	RWB1c	164.97	1.7	0.023	15.3	389.95	1.7	2.73	2.4	< 0.017	40.5	< 0.021	391.7	40.25	0.9	6.54	3.8	0.04	8.3	0.04	9.8
	Rooiwaal	RWB5	41.90	0.6	< 0.005	115.5	98.09	2.2	13.30	2.4	8.43	2.7	0.238	8.2	15.67	1.6	9.87	1.6	0.04	6.6	0.27	8.4
	Vaalbank	VBB1	49.73	1.8	< 0.005	53.5	406.40	1.5	2.59	3.3	< 0.017	85.8	< 0.021	307.4	7.19	1.1	10.04	1.1	0.02	11.2	0.04	18.2
	La Rochelle	LRB2	34.33	1.3	< 0.005	33.9	42.58	1.1	0.24	4.1	9.93	0.8	0.208	5.7	0.04	39.6	0.20	5.0	0.04	18.4	0.03	24.1
Trompsburg	Vlakfontein	VFB1	6813.93	0.7	< 0.005	135.8	3065.51	1.7	8.77	2.1	0.03	21.1	< 0.021	37.9	2.09	4.5	3.86	2.8	0.01	0.5	0.03	12.3
	Vlakfontein	VFB2	39.08	1.7	< 0.005	14.2	55.22	2.1	0.78	3.9	12.50	0.7	0.176	15.8	0.25	4.2	1.46	3.3	0.05	12.9	0.09	22.1
Florisbad	Florisbad Spa	FLS1	842.81	3.0	< 0.005	41.6	2030.81	2.1	5.47	3.6	0.05	6.7	0.105	1.0	2.69	2.3	4.08	0.8	0.01	16.2	0.05	12.7
	Farm	FLB5	18.05	2.0	0.012	18.7	72.26	0.5	8.02	2.8	7.84	1.3	0.584	1.9	1.65	1.1	18.13	1.2	0.05	3.2	0.29	1.4
Merweville	Soekor borehole	SA1/66																				
	Farm	MWB2	264.79	2.0	< 0.005	30.7	223.96	3.9	3.39	5.0	0.61	4.0	< 0.021	37.7	77.31	1.1	3.22	4.7	0.13	2.2	0.30	9.2

RSD: Relative Standard Deviation

continued....

Town	Location	Sample No.	STELLENBOSCH UNIVERSITY																			
			Cu		Zn		Ar		Se		Sr		Mo		Cd		Ba		Pb		U	
			µg/L	%RSD	µg/L	%RSD	µg/L	%RSD	µg/L	%RSD	µg/L	%RSD	µg/L	%RSD	µg/L	%RSD	µg/L	%RSD	µg/L	%RSD	µg/L	%RSD
Leeu Gamka	Kruidfontein	WP 508	0.022	7.2	1.027	6.1	0.042	33.0	0.245	16.3	2427.793	0.9	1.221	1.6	< 0.01	32.2	41.568	1.5	0.054	7.5	0.664	2.4
	Groot Kruidfontein	WP 502	0.926	6.4	2.295	8.4	2.348	2.5	0.492	27.5	1754.808	1.0	7.408	0.6	< 0.01	109.0	48.241	1.5	0.032	6.1	4.118	1.5
	Groot Kruidfontein	WP 505	0.010	12.9	1.731	7.5	0.102	20.3	< 0.22	47.0	2639.927	1.9	1.982	2.7	< 0.01	173.2	40.913	0.8	0.009	10.5	0.544	1.8
Cradock	Cradock Spa	CRS1	0.028	9.3	2.581	3.2	1.379	2.4	< 0.22	77.4	67.526	1.0	1.158	3.0	< 0.01	91.9	2.064	0.5	0.023	9.4	0.048	2.9
	Waaikraal Farm	DRB4	1.184	1.0	0.374	22.6	27.588	3.5	2.699	22.4	582.018	2.4	26.815	4.3	< 0.01	102.3	33.328	2.4	0.016	6.5	26.558	5.6
Fort Beaufort	Sulphur Baths	BFB1	0.028	7.2	0.327	12.0	0.557	6.9	< 0.22	100.0	306.898	0.8	0.354	2.2	< 0.01	42.9	26.863	3.0	0.060	4.7	0.001	12.0
	Sulphur Baths	BFB2	0.007	26.8	0.204	11.0	2.825	3.0	< 0.22	57.0	2224.480	2.0	0.064	11.5	< 0.01	132.9	160.323	0.4	0.012	2.4	1.310	1.8
	Rocky Ridge	RRB1	3.104	0.8	31.151	1.0	0.707	8.0	3.095	9.5	1936.248	1.6	1.169	3.2	0.022	49.1	13.022	1.4	0.179	1.7	11.784	0.9
Aliwal North	Aliwal North Spa (inside)	ANS1	0.215	4.7	1.027	3.6	0.078	17.1	< 0.22	60.1	1103.745	2.0	0.598	6.0	< 0.01	115.7	19.585	0.9	0.018	3.7	0.004	11.4
	Aliwal North Farm	ANBH1	0.291	6.6	1.321	6.7	0.059	14.8	< 0.22	81.6	536.067	2.1	2.105	2.0	< 0.01	76.6	372.388	1.6	0.028	1.6	0.003	6.1
Venterstad	Rooiwaal	RWB1c	0.027	11.8	0.346	14.3	0.018	20.2	0.202	31.5	921.319	1.3	0.145	0.2	< 0.01	N/A	36.262	0.4	0.032	8.0	0.023	5.5
	Rooiwaal	RWB5	1.738	3.4	3.730	3.4	0.944	4.9	0.855	32.6	780.943	1.2	1.616	1.9	0.010	15.7	76.477	2.4	0.144	1.7	40.851	3.5
	Vaalbank	VBB1	0.843	1.8	0.963	8.9	0.065	12.3	< 0.22	88.7	244.432	0.6	0.116	10.9	< 0.01	173.2	7.242	3.8	0.040	5.2	0.040	1.5
	La Rochelle	LRB2	0.417	5.3	2.275	5.6	3.448	0.4	0.809	39.1	511.728	0.9	1.160	1.6	< 0.01	91.4	29.450	1.4	0.186	0.9	3.141	3.0
Trompsburg	Vlakfontein	VFB1	0.052	14.8	< 0.33	30.8	< 0.012	56.2	< 0.22	60.8	12435.787	0.9	23.384	2.1	< 0.01	68.3	71.879	1.5	0.010	9.9	0.002	10.6
	Vlakfontein	VFB2	0.691	1.6	69.593	1.2	3.125	2.4	1.119	12.5	526.257	0.8	1.959	2.6	< 0.01	47.0	112.157	1.1	0.233	0.7	3.594	2.3
Florisbad	Florisbad Spa	FLS1	0.056	5.1	0.588	4.2	0.014	37.6	< 0.22	65.2	3205.623	1.2	0.391	1.3	< 0.01	173.2	214.245	1.0	0.029	5.9	0.004	13.6
	Farm	FLB5	3.009	1.5	16.623	1.7	0.934	4.2	1.829	13.1	438.443	1.9	0.333	4.4	0.021	38.1	11.683	2.4	0.249	0.9	2.536	2.3
Merweville	Soekor borehole	SA1/66																				
	Farm	MWB2	7.532	1.8	37.311	2.8	0.642	6.6	1.105	12.9	5862.800	2.0	6.175	2.2	0.036	23.1	69.703	1.7	0.051	4.3	15.070	3.4

Appendix 5b. Duke University Data

Town	Location	Sample No.	F^-	Cl^-	Br^-	NO_3^{2-}	SO_4^{2-}	HCO_3^-	Ca^+	Mg^+	K^+	Na^+	CB	δ^2H	$\delta^{18}O$	$\delta^{13}C$-DIC	$\delta^{11}B$	$^{87}Sr/^{86}Sr$	^{226}Ra	^{228}Ra	$^{228/226}Ra$
			mg/L						mg/L				%	‰ SMOW		PDB	‰		Bq/L		
Leeu Gamka	Kruidfontein	WP 508	2.2	76.2	0.33	0.04	150.3	211.8	37.5	2.6	1.5	166.4	3.3	-29.9	-4.3	-15.1	8.9	0.71158			
	Groot Kruidfontein	WP 502	0.9	24.1	0.10	3.73	42.4	236.0	39.2	10.2	1.0	62.4	0.5	4.3	0.7	-11.1		0.71160	0.0017	0.0118	6.94
	Groot Kruidfontein	WP 505	3.7	91.7	0.43	0.07	278.0	232.0	23.6	0.5	1.4	255.1	0.7	-29.8	-4.2	-17.6	9.3	0.71117			
Cradock	Cradock Spa	CRS1	7.0	20.9	0.08	0.03	8.1	55.2	3.4	0.0	0.1	57.0	22.8	-41.5	-6.7	-3.1		0.70985			
	Waaikraal Farm	DRB4	1.2	42.3	0.20	21.59	60.6	764.1	30.0	52.3	0.6	286.8	8.9	-12.3	-1.7	-15.4	32.9	0.71233			
Fort Beaufort	Sulphur Baths	BFB1	16.1	174.0	0.64	0.25	17.1	62.7	4.6	0.0	0.3	160.1	6.7	-41.6	-6.0	16.4	5.4	0.71005	0.0016	0.0042	2.63
	Sulphur Baths	BFB2	3.4	435.8	1.51		24.0	402.6	81.2	37.1	1.6	303.2	2.4	-25.5	-4.3	-13.3	19.9	0.70893			
	Rocky Ridge	RRB1	1.3	523.6	2.01	17.86	89.3	622.2	165.0	71.3	1.7	384.8	6.6	-25.7	-4.0	-11.2	35.1	0.70963			
Aliwal North	Aliwal North Spa (inside)	ANS1	4.5	664.6	1.44	0.29	2.3	19.9	99.1	0.0	1.1	408.2	8.6	-36.7	-6.0	-11.6	9.5	0.71208	0.0076	0.0123	1.62
	Aliwal North Farm	ANBH1	3.8	545.9	1.24	0.05	1.2	72.8	17.9	1.5	0.6	392.6	4.3	-37.0	-5.6	-19.8	15.2	0.71211			
Venterstad	Rooiwaal	RWB1c	2.5	26.9	0.17	0.04	22.4	226.7	22.2	3.2	0.4	101.5	8.0	-30.9	-4.9	-4.7	6.5	0.71020			
	Rooiwaal	RWB5	0.4	20.2	0.18	0.46	44.0	465.4	73.4	28.1	0.6	45.2	-6.6	-28.3	-4.4	-12.3		0.71045			
	Vaalbank	VBB1	3.1	77.3	0.32	0.08	2.4	167.3	16.5	3.1	0.3	112.6	9.2	-32.5	-4.7	-9.0	5.9	0.71057	0.0068	0.0063	0.93
	La Rochelle	LRB2	0.3	10.1	0.09	11.34	21.1	339.1	54.0	19.6	0.4	28.3	-7.5	-27.3	-4.2	-9.6		0.71004			
Trompsburg	Vlakfontein	VFB1	3.7	4076.4	23.39	0.83	870.2	24.5	553.7	0.1	11.5	2469.6	0.7	-39.1	-6.5	-19.1	29.9	0.77177			
	Vlakfontein	VFB2	0.6	12.0	0.09	23.98	24.3	283.5	37.4	12.8	0.3	17.6	-22.6	-29.0	-3.7	-9.4		0.71067	0.0019	0.0096	5.05
Florisbad	Florisbad Spa	FLS1	5.7	1334.4	4.01	3.88	2.6	21.8	101.9	0.1	2.8	806.3	2.7	-37.7	-5.8	-32.3	23.2	0.75394			
	Farm	FLB5	0.9	135.6	0.77	93.14	82.9	444.2	97.5	49.1	0.8	83.2	-6.4	-21.5	-3.6	-4.7	32.9	0.71838			
Merweville	Soekor borehole	SA1/66	5.6	3606.5	13.43	0.12	130.1		129.2	4.0	12.8	530.6					23.9				
	Farm	MWB2	0.6	102.9	0.46	16.44	98.0	347.0	87.3	19.6	1.5	91.1	-4.3	-30.6	-4.8	-13.5	26.9	0.71056	0.0061	0.0146	2.39

continued.....

Sample No.	Li	Be	B	Mg	Al	Ca	V	Cr	Mn	Fe	Co	Ni	Cu	Zn	As	Se	Rb	Sr	Mo	Ag	Cd	Sb	Ba	Tl	Pb	Th	U
	µg/L																										
WP 508	533.07	0.03	391.61	5.89	0.88	39.65	0.74	1.92	37.93	57.64	0.04	0.60	8.55	1.11	0.12	0.00	6.26	2379.10	1.95	0.00	0.00	0.00	39.32	0.00	0.00	0.00	0.66
WP 502	110.82	0.00	124.30	10.00	1.62	44.08	1.74	0.62	1.79	84.39	0.09	0.92	0.91	1.84	2.13	0.36	1.17	1696.75	7.10	0.00	0.01	0.15	46.32	0.00	0.00	0.00	4.02
WP 505	438.29	0.01	616.41	1.17	0.00	24.28	0.72	1.94	14.81	23.39	0.03	0.00	0.02	0.09	0.13	0.11	3.49	2189.84	0.88	0.00	0.02	0.00	31.22	0.00	0.00	0.00	0.30
CRS1	163.64	0.01	479.72	0.02	20.46	2.78	0.21	0.41	0.01	1.70	0.00	0.13	0.00	0.00	0.95	0.00	0.76	63.72	1.11	0.00	0.00	0.08	2.05	0.00	0.00	0.00	0.00
DRB4	17.39	0.00	973.14	62.80	0.00	28.99	100.28	6.47	0.00	38.14	0.12	0.67	1.10	0.00	20.64	0.85	0.22	594.16	26.42	0.01	0.07	0.00	31.35	0.00	0.00	0.00	31.40
BFB1	344.95	0.01	1025.38	0.02	10.74	4.93	1.50	4.31	0.26	2.25	0.01	0.00	1.02	0.34	0.96	0.51	3.54	312.84	0.18	0.00	0.02	0.14	23.84	0.01	0.03	0.00	0.00
BFB2	193.09	0.09	935.05	39.18	0.00	84.62	3.68	11.04	219.01	209.43	0.13	1.66	0.00	0.00	4.88	3.57	1.46	2311.01	0.00	0.00	0.01	0.00	143.33	0.04	0.00	0.00	1.21
RRB1	48.18	0.00	363.74	72.38	0.00	165.34	5.43	11.97	0.00	300.59	0.24	3.23	2.57	27.68	1.44	6.66	2.82	2066.06	0.45	0.01	0.00	0.00	12.01	0.02	0.15	0.00	11.34
ANS1	557.13	0.01	1098.04	0.04	6.01	82.34	4.54	13.41	1.32	132.34	0.13	1.39	0.00	2.27	1.16	2.53	6.34	1127.16	0.00	0.00	0.05	0.05	18.83	0.01	0.03	0.00	0.00
ANBH1	479.91	0.01	689.79	2.88	12.87	15.55	4.26	12.52	86.59	26.69	0.36	0.35	0.20	1.04	1.15	3.76	0.98	560.73	1.99	0.00	0.00	0.00	310.57	0.00	0.07	0.00	0.00
RWB1c	139.74	0.01	472.09	6.64	9.34	21.72	0.39	0.72	24.67	57.30	0.04	0.36	0.00	0.71	0.07	0.00	0.88	563.06	0.00	0.00	0.00	0.00	22.73	0.00	0.05	0.00	0.10
RWB5	44.71	0.01	133.76	32.66	0.00	82.96	8.62	0.73	20.77	152.46	0.13	1.89	0.70	1.49	0.87	0.00	0.26	746.13	1.55	0.00	0.01	0.03	71.38	0.01	0.01	0.00	41.65
VBB1	47.60	0.01	421.79	5.95	0.99	15.40	0.70	1.92	9.71	25.71	0.03	0.26	0.00	0.52	0.14	0.26	0.88	241.94	0.00	0.00	0.00	0.00	6.95	0.01	0.00	0.00	0.00
LRB2	35.09	0.00	51.23	21.98	0.00	65.79	10.15	0.31	0.00	119.66	0.10	1.46	0.57	2.02	3.00	0.19	1.04	506.33	0.97	0.00	0.00	0.05	27.16	0.00	0.00	0.00	3.26
VFB1	3749.56	0.00	4375.18	0.28	4.64	490.09	25.98	78.42	2.86	903.55	0.64	7.62	0.00	16.13	7.29	28.67	83.71	14206.90	18.93	0.01	0.11	0.00	59.91	0.00	0.16	0.00	0.00
VFB2	35.92	0.00	64.64	16.90	0.00	54.65	12.22	0.49	0.00	90.18	0.08	0.96	0.17	57.85	2.82	0.38	1.52	475.64	1.85	0.00	0.00	0.07	99.10	0.00	0.00	0.00	3.37
FLS1	871.99	0.00	2453.68	0.15	7.81	98.18	8.43	24.95	2.15	142.30	0.11	0.93	0.00	261.57	2.36	13.15	84.47	3450.16	0.00	0.01	0.00	0.00	192.61	0.00	0.00	0.00	0.00
FLB5	68.98	0.02	369.43	100.81	2.14	169.66	34.04	5.52	0.11	324.64	0.46	3.73	1.16	71.91	3.57	8.48	6.84	1675.26	0.58	0.00	0.00	0.14	41.12	0.00	0.14	0.00	10.06
SA1/66	1906.05	0.13	7188.75	6.31	1.14	106.37	24.10	72.26	134.34	162.73	0.65	5.25	1.48	7.59	9.43	39.37	201.70	13719.04	33.68	0.01	0.11	0.65	336.63	0.00	0.65	0.00	0.19
MWB2	101.46	0.00	322.04	18.21	0.00	104.35	2.12	4.10	1.71	178.16	0.13	1.76	23.00	55.68	0.94	2.37	1.60	2479.10	5.38	0.01	0.04	0.01	73.13	0.00	0.07	0.00	13.52

Appendix 5c. Ohio State University Data

Town	Location	Sample No.	OHIO STATE UNIVERSITY											
			^4He	Ar	CH_4	N_2	O_2	Total CO_2	H_2S	R/R_0	N_2/Ar	C_1/C_2^+	$\delta^{13}C$-CH_4	$\delta^{13}C$-CO_2
			µcc/kg	cc/kg	cc/kg	cc/kg	cc/kg	cc/kg	µcc/kg				‰	PDB
Leeu Gamka	Kruidfontein	WP 508	14 146.4	0.389	0.07	14.2	0.003	16.8	3.03	0.011	36.6	7990	bdl	-11.38
	Groot Kruidfontein	WP 502	638.6	0.466	1.14	15.9	0.001	18.5	0.09	0.344	34.2	12484	-74.45	-16.37
	Groot Kruidfontein	WP 505	62 531.5	0.351	0.27	11.6	0.023	19.3	5.23	0.018	33.2	9451	-62.64	-10.62
Cradock	Cradock Spa	CRS1	411.9	0.389	0.22	14.4	0.011	1.2	5.23	0.265	37.0	15247	-72.11	-13.46
	Waaikraal Farm	DRB4	987.0	0.424	3.07	16.5	0.049	34.8	0.03	0.211	38.8	16247	-70.14	-19.28
Fort Beaufort	Sulphur Baths	BFB1	71.2	0.305	0.01	16.3	0.094	0.1	7.77	1.016	53.6	bdl	bdl	-13.24
	Sulphur Baths	BFB2	84 512.7	0.311	23.53	13.8	0.074	12.1	4.22	0.024	44.3	5165	-55.36	-11.92
	Rocky Ridge	RRB1	10 153.3	0.348	3.67	13.5	0.017	37.5	0.19	0.012	38.7	4879	-55.88	-10.35
Aliwal North	Aliwal North Spa (inside)	ANS1	235 141.2	0.287	35.29	11.0	0.005	0.3	47.34	0.088	38.5	4570	-64.98	-12.77
	Aliwal North Farm	ANBH1	120 582.8	0.408	39.07	17.1	0.012	0.6	0.16	0.097	41.9	5149	-65.61	-17.61
Venterstad	Rooiwaal	RWB1c	39 636.1	0.359	2.91	14.3	0.047	15.6	23.58	0.018	39.7	3655	-50.68	-12.20
	Rooiwaal	RWB5	87.1	0.272	0.01	15.4	0.085	17.4	0.78	0.713	56.5	bdl	bdl	-15.25
	Vaalbank	VBB1	6 752.7	0.369	5.31	14.9	0.001	1.1	18.22	0.042	40.3	2877	-49.54	-10.34
	La Rochelle	LRB2	980.2	0.351	1.61	13.8	0.003	19.1	0.08	0.159	39.3	16547	-73.14	-17.45
Trompsburg	Vlakfontein	VFB1	40 631.8	0.543	1.00	24.8	0.010	0.3	15.92	0.052	45.6	5915	-65.65	-12.72
	Vlakfontein	VFB2	185.6	0.413	1.21	15.6	0.000	17.0	0.06	0.441	37.7	9869	-72.14	-18.02
Florisbad	Florisbad Spa	FLS1	483 492.8	0.435	31.95	13.5	0.040	0.5	28.36	0.027	31.1	2417	-50.90	-13.12
	Farm	FLB5	7 567.8	0.348	3.40	13.7	0.052	23.7	0.07	0.115	39.4	2988	-51.60	-16.36
Merweville	Soekor borehole	SA1/66												
	Farm	MWB2	189.0	0.397	1.05	14.8	0.069	24.6	0.07	0.657	37.1	14120	-74.61	-19.84

bdl: below detection limits

Appendix 5d. Australian National University, University of Cape Town, iThemba Labs and Beta Analytic Laboratory data

Town	Location	Sample No.	AUSTRALIAN NATIONAL UNIVERSITY			UCT	iThemba LABS and Beta Analytic						
			$^{36}Cl \times 10^{-12}$	$^{36}Cl/Cl$ (x10 $^{-15}$)	Error	$^{87}Sr/^{86}Sr$	$\delta^{2}H$	$\delta^{18}O$	$\delta^{13}C$	Tritium		C^{14}	
							‰ SMOW		PDB	TU	±	pMC	±
Leeu Gamka	Kruidfontein	WP 508	17.6	333.2	11.3	0.71157	-29	-5.0	-14.8	0.1	0.2	56.7	2.1
	Groot Kruidfontein	WP 502	21.5	499.1	18.0	0.71158	3	0.4	-10.3	3.5	0.3	89.2	2.4
	Groot Kruidfontein	WP 505	10.2	287.4	10.2	0.71119	-26	-4.7		0.4	0.2		
Cradock	Cradock Spa	CRS1	2.3	125.7	6.3	0.71006	-39	-7.7	-7.2	0.5	0.2	23.0	0.1
	Waaikraal Farm	DRB4	24.4	728.5	24.7	0.71233	-13	-2.4	-13.6	3.1	0.3	90.5	2.5
Fort Beaufort	Sulphur Baths	BFB1	7.9	65.4	3.2	0.71004	-36	-7.2	4.7	0.0	0.2	20.2	0.1
	Sulphur Baths	BFB2	40.1	122.6	4.9	0.70887	-24	-4.9	-12.9	0.4	0.2	62.3	2.2
	Rocky Ridge	RRB1	44.6	112.7	4.6	0.70962	-24	-4.8	-11.6	0.5	0.2	74.4	2.3
Aliwal North	Aliwal North Spa (inside)	ANS1	19.9	38.6	2.2	0.71206	-36	-6.8		0.5	0.2		
	Aliwal North Farm	ANBH1	22.2	40.6	2.4	0.71206	-36	-6.7		0.1	0.2		
Venterstad	Rooiwaal	RWB1c	17.4	830.9	28.0	0.71016	-32	-5.4	-11.3	0.9	0.3	73.9	2.3
	Rooiwaal	RWB5	27.2	1701.7	54.8	0.71043	-26	-4.9	-11.7	1.2	0.3	93.7	2.5
	Vaalbank	VBB1	7.6	137.2	6.8	0.71054	-29	-5.7	-11.5	0.6	0.2	49.7	0.2
	La Rochelle	LRB2				0.71003	-26	-4.8	-9.2	1.2	0.3	84.2	2.4
Trompsburg	Vlakfontein	VFB1	77.6	20.1	1.6	0.77719	-39	-7.5	-25.5	0.1	0.2	53.1	0.2
	Vlakfontein	VFB2	21.3	2294.0	81.9	0.71066	-28	-4.8	-8.6	1.0	0.3	89.7	2.5
Florisbad	Florisbad Spa	FLS1	34.1	34.5	2.0	0.75392	-37	-6.9	-26.0	1.6	0.3	47.3	0.2
	Farm	FLB5	64.7	619.3	19.9	0.71840	-21	-3.4	-4.6	1.3	0.3	94.0	2.5
Merweville	Soekor borehole	SA1/66											
	Farm	MWB2	50.7	624.2	21.4	0.71031	-28	-5.2	-13.3	1.4	0.3	86.9	2.4

UCT: University of Cape Town

Appendix 6. Data set used in the final analyses

Town	Location	Sample No.	FIELD			STELLENBOSCH UNIVERSITY					DUKE U.		STELLENBOSCH UNIVERSITY								
						Anions							Cations					Trace Elements			
						Cl^-	Br^-	NO_3^-	PO_4^{3-}	SO_4^{2-}	F^-	HCO_3^-	Ca^{2+}	K^+	Mg^{2+}	Na^+	CB	Li	B	V	U
			°C		mS/m	mg/L							mg/L				%	µg/L			
Deep																					
Cradock	Cradock Spa	CRS1	29.4	9.8	21	24	<1	<1	<2	7	7.0	55	3	0.3	0.01	43	7.2	166.9	473.5	0.506	0.048
Fort Beaufort	Sulphur Baths	BFB1	23.5	10.0	82	191	<1	<1	<2	23	16.1	63	4	2.0	0.01	144	-2.8	650.0	1 909.3	< 0.017	0.001
Aliwal North	Aliwal North Spa	ANS1	30.0	9.1	201	515	<1	<1	<2	<2	4.5	20	78	1.8	0.03	314	8.5	539.6	924.6	< 0.017	0.004
Aliwal North	Aliwal North Farm	ANBH1	21.6	7.5	190	484	<1	<1	<2	<2	3.8	73	14	1.0	1.25	350	4.0	540.5	670.1	0.030	0.003
Trompsburg	Vlakfontein	VFB1	29.5	9.2	1 019	3 869	<1	<1	<2	956	3.7	24	432	17.2	0.14	2 363	-1.8	6 813.9	3 065.5	0.031	0.002
Florisbad	Florisbad Spa	FLS1	28.7	9.4	362	1 034	<1	<1	<2	<2	5.7	22	86	7.2	0.07	696	8.2	842.8	2 030.8	0.047	0.004
Merweville	Soekor Borehole	SA1/66	21.9	7.6	1 202	3 858	12.02	0.12		237			110	37.5	7.52	2 584	2.4		23 057.3		<0.006
Mixed																					
Leeu Gamka	Kruidfontein	WP 508	26.5	8.1	93	83	<1	<1	<2	101	2.2	212	34	2.9	2.37	144	1.7	540.4	333.4	< 0.017	0.664
Leeu Gamka	Groot Kruidfontein	WP 505	23.5	8.2	133	80	<1	<1	<2	219	3.7	232	22	2.2	0.56	233	3.4	945.8	664.5	< 0.017	0.544
Fort Beaufort	Sulphur Baths	BFB2	21.2	7.4	200	452	<1	<1	<2	<2	3.4	403	76	1.5	39.10	266	-1.9	170.4	760.9	0.049	1.310
Venterstad	Rooiwaal	RWB1c	25.7	8.0	49	32	<1	<1	<2	18	2.5	227	20	0.5	2.88	81	-2.0	165.0	389.9	< 0.017	0.023
Venterstad	Vaalbank	VBB1	18.2	8.4	54	85	<1	<1	<2	<2	3.1	167	14	0.6	2.65	88	-4.0	49.7	406.4	< 0.017	0.040
Shallow																					
Leeu Gamka	Groot Kruidfontein	WP 502	20.3	7.9	53	30	<1	<1	<2	32	0.9	236	39	2.7	10.11	58	-0.1	99.1	110.6	1.491	4.118
Cradock	Waaikraal Farm	DRB4	16.2	7.8	162	62	<1	<1	<2	48	1.2	764	26	3.8	60.09	242	5.0	14.5	753.4	93.181	26.558
Fort Beaufort	Rocky Ridge	RRB1	21.2	7.1	249	463	2.3	15.8	<2	74	1.3	622	148	5.0	72.64	280	0.6	43.7	295.1	1.240	11.784
Venterstad	Rooiwaal	RWB5	18.1	7.4	85	26	<1	<1	<2	32	0.4	465	77	1.6	34.07	42	-2.7	41.9	98.1	8.426	40.851
Venterstad	La Rochelle	LRB2	17.3	7.5	58	17	<1	7.8	<2	14	0.3	339	63	0.9	23.30	26	-2.6	34.3	42.6	9.929	3.141
Trompsburg	Vlakfontein	VFB2	18.2	7.7	50	12	<1	14.9	<2	17	0.6	284	57	1.5	20.58	23	-2.2	39.1	55.2	12.499	3.594
Florisbad	Farm	FLB5	19.2	7.7	138	196	<1	53.9	<2	62	0.9	444	92	17.2	58.14	75	-9.7	18.0	72.3	7.837	2.536
Merweville	Farm	MWB2	21.5	7.1	107	114	<1	<1	<2	84	0.6	347	93	2.2	18.94	79	-4.7	264.8	224.0	0.610	15.070

SA1/66: Sample taken in September 2013 and analysesd at the Institute for Groundwater Studies laboratory
< below detection limits
Blank cell: not analysed

continued....

Town	Location	Sample No.	iThemba LABS and Beta Analytic							UCT	SU		AUSTRALIAN NATIONAL U.	
			δ^2H	$\delta^{18}O$	$\delta^{13}C$	Tritium		C^{14}		$^{87}Sr/^{86}Sr$	Radon		$^{36}Cl \times 10^{-12}$	$^{36}Cl/Cl (\times 10^{-15})$
			‰ SMOW		PDB	TU	±	pMC	±		Bq/L	±		
Deep														
Cradock	Cradock Spa	CRS1	-39	-7.7	-7.2	0.5	0.2	23.0	0.1	0.71006	2.1	1.0	2.3	125.7
Fort Beaufort	Sulphur Baths	BFB1	-36	-7.2	4.7	0.0	0.2	20.2	0.1	0.71004	3.4	1.2	7.9	65.4
Aliwal North	Aliwal North Spa	ANS1	-36	-6.8		0.5	0.2			0.71206	1.3	0.8	19.9	38.6
Aliwal North	Aliwal North Farm	ANBH1	-36	-6.7		0.1	0.2			0.71206	57.6	4.4	22.2	40.6
Trompsburg	Vlakfontein	VFB1	-39	-7.5	-25.5	0.1	0.2	53.1	0.2	0.77719	2.5	1.0	77.6	20.1
Florisbad	Florisbad Spa	FLS1	-37	-6.9	-26.0	1.6	0.3	47.3	0.2	0.75392	9.1	1.8	34.1	34.5
Merweville	Soekor Borehole	SA1/66												
Mixed														
Leeu Gamka	Kruidfontein	WP 508	-29	-5.0	-14.8	0.1	0.2	56.7	2.1	0.71157	1.1	0.8	17.6	333.2
Leeu Gamka	Groot Kruidfontein	WP 505	-26	-4.7		0.4	0.2			0.71119	1.2	0.7	10.2	287.4
Fort Beaufort	Sulphur Baths	BFB2	-24	-4.9	-12.9	0.4	0.2	62.3	2.2	0.70887	5.7	1.4	40.1	122.6
Venterstad	Rooiwaal	RWB1c	-32	-5.4	-11.3	0.9	0.3	73.9	2.3	0.71016	20.7	2.6	17.4	830.9
Venterstad	Vaalbank	VBB1	-29	-5.7	-11.5	0.6	0.2	49.7	0.2	0.71054	17.5	2.4	7.6	137.2
Shallow														
Leeu Gamka	Groot Kruidfontein	WP 502	3	0.4	-10.3	3.5	0.3	89.2	2.4	0.71158	13.6	2.1	21.5	499.1
Cradock	Waaikraal Farm	DRB4	-13	-2.4	-13.6	3.1	0.3	90.5	2.5	0.71233	34.7	3.5	24.4	728.5
Fort Beaufort	Rocky Ridge	RRB1	-24	-4.8	-11.6	0.5	0.2	74.4	2.3	0.70962	38.6	3.5	44.6	112.7
Venterstad	Rooiwaal	RWB5	-26	-4.9	-11.7	1.2	0.3	93.7	2.5	0.71043	39.1	3.6	27.2	1701.7
Venterstad	La Rochelle	LRB2	-26	-4.8	-9.2	1.2	0.3	84.2	2.4	0.71003	43.5	4.0		
Trompsburg	Vlakfontein	VFB2	-28	-4.8	-8.6	1.0	0.3	89.7	2.5	0.71066	48.6	4.0	21.3	2294.0
Florisbad	Farm	FLB5	-21	-3.4	-4.6	1.3	0.3	94.0	2.5	0.71840	152.3	8.0	64.7	619.3
Merweville	Farm	MWB2	-28	-5.2	-13.3	1.4	0.3	86.9	2.4	0.71031	163.5	7.0	50.7	624.2

continued....

Town	Location	Sample No.	DUKE UNIVERSITY				OHIO STATE UNIVERSITY											
			$\delta^{11}B$	^{226}Ra	^{228}Ra	$^{228}Ra/^{226}Ra$	^{4}He	Ar	CH_4	N_2	O_2	Total CO_2	H_2S	$^{3}He/^{4}He$ as R/R_0	N_2/Ar	C_1/C_2^+	$\delta^{13}C$-CH_4	$\delta^{13}C$-CO_2
			‰	Bq/L			µcc/kg	cc/kg	cc/kg	cc/kg	cc/kg	cc/kg	µcc/kg				‰	PDB
Deep																		
Cradock	Cradock Spa	CRS1					412	0.389	0.22	14.4	0.011	1.2	5.23	0.265	37.0	15 247	-72.1	-13.5
Fort Beaufort	Sulphur Baths	BFB1	5.4	0.002	0.004	2.63	71	0.305	0.01	16.3	0.094	0.1	7.77	1.016	53.6	bdl	bdl	-13.2
Aliwal North	Aliwal North Spa	ANS1	9.5	0.008	0.012	1.62	235 141	0.287	35.29	11.0	0.005	0.3	47.34	0.088	38.5	4 570	-65.0	-12.8
Aliwal North	Aliwal North Farm	ANBH1	15.2				120 583	0.408	39.07	17.1	0.012	0.6	0.16	0.097	41.9	5 149	-65.6	-17.6
Trompsburg	Vlakfontein	VFB1	29.9				40 632	0.543	1.00	24.8	0.010	0.3	15.92	0.052	45.6	5 915	-65.7	-12.7
Florisbad	Florisbad Spa	FLS1	23.2				483 493	0.435	31.95	13.5	0.040	0.5	28.36	0.027	31.1	2 417	-50.9	-13.1
Merweville	Soekor Borehole	SA1/66	23.9															
Mixed																		
Leeu Gamka	Kruidfontein	WP 508	8.9				14 146	0.389	0.07	14.2	0.003	16.8	3.03	0.011	36.6	7 990	bdl	-11.4
Leeu Gamka	Groot Kruidfontein	WP 505	9.3				62 532	0.351	0.27	11.6	0.023	19.3	5.23	0.018	33.2	9 451	-62.6	-10.6
Fort Beaufort	Sulphur Baths	BFB2	19.9				84 513	0.311	23.53	13.8	0.074	12.1	4.22	0.024	44.3	5 165	-55.4	-11.9
Venterstad	Rooiwaal	RWB1c	6.5				39 636	0.359	2.91	14.3	0.047	15.6	23.58	0.018	39.7	3 655	-50.7	-12.2
Venterstad	Vaalbank	VBB1	5.9	0.007	0.006	0.93	6 753	0.369	5.31	14.9	0.001	1.1	18.22	0.042	40.3	2 877	-49.5	-10.3
Shallow																		
Leeu Gamka	Groot Kruidfontein	WP 502		0.002	0.012	6.94	639	0.466	1.14	15.9	0.001	18.5	0.09	0.344	34.2	12 484	-74.5	-16.4
Cradock	Waaikraal Farm	DRB4	32.9				987	0.424	3.07	16.5	0.049	34.8	0.03	0.211	38.8	16 247	-70.1	-19.3
Fort Beaufort	Rocky Ridge	RRB1	35.1				10 153	0.348	3.67	13.5	0.017	37.5	0.19	0.012	38.7	4 879	-55.9	-10.4
Venterstad	Rooiwaal	RWB5					87	0.272	0.01	15.4	0.085	17.4	0.78	0.713	56.5	bdl	bdl	-15.3
Venterstad	La Rochelle	LRB2					980	0.351	1.61	13.8	0.003	19.1	0.08	0.159	39.3	16 547	-73.1	-17.5
Trompsburg	Vlakfontein	VFB2		0.002	0.01	5.05	186	0.413	1.21	15.6	0.000	17.0	0.06	0.441	37.7	9 869	-72.1	-18.0
Florisbad	Farm	FLB5	32.9				7 568	0.348	3.40	13.7	0.052	23.7	0.07	0.115	39.4	2 988	-51.6	-16.4
Merweville	Farm	MWB2	26.9	0.006	0.015	2.39	189	0.397	1.05	14.8	0.069	24.6	0.07	0.657	37.1	14 120	-74.6	-19.8

Appendix 7. Assessment and Selection of Data for Use in the Final Analyses

1. PREAMBLE

As part of the mandate for the Karoo deep groundwater project, a wide range of geochemical tracers have been collected from various different analytical laboratories. The data obtained has been compiled into a database that formed the basis for the assessment of groundwater characteristics of shallow vs deep groundwater in the Karoo Basin. Samples have also been collected in two field seasons, one in summer and one in winter, to evaluate any seasonal variation. However, in some cases, multiple datasets of the same tracer have been obtained from different laboratories. The purpose of this document is to summarise what data has been obtained and where and how the final dataset was compiled.

2. DATA OBTAINED

An initial round of analyses was obtained from the first sampling trip (March 2014). The purpose of these analyses was to provide a framework to make decisions as to which boreholes and springs should be sampled during the second sampling trip (June/July 2014). 33 sites were sampled during the first trip and analysis focussed on standard geochemical tracers. This included cations, anions, trace elements and stable isotopes of oxygen and hydrogen. A decision was made to also obtain REE data. At each sampling location, additional 250ml plus 1000ml bottles were collected as backups. After assessment of the data obtained during the first field trip, a reduced number of sampling locations were identified for sampling in the second sampling trip. 20 sites were selected for the second season sampling. However, only 19 samples were collected as the old Soekor borehole in Merweville, SA1/66, could not be sampled due to a lack of water pressure. Note that a sample collected from the SA1/66 borehole by Dr Ricky Murray in 2013, which had been stored in a fridge but was not a full container, was analysed by Duke University for some geochemical parameters. The second sampling trip was set up as the “main” sampling trip during which most of the geochemical tracers that were to be used in the project were obtained. However, because 250ml bottles had been collected as backups in the summer round, once the selection of sampling locations had been made, these bottled were used to do Sr isotope analyses at UCT before the winter sampling trip began and contributed to refinements of the final sampling site list.

In some cases, a laboratory did not provide a full dataset because they were being used as a check on data quality. For example, the IGS data was not intended to be an integral part of the project results but was obtained to better understand why the first round of cation and anion analyses from Stellenbosch University had problems with charge balances being above acceptable levels. In the case of $\delta^{18}O$ and $\delta^{2}H$ data, three datasets have been obtained, one from the first round of sampling

used to help decide on final sampling sites and then another two sets from the second sampling trip. Table 1 summarises the data that were obtained from which laboratories.

Table 25: *Summary of data collected.*

Geochemical Tracer	SU		IGS	UKZN	UCT	iThemba Labs	Duke University	Ohio State University	ANU	Beta Analytic
	Sum	Win	Sum	Sum	Sum	Win	Win	Win	Win	Win
Cations	X	X	o				X			
Anions	X	X	X				X			
Field Alkalinity	X	X								
Lab Alkalinity	X						X			
Trace elements	X	X					X			
REE	X									
$\delta^{18}O$ and $\delta^{2}H$				X		X	X			
$\delta^{13}C$						o				o
Sr Isotopes					X		X			
Radon	X	X								
Radium							o			
^{14}C						o				o
Tritium						X				
^{36}Cl									X	
B Isotopes							o			
Noble Gases								X		
$\delta^{13}C$ in methane								X		

Notes: X = results received, o = results received but not full dataset, Sum = summer field trip (March 2014), Win = winter field trip (June/July 2014).

3. DATA VALIDATION

In this report only one set of data per geochemical tracer is used in the final database (Appendix 6). Where there are multiple sets of the same tracer have a decision was made as to which will be included in the final database. In some cases there are two sets of data, one from the first trip in March and one from the second trip in June/July but from different laboratories. This makes the assessment of the data difficult because it is not easy to determine if differences are due to seasonal variation or laboratory bias. In the sections below, the data that has been obtained for each tracer is outlined and its validity assessed. The decision making process for which dataset is included in the final database is then explained. In general the data from the second trip were used, unless there was a good reason not to do so.

3.1 Cations and Anions including Alkalinity

Cations from the first field trip were analysed at via an Agilent 7700 ICP-MS in the ICP-MS/AES Laboratory of the Central Analytical Facility (CAF) at Stellenbosch University. The anion analysis was performed using a Waters IC-Pak 717 Autosample-conductivity detector-Agillent 1120 pump in the Mass Spectrometry laboratory also of the CAF at Stellenbosch University. The data received from these two laboratories was then compiled and processed. For a number of the samples the charge balance was above acceptable levels (10%) and the anion analyses were repeated using different dilutions. However, the charge balance problem persisted. A decision was made to send the all of the anion samples and some of the cation samples to the IGS laboratory at the University of the Free State in order to provide an independent check of the data. The results of the cations were almost identical to that obtained from the CAF laboratory at Stellenbosch University, som of them exactly the same to the decimal place. The anion results from IGS were slightly different from SU, most likely due to a laboratory bias. However, the charge balance of the ions from IGS was poorer than that of the SU data. The cations and anions from the second field trip were analysed at the same analytical facilities at SU, as well as at Duke University where the Major anions were determined by ion chromatography on a Dionex IC DX-2100. A systematic error between the HCO_3^- and Cl^- values from both laboratories was observed, and there were still some problems with the charge balances from both laboratories. Therefore, the Cl analyses were repeated at SU again using a different range of dilutions. This improved the charge balance slightly and decreased the difference between the two laboratories.

The alkalinity was measured in the field during both field trips using a Hatch Digital Titrator. Lab alkalinity was measured at SU after the first field trip. When the field alkalinity value was replaced with the lab alkalinity value, the charge balance was significantly improved. Therefore, the data from the first field trip includes the cations, anions and lab alkalinity from SU. Lab alkalinity was measured after the second field trip at Duke University. When the field alkalinity was replaced with the lab alkalinity, the charge balance was again significantly improved. Therefore, Appendix 6 uses cations and anions from SU and the lab alkalinity from Duke University. A summary of the charge balances from each laboratory is shown in table 2.

3.2 Trace Elements

The trace and rare earth (REE) elements from both field trips were analysed using an Agilent 7700 ICP-MS in the ICP-MS/AES Laboratory of the Central Analytical Facility at Stellenbosch University. However, additional samples were collected by A Vengosh for analysis at Duke University. The instrument used at this laboratory is DCP-OES and ICP-MS. The results from the two laboratories are quite different. Appendix 6 uses the trace elements from the second sampling trip analysed at SU.

3.3 $\delta^{18}O$ and $\delta^{2}H$

Stable isotopes of $\delta^{18}O$ and $\delta^{2}H$ from the first field trip were analysed at the University of KwaZulu-Natal (UKZN) using a Los Gatos laser. The samples collected during the second field trip were analysed at iThemba LABS in Johannesburg using a duel inlet gas source from a Finnigan GasBench II mass spectrometer. Samples from the second sampling run were also analysed at the Environmental Isotope Laboratory at Duke University using thermochemical elemental analysis/continuous flow isotope ratio mass spectrometry (TCEA-CFIRMS) and a ThermoFinnigan TCEA and Delta+XL mass spectrometer. Appendix 6 uses the of $\delta^{18}O$ and $\delta^{2}H$ results from iThemba LABS.

3.4 Sr Isotopes

Two sets of Sr isotope data are available. The first was obtained from the MC-ICP-MS facility at UCT which is run and maintained by Dr Petrus le Roux. The second set of data was analysed at Duke University. Both sets of data are very similar to one another, with some being exactly the same. Given the similarity in the data there was no advantage of one laboratory over the other. The UCT data was included in the final data set (Appendix 6) as this was received much earlier and used in the preliminary data interpretation.

Table 26: *Summary of charge balance from each laboratory.*

Town	Location	Sample No.	Charge Balance				
			SU Summer	IGS Summer	SU Winter	DU Winter	SU Win with DU HCO_3
Leeu Gamka	Kruidfontein	WP 507	2.60	3.81			
	Kruidfontein	WP 506	3.26	7.42			
	Kruidfontein	WP 508	1.37	2.22	9.69	3.34	1.68
	Groot Kruidfontein	WP 497	2.71	3.31			
	Groot Kruidfontein	WP 496	3.77	3.34			
	Groot Kruidfontein	WP 502	5.72	8.63	10.69	0.51	-0.13
	Groot Kruidfontein	WP 505	2.23	2.12	7.70	0.68	3.36
Cradock	Cradock Spa	CRS1	-7.25		21.88	22.78	7.25
	Agri School Farm	DRB2	-5.64			8.94	
	Agri School Farm	DRB1	-9.12				
	Waaikraal Farm	DRB4	8.05		13.87		5.03
Fort Beaufort	Sulphur Baths	BFB1	3.24		1.28	6.69	-2.77
	Sulphur Baths	BFB2	-0.16		5.32	2.45	-1.89
	Rocky Ridge	RRB1			7.72	6.62	0.65
Aliwal North	Aliwal North Spa (inside)	ANS1	-2.64		8.28	8.60	8.51
	Aliwal North Spa (outside)	ANS2	-5.10				
	Aliwal North Farm	ANBH1	0.41	10.70	6.75	4.30	4.04
Venterstad	Wildebeest Valley	DB11a	7.26	13.60			
	Wildebeest Valley	WVB1	6.45	9.66			
	Wildebeest Valley	WVB3	0.13	6.38			
	Rooiwaal	RWB1c	0.54	14.37	8.29	8.03	-2.00
	Rooiwaal	RWB5	3.28		17.65	-6.64	-2.74
	Vaalbank	VBB1	-3.04		9.26	9.19	-4.01
	Vaalbank	VBB2	3.60				
	La Rochelle	LRB1	6.57			-10.46	
	La Rochelle	LRB2	0.78		15.58	-7.47	-2.62
Trompsburg	Vlakfontein	VFB1	4.73		-1.73	0.67	-1.80
	Vlakfontein	VFB2	6.82		25.52	-22.61	-2.21
	Vlakfontein	VFB3	8.41				
	Vlakfontein	VFB4	5.28			-13.04	
Florisbad	Florisbad Spa	FLS1	-2.29		8.76	2.68	8.21
	Florisbad Resort	FLB4	3.00				
	Farm	FLB5			2.16	-6.43	-9.69
Merweville	Farm	MWB1	4.80				
	Farm	MWB2	2.72		3.21	-4.31	-4.69

3.5 Radon

The radon was measured in the field during the first field trip using two detectors (Det. A and B). During the second field trip, one of the same detectors from the first field trip (Det. B) and a new detector (Det. C) were used. However, the samples were not analysed in the field, but instead were collected in bottles and the analysis occurred at the end of each day. After each field trip the results of each detector were analysed and processed. It was decided that the results from the detector with the lowest relative humidity reading would be used. When the humidity values were the same, an average result from both detectors was calculated. The results from the second field trip are considered to be more reliable because both detectors were used and compared to one another. The final data set (Appendix 6) include the radon results from the second field trip calculated as described above.

3.6 Soekor borehole data

As mentioned in section 2 above, the deep site in Merweville, SA1/66, could not be sampled at the time of either field trip. Prior to this two samples were collected by Mr Fanie de Lange and Prof Gerrit van Tonder from the IGS at the University of the Free State, and analysed at their laboratory. These were in November 2012 and September 2013. Gerrit van Tonder gave us permission to use the results of these analyses, and he also gave a ~200 mL sample to Dr Ricky Murray who kept it refrigerated before giving it to Prof Avner Vengosh from Duke University in July 2014 who later analysed it (see the results in Appendix 5). For the final data set (Appendix 6) it was decided to use the September 2013 analysed at the IGS laboratory because the sample analysed by Duke was old and the preservation of the sample (after sampling in 2013) is unknown.

3.7 Temperature of Florisbad warm spring

The temperature measured at the warm spring in Florisbad (FLS1), was 20°C during the second sampling round. However, during the first sampling round a temperature of 29°C was recorded. Appendix 3 presents historical water quality assessments of the spring. Temperatures of approximately 29°C have been recorded between 1915 and 1999. Therefore, a decrease of 9°C within three months is improbable. Potential reasons for measuring 20°C could be the cool air temperature of 13.5°C, as well as the extended sampling time due to the site being the first site of the sampling trip. A decision was made to use the temperature recorded during the first sampling trip of 29°C for the final dataset (Appendix 6).

4. CONCLUSION

Multiple sets of data have been obtained from different laboratories for various geochemical tracers. All of the results are presented in Appendices 5a-d. However, the final dataset used in the data analysis part of this report (chapters 5, 6 and 7) is the merged dataset presented in Appendix 6. The

set of anion, cation and alkalinity data with the best charge balance was obtained using the results from Stellenbosch University collected during the second field trip and the laboratory alkalinity from Duke University (also collected during the second field trip). Trace elements were analysed at both Stellenbosch and Duke Universities. There are significant differences in the two sets of data and the final dataset selected is that from Stellenbosch University from the second field trip. The final data set includes the stable isotopes of O and H analysed at iThemba LABS, the Sr isotope analyses obtained from UCT and radon values measured during the second field trip using the detector with the lowest relative humidity.